



Molecular-Based Optical Diagnostics for Hypersonic Nonequilibrium Flows



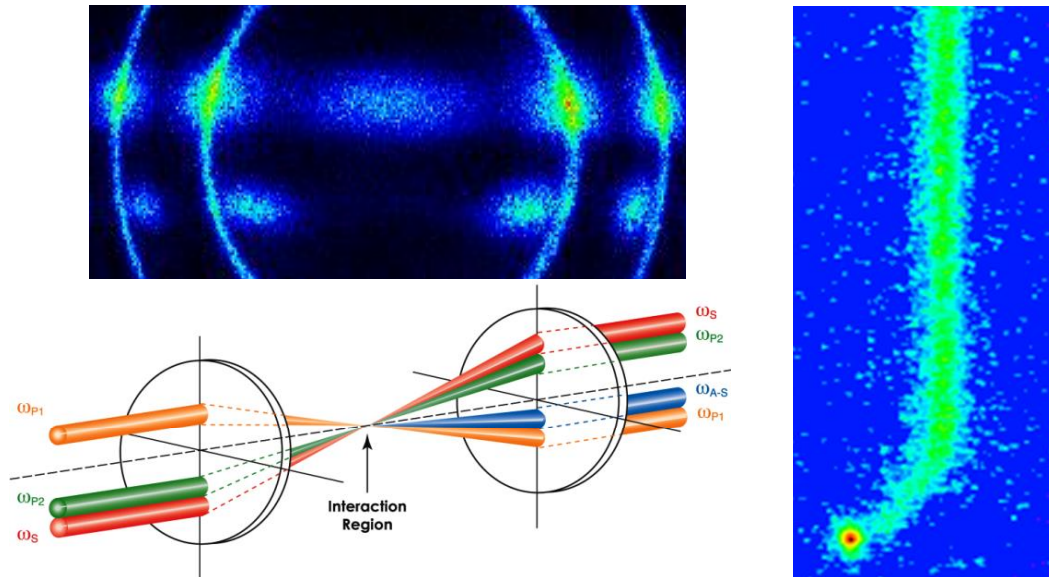
Paul Danehy and Brett Bathel, NASA Langley Research Center, Virginia, USA

Craig Johansen, The University of Calgary, Canada

Michael Winter, University of Kentucky, Kentucky, USA

Sean O'Byrne, University of New South Wales Canberra, Canberra, Australia

Andrew Cutler, The George Washington University, USA



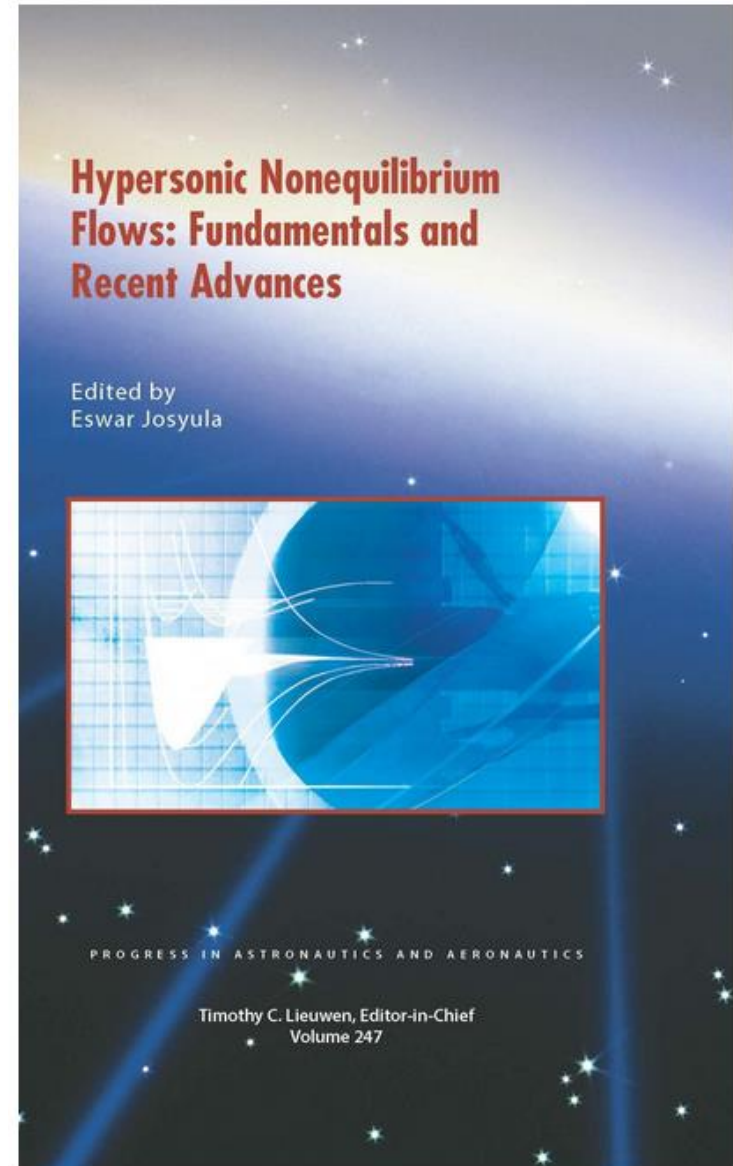
Trade names and trademarks are used in this report for identification only. Their usage does not constitute an official endorsement, either expressed or implied, by the National Aeronautics and Space Administration

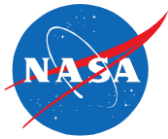


“Paul, Why are you doing this special session?”



- Multi-purpose:
 - Educate those new to field of laser based measurements (students)
 - Let collaborators from other fields know what is possible to measure
 - Provide some updates and ideas for those already working in measurement technology
- Special session is coordinated with the launch of a new AIAA Progress Series Book
 - Pedagogical treatment
 - Came out of a Fluids TC Working group led by E. Josyula
 - Our chapter: *Molecular-Based Optical Diagnostics for Hypersonic Nonequilibrium Flows*





HYPERSONIC NONEQUILIBRIUM FLOWS: FUNDAMENTALS AND RECENT ADVANCES



[Most Recent Book](#)
[Available Books](#)

Progress in Astronautics and Aeronautics

Hypersonic Nonequilibrium Flows: Fundamentals and Recent Advances

Eswar Josyula, U.S. Air Force Research Laboratory, Wright-Patterson Air Force Base, Ohio
eISBN: 978-1-62410-329-2
print ISBN: 978-1-62410-328-5
DOI: 10.2514/4.103292

© 2015 American Institute of Aeronautics and Astronautics
[Download the Full PDF](#)

About the Book

The high-temperature environment poses an unusual challenge in understanding the basic physics of hypersonic flight. A lack of such understanding can lead to risks and uncertainties in the design of aerospace vehicles. *Hypersonic Nonequilibrium Flows* documents recent, unprecedented scientific advances in the field of nonequilibrium processes for aerospace applications. These advances have been driven primarily by interest in space access and exploration, or in developing military technologies involving hypersonic flight regimes.

In the modeling of hypersonic flows, the last decade has witnessed a reexamination of fundamental principles of kinetic theory and quantum chemistry to describe the kinetic and thermal states, respectively, of the individual gas particles. Modern aerospace programs where nonequilibrium energy transfer processes play a major role may broadly be categorized as exo- and endo-atmospheric. The exo-atmospheric flight programs consist of Earth and planetary reentry programs, as well as access to space programs for applications that include space exploration, flight experiments and demonstrations, missile defense, and the nascent space tourism industry. The endo-atmospheric flight programs are primarily motivated by hypersonic military applications requiring high-precision engagement for tactical, theater and strategic defense, as well as applications involving intelligence, surveillance, and reconnaissance.

The nonequilibrium processes considered in this volume are generally associated with flight Mach numbers between 7 and 25, where the shock-layer temperatures range from 3000 to 25,000 K.

Hypersonic Nonequilibrium Flows includes fundamental governing equations of nonequilibrium fluid transport and computational approach to calculation of rates and cross-sections in quantized energy states; DSMC approach; radiative heat transfer; a CFD perspective; surface chemistry, with additional chapters on high enthalpy facilities and the associated diagnostic techniques.

PRICES

PDF

Member: \$79.95
List: \$116.95

[Add to Cart](#)

Hardback

Member: \$89.95
List: \$129.95

[Add to Cart](#)



Hypersonic Nonequilibrium Flows: Fundamentals and Recent Advances

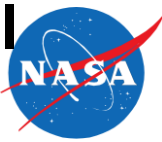


Edited by Eswar Josyula

Table of Contents:

1. *Fundamental Fluid Transport Equations for Hypersonic Nonequilibrium Flows, Eswar Josyula, Prakash Vedula*
2. *Computation of Hypersonic Nonequilibrium Flows using the Direct Simulation Monte Carlo Method, Iain D. Boyd*
3. *First Principles Calculation of Heavy Particle Rate Coefficients, Richard L. Jaffe, David W. Schwenke, Marco Panesi*
4. *Radiation from Hypersonic Bodies—A Window on Non-Equilibrium Processes, Deborah A. Levin*
5. *CFD Methods for Hypersonic Flows and Aerothermodynamics, Graham V. Candler, Pramod K. Subbareddy, Ioannis Nompelis*
6. *Surface Chemistry in Non-Equilibrium Flows, Jochen Marschall, Matthew MacLean, Paul E. Norman, Thomas E. Schwartzentruber*
7. *High-Enthalpy Facilities and Plasma Wind Tunnels for Aerothermodynamics Ground Testing, Olivier Chazot, Francesco Panerai*
8. *Molecular-Based Optical Diagnostics for Hypersonic Nonequilibrium Flows, Paul M. Danehy, Brett F. Bathel, Craig T. Johansen, Michael Winter, Sean O'Byrne, Andrew D. Cutler*

Introduction and Application Considerations for Optical Diagnostics in Hypersonic Nonequilibrium Flows



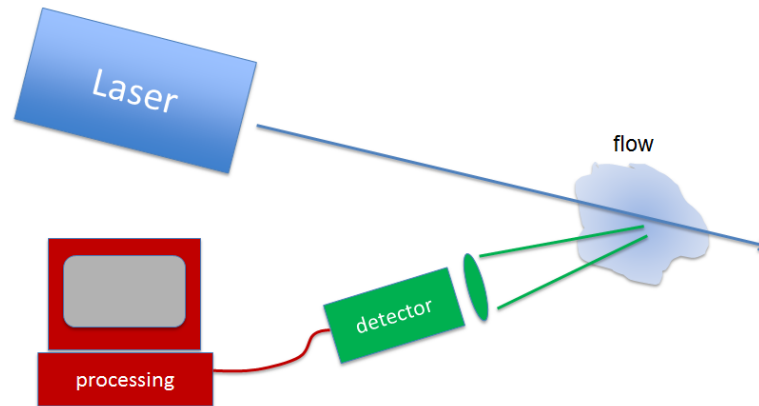
Paul Danehy and Brett Bathel, NASA Langley Research Center, Virginia, USA

Craig Johansen, The University of Calgary, Canada

Michael Winter, University of Kentucky, Kentucky, USA

Sean O'Byrne, University of New South Wales Canberra, Canberra, Australia

Andrew Cutler & Samantha Hurley, The George Washington University, USA





Outline for 1st Talk



Introduction and Application Considerations for Optical Diagnostics in Hypersonic Nonequilibrium Flows

- Temperature, equilibrium and nonequilibrium
- Characteristics of hypersonic nonequilibrium flow
 - What needs measuring?
- Advantages of spectroscopic measurement
- Aspects of a good measurement technique
- Choosing which measurement technique to use.



Temperature and Equilibrium



- Temperature

- Classical thermodynamics

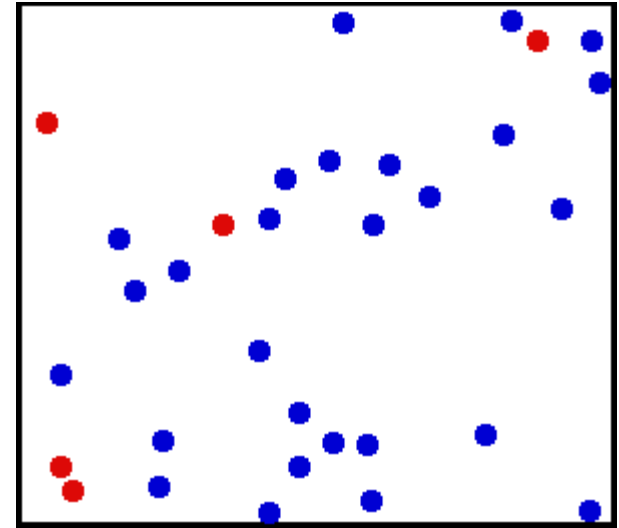
- Heat flowing from object A to B $\rightarrow T_A > T_B$

- Statistical thermodynamics

- Describe by Boltzmann distribution

- e.g. Maxwellian Velocity Distribution

width $\sim \sqrt{T}$



<http://en.wikipedia.org/wiki/Temperature>
Greg L at the [English language Wikipedia](http://en.wikipedia.org/wiki/Temperature)

- Equilibrium

- Classical thermodynamics

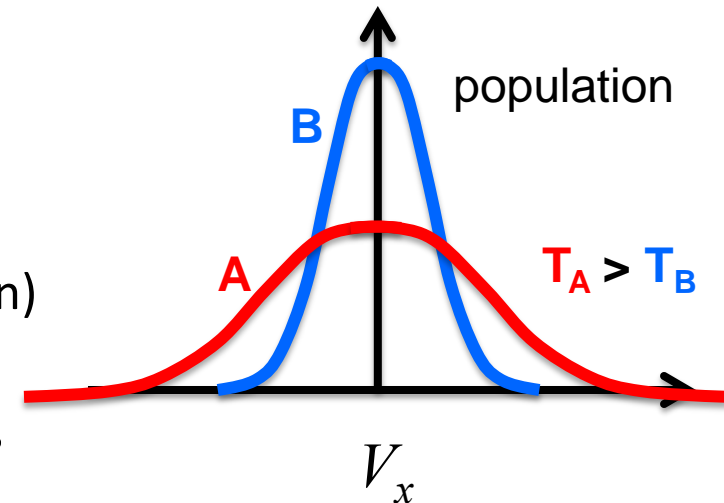
- Thermal equilibrium: $T_A = T_B$

- Statistical thermodynamics

- One temperature can describe all the different energy modes (via Boltzmann)

- Chemical equilibrium:

- Reactants and product concentrations don't further change with time

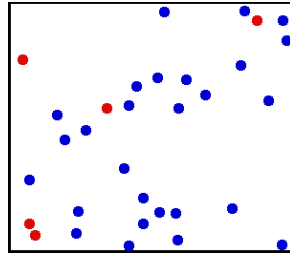




Energy Modes



- Translation



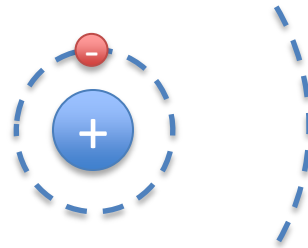
- Rotation



- Vibration



- Electronic



- These can all be described by a temperature:

- T_{trans} T_{rot} T_{vib} T_{elec}

- Thermal equilibrium: these T 's are all equal

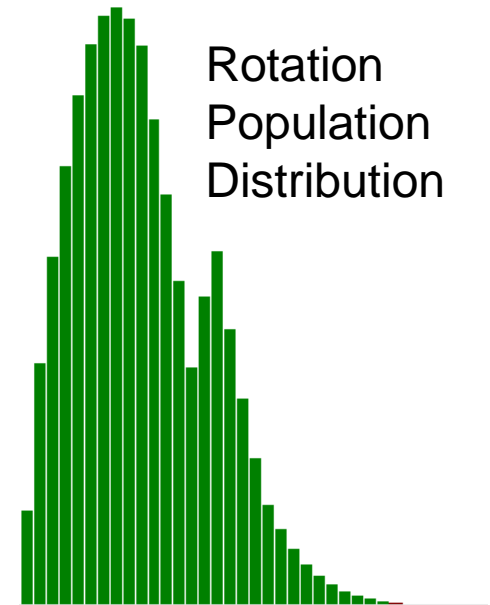
All these states are quantized!
1, 2, 3, ...



Nonequilibrium



- Thermal Nonequilibrium:
 - Different energy modes described by different T 's
 - e.g.: $T_{rot} \neq T_{vib}$
 - Or, the distribution of population can't be described by Maxwell-Boltzmann statistics (“non-thermal” distribution)
- Chemical Nonequilibrium:
 - Products and reactants are in a state of change
 - If held at those conditions (P, T) the composition will change.
- Equilibrium occurs via *collisions*



Rotational Quantum Number, J

Computed using LIFBASE
(J. Luque, SRI International)



Hypersonic Flows and Noneq.



- Hypersonic vehicles fly at high altitude (low P) and high speed ($M > 5$) resulting in gas and vehicle heating (high T)



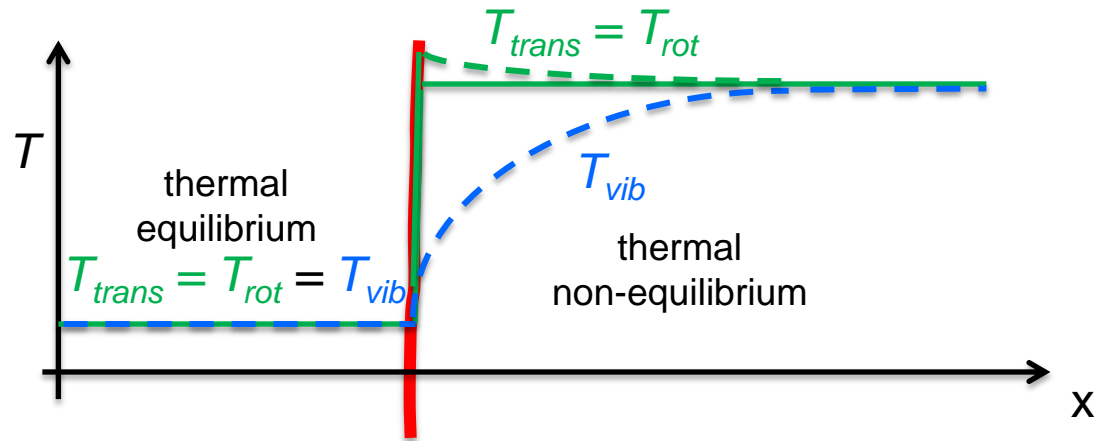
- Collisions rate scales as P/\sqrt{T}
- *Low collision rate causes nonequilibrium*
- At STP for O_2 : Trans: 10; Rot: 10; Vib: 20,000; Dissoc: 200,000 collisions to equilibrate!
 - 10 coll. ~ 1 ns; 20,000 coll. $\sim 2 \mu s$ at STP
- Hypersonic flows are also characterized by:
 - Steep gradients (shocks, boundary layers, expansions)
 - Combustion (in scramjets)
 - Dissociation / recombination



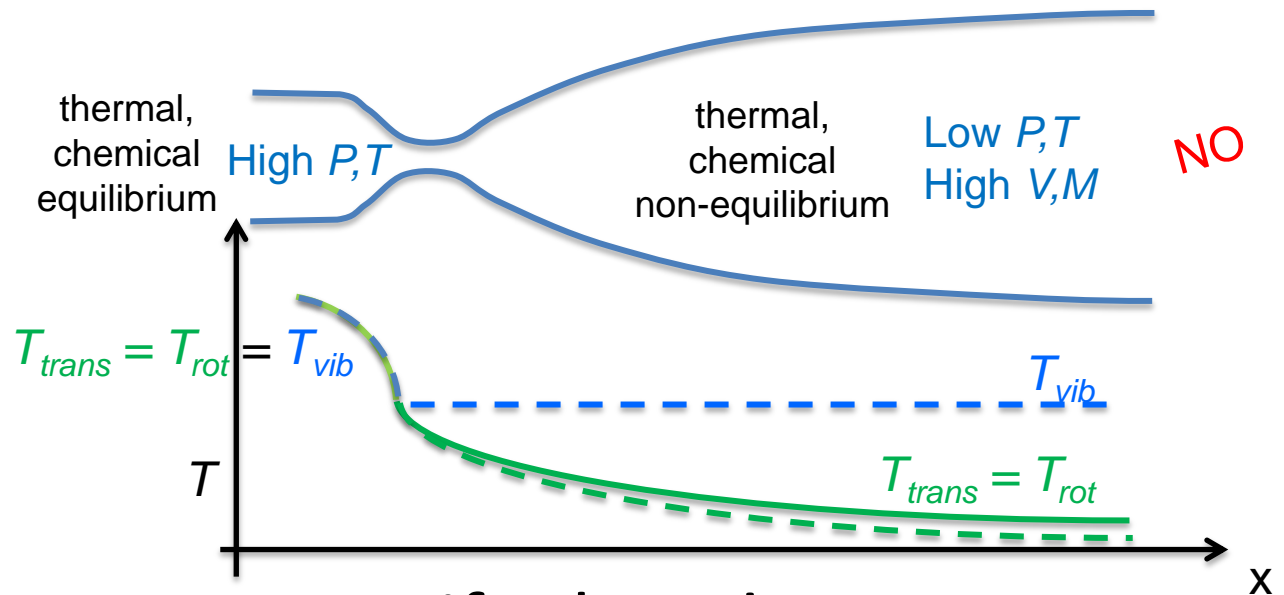


Some Hypersonic Nonequilibrium Flows

- Shock wave:



- Expansion:



- We can measure, quantify these!



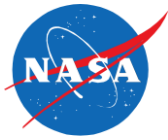
Parameters to measure



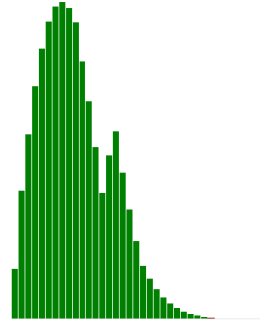
- Typical parameters of interest in Hypersonic Nonequilibrium Flows:
 - Velocity, Pressure, Density, Temperature_s, Species
 - *Non-thermal population distributions*
 - *How is energy in flow partitioned in terms of:*
 - thermal energy (T)
 - chemical energy (species) and
 - kinetic energy (V)?
- (O and N atom LIF at NASA ARC)*



Some advantages of Spectroscopic Measurement Techniques



- Non-intrusive
 - No probes, particles perturb the flow
- Remote detection
 - Can be used in hostile environments
- Can measure multiple parameters, states:
 - Sometimes simultaneously
 - Can be instantaneous (<10 ns) and high freq. (MHz)
 - Can be precise, accurate, high spatial res. (2D, 3D)
- *But...* No one measurement technique can meet all requirements
 - Can have more complicated theory, expensive and complex equipment, more difficult data analysis
 - May require seeding of (sometimes toxic) gases, more expertise, slower data acquisition, analysis





Scope of the Content



- Content focuses on molecular based, quantitative, mostly spectroscopic measurement techniques previously applied in or may be applicable to non-equilibrium flows. Many examples in equilibrium.
 - Content of lectures and manuscript are not exhaustive. Not all the ‘first’ or ‘most important’ references are given. Instead they there is an emphasis on describing how the techniques work and how they can be used to measure.
 - Also there is an admitted bias towards the authors’ own work.
- Content excludes the many relevant particle-based (PIV, LDV), probe-based and surface-based measurement techniques that could be used to study non-equilibrium flows; mostly no ‘flow vis’. (No schlieren.)



What makes a good measurement technique?

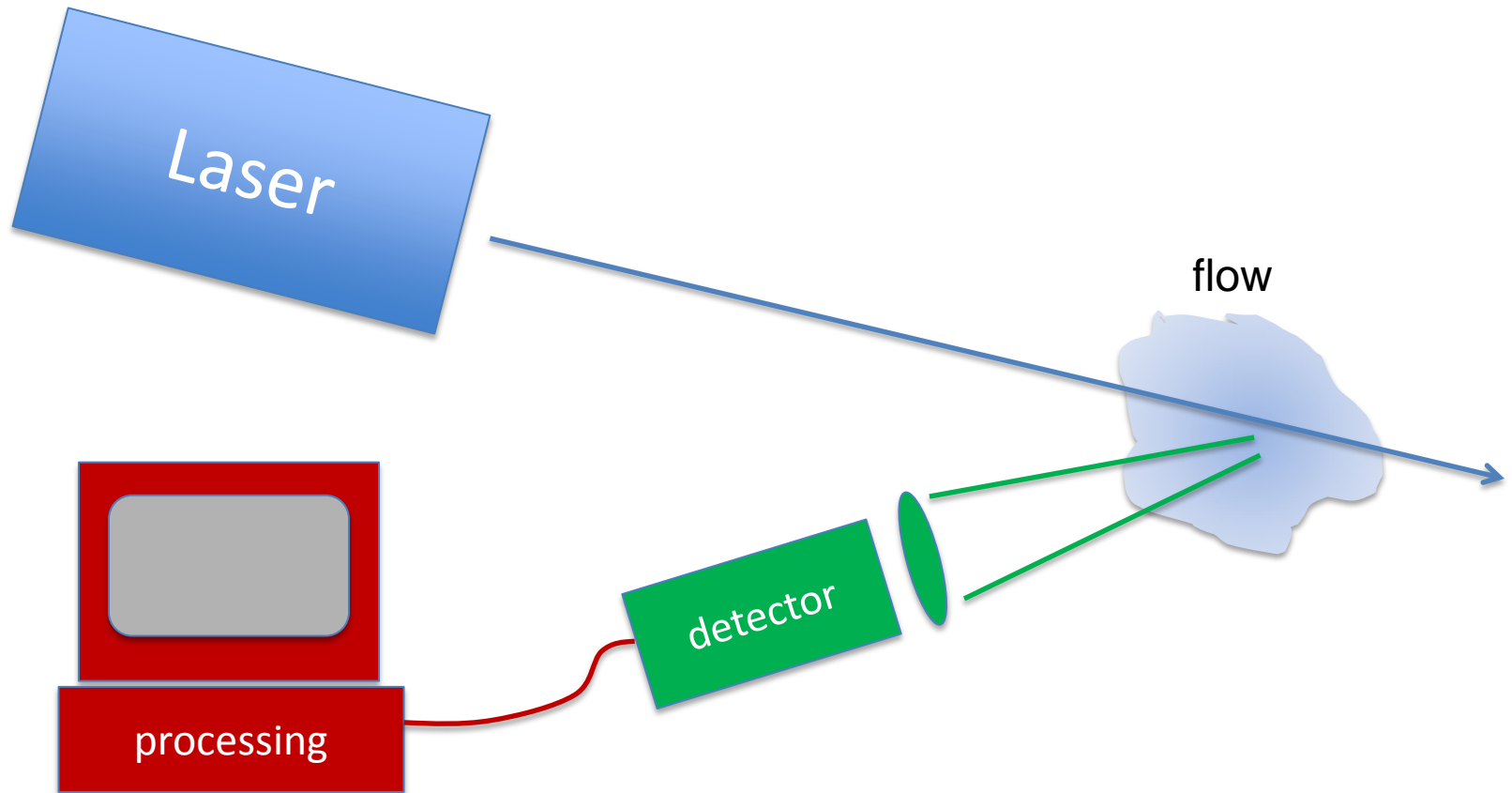


- A reliable measurement system matched with well-understood physics to make a quantified measurement that meets a customer's requirements.

Explore each of these...



Typical Measurement System



- Need to understand equipment and physics of process to make a measurement
 - Emission, Abs., LIF, Rayleigh, Raman, CARS, etc.



Measurement System: Lasers



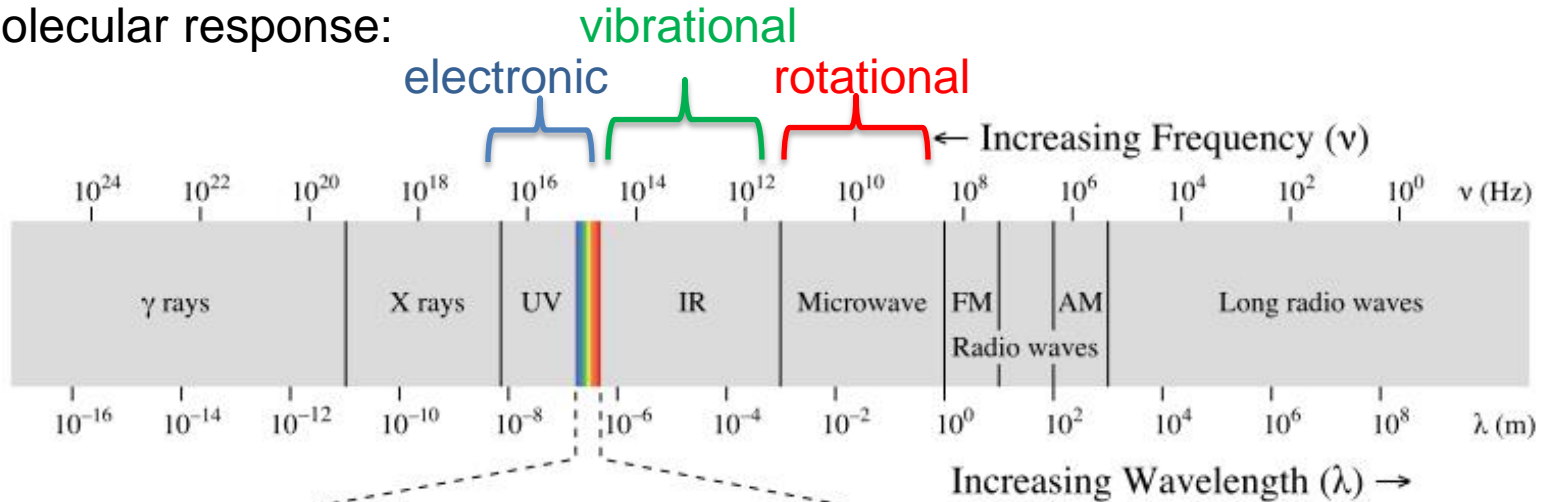
- Lasers: pulsed vs. continuous wave (cw)
 - Continuous wave: lower power (mW to Watt)
 - Pulsed:
 - 10 ns, picosecond, femtosecond all commercially available
 - ‘Freeze’ the flow
 - Much higher power vs cw (MWatt-GWatt, even TWatt)
 - Frequency conversion (useful in linear techniques such as Raman, Rayleigh, LIF)
 - Provide high powers for nonlinear techniques (CARS)
 - Repetition rate: 10-100 Hz, 16 kHz, 1 MHz, 80 MHz...
- What colors of laser light do we need?



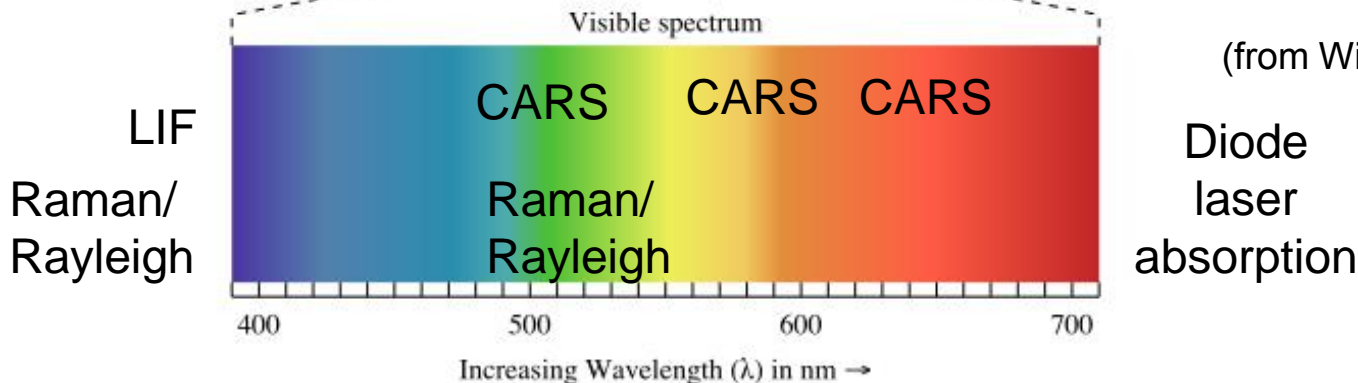
Colors of Light: Spectroscopy



Molecular response:



(from Wikipedia, "frequency")



<http://creativecommons.org/licenses/by-sa/3.0/deed.en>

- Many different colors can be useful for spectroscopy
- As energy increases, more modes can be excited
 - LIF: can see electronic, vibrational and rotational structure



Measurement System 2



- Detectors:

- Single point detectors:

- Photomultiplier tubes (PMT) and photodiodes

- Camera technology is rapidly evolving:

- CCDs provide 'scientific grade' (low noise, linear, etc.)

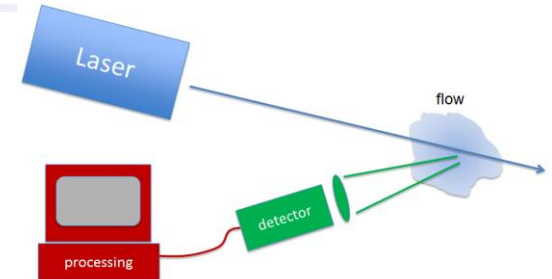
- CMOS cameras are faster

- Commercially available cameras at up to 10's, 100's of kHz steady streaming or MHz for short bursts or few pix

- Fiber optics and fiber-optic bundles often used for either transmitting laser or collecting signal

- Processing:

- Some data processing codes are available (CARSFT, LIFBASE) but many are proprietary.





What makes a good measurement technique?



- A reliable measurement system matched with well-understood physics to make a quantified measurement that meets a customer's requirements.



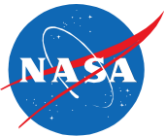
SKIP



Explore each of these...



Quantified Measurements



- Accuracy and precision of a measurement must be quantified to be useful, for example when comparing to a code
 - Qualitative measurements (flow vis) can be useful
- Quantified measurement:
 - Accuracy and precision are well characterized



Accurate but
not precise



Precise but
not accurate

(from Wikipedia,
“accuracy and precision”)

- Accuracy: compared to a ‘standard’ or ‘accepted’
- Precision: 1σ of large sample of measurements
 - Averaging reduces precision’s contribution to uncertainty
 - High precision required to quantify fluctuations (turbulence)



Customer Requirements







Interview the customer... (sometime the customer is you!)

- Simultaneous measurements to obtain correlations: $T'u'$, $\rho u'v'$
- Time resolution ($< \mu\text{sec}$), and frequency response ($> \text{MHz}$)
- Spatial resolution: near walls; smallest scales in shear layer
- Where are the measurement to be made?
 - Inflow to establish B.C., exit, near walls?
 - Point, line, plane, volume?
- Accuracy and precision requirement?
- What quantity of data is required? Uncertainty required?
- When is the data needed? Is “real-time” data required?
- What type of optical access is available?
- Can (toxic) seed gases be introduced? Will they influence the properties being measured? Can particles be used?
- What is the ordered priority of the above requirements?



What makes a good measurement technique?



- A reliable measurement system 
matched with well-understood physics 
to make a quantified measurement 
that meets a customer's requirements. 
- Now the lectures will focus on different measurement systems, introducing the physics.
 - How's the basic physics of the method work?
 - Can the measurements be made instantaneously (aka. single-shot) at high frequencies?
 - What accuracy and precision can be obtained?



Customer Requirements



- Consider a customer with arbitrary measurement requirements:
 - Would like a particular parameter measured
 - Would like the measurement at some conditions (P, T)
 - Many measurement technique signals scale as P_{static}, T_{static}
- Parameters to be measured:
 - Velocity, temperature, density, pressure, species (concentration or mole fraction)
- Can base choice of measurement technique (in part) on prior success by others:
 - We compiled past work into graphics that show static pressure and temperature of demonstrated measurements
 - Use these charts to find appropriate measurement methods



Backup Charts



Explanation of Parameter Charts



Overview:

This appendix shows the static conditions (temperature and pressure) at which various measurement techniques have been successfully demonstrated. When planning a new experiment to occur at a specified temperature and pressure, these graphs might be useful to see what measurements have previously been demonstrated at those conditions. The numerals used as data points indicate the reference in the attached reference list. The different measurement techniques are denoted by the colors indicated. Pressure is plotted on a logarithmic axis while temperature is on a linear axis.

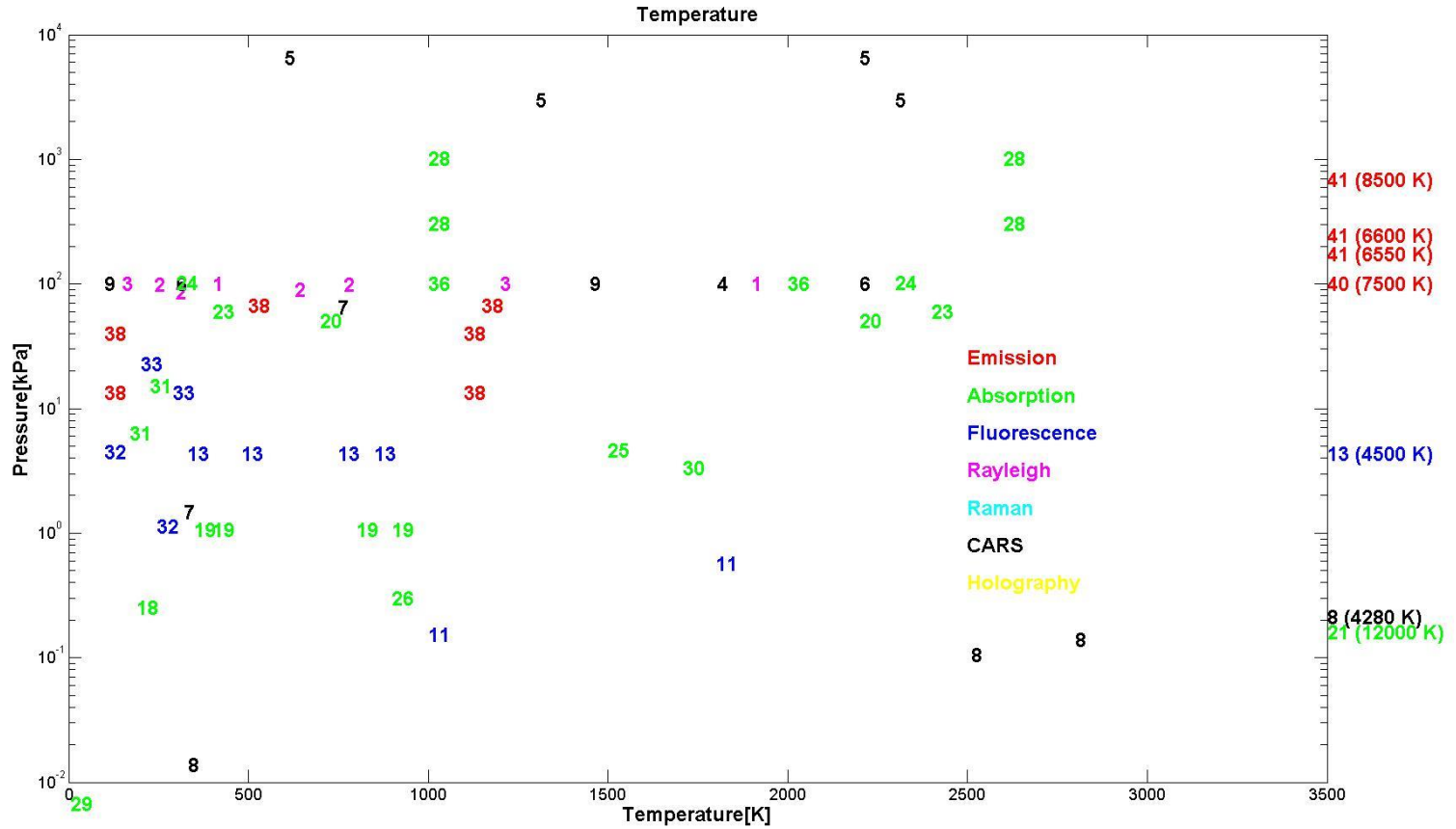
Caveats:

- The data includes both references contained in the manuscript as well as additional works.
- The reference numbers in the manuscript are different from those in this appendix.
- This study is not meant to be exhaustive; it provides a partial sampling of the data available in the literature.
- Some data points overlap. This is particularly true at room temperature and atmospheric pressure. Some data has been omitted to avoid overlaps.
- For temperatures greater than 3500 K, the reference number is plotted to the right of the chart with the static temperature in parentheses.
- “Species” includes either species concentrations or species mole fraction measurements.

(Not included in AIAA Progress Series manuscript)

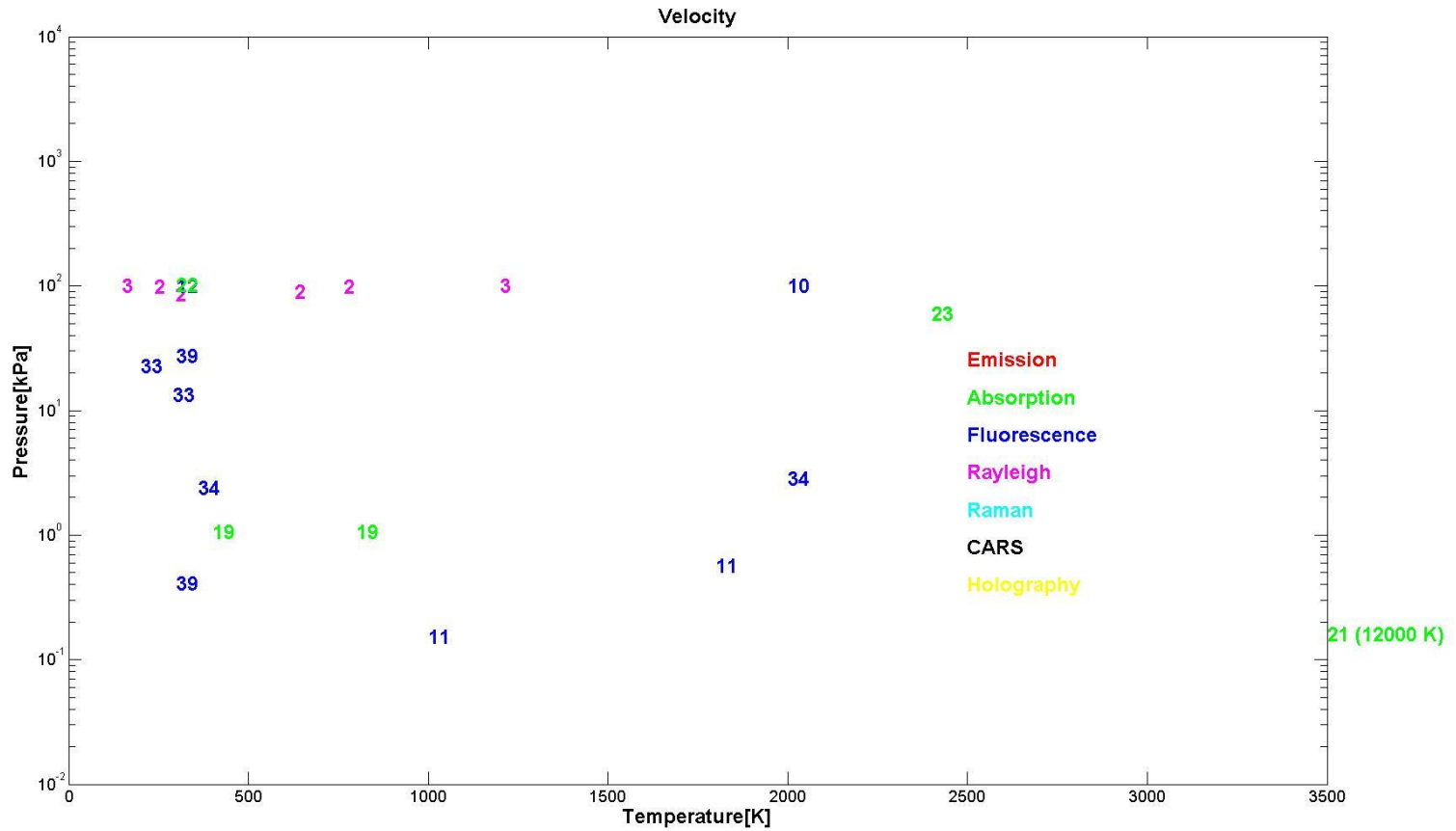


Temperature



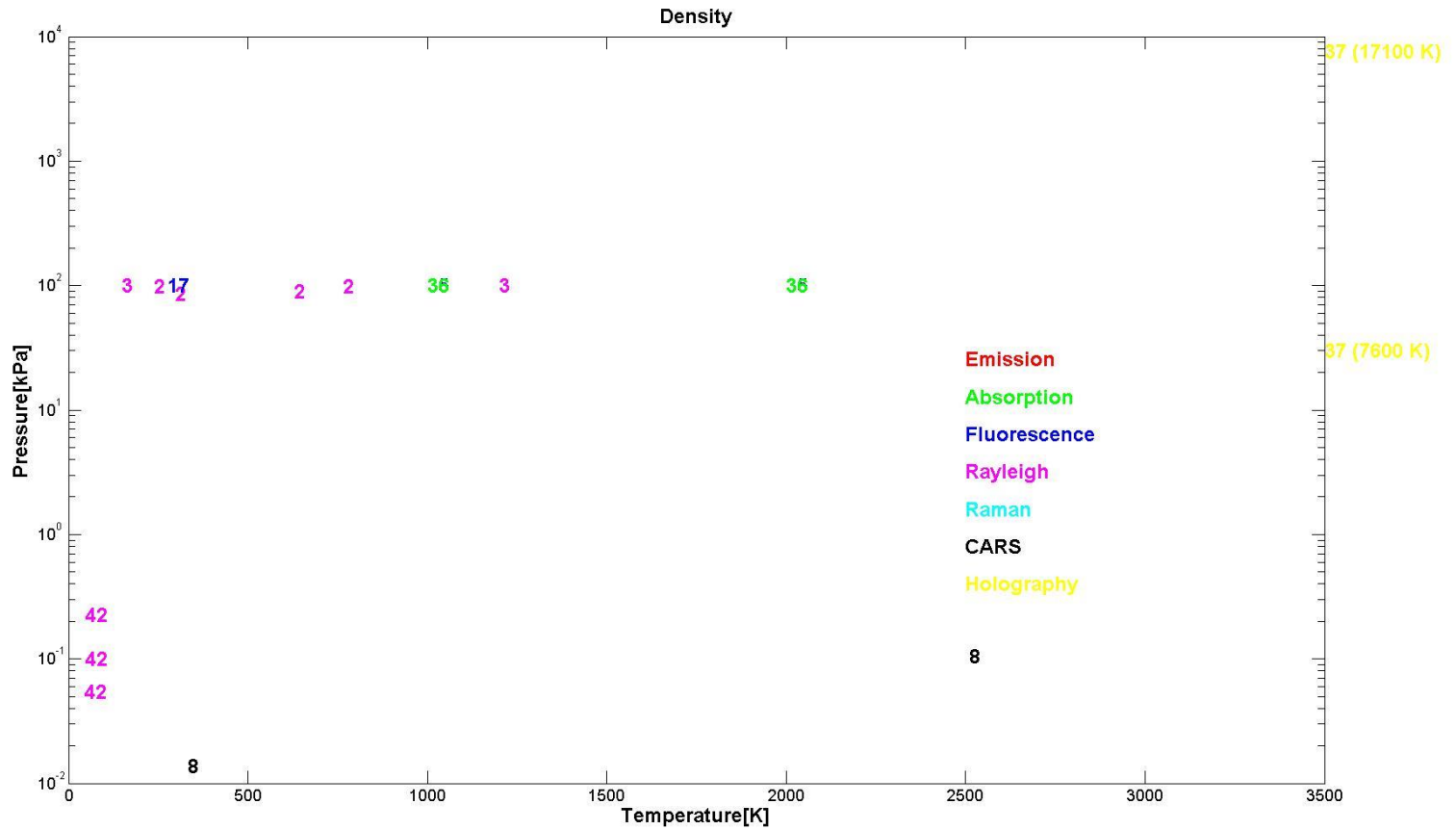
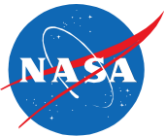


Velocity



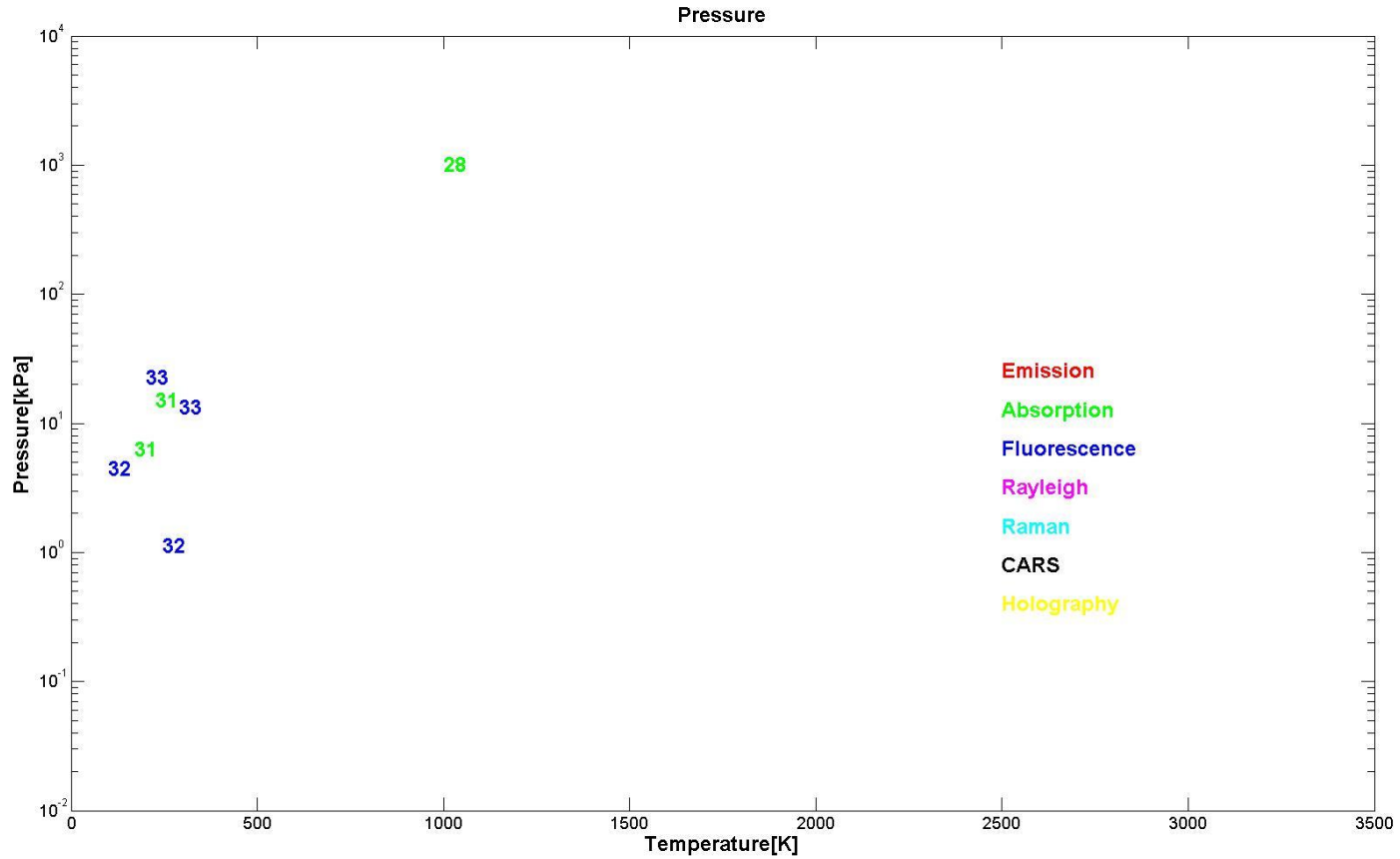


Density



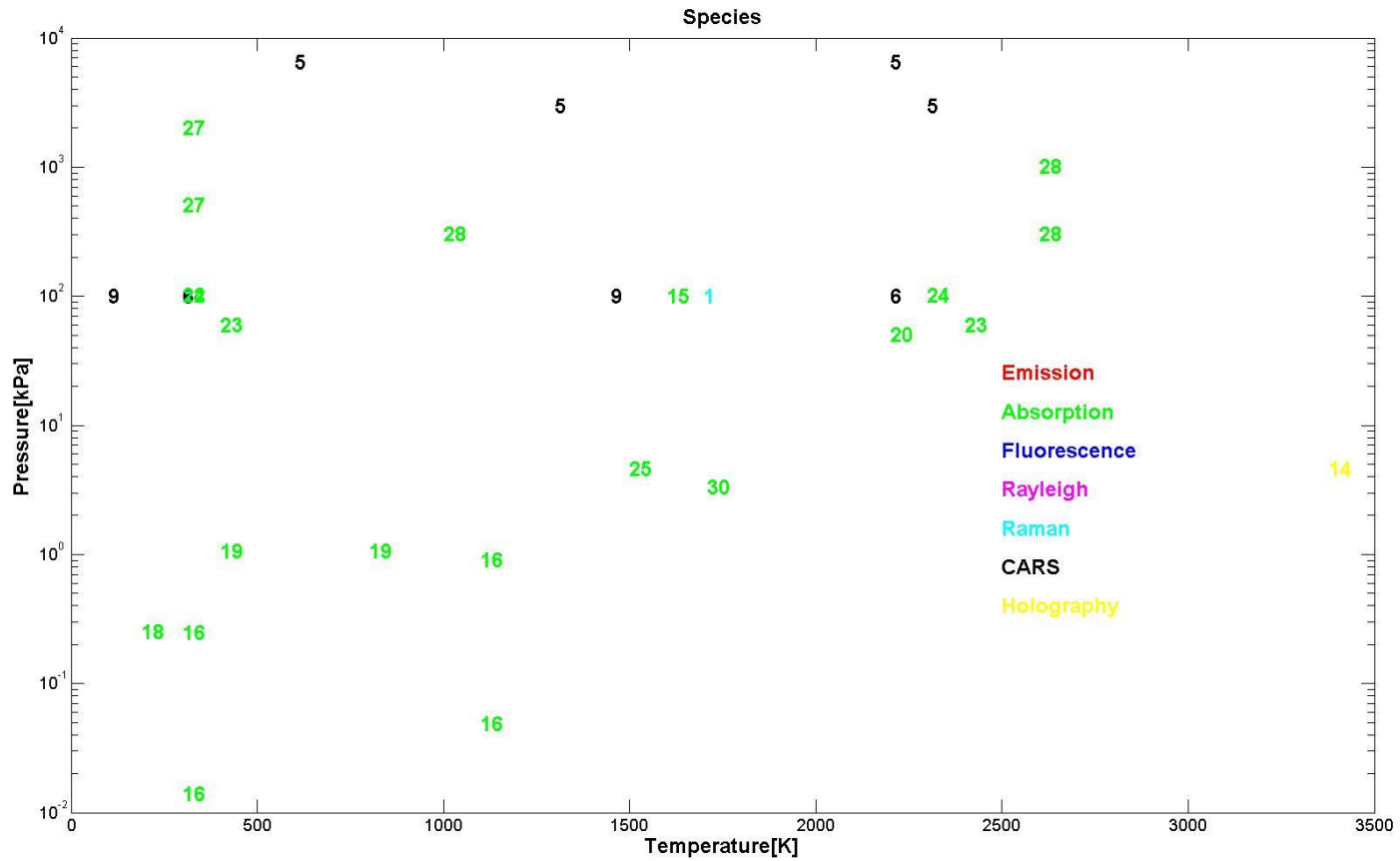


Pressure



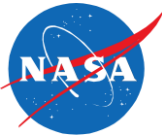


Species





References



- 1 Bergmann, V., W. Meier, D. Wolff, and W. Stricker. "Application of spontaneous Raman and Rayleigh scattering and 2D LIF for the characterization of a turbulent CH₄/H₂/N₂ jet diffusion flame." *Applied Physics B* 66, no. 4 (1998): 489-502.
- 2 Mielke, Amy F., Kristie A. Elam, and Chih-Jen Sung. "Multi-Property Measurements at High Sampling Rates Using Rayleigh Scattering." *AIAA journal* 47, no. 4 (2009): 850-862.
- 3 Mielke, Amy F., and Kristie A. Elam. "Dynamic measurement of temperature, velocity, and density in hot jets using Rayleigh scattering." *Experiments in fluids* 47, no. 4-5 (2009): 673-688.
- 4 Bohlin, Alexis, Brian D. Patterson, and Christopher J. Kliewer. "Communication: Simplified two-beam rotational CARS signal generation demonstrated in 1D." *The Journal of chemical physics* 138, no. 8 (2013): 081102.
- 5 Grisch, Frédéric, Paul Bouchardy, and Walter Clauss. "CARS thermometry in high pressure rocket combustors." *Aerospace science and technology* 7, no. 4 (2003): 317-330.
- 6 O'Byrne, S., P. M. Danehy, S. A. Tedder, and A. D. Cutler. "Dual-pump CARS temperature and species concentration measurements in a supersonic combustor." *AIAA Journal* (2007).
- 7 Fraval, Elliot, P. M. Danehy, and A. F. P. Houwing. "Single-shot broadband coherent anti-stokes raman scattering measurements in a free piston shock tunnel nozzle expansion." In *The Proceedings of the 23rd International Symposium on Shock Waves*, vol. 23, pp. 396-402. 2001.
- 8 Grisch, F., P. Bouchardy, V. Joly, C. Marmignon, U. Koch, A. G-uacute, and Ihan. "Coherent Anti-Stokes Raman Scattering measurements and computational modeling of nonequilibrium flow." *AIAA journal* 38, no. 9 (2000): 1669-1675.
- 9 Hsu, Paul S., Anil K. Patnaik, James R. Gord, Terrence R. Meyer, Waruna D. Kulatilaka, and Sukesh Roy. "Investigation of optical fibers for coherent anti-Stokes Raman scattering (CARS) spectroscopy in reacting flows." *Experiments in fluids* 49, no. 4 (2010): 969-984.
- 10 Miles, Richard, Matthew R. Edwards, James B. Michael, Nathan D. Calvert, and Arthur Dogariu. "Femtosecond Laser Electronic Excitation Tagging (FLEET) for Imaging Flow Structure in Unseeded Hot or Cold Air or Nitrogen." In *51st AIAA Aerospace Sciences Meeting including the New Horizons Forum and Aerospace Exposition*. 2013.
- 11 Grinstead, Jay H., Christopher L. Harris, Dickson Yeung, Gregg P. Scott, Barry J. Porter, Peter Graube, and Reid B. Greenberg. "Next-Generation Laser-Induced Fluorescence Diagnostic Systems for NASA Arc Jet Facilities." In *47th AIAA Aerospace Sciences Meeting*.
- 12 Danehy, Paul M., Sean O', Byrne, A. Frank P. Houwing, Jodie S. Fox, and Daniel R. Smith. "Flow-tagging velocimetry for hypersonic flows using fluorescence of nitric oxide." *AIAA journal* 41, no. 2 (2003): 263-271.
- 13 Palma, Philip C., Paul M. Danehy, and A. F. P. Houwing. "Fluorescence imaging of rotational and vibrational temperature in shock-tunnel nozzle flow." *AIAA journal* 41, no. 9 (2003): 1722-1732.
- 14 Bishop, Alexis Ivan, B. N. Littleton, T. J. McIntyre, and Halina Rubinsztein-Dunlop. "Near-resonant holographic interferometry of hypersonic flow." *Shock Waves* 11, no. 1 (2001): 23-29.
- 15 Stancu, Gabi D., Mario Janda, Farah Kaddouri, Deanna A. Lacoste, and Christophe O. Laux. "Time-Resolved CRDS Measurements of the N₂ (A₃Σ^{u+}) Density Produced by Nanosecond Discharges in Atmospheric Pressure Nitrogen and Air." *The Journal of Physical Chemistry A* 114, no. 1 (2009): 201-208.



References (cont.)



- 16 Stancu, G. D., M. Simeni Simeni, and C. O. Laux. "Study of nitric oxide and carbon monoxide production in plasma assisted combustion by Quantum Cascade Laser Absorption Spectroscopy." 21st International Symposium on Plasma Chemistry (ISPC 21), 4 August – 9 August 2013, Cairns Convention Centre, Queensland, Australia
- 17 Stancu, G. D., F. Kaddouri, D. A. Lacoste, and C. O. Laux. "Investigations of rapid plasma chemistry generated by nanosecond discharges in air at atmospheric pressure using advanced optical diagnostics." In 47th AIAA Aerospace Sciences Meeting, 2009.
- 18 Parker, R.A., Wakeman, T., MacLean, M., and Holden, M., "Measuring nitric oxide freestream concentration using quantum cascade lasers at CUBRC," AIAA Paper 2006-926, 44th AIAA Aerospace Sciences Meeting and Exhibit, Jan 2006.
- 19 Wehe, S.D., Baer, D.S., and Hanson, R.K., "Tunable diode-laser absorption measurements of temperature, velocity, and H₂O in hypervelocity flows," AIAA Paper 97-3267, 33rd Joint Propulsion Conference and Exhibit, Seattle, WA, 1997.
- 20 Goldstein, C.S., Schultz, I.A., Jeffries, J.B., and Hanson, R.K., "Tunable diode laser absorption sensor for measurements of temperature and water concentration in supersonic flows," AIAA Paper 2011-1094, 49th AIAA Aerospace Sciences Meeting including the New Horizons Forum and Aerospace Exposition, Orlando FL, Jan 4-7, 2011.
- 21 Lin, X., Yu, X.L., Li, F., Zhang, S.H., Xin, J.G., and Chang, X.Y., "CO concentration and temperature measurements in a shock tube for Martian mixtures by coupling OES and TDLAS," Applied Physics B. 2012
- 22 Lyle, K. H., Jeffries, J.B. and Hanson, R. K. "Diode-laser sensor for air-mass flux 1: design and wind tunnel validation." AIAA Journal Vol. 45, No. 9 pp. 2204-2212, 2007.
- 23 Mohamed, A.K., Henry, D., Falni, J. P., Sagnier, P., Soutad, J., Beck, W.H., and Martinez Schramm, J., "Infrared diode laser absorption spectroscopy measurements in the S4MA, F4, and HEG Hypersonic Flows," International Symposium on Atmospheric Reentry Vehicles and Systems, 16-18 March 1999, Arcachon, France
- 24 L. Ma, X. Li, S. T. Sanders, A. W. Caswell, S. Roy, D. H. Plemmons, and J. R. Gord, "50-kHz-rate 2D imaging of temperature and H₂O concentration at the exhaust plane of a J85 engine using hyperspectral tomography," Optics Express, Vol. 21, Issue 1, pp. 1152-1162, 2013.
- 25 Scherer, J. J., and D. J. Rakestraw. "Cavity ringdown laser absorption spectroscopy detection of formyl (HCO) radical in a low pressure flame." Chemical physics letters 265, no. 1 (1997): 169-176.
- 26 Briefi, S., C. Wimmer, and U. Fantz. "Correction factors for saturation effects in white light and laser absorption spectroscopy for application to low pressure plasmas." Physics of Plasmas (1994-present) 19, no. 5 (2012): 053501.
- 27 Sun, K., X. Chao, R. Sur, J. B. Jeffries, and R. K. Hanson. "Wavelength modulation diode laser absorption spectroscopy for high-pressure gas sensing." Applied Physics B 110, no. 4 (2013): 497-508.
- 28 Spearrin, R. M., C. S. Goldenstein, J. B. Jeffries, and R. K. Hanson. "Fiber-coupled 2.7 μ m laser absorption sensor for CO₂ in harsh combustion environments." Measurement Science and Technology 24, no. 5 (2013): 055107.
- 29 Jin, Pei, Hong Wang, Susan Oatis, Gregory E. Hall, and Trevor J. Sears. "Very-Low-Temperature Infrared Laser Absorption Spectroscopy of N₂O, NO, and NO₂." Journal of Molecular Spectroscopy 173, no. 2 (1995): 442-451.



References (cont.)

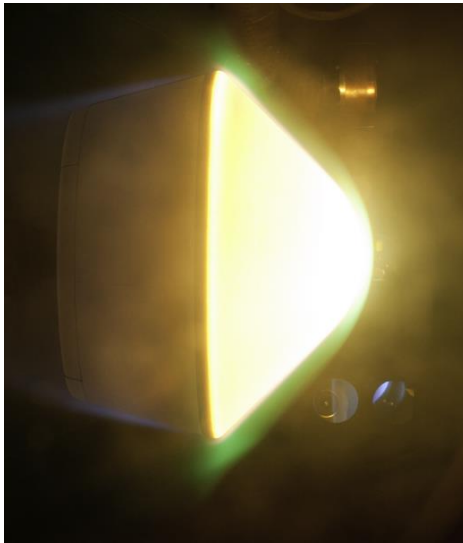


- 30 Luque, J., J. B. Jeffries, G. P. Smith, D. R. Crosley, and J. J. Scherer. "Combined cavity ringdown absorption and laser-induced fluorescence imaging measurements of CN (BX) and CH (BX) in low-pressure CH₄-O₂-N₂ and CH₄-NO-O₂-N₂ flames." *Combustion and flame* 126, no. 3 (2001): 1725-1735.
- 31 Hart, Roger C., Gregory C. Herring, and R. Jeffrey Balla. "Pressure measurement in supersonic air flow by differential absorptive laser-induced thermal acoustics." *Optics letters* 32, no. 12 (2007): 1689-1691.
- 32 Lachney, E. R., and N. T. Clemens. "PLIF imaging of mean temperature and pressure in a supersonic bluff wake." *Experiments in Fluids* 24, no. 4 (1998): 354-363.
- 33 Hiller, Bernhard, and Ronald K. Hanson. "Simultaneous planar measurements of velocity and pressure fields in gas flows using laser-induced fluorescence." *Applied Optics* 27, no. 1 (1988): 33-48.
- 34 Danehy, Paul M., Sean O', Byrne, A. Frank P. Houwing, Jodie S. Fox, and Daniel R. Smith. "Flow-tagging velocimetry for hypersonic flows using fluorescence of nitric oxide." *AIAA journal* 41, no. 2 (2003): 263-271.
- 35 G.D. Stancu, F. Kaddouri, D.A. Lacoste, C.O. Laux, Investigations of the rapid plasma chemistry induced by nanosecond discharges in atmospheric pressure air using advanced optical diagnostics, AIAA, 40th Plasmadynamics and Lasers Conference, San Antonio TX, 10.2514/6.2009-3593, (2009) USA
- 36 G.D. Stancu, M. Janda, F. Kaddouri, D.A. Lacoste, C.O. Laux, Time-resolved CRDS measurements of the N₂(A³S + u) density produced by nanosecond discharges in atmospheric pressure nitrogen and air, *J. Phys. Chem. A*, 114, (1) (2010) 201-208 (doi: 10.1021/jp9075383)
- 37 McIntyre, Timothy J., Margaret J. Wegener, Alexis I. Bishop, and Halina Rubinsztein-Dunlop. "Simultaneous two-wavelength holographic interferometry in a superorbital expansion tube facility." *Applied optics* 36, no. 31 (1997): 8128-8134.
- 38 Belostotskiy, Sergey G., Tola Ouk, Vincent M. Donnelly, Demetre J. Economou, and Nader Sadeghi. "Gas temperature and electron density profiles in an argon dc microdischarge measured by optical emission spectroscopy." *Journal of applied physics* 107, no. 5 (2010): 053305.
- 39 Bathel, Brett F., Paul M. Danehy, Craig T. Johansen, Stephen B. Jones, and Christopher P. Goyne. "Hypersonic Boundary Layer Measurements with Variable Blowing Rates Using Molecular Tagging Velocimetry." *AIAA Paper2886* (2012): 25-28.
- 40 Laux, C. O., T. G. Spence, C. H. Kruger, and R. N. Zare. "Optical diagnostics of atmospheric pressure air plasmas." *Plasma Sources Science and Technology* 12, no. 2 (2003): 125.
- 41 D. G. Fletcher, "Nonintrusive diagnostic strategies for arcjet stream characterization." NASA Ames Research Center, Moffett Field CA .Paper presented at the RTO AVT Course on "Measurement Techniques for High Enthalpy and Plasma Flows", held in Rhode-Saint-Gen~se, Belgium, 25-29 October 1999, and published in RTO EN-8.
- 42 Balla, R. Jeffrey, and Joel L. Everhart. "Rayleigh scattering density measurements, cluster theory, and nucleation calculations at Mach 10." *AIAA journal* 50, no. 3 (2012): 698-707.

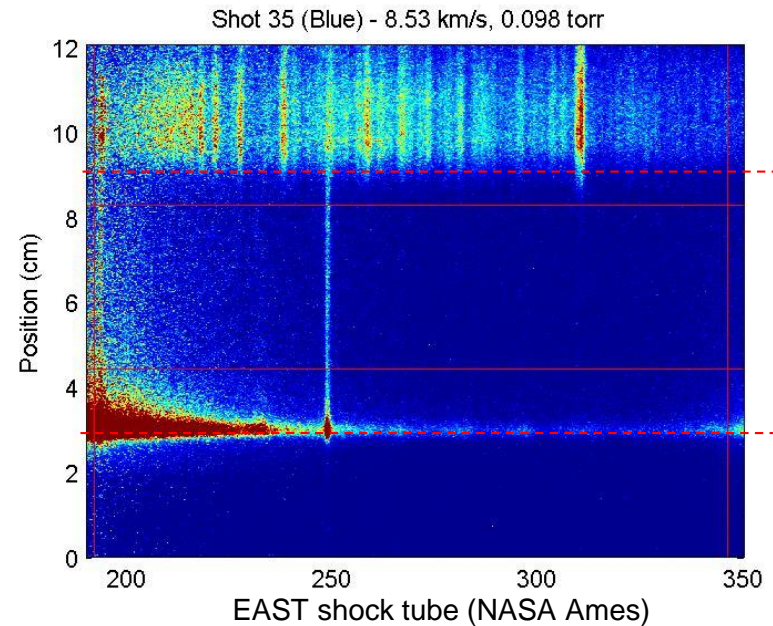
Intro to Optical Emission Spectroscopy for Hypersonic Nonequilibrium Flows



Michael Winter, University of Kentucky, Kentucky, USA
Paul Danehy, NASA Langley Research Center, Virginia, USA



PICA at NASA Ames (SPRITE)



Outline:

- Introduction to emission spectroscopy
- Excitation of Atoms and Molecules (electronic, vibrational, rotational)
- Line broadening
- Spatial resolution
- Application examples of emission spectroscopy



Applications of emission spectroscopy



- *Astronomy !!!* - composition and velocity of celestial bodies
- *Diagnostics for gases at high temperatures*
 - re-entry (ground test and flight)
 - electric propulsion characterization
 - plasma processing (coating, edging, ...)
 - combustion (though temperatures might be too low)
 - material analysis (laser ablation of surface material → radiation)
- *Radiation transport in gases at high temperatures*
 - re-entry radiation heat flux to the spacecraft (ground test and flight)
 - radiation transport within the flow field (source term in energy equation)
→ particular importance of VUV radiation

Goals:

- *Identification of elements*
- *Radiation heat flux determination*
- *Temperature determination*
 - ratios of atomic lines (electronic excitation temperature)
 - rotational and vibrational temperature of molecules (line ratios or comparison with spectral simulation)
 - translational temperature from line broadening (Doppler effect)
 - glowing surfaces (Planck blackbody radiation)
- *Chemical composition (usually under equilibrium conditions)*

Typically valid in nonequilibrium

} Equilibrium assumed but may measure thermal nonequilibrium

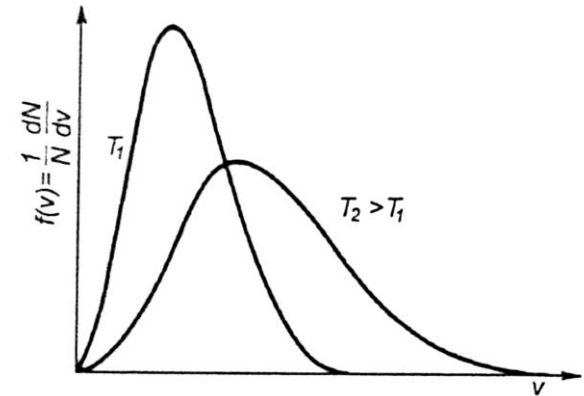
Typically equilibrium required



Introduction

- Each particle in a gas has a specific undirected velocity and, therefore, a kinetic energy.
- Definition of translational temperature: for the sum of all particles, a statistic distribution function can be formulated (Maxwellian velocity distribution):

$$\text{Maxwellian velocity distribution}$$
$$f(v) = \frac{dN}{N} = \frac{4}{\sqrt{\pi}} \frac{v^2}{(2RT)^{3/2}} e^{-\frac{v^2}{2RT}} dv$$



- Similar distribution functions can be formulated for other energies such as vibrational, rotational and electronic excitation (i.e. Boltzmann distributions).
- Energy is constantly exchanged through collisions.
- Electrons are lighter and more movable than heavy particles → more collisions possible → possibly different energy distribution → distinctive temperature
- For each form of energy, a temperature can be defined which controls the corresponding energy distribution (T_{vib} , T_{rot} , T_{elec} , ...).
- **For many plasmas, the distribution parameters (i.e. temperatures) might all be different → $T_{\text{trans}} \neq T_{\text{el}} \neq T_{\text{rot}} \neq T_{\text{vib}}$ → non-equilibrium.**



Emission of Atoms and Molecules

- Line position
- Line strength/intensity
- Line shape

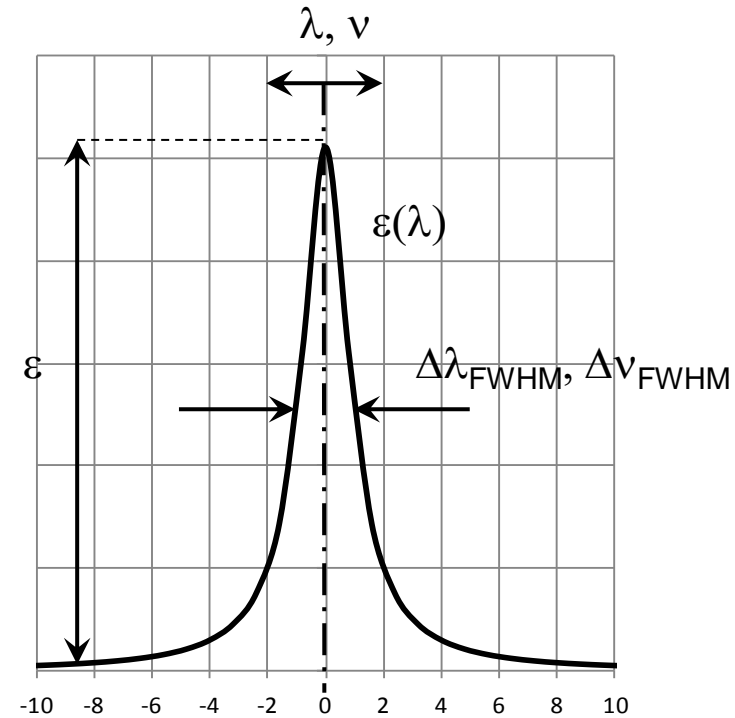
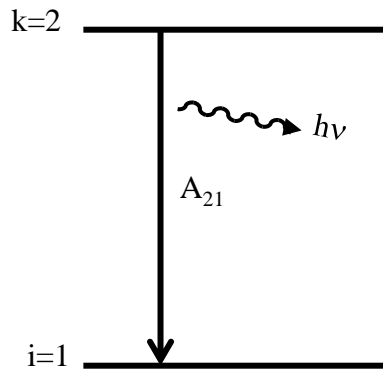
from $\Delta E = E_{\text{upper}} - E_{\text{lower}} = h \nu$,
 $\rightarrow \nu$ or λ for known energy levels

valid in general (atoms and molecules)

$$\epsilon_{21} = \frac{h\nu}{4\pi} A_{21} n_2$$

number of transitions
 \rightarrow depends on energy of the upper state

one photon/transition
 \rightarrow depends on energy difference



In equilibrium, the density n_k is related to n through the Boltzmann distribution:



Emission of Atoms: Electronic Excitation



- Line position
- Line strength/intensity
- Line shape

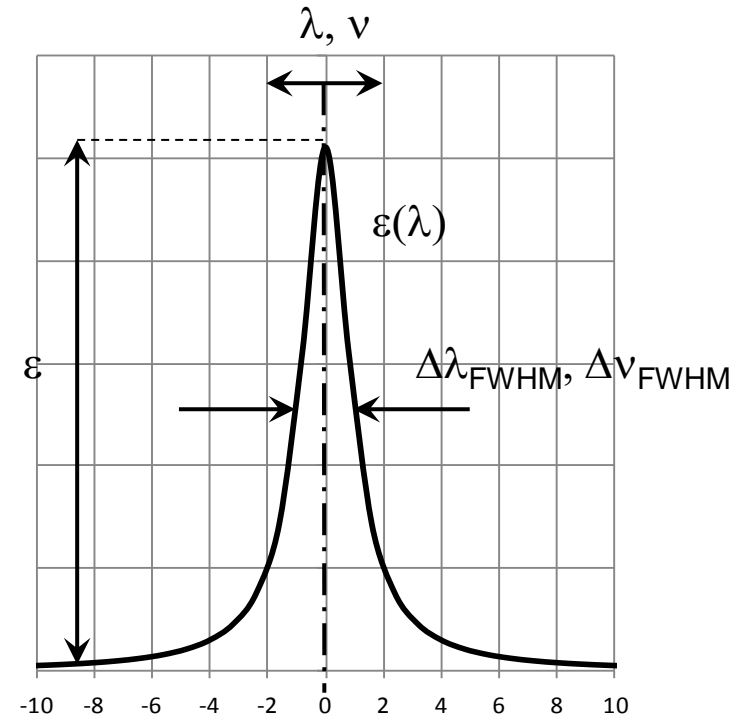
from $\Delta E = E_{\text{upper}} - E_{\text{lower}} = h \nu$,
 $\rightarrow \nu$ or λ for known energy levels

valid in general (atoms and molecules)

$$\epsilon = \frac{h\nu}{4\pi} A_{ki} n_k$$

Number of different states which share the same energy
 Depends on the total angular momentum J which is the value of the vector addition of the orbital angular momentum L and the spin momentum S
 $g = 2J + 1$

Degeneracy of the state k



Population density of the excited state k

$$n_k = \frac{g_k}{U(T_{ex})} n_0 \exp\left(-\frac{E_k}{kT_{ex}}\right)$$

excitation energy of the state k

electronic excitation temperature (in equilibrium gas temperature)

Partition function

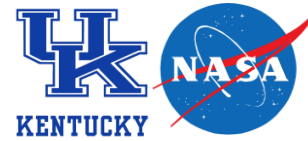
$$U(T_{ex}) = \sum_i g_i \exp\left(-\frac{E_i}{kT_{ex}}\right)$$

Total density of the species under consideration

In equilibrium, the density n_k is related to n through the Boltzmann distribution:



Emission of Atoms: Electronic Excitation



- Line position
- Line strength/intensity
- Line shape

from $\Delta E = E_{\text{upper}} - E_{\text{lower}} = h \nu$,

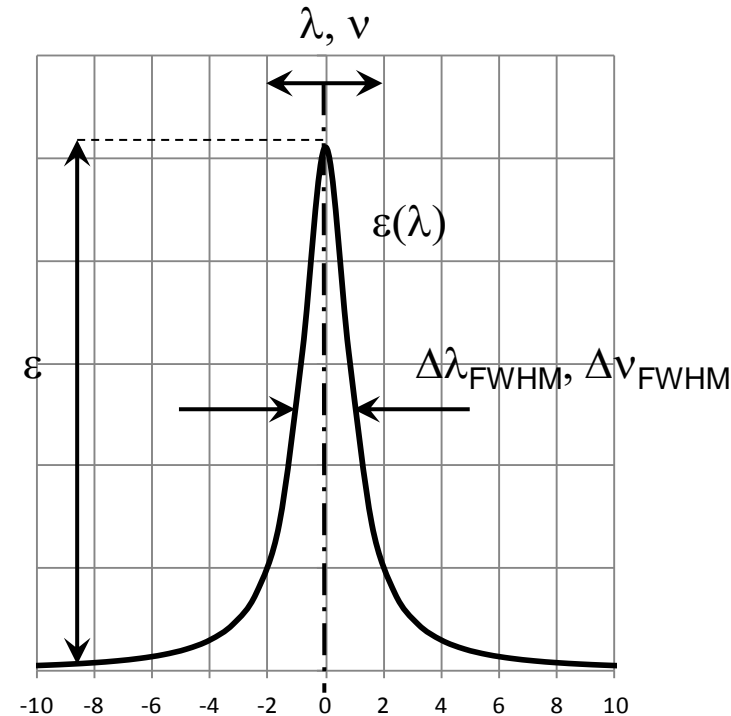
→ ν or λ for known energy levels

valid in general (atoms and molecules)

$$\varepsilon = \frac{h \nu}{4 \pi} A_{ki} n_k$$

$$= \frac{h \nu}{4 \pi} A_{ki} \frac{g_k}{U(T_{ex})} n_0 \exp\left(-\frac{E_k}{k T_{ex}}\right)$$

for electronic excitation in equilibrium



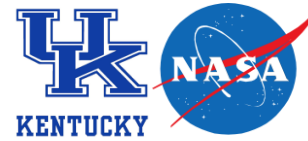
information on the transition (from quantum mechanics, e.g. from tables)

information about the thermodynamic condition of the plasma

In equilibrium, the density n_k is related to n through the Boltzmann distribution:



Electronic Excitation Temperature

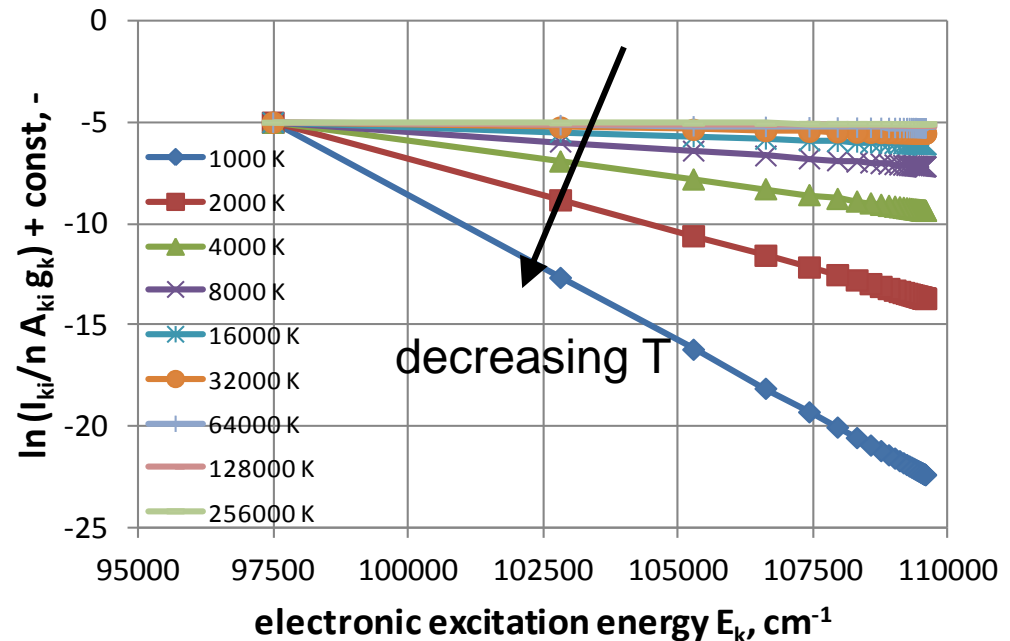


Theoretically, the ratio of two lines would be sufficient to determine the excitation temperature, but it is often in doubt if the electronic excitation is in equilibrium.

$$\ln\left(\frac{I_{ki}}{\nu A_{ki} g_k}\right) + const = -\frac{E_k}{kT_{ex}} \quad \rightarrow \text{Plot } \ln\left(\frac{I_{ki}}{\nu A_{ki} g_k}\right) \text{ vs } E_k \rightarrow \text{straight line with slope } 1/-kT \text{ (Boltzmann Plot)}$$

If points are indeed on a straight line \rightarrow Boltzmann valid \rightarrow T can be determined

BUT: Even if Boltzmann seems valid, the apparent excitation temperature might not be an equilibrium temperature:





Electronic Excitation Temperature



Theoretically, the ratio of two lines would be sufficient to determine the excitation temperature, but it is often in doubt if the electronic excitation is in equilibrium.

$$\ln\left(\frac{I_{ki}}{\nu A_{ki} g_k}\right) + const = -\frac{E_k}{kT_{ex}} \quad \rightarrow \text{Plot } \ln\left(\frac{I_{ki}}{\nu A_{ki} g_k}\right) \text{ vs } E_k \rightarrow \text{straight line with slope } 1/-kT \text{ (Boltzmann Plot)}$$

If points are indeed on a straight line \rightarrow Boltzmann valid \rightarrow T can be determined

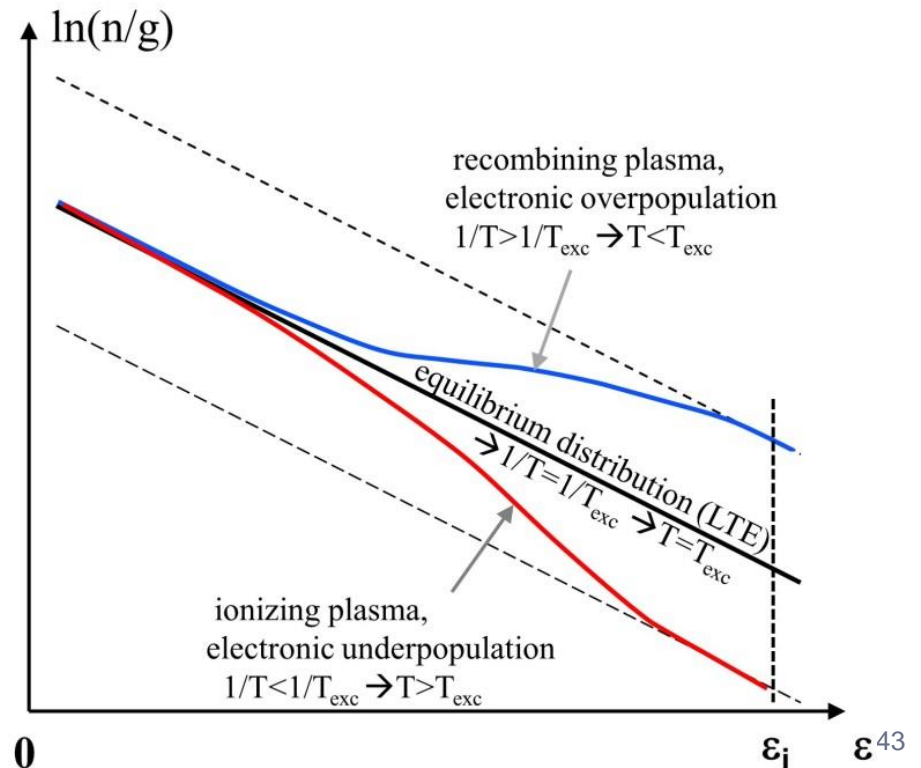
BUT: Even if Boltzmann seems valid, the apparent excitation temperature might not be an equilibrium temperature:

Recombining plasma

- high energy states will be populated through recombining ions
- \rightarrow flat distribution
- \rightarrow high excitation temperature

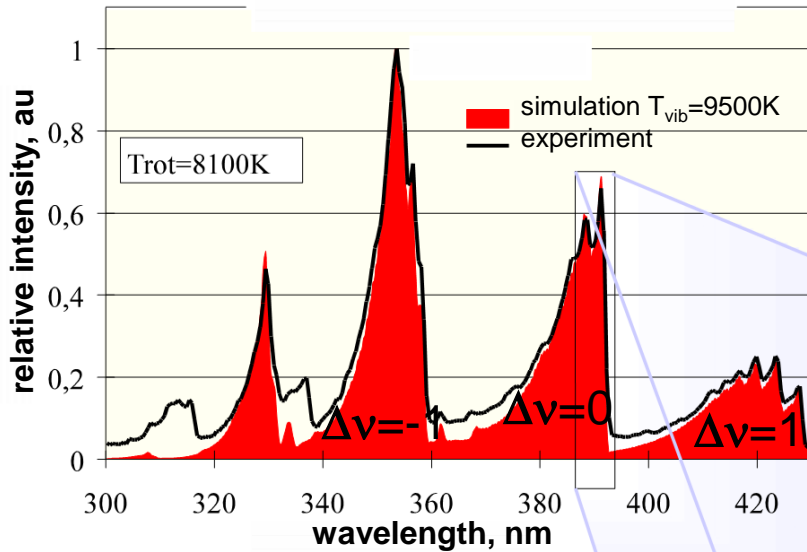
Ionizing plasma

- high energy states will be depopulated through ionizing neutrals
- \rightarrow steep distribution
- \rightarrow low excitation temperature





Emission from Molecules

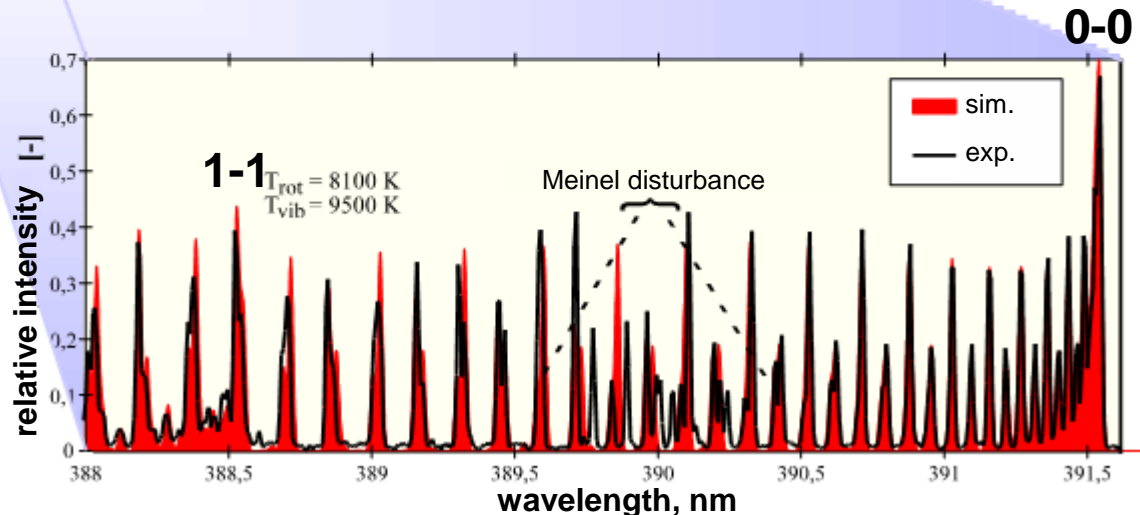


Molecule emission shows some shape but looks like a continuum

- Ratio of the different vibrational systems governed by T_{vib}
- Ratio within one vibrational transition (e.g. $0-0 \rightarrow V_u=0, V_l=0$) governed by T_{rot}

High spectral resolution
 → Single lines like atoms
 but more ...

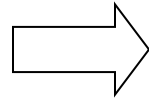
→ rotation and vibration





Emission from Molecules

Radiation of molecules is caused by changes of the electronic level, the vibrational level, and the rotational level of excitation, often simultaneously.



$$\tilde{\nu} = \frac{1}{hc} (\Delta E_{el} + \Delta E_{vib} + \Delta E_{rot})$$

Born-Oppenheimer approximation: The total energy is the sum of the different excitations which can be computed separately.

Electronic excitation works similar to the atoms ...



Emission from Molecules

- For diatomic molecules, **rotation** and only **one vibrational mode** need to be accounted for.
- Already for tri-atomic molecules, several vibrational modes are possible.

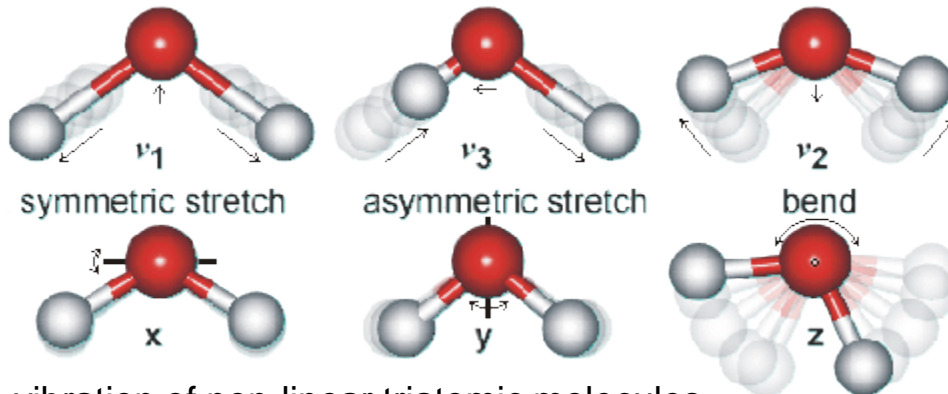


linear triatomic symmetric stretch mode

linear triatomic asymmetric stretch mode



- Different modes for linear and non-linear molecules



vibration of non-linear triatomic molecules

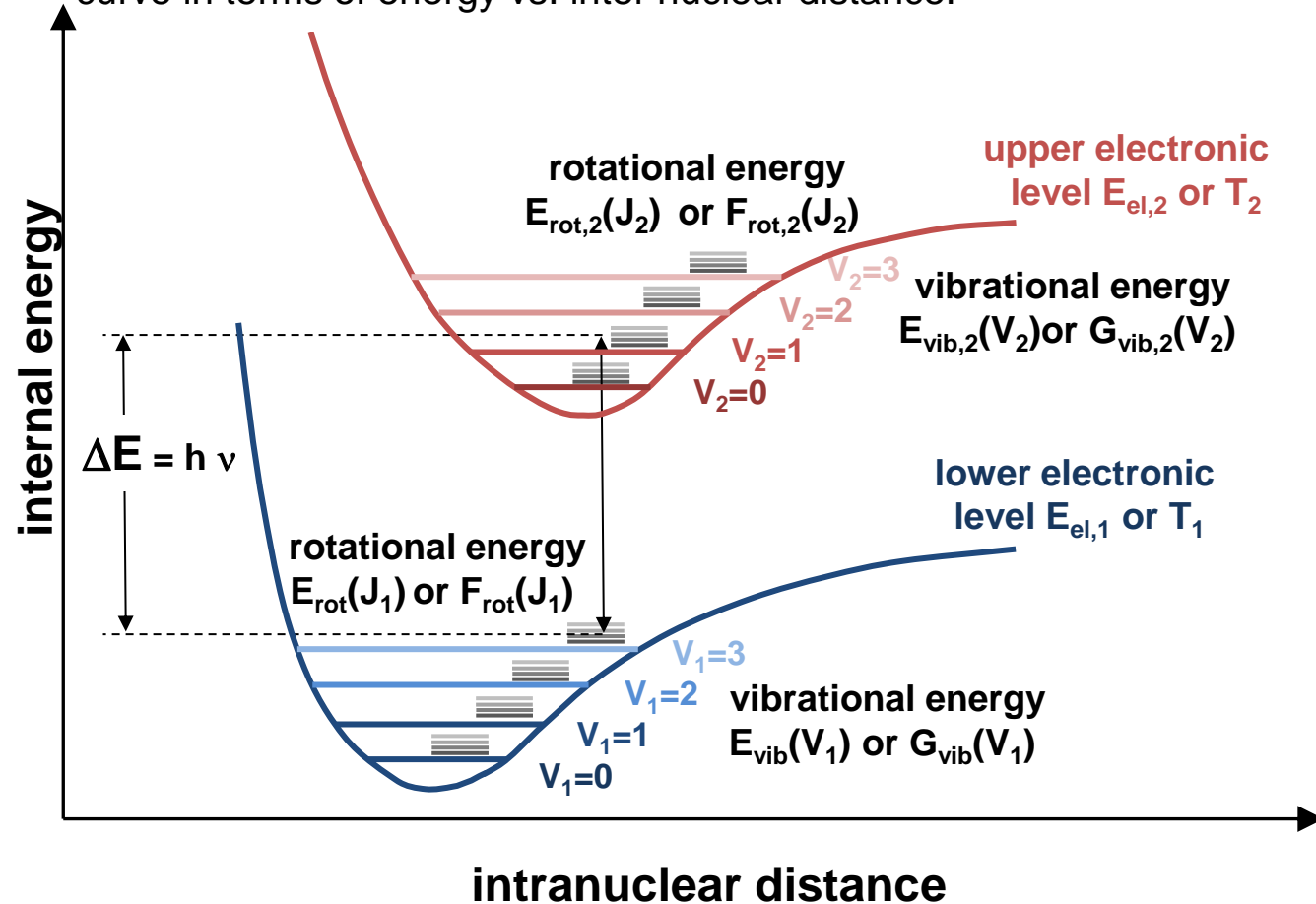
diatomic molecules

- Rotation and vibration energies are discrete and not continuous and are obtained from solutions of the Schroedinger equation.
- For diatomic molecules, each energy is characterized through one quantum number (J for rotation, V for vibration).
- In addition, molecules may be electronically excited (same process as for atoms).



Emission from Molecules

- Each electronic level of a molecule is described by a potential curve in terms of energy vs. inter nuclear distance.



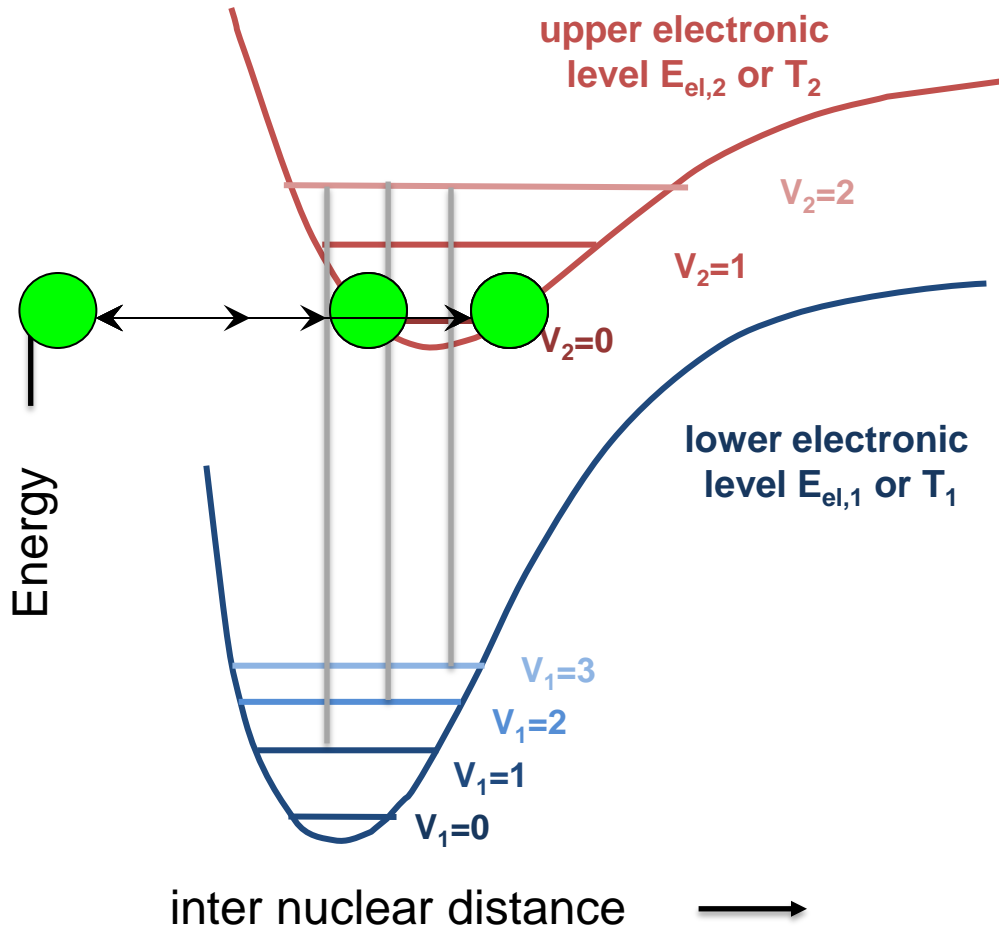
- Different vibrational energies appear as lines of constant energy on these potentials
- Excitation of the levels can happen through collisions (one major partner are electrons) or absorption of radiation.
- From one upper level, transitions to different lower levels are possible, each one resulting in a different emission line
- Usually, rotational energy changes in the same transition, possibly electronic excitation does, too, therefore contribution to the transition energy and the line position.

$$\tilde{\nu} = \frac{1}{hc} (\Delta E_{el} + \Delta E_{vib} + \Delta E_{rot})$$



Emission from Molecules

- Each electronic level of a molecule is described by a potential curve in terms of energy vs. inter nuclear distance.



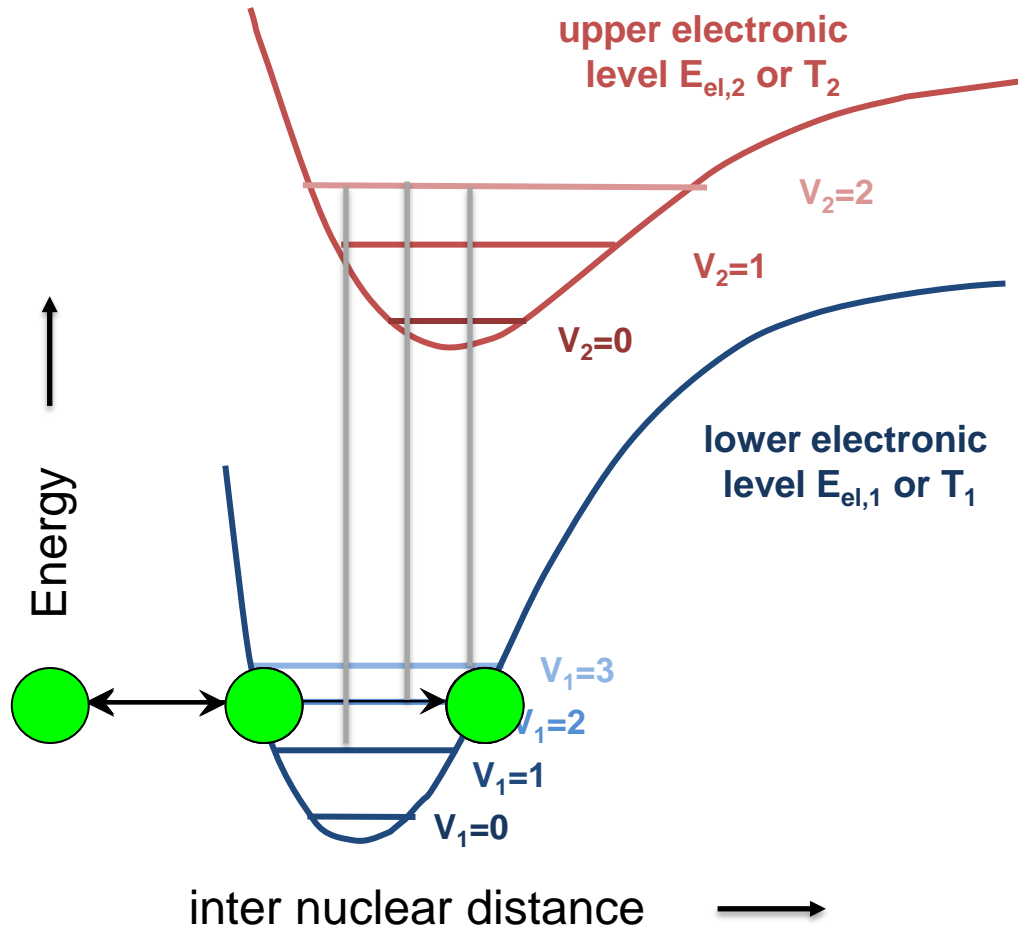
- Different vibrational energies appear as lines of constant energy ion these potentials
- Excitation of the levels can happen through collisions (one major partner are electrons) or absorption of radiation.
- From one upper level, transitions to different lower levels are possible, each one resulting in a different emission line
- Usually, rotational energy changes in the same transition, possibly electronic excitation does, too, therefore contribution to the transition energy and the line position.

Vibrational Excitation of diatomic molecules



Emission from Molecules

- Each electronic level of a molecule is described by a potential curve in terms of energy vs. inter nuclear distance.



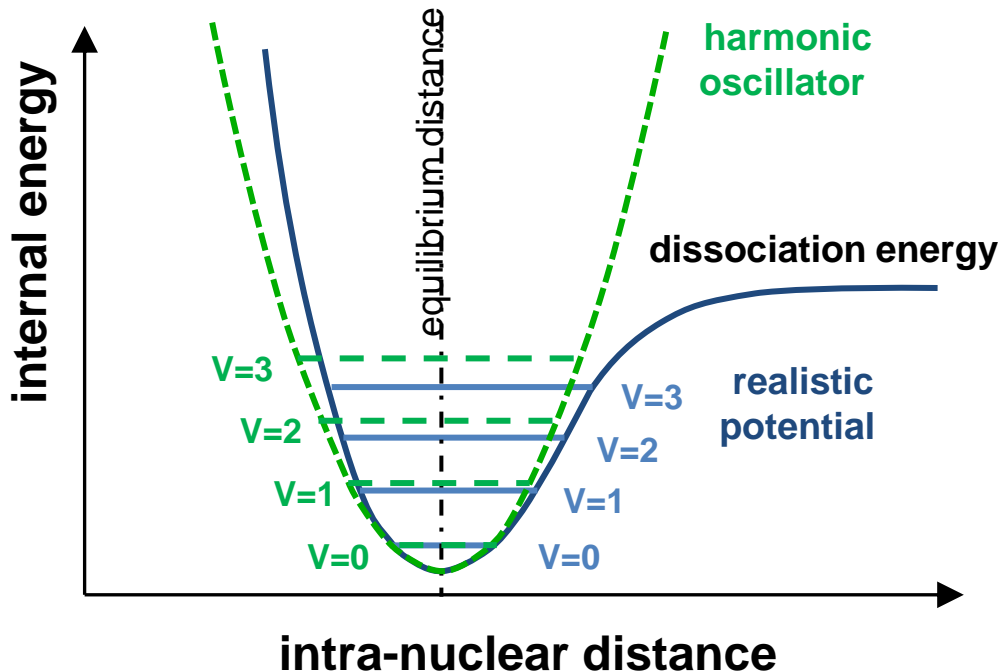
- Different vibrational energies appear as lines of constant energy on these potentials
- Excitation of the levels can happen through collisions (one major partner are electrons) or absorption of radiation.
- From one upper level, transitions to different lower levels are possible, each one resulting in a different emission line
- Usually, rotational energy changes in the same transition, possibly electronic excitation does, too, therefore contribution to the transition energy and the line position.

Vibrational Excitation of diatomic molecules



Emission from Molecules

- Rigid Rotator and Harmonic Oscillator
 - simple model, mainly to be used to account for rotational and vibrational energies in CFD codes → energy conservation
 - not suitable (at least the harmonic oscillator for spectral simulation)
 - The harmonic oscillator, however, does not describe real molecules:
 - for $r \sim \text{inf.}$ → $E = \text{dissociation energy}$
 - for $r \sim 0$ → $E \sim \text{inf.}$



Morse Potential

$$U(x) = D_e \left(1 - e^{-\beta x}\right)^2$$

- x : distance to r_e (re: equilibrium distance between the nuclei)
- D_e : Well depth of the potential (dissociation energy- energy at minimum)

$$\beta = 1,2177 \cdot 10^{-7} \omega_e \sqrt{\frac{\mu_A}{D_e}}$$

- μ_A : reduced mass of the molecule

vibrational energy increment from V to $V+1$ now decreases with V :

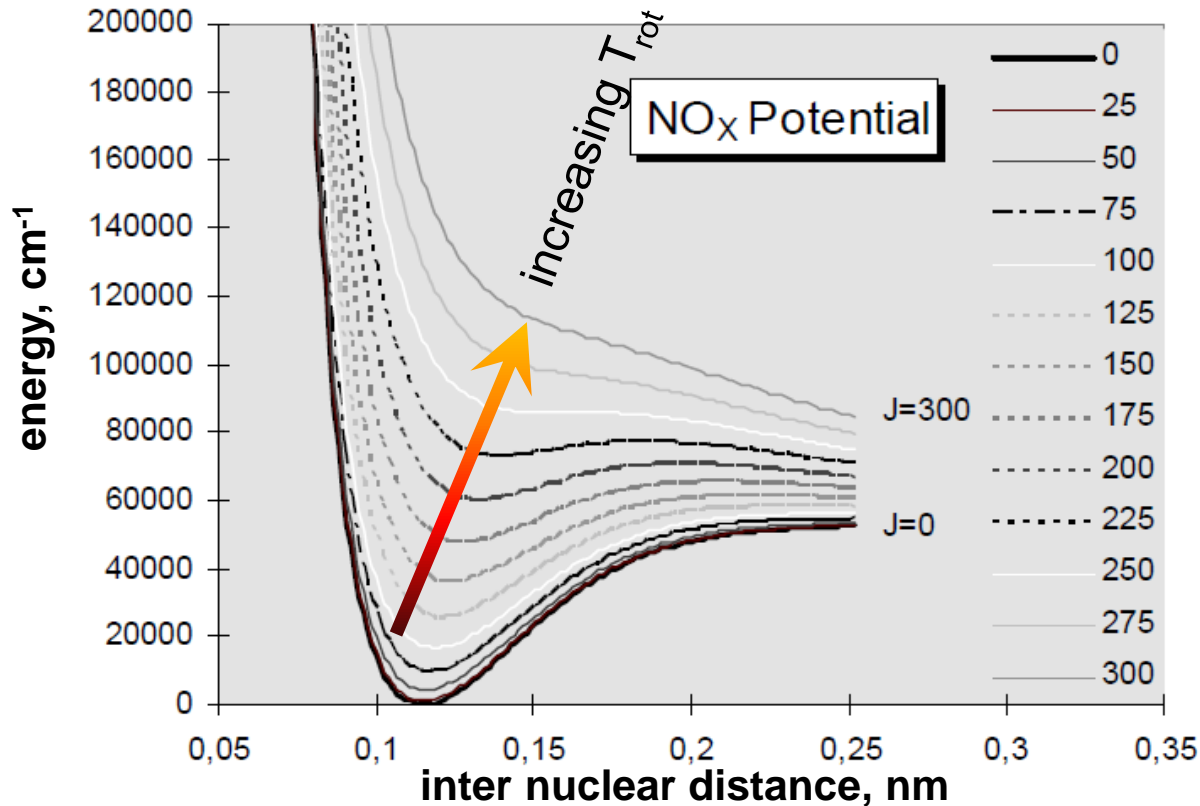
$$G(V) = \omega_e \left(V + \frac{1}{2}\right) - \omega_e x_e \left(V + \frac{1}{2}\right)^2$$



Emission from Molecules

- Separation of rotational and vibrational excitation is not completely possible.
- In fact, the whole molecular potential changes shape with rotational quantum number.
- For rotationally highly excited states, only low vibrational excitation possible $\rightarrow V_{\max}(J)$
- Or: limiting rotational quantum numbers different for each vibrational state $\rightarrow J_{\max}(V)$

Molecular potential with rotational excitation



- limiting case:
no more potential well
 \rightarrow not stable
- will be different for each electronic state



Theoretical Simulation of Molecule Radiation

➤ Intensity of one emission line:

$$\varepsilon = \frac{N' A_{\rightarrow} \Delta E_{\rightarrow}}{4\pi} = \underbrace{N'}_{\substack{\text{Particle density} \\ \text{in the level } e' V' J'}} \frac{16\pi^3 c \bar{\nu}^4}{3} \underbrace{(R_e(\bar{r}_{VV''}))^2}_{\substack{\text{Electronic} \\ \text{transition moment}}} q_{VV''} \frac{S_{J''\Lambda''}^{J'\Lambda'}}{2J'+1} \quad \text{Hönl London Factor}$$

Assumption of Boltzmann distributions

$$\frac{N_{e'V'J'}}{N_{total}} = \frac{Q_{el}^{e'} Q_{vib}^{e'V'} Q_{rot}^{e'V'J'}}{\sum_{e'V'J'} Q_{el}^{e'} Q_{vib}^{e'V'} Q_{rot}^{e'V'J'}}$$

with the total partition function:

$$Q = \sum_{e'V'J'} Q_{el}^{e'} Q_{vib}^{e'V'} Q_{rot}^{e'V'J'}$$

$$N_{e'V'J'}(T_{el}, T_{vib}, T_{rot}) = N_{total} \frac{g_{e'} (2J'+1)}{Q} \exp\left(-\frac{E_{el}^{e'}}{kT_{el}}\right) \exp\left(-\frac{E_{vib}^{e'V'}}{kT_{vib}}\right) \exp\left(-\frac{E_{rot}^{e'V'J'}}{kT_{rot}}\right)$$

electronic

$$Q_{el}^{e'} = g_{e'} \exp\left(-\frac{E_{el}^{e'}}{kT_{el}}\right)$$

vibrational

$$Q_{vib}^{e'V'} = \exp\left(-\frac{E_{vib}^{e'V'}}{kT_{vib}}\right)$$

rotational

$$Q_{rot}^{e'V'J'} = (2J'+1) \exp\left(-\frac{E_{rot}^{e'V'J'}}{kT_{rot}}\right)$$



Emission from Molecules

Theoretical Simulation of Molecule Radiation

➤ Intensity of one emission line:

$$\varepsilon = \frac{N' A_{\rightarrow} \Delta E_{\rightarrow}}{4\pi} = N' \frac{16\pi^3 c \bar{\nu}^4}{3} \underbrace{(R_e(\bar{r}_{VV''}))^2}_{\text{Electronic transition moment}} q_{VV''} \frac{S_{J'\Lambda'}}{2J'+1}$$

Particle density
in the level e' V' J'

Electronic
transition moment

Hönl London Factor

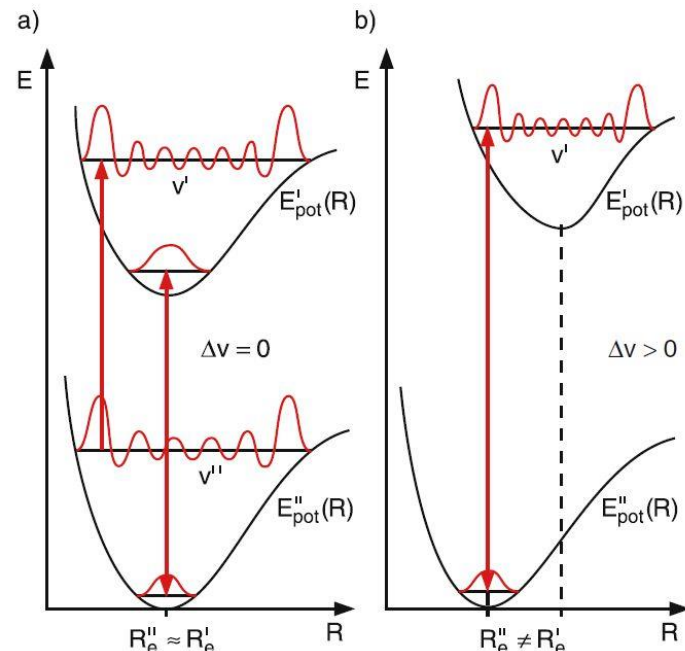
• The electronic transition is fast in comparison to the motion of the nuclei during vibration.

→ The position of the nuclei relative to each other will not change during the transition.

→ The higher the overlap between the upper and lower potential, the higher the probability of the transition.

→ If wave functions are analyzed, this probability can be expressed in the electronic transition moment containing the Franck-Condon factor.

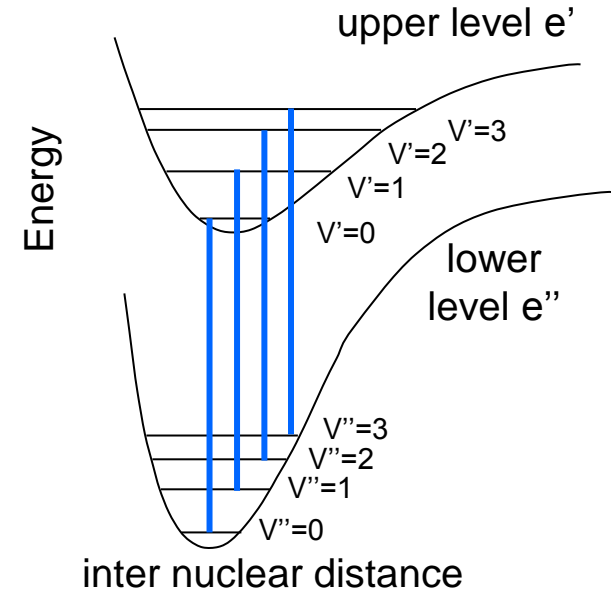
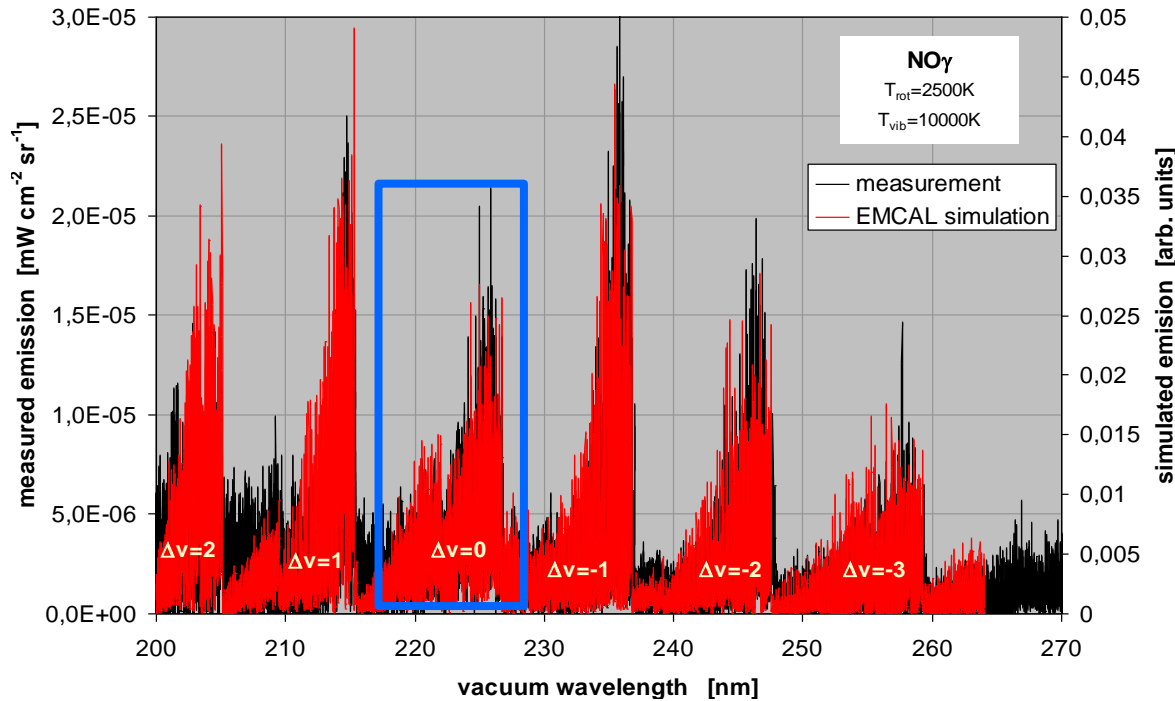
Frank-Condon Principle

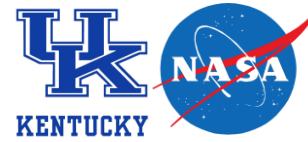




Molecular Band Structure

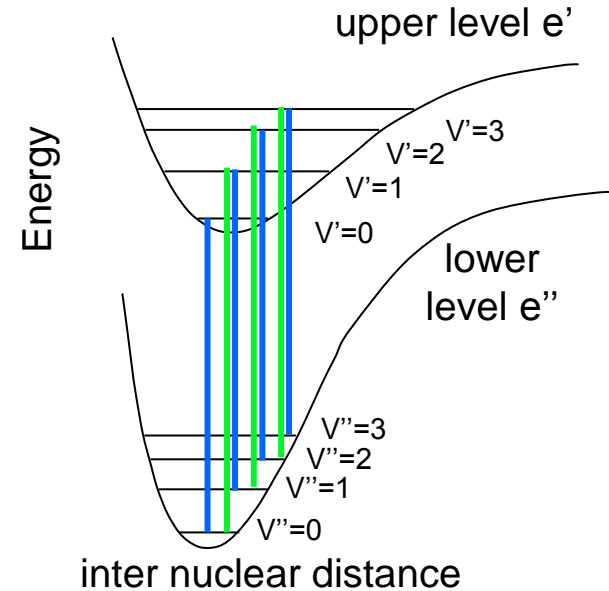
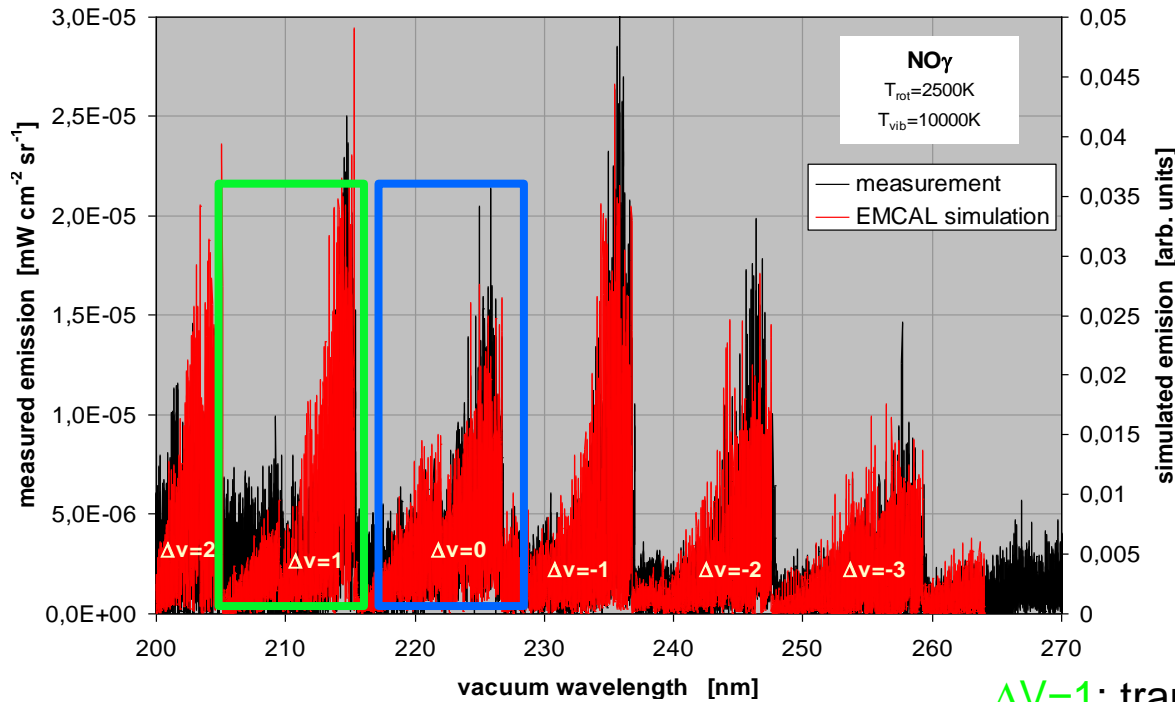
- Transition energies with the same difference in vibrational quantum number Δv are similar
→ The different vibrational transitions tend to group for the same Δv .
- $\Delta V = 0$: 0-0, 1-1, 2-2, 3-3, ...





Molecular Band Structure

- Transition energies with the same difference in vibrational quantum number Δv are similar
→ The different vibrational transitions tend to group for the same Δv .
- $\Delta V = 1$: 1-0, 2-1, 3-2, 4-3, ... → higher ΔE → lower λ

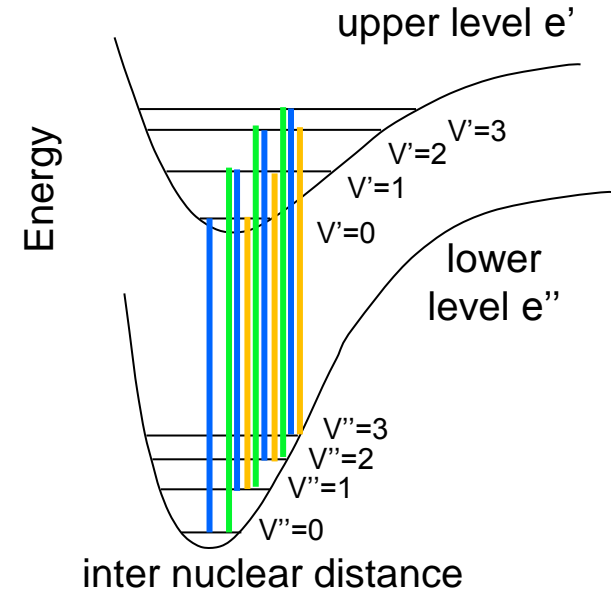
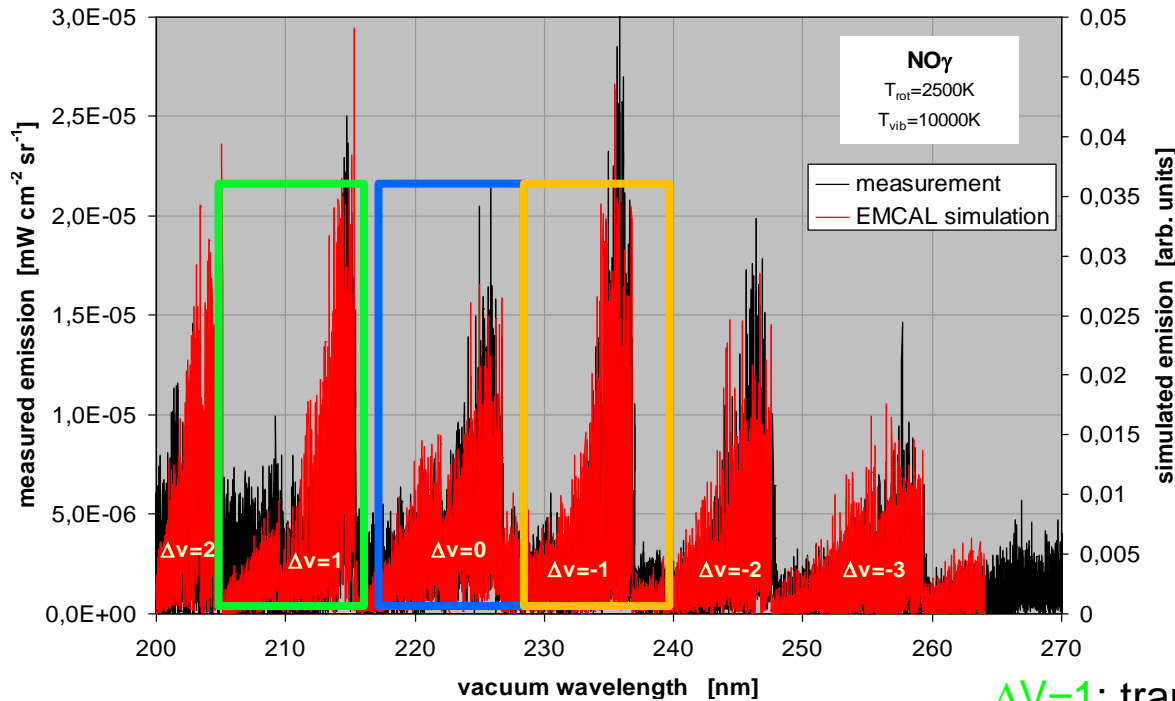


$\Delta V=1$: transition energy higher than $\Delta V=0$



Molecular Band Structure

- Transition energies with the same difference in vibrational quantum number Δv are similar
→ The different vibrational transitions tend to group for the same Δv .
- $\Delta V = -1$: 0-1, 1-2, 2-3, 3-4, ... → lower ΔE → higher λ



$\Delta V = 1$: transition energy higher than $\Delta V = 0$

$\Delta V = -1$: transition energy lower than $\Delta V = 0$



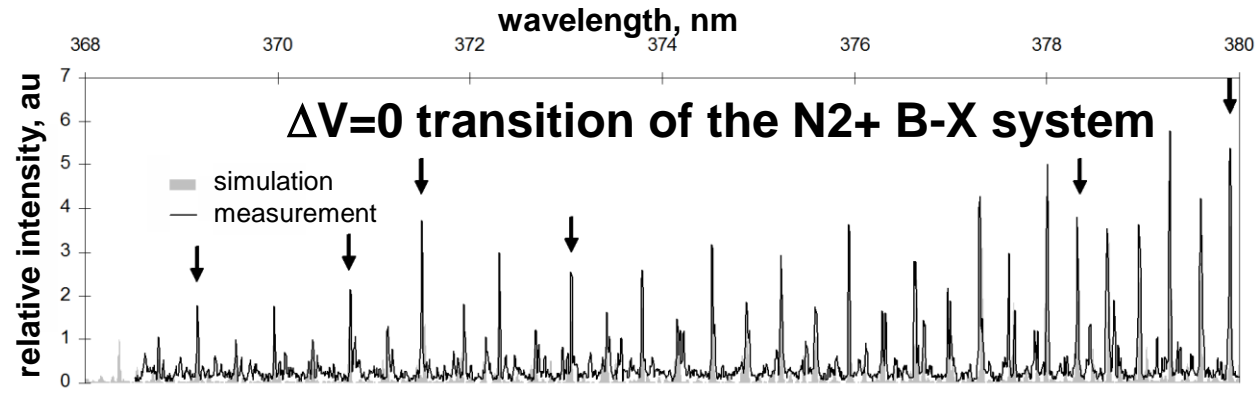
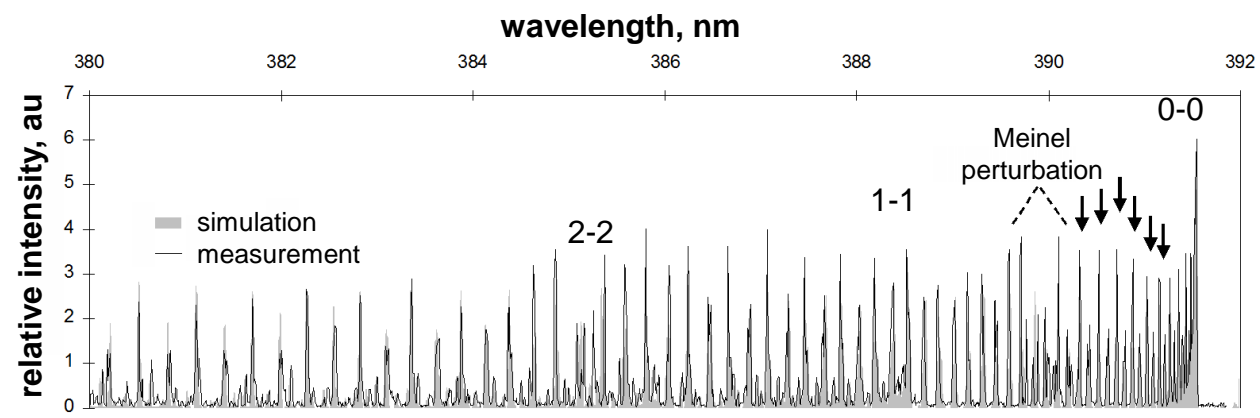
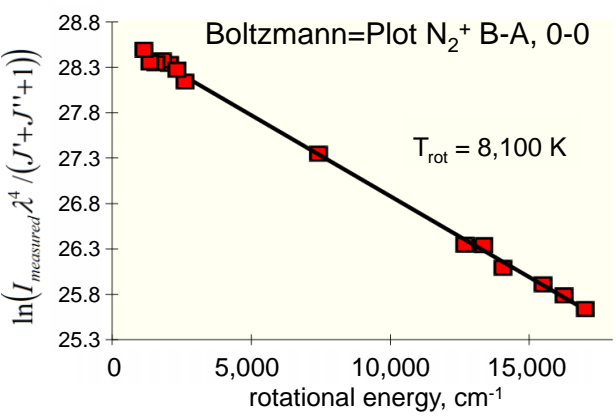
Emission from Molecules



Temperature determination from molecular radiation

- Within one vibrational transition, a large number of rotational lines is present
→ rovibrational lines (may shift to lower or higher wavelengths, depending on B)
- Similar to the atoms, a Boltzmann plot can be performed to determine T_{rot} .

$$Q_{rot}^{e'v'J'} = (2J'+1) \exp\left(-\frac{E_{rot}^{e'v'J'}}{kT_{rot}}\right)$$





Abel-Inversion

- emission spectroscopy is a line of sight method
→ only integrated data, no spatial resolution

Abel integral equation:

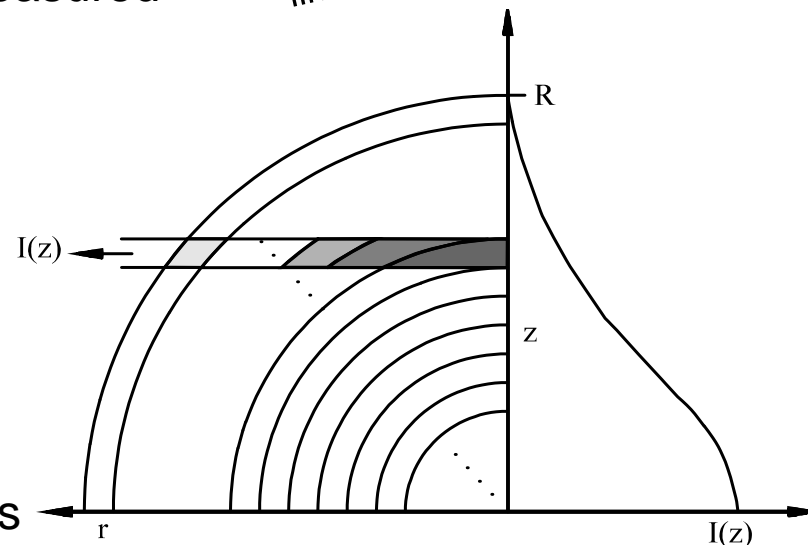
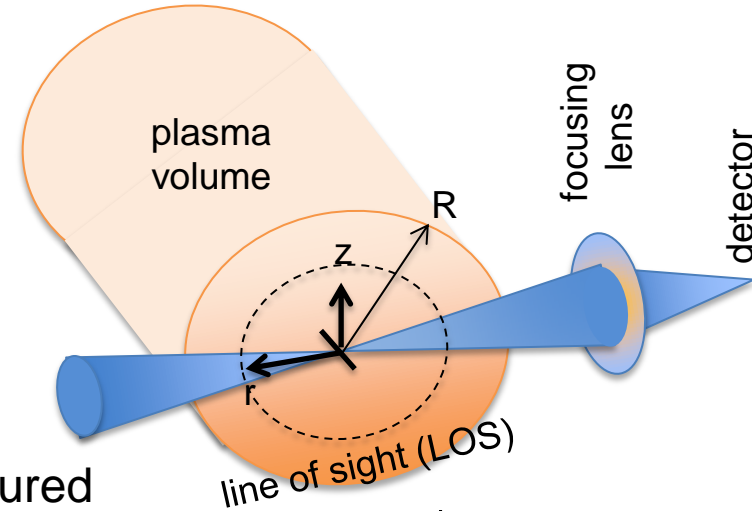
$$I(z) = 2 \int_{r=z}^R \frac{r}{\sqrt{r^2 - z^2}} \varepsilon(r) dr$$

Typically, integrals along the line of sight are measured
→ the local emission is desired.

$$\varepsilon(r) = -\frac{1}{\pi} \int_{z=r}^{\infty} \frac{(dI/dz)}{\sqrt{z^2 - r^2}} dz$$

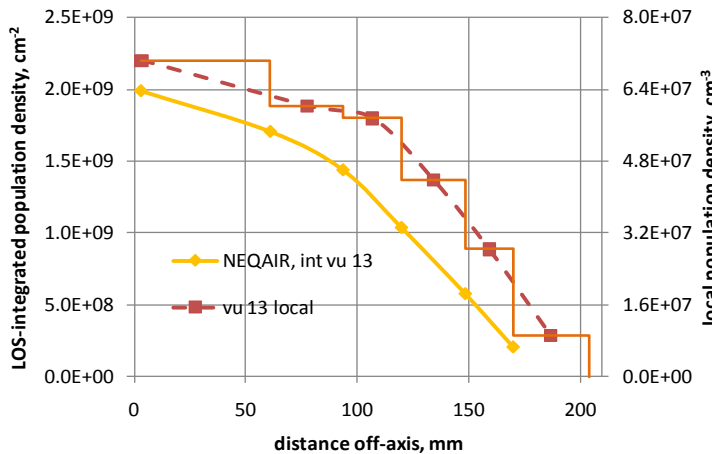
Solving this equation is usually only possible in special cases (e.g. a constant local distribution $\varepsilon(r)=\text{const.}$ yields and elliptical profile in $I(z)$)

Under the assumptions of rotational symmetry and optically thin medium, local emission values can be obtained from an Abel-Inversion.



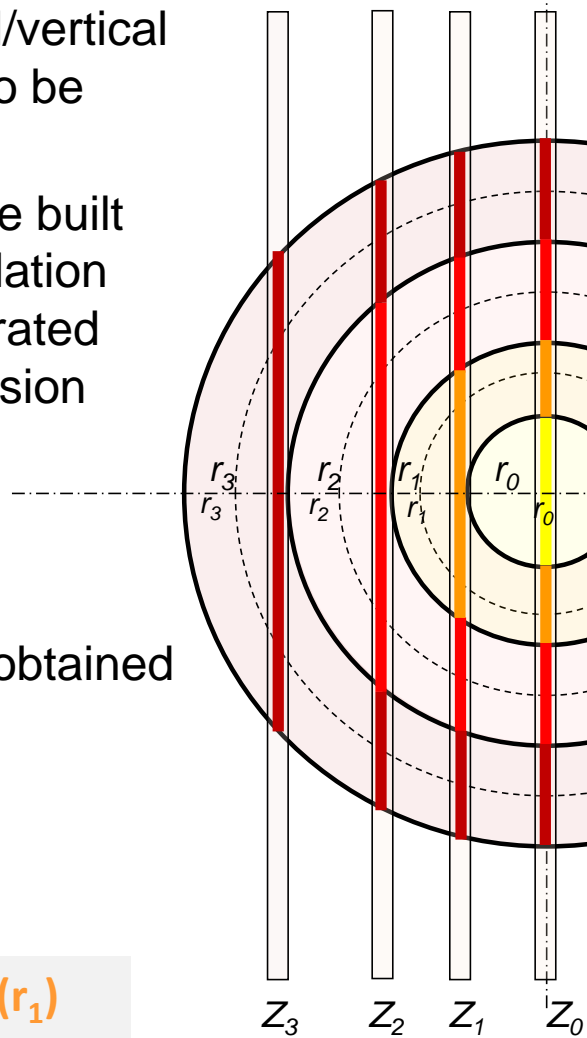


Approximate Abel-Inversion



- Different radial/vertical positions are to be measured
- A matrix can be built that gives a relation between integrated and local emission

- The matrix simplifies significantly if only few measurement positions are taken into account.
- constant local intensity in each ring assumed
- A very simple system of linear equations can be obtained and solved recursively

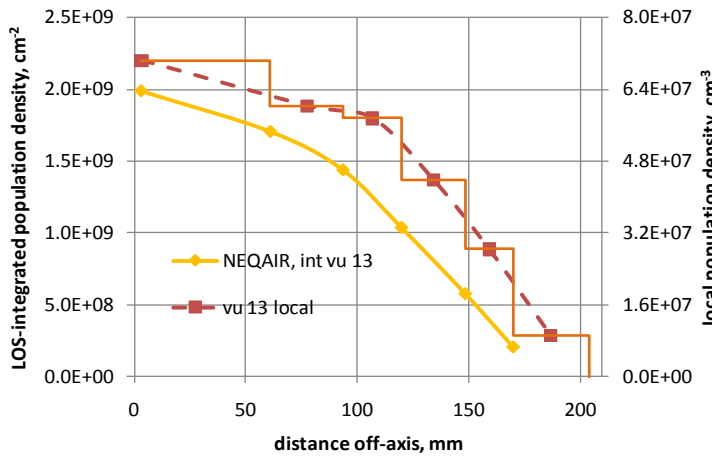


$$\begin{aligned}
 I_{3,int}(Z_3) &= \epsilon(r_3) * L_3(r_3) \\
 I_{2,int}(Z_2) &= \epsilon(r_3) * L_2(r_3) + \epsilon(r_2) * L_2(r_2) \\
 I_{1,int}(Z_1) &= \epsilon(r_3) * L_1(r_3) + \epsilon(r_2) * L_1(r_2) + \epsilon(r_1) * L_1(r_1) \\
 I_{0,int}(Z_0) &= \epsilon(r_3) * L_0(r_3) + \epsilon(r_2) * L_0(r_2) + \epsilon(r_1) * L_0(r_1) + \epsilon(r_0) * L_0(r_0)
 \end{aligned}$$

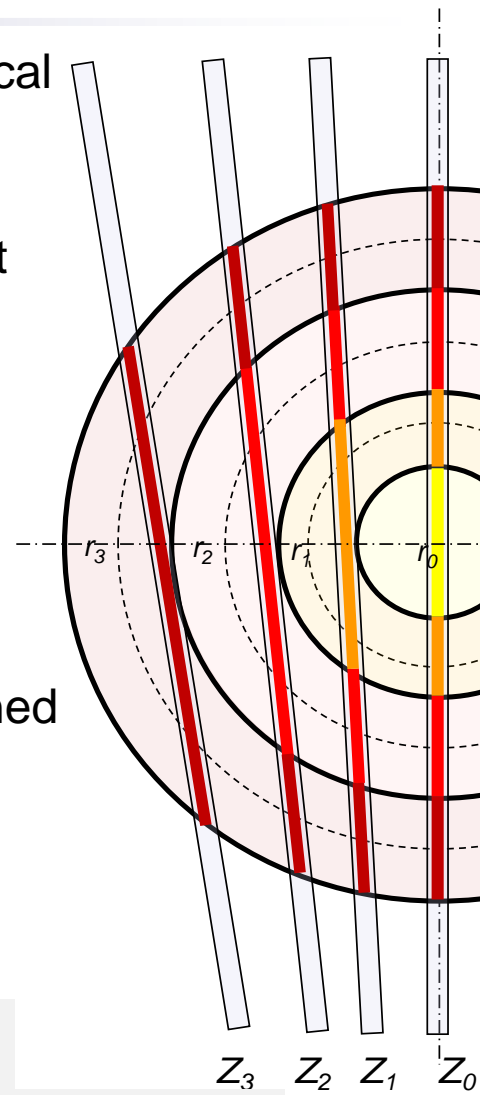
Winter, M. W., Prabhu, D. K., "Excited State Chemistry in the Free Stream of the NASA IHF Arc Jet Facility Observed by Emission Spectroscopy," 42nd AIAA Thermophysics Conference in Honolulu, Hawaii, 27 - 30 Jun 2011.



Approximate Abel-Inversion



- Different radial/vertical positions are to be measured
- A matrix can be built that gives a relation between integrated and local emission



- The matrix simplifies significantly if only few measurement positions are taken into account.
- constant local intensity in each ring assumed
- A very simple system of linear equations can be obtained and solved recursively

$$\begin{aligned}
 I_{3,int}(Z_3) &= \epsilon(r_3) * L_3(r_3) \\
 I_{2,int}(Z_2) &= \epsilon(r_3) * L_2(r_3) + \epsilon(r_2) * L_2(r_2) \\
 I_{1,int}(Z_1) &= \epsilon(r_3) * L_1(r_3) + \epsilon(r_2) * L_1(r_2) + \epsilon(r_1) * L_1(r_1) \\
 I_{0,int}(Z_0) &= \epsilon(r_3) * L_0(r_3) + \epsilon(r_2) * L_0(r_2) + \epsilon(r_1) * L_0(r_1) + \epsilon(r_0) * L_0(r_0)
 \end{aligned}$$

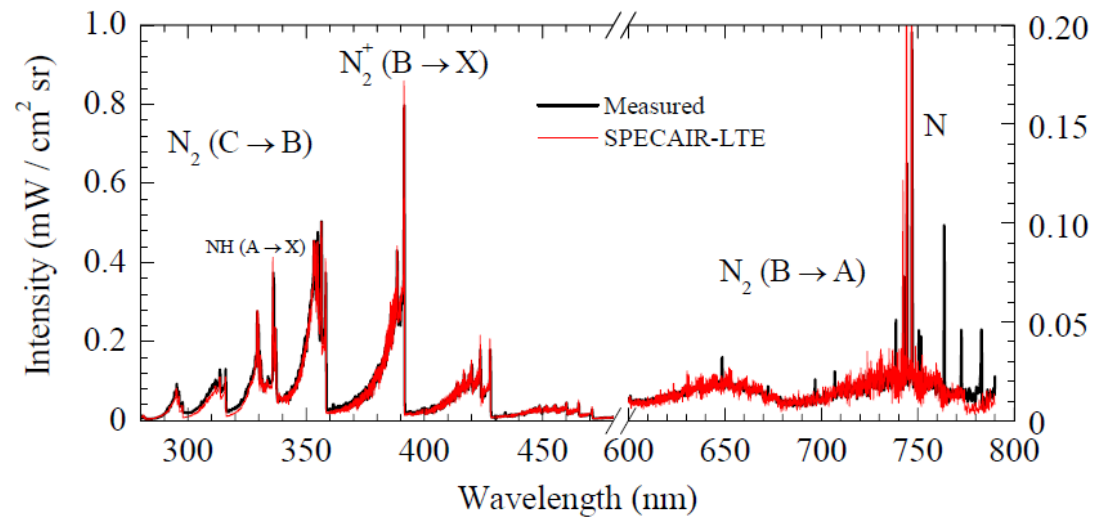
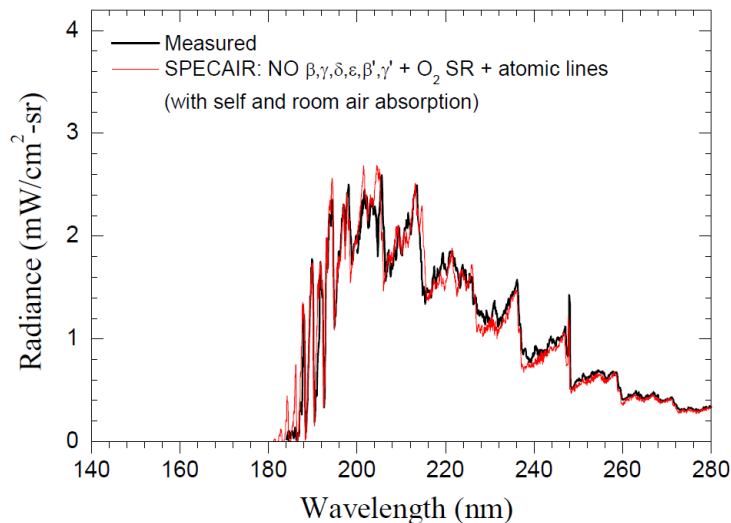


Application examples



Measurements in an atmospheric, inductively coupled plasma torch
(C. Laux, Stanford University, now Ecole Centrale, Paris)

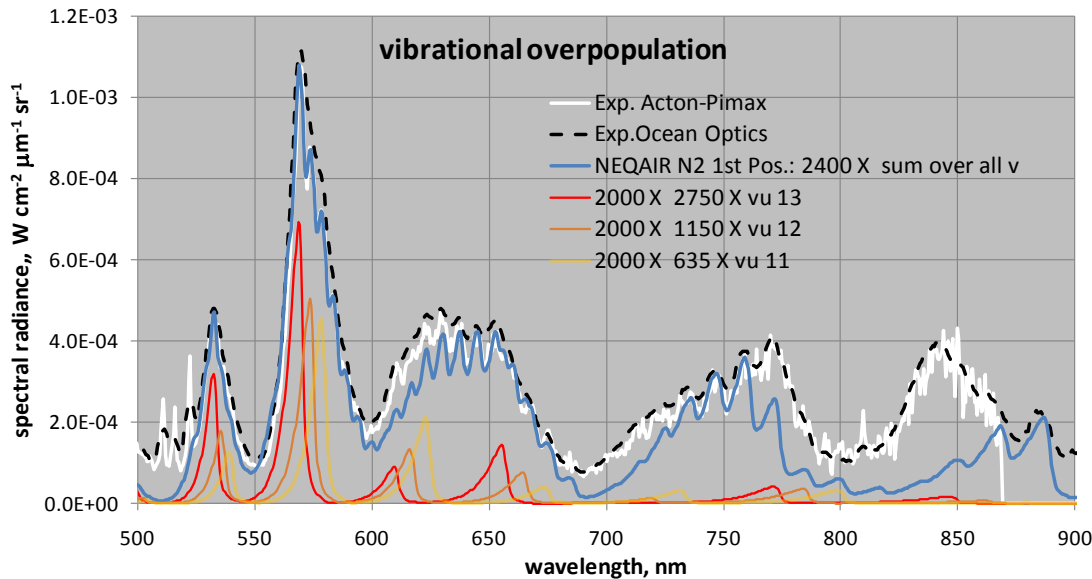
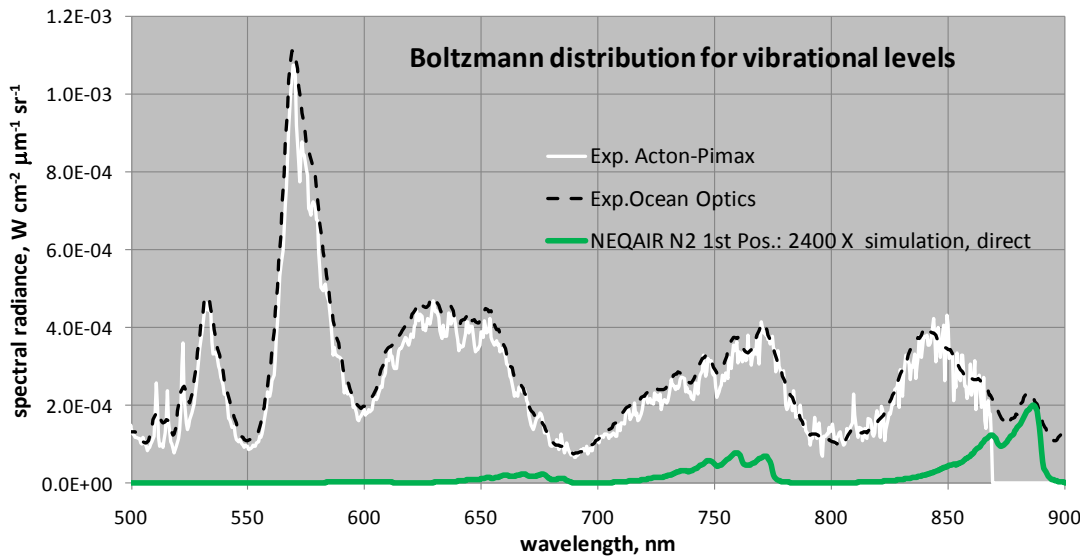
- Equilibrium plasma at up to 6000 K
→ chemistry well defined
- Used for the development of radiation models
- Excellent agreement between experiment and simulation can be achieved.
- After equilibrium characterization, used for non-equilibrium investigation.



- Laux C. O.: Radiation and Nonequilibrium Collisional-Radiative Models, VKI Special Course on Physico-Chemical Models for High Enthalpy and Plasma Flows Modeling, Belgium, June 4-7, 2002. See also Laux, C.O., Pierrot, L., and Gessman, R.J., "State-to-state modeling of a recombining nitrogen plasma experiment," Chemical Physics, Vol. 398, pp. 46-55, DOI: 10.1016/j.chemphys.2011.10.028, 2012.
- Laux, C. O., "Radiation and nonequilibrium collisional-radiative models" in "Physico-chemical Models for High Enthalpy and Plasma Flows, VKI LS 2002-07, edited by D. G. Fletcher et al., Rhode-Saint-Genèse, Belgium, 2002.



NASA Ames IHF: Free Stream Investigation



Comparison of free stream spectra at high condition with LTE simulation (VIS/NIR):

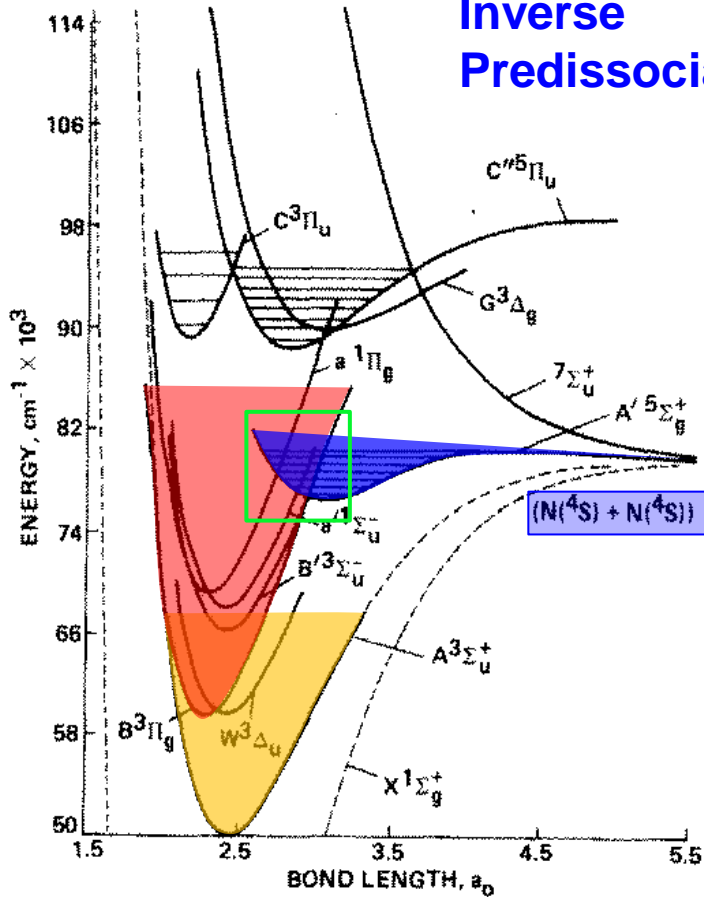
- Spectra dominated by emission of N2 B-A (1st Pos.)
- Thermodynamic quantities from CFD solution used as input for NEQAIR
- Spectra integrated along the line of sight
- Simulation and experiment do not even agree qualitatively
- If individual vibrational states are computed separately, the spectrum can be fitted by scaling these upper populations
→ massive overpopulation of the high vibrational levels peaking at $v_{\text{upper}} = 13$



Application examples

Inverse Predissociation

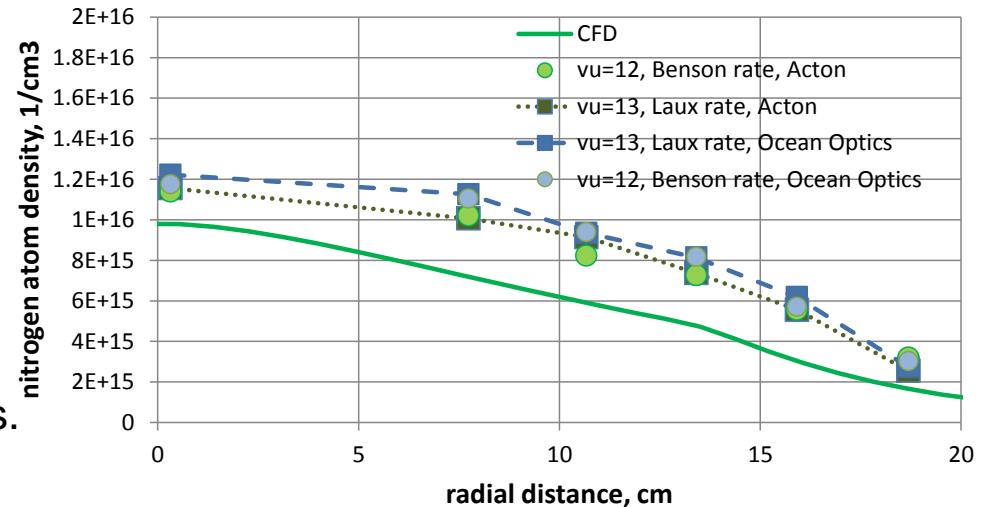
level crossing with $N_2 B^3\Pi_g$ at v between 10 and 13



→ Population of the excited state is not caused by thermal excitation of the ground state but by recombination of atoms in an excited N_2 state

→ Molecule emission can be used to determine atom ground state densities.

- Observed radiation comes from the 1st Pos. System ($N_2 B^3\Pi_g \rightarrow A^3\Sigma_u^+$) with electronic excitation energies around 8eV to 10eV.



Harry Partridge, Stephen R. Langhoff, and Charles W. Bauschlicher, Jr., and David W. Schwenke, "Theoretical study of the $A^5\Sigma_g^+$ and $C''^5\Pi_u$ states of N_2 : Implications for the N_2 afterglow," J. Chem. Phys. 88 (5), 1 March 1988. Figure reproduced with permission from the authors.

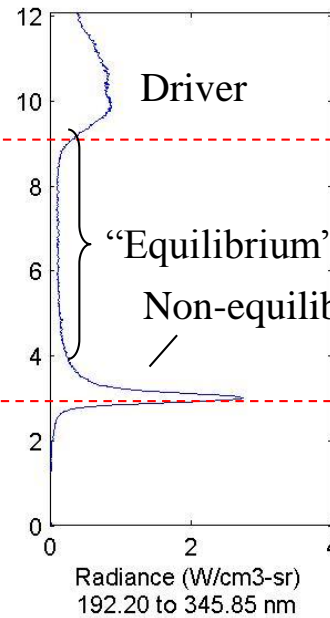
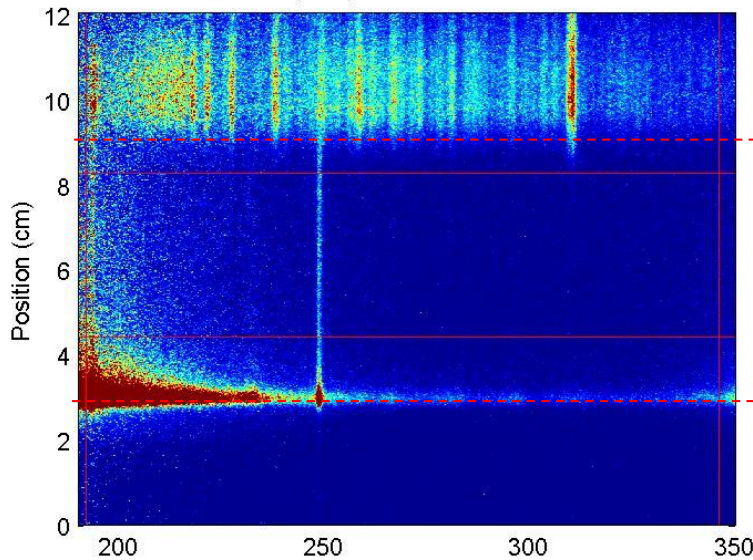
Winter, M, Srinivasan, C., Charnigo, R., "Non-Equilibrium Analysis of Emission Spectroscopy Data Taken in the Freestream of the NASA IHF Arc Jet Facility," AIAA AVIATION 2015, Dallas, Texas, June 2015.



Application examples

Quantify radiation loads to spacecraft during atmospheric entry in impulse facilities

Shot 35 (Blue) - 8.53 km/s, 0.098 torr



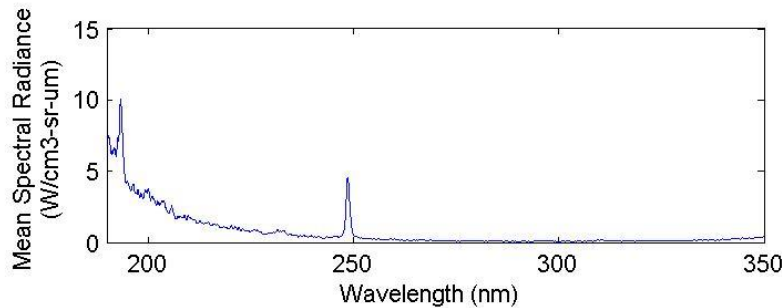
Contact Front
Shock Front

EAST shock tube (NASA Ames):

- reproduction of flight conditions
- no model testing
- 130nm – 8μm in various intervals
- simultaneous measurements with 4 spectrometers possible
- one dimension resolves spectrally, the other spatially → shock and post-shock region are covered in one image

Goals:

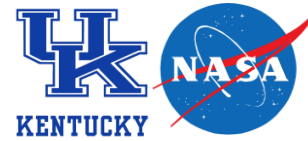
- quantify radiation from shock and post shock → radiation heat flux from the plasma upstream of the spacecraft after spectral integration
- empirical correlation for radiation heat flux



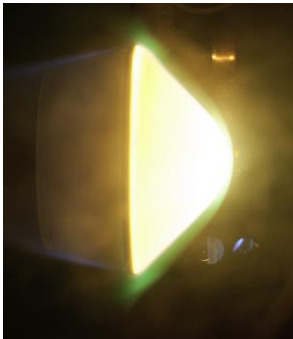
- Cruden, B., Martinez, R., Grinstead, J. H., Olejniczak, J., "Simultaneous Vacuum Ultraviolet through Near IR Absolute Radiation Measurement with Spatiotemporal Resolution in an Electric Arc Shock Tube," AIAA 2009-4240, 41st AIAA Thermophysics Conference, 22 - 25 June 2009, San Antonio, Texas.
 - Aaron Brandis, Christopher Johnston, Marco Panesi, Brett Cruden, Dinesh Prabhu, Deepak Bose, "Investigation of Nonequilibrium Radiation for Mars Entry," AIAA 2013-1055, 51st AIAA Aerospace Sciences Meeting including the New Horizons Forum and Aerospace Exposition, 2013.



Application examples



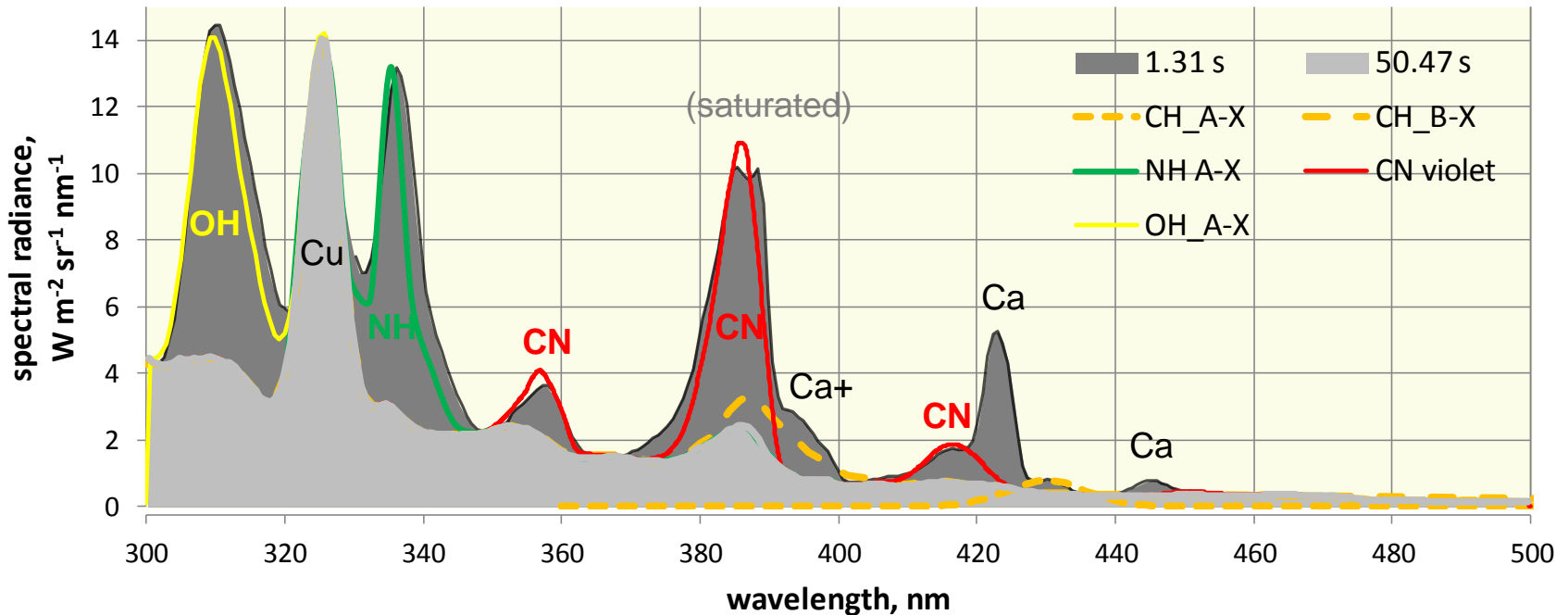
Monitoring of ablation species through optical methods



Testing of PICA at NASA Ames (SPRITE) showed the appearance of ablation products in emission spectra inside the boundary layer:

- CN, OH, NH, Ca, (Na, K)

Combination of pyrolysis products themselves and interactions with the plasma.





Application examples

Remote recession measurements of ablating TPS material

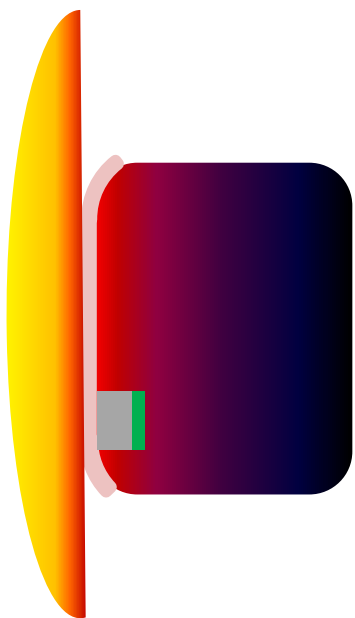
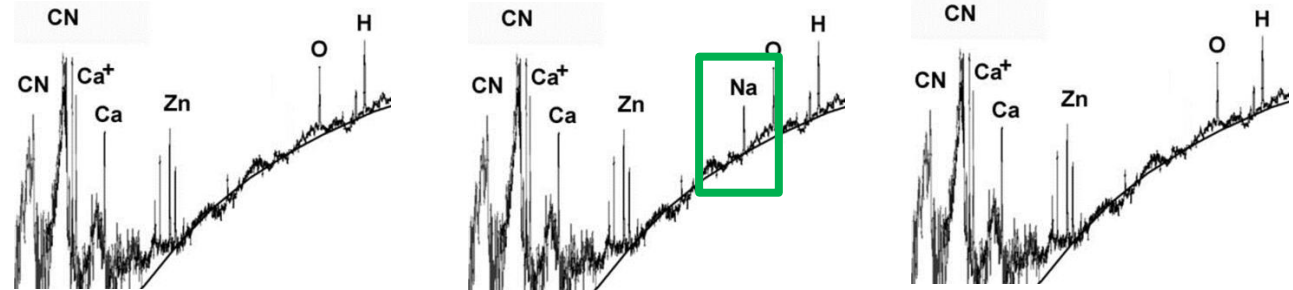


Tracer element (Coating/paint)

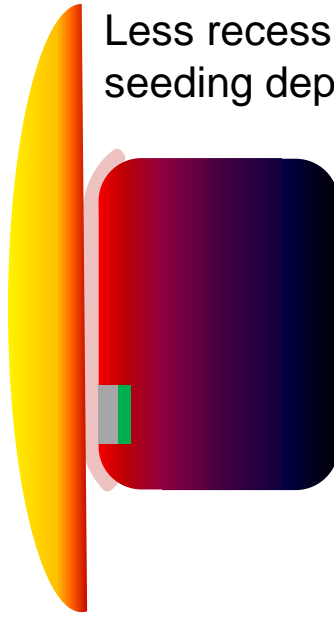
(on ground and in flight)



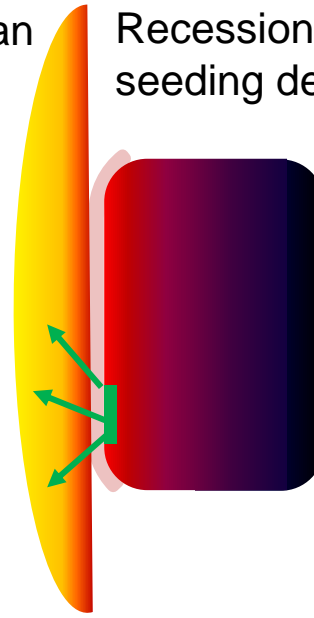
Tracer plug (e.g. PICA)



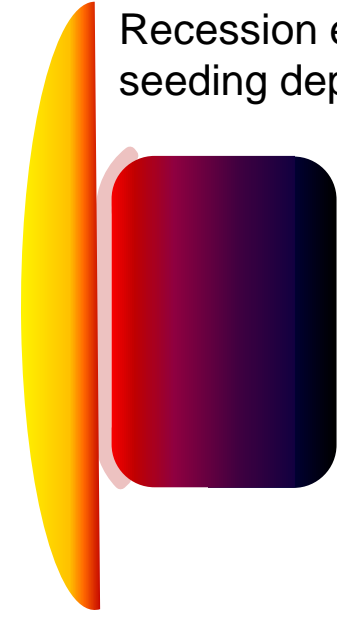
Less recession than seeding depth



Recession reaches seeding depth



Recession exceeds seeding depth





Conclusions



- Optical emission spectroscopy is a useful tool to access information on thermal characteristics and composition of a plasma.
- Applications for which the assumption of **equilibrium** is rather **uncritical**:
 - identification of species;
 - total radiation flux (in the wavelength covered and if properly calibrated);
 - quantities from line broadening (e.g. Doppler temperature, electron density);
 - identification of thermal non-equilibrium.
- Applications for which the assumption of **equilibrium** is rather **crucial**:
 - determination of particle densities from thermal excitation;
 - measurement of excitation temperatures from line ratios.
- Proper calibration is imperative.
- Comparison with simulation (non-equilibrium chemistry and excitation, e.g. though collisional radiative models) seems the best approach as soon as these models are validated.

Thanks for your attention!

Open for

Questions ?

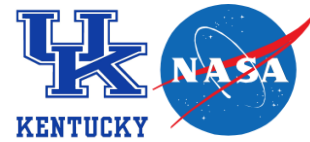


Back-up Slides





Selection of Simulation Codes (Line-byLine)

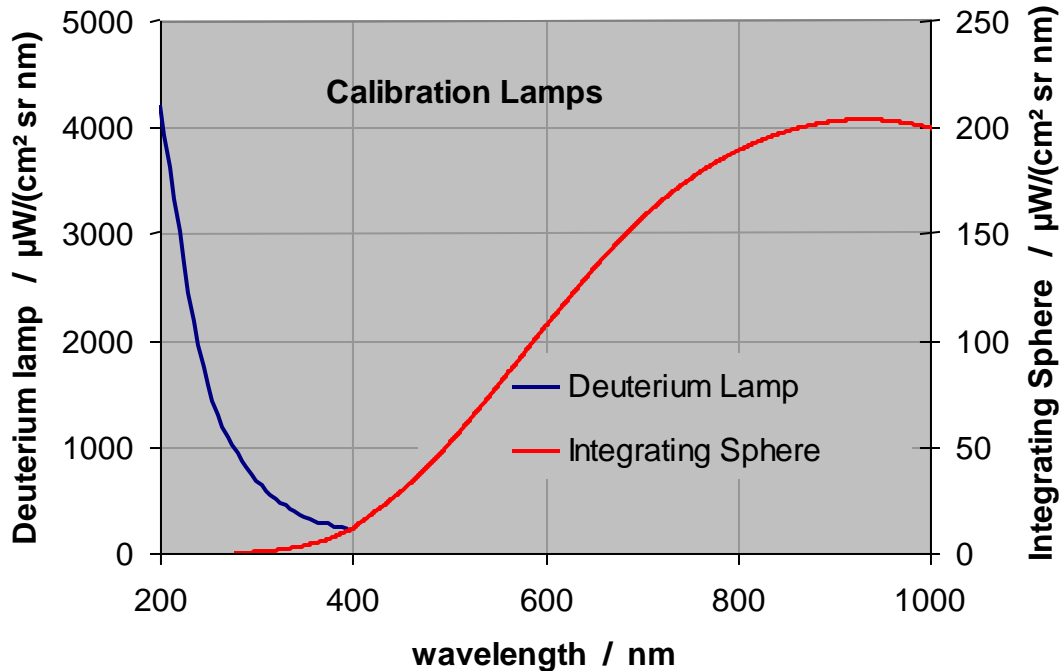
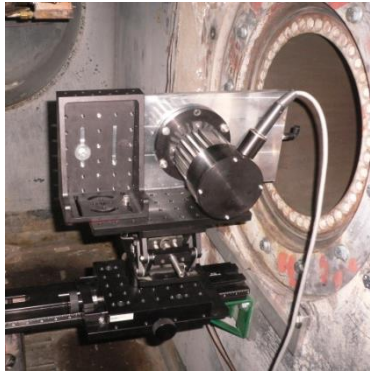


- **NEQAIR (Non Equilibrium ...)** - NASA Ames EAR restricted
FORTRAN, non-eq. (QSS + multi T), air and CO₂ plasma related species + H, radiation transport capabilities
Whiting, E E, Park, C, Liu, Y, Arnold, J O, and Paterson, J A, "NEQAIR96, Nonequilibrium and Equilibrium Radiative Transport and Spectra Program: User's Manual," NASA RP-1389, NASA, December 1996.
- **HARA (...)** – NASA Langley EAR restricted
FORTRAN, non-eq. (QSS + multi T), air and CO₂ plasma related species, radiation transport capabilities
Johnston, C. O., Hollis, B. R., and Sutton, K., "Spectrum Modeling for Air Shock-Layer Radiation at Lunar-Return Conditions," Journal of Spacecraft and Rockets, Sep.-Oct. 2008.
- **SPRADIAN/RADIPAC** – Japan/South Korea available on request to JAXA
FORTRAN, non-eq. (QSS + multi T), air + ablation related species , radiation transport capabilities
Fujita, K., and Abe, T., "SPRADIAN, Structured Package for Radiation Analysis: Theory and Application," The Institute of Space and Astronautical Science Report No. 669, July 1997.
- **PARADE** – European Space Agency ESA available on request to ESA
FORTRAN, non-eq. (QSS + multi T), air + CO₂ plasma related species , rad. transport capabilities (HERTA)
Smith, A. J., Wood, A., Dubois, J., Fertig, M., Pfeiffer, B.: *Plasma Radiation Database PARADE V22 Final Report Issue 3*, ESTEC contract 11148/94/NL/FG, FGE TR28/96, Issue 3, Oktober 2006.
- **SPECAIR** – Ecole Centrale Paris Windows version available by download
air, multi T, no radiation transport
Laux, C. O. , "Radiation and nonequilibrium collisional-radiative models" in "Physico-chemical Models for High Enthalpy and Plasma Flows," VKI LS 2002-07, edited by D. G. Fletcher et al., Rhode-Saint-Genèse, Belgium, 2002.
<http://www.specair-radiation.net>
- **LIFBASE** - Stanford Research Institute SRI Windows version available by download
LIF related diatomic molecules (CH, NH, OH, CO, NO, ...), no radiation transport
J. Luque and D.R. Crosley, "LIFBASE: Database and spectral simulation (version 1.5)", SRI International Report MP 99-009 (1999)
<http://www.sri.com/psd/lifbase/>

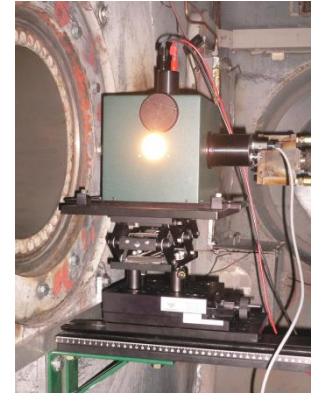


Intensity Calibration – How?

Deuterium Lamp



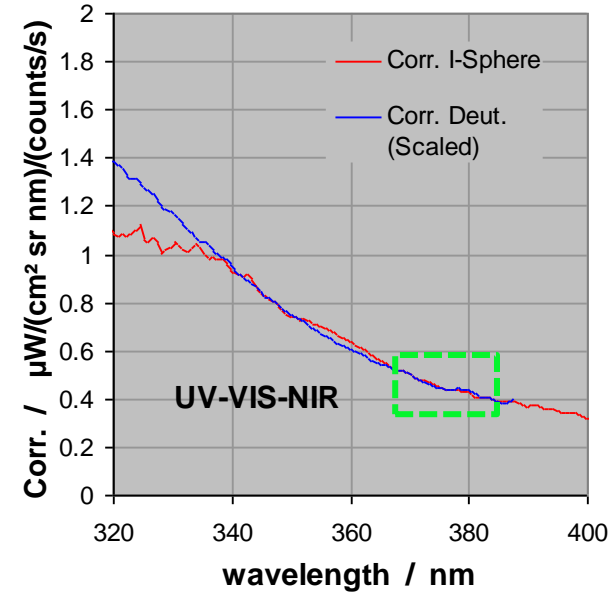
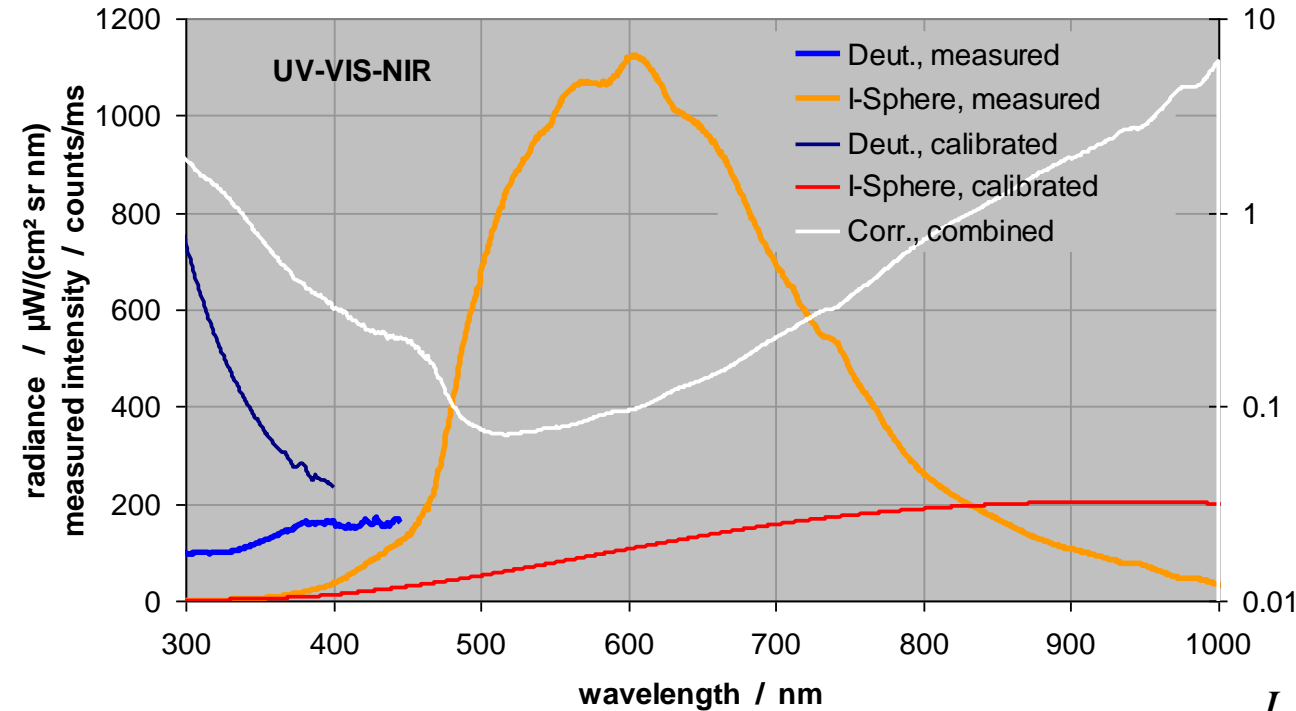
Integrating Sphere



- Calibration with an integrating sphere (halogen bulbs - UV-VIS-NIR) and a Deuterium lamp (UV) both calibrated to spectral radiance in $\mu\text{W}/(\text{cm}^2 \text{sr nm})$
- Correction factor: ratio of factory calibration value and measurement of calibration lamp
- Deuterium lamp (UV) can not easily be used for absolute calibration
→ scaling of Deuterium correction factor to the I-Sphere in overlapping region.
- Best calibration: place the calibration lamp at the location of the measured plasma
→ all set-up influences are covered and direct calibration is possible.
 - **Lamp area must be larger than measurement spot !!!**



Intensity Calibration – How?



VIS: direct

$$I_{pl,cal}(\lambda) = corr(\lambda) I_{pl,meas}(\lambda) = \frac{I_{BB,theory}(\lambda)}{I_{BB,meas}(\lambda)} I_{pl,meas}(\lambda)$$

UV: scaled

$$I_{pl,cal}(\lambda) = \frac{corr_{BB}}{corr_{Deut}} \Big|_{\Delta\lambda_{scaling}} \frac{I_{Deut,theory}(\lambda)}{I_{Deut,meas}(\lambda)} I_{pl,meas}(\lambda)$$

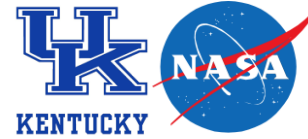
→ Correction factor $corr(\lambda)$ which is the inverse sensitivity of the set-up.

→ Use of Deuterium lamp only for qualitative calibration

followed by scaling (cross calibration) through halogen lamp/black-body.

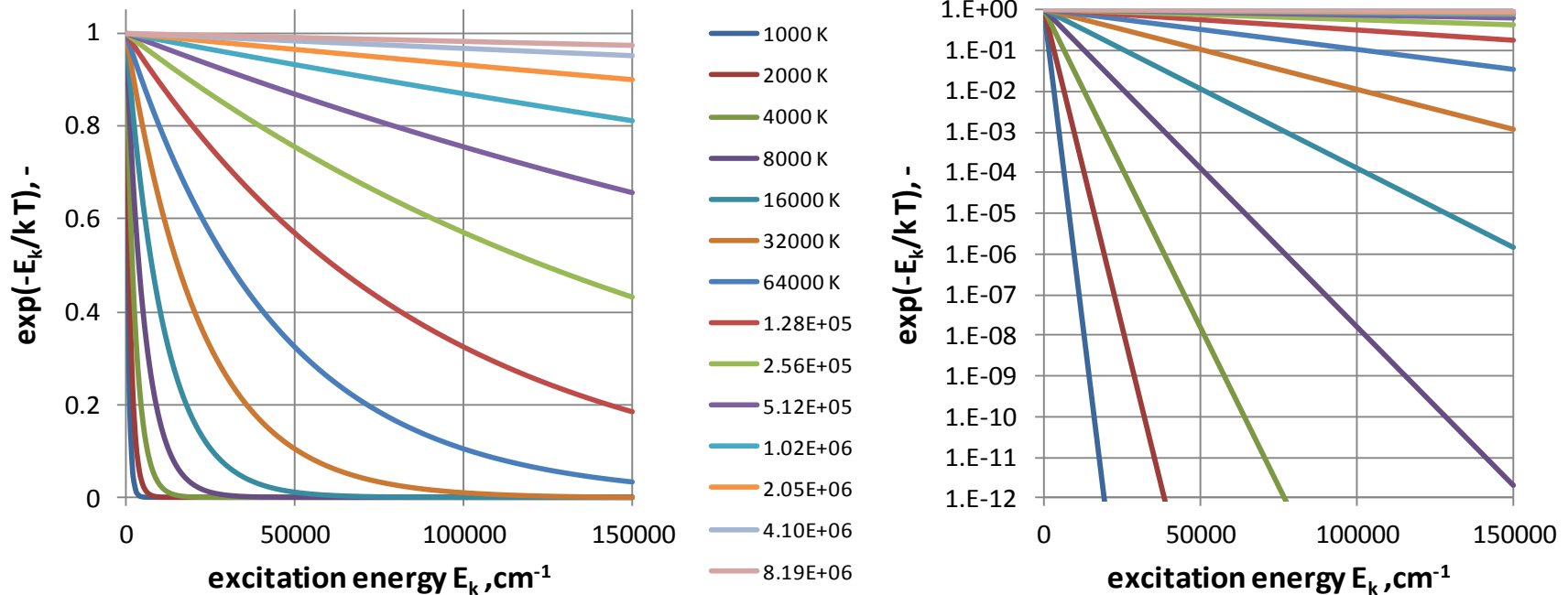


Emission of Atoms: Electronic Excitation



$$\varepsilon = \frac{h\nu}{4\pi} A_{ki} n_k = \frac{h\nu}{4\pi} A_{ki} \frac{g_k}{U(T_{ex})} n_0 \exp\left(-\frac{E_k}{kT_{ex}}\right)$$

- For low temperatures, only the first energy levels are populated.
- With temperature going to infinity, all levels would be populated according to g_k/U .



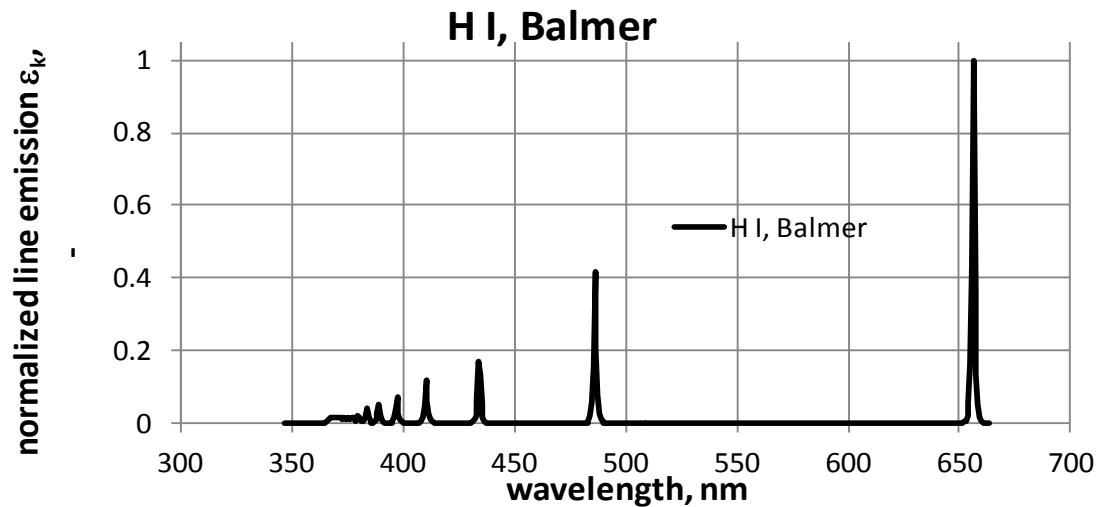


Electronic Excitation of Hydrogen



$$\varepsilon = \frac{h\nu}{4\pi} A_{ki} n_k = \frac{h\nu}{4\pi} A_{ki} \frac{g_k}{U(T_{ex})} n_0 \exp\left(-\frac{E_k}{kT_{ex}}\right)$$

Balmer spectrum of hydrogen



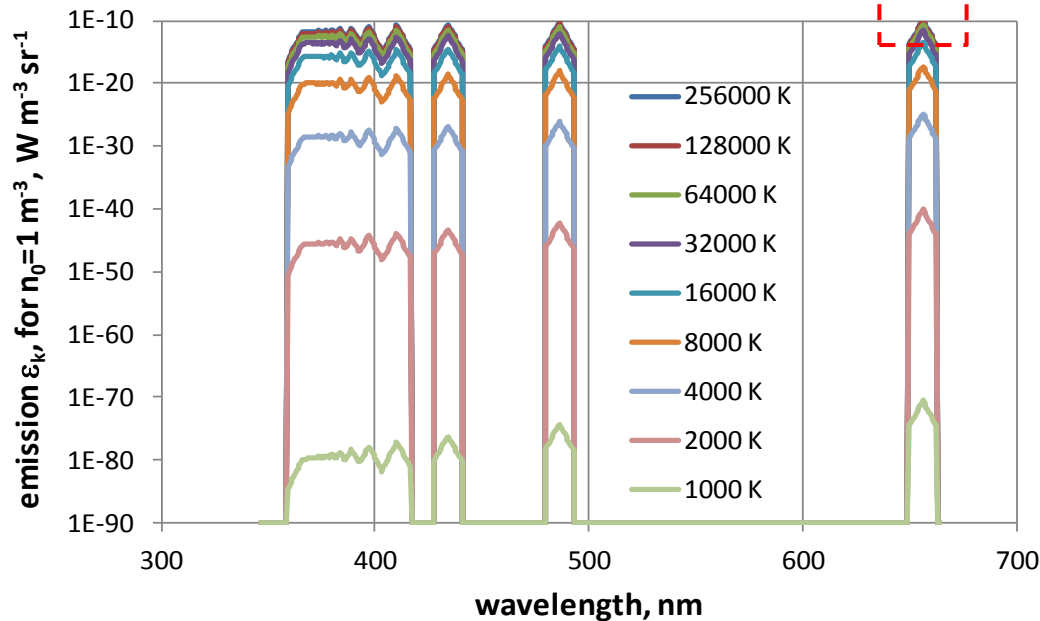


Electronic Excitation of Hydrogen



$$\varepsilon = \frac{h\nu}{4\pi} A_{ki} n_k = \frac{h\nu}{4\pi} A_{ki} \frac{g_k}{U(T_{ex})} n_0 \exp\left(-\frac{E_k}{kT_{ex}}\right)$$

Balmer spectrum of hydrogen for different temperatures:
(logarithmic scale)



- Emission increases by 60 orders of magnitude between 1000K and 8000K
- Ratio of different lines in the Balmer series changes with temperature (hard to see on log scale).
- To illustrate the ratios, we normalize the spectrum to the H_α line.



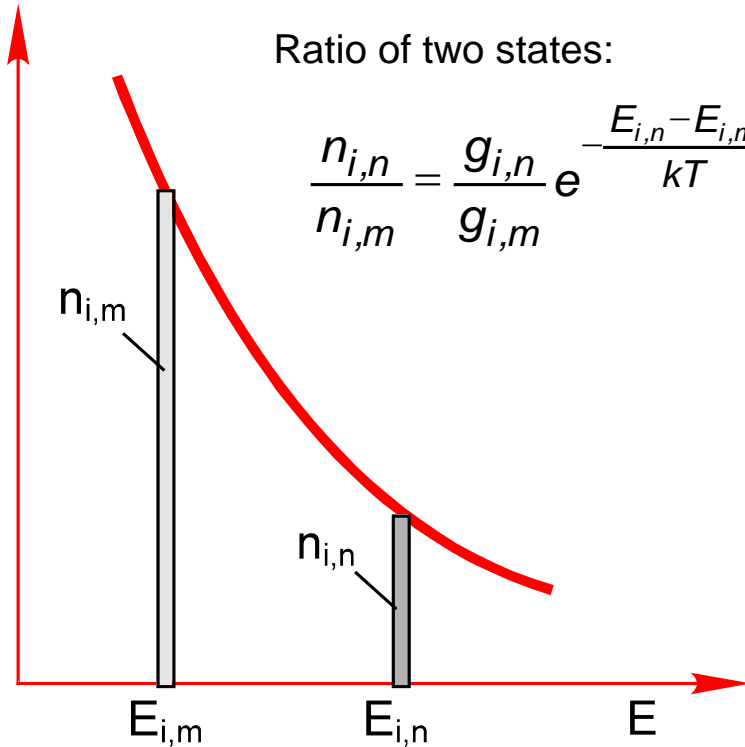
Electronic Excitation of Hydrogen



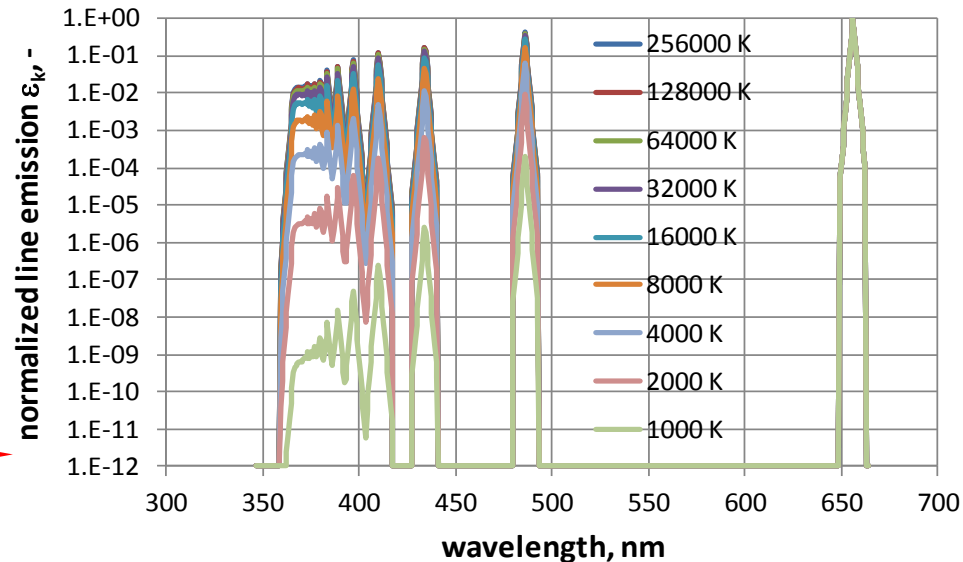
$$\varepsilon = \frac{h\nu}{4\pi} A_{ki} n_k = \frac{h\nu}{4\pi} A_{ki} \frac{g_k}{U(T_{ex})} n_0 \exp\left(-\frac{E_k}{kT_{ex}}\right)$$

Ratio of two states:

$$\frac{n_{i,n}}{n_{i,m}} = \frac{g_{i,n}}{g_{i,m}} e^{-\frac{E_{i,n}-E_{i,m}}{kT}}$$



Spectrum **normalized to H α** to illustrate the influence on the line ratios:





Emission of Atoms and Molecules



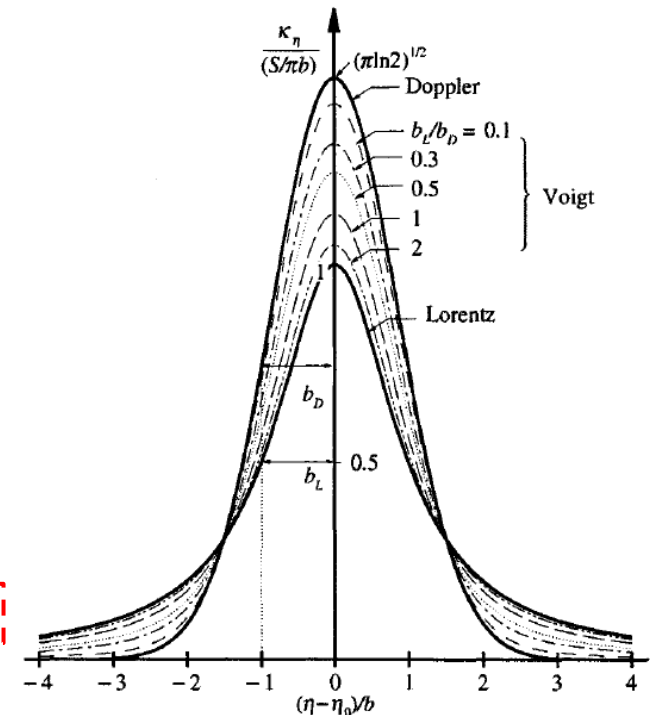
Line Broadening

Emission and absorption lines can be broadened through different processes:

- natural broadening (Heisenberg uncertainty principle)
- Doppler broadening (thermal motion)
- Collision broadening
 - Van-der-Waals: collisions with neutrals
 - Resonance: collisions with the 'like' species particles (perturber's state connected by an allowed transition to the upper or lower state of the transition under consideration)
 - Stark for interactions with ions or electrons, specific for each transition/line
- (Zeeman effect - interaction with magnetic fields)

- Each of these processes is actually a line shift for one photon.
- The integration over many photons with different shifts produces a broadening.
 - distributing the transition energy over a certain wavelength/wavenumber range

- Depending on the physical effect, the final line shape will follow a Gauss or a Lorentz profile.
- Usually, the broadening is described by the line width at its half maximum (full width FWHM, or half width HWHM).
- Half widths of Lorentz profile can be summed up linearly.
- Half widths of Gauss profiles can be combined quadratically through $FWHM_{G,total} = \sqrt{FWHM_{G,1}^2 + FWHM_{G,2}^2}$.





Emission of Atoms and Molecules

Line Broadening

Collision broadening (Lorentz)

$$\kappa_\eta = \frac{S}{\pi} \frac{b_c}{(\eta - \eta_0)^2 + b_c^2}, \quad S \equiv \int_{\Delta\eta} \kappa_\eta d\eta,$$

HWHM decreases with T

$$b_c = b_{c0} \left(\frac{p}{p_0} \right) \sqrt{\frac{T_0}{T}},$$

Doppler broadening (Gauss)

$$\kappa_\eta = \sqrt{\frac{\ln 2}{\pi}} \left(\frac{S}{b_D} \right) \exp \left[-(\ln 2) \left(\frac{\eta - \eta_0}{b_D} \right)^2 \right]$$

HWHM increases with T

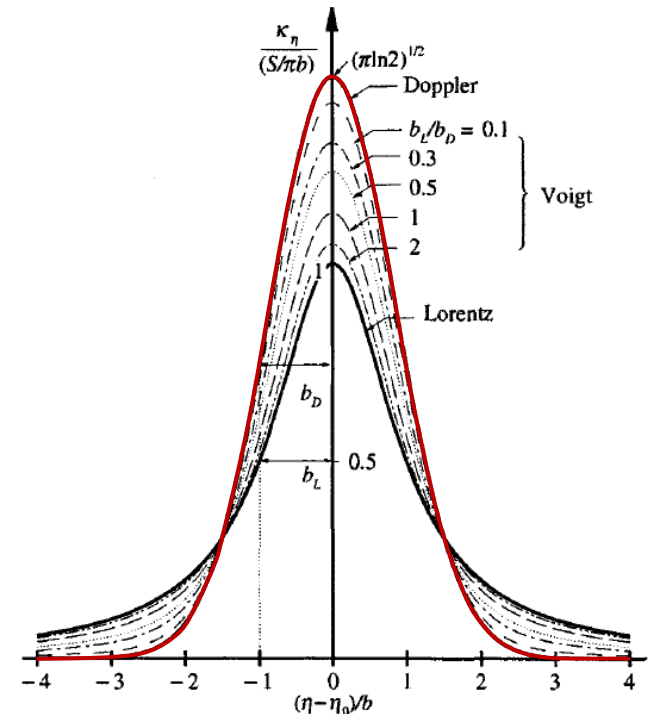
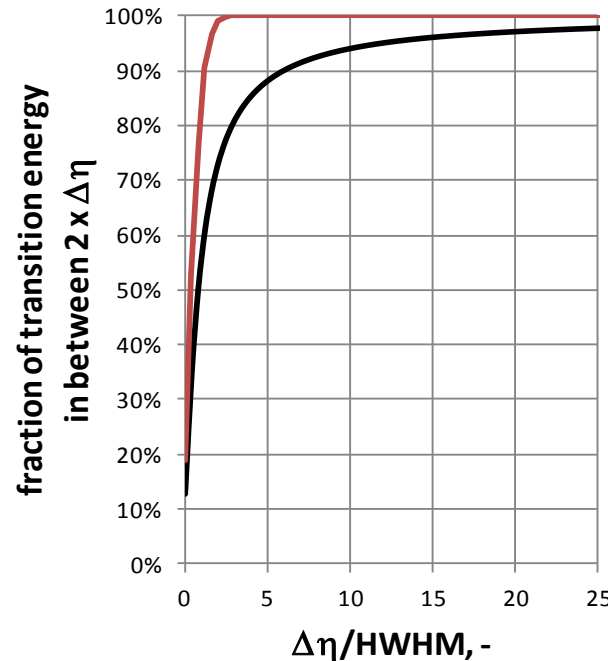
$$b_D = \frac{\eta_0}{c_0} \sqrt{\frac{2kT}{m} \ln 2}.$$

Lorentz:

- 90% of the transition energy within 6 HWHM
- 99% is reached after ~ 50 HWHM

Gauss:

- 99% in 2 HWHM





Emission from Molecules

The Anharmonic Oscillator – Higher Order Potentials

- Higher order potentials
Lippincott – 3 parameter fit
Hulbert-Hirschfelder – 5 parameter fit
- may provide better agreement with experimental data

Morse Potential

$$U(x) = D_e \left(1 - e^{-\beta x}\right)^2$$

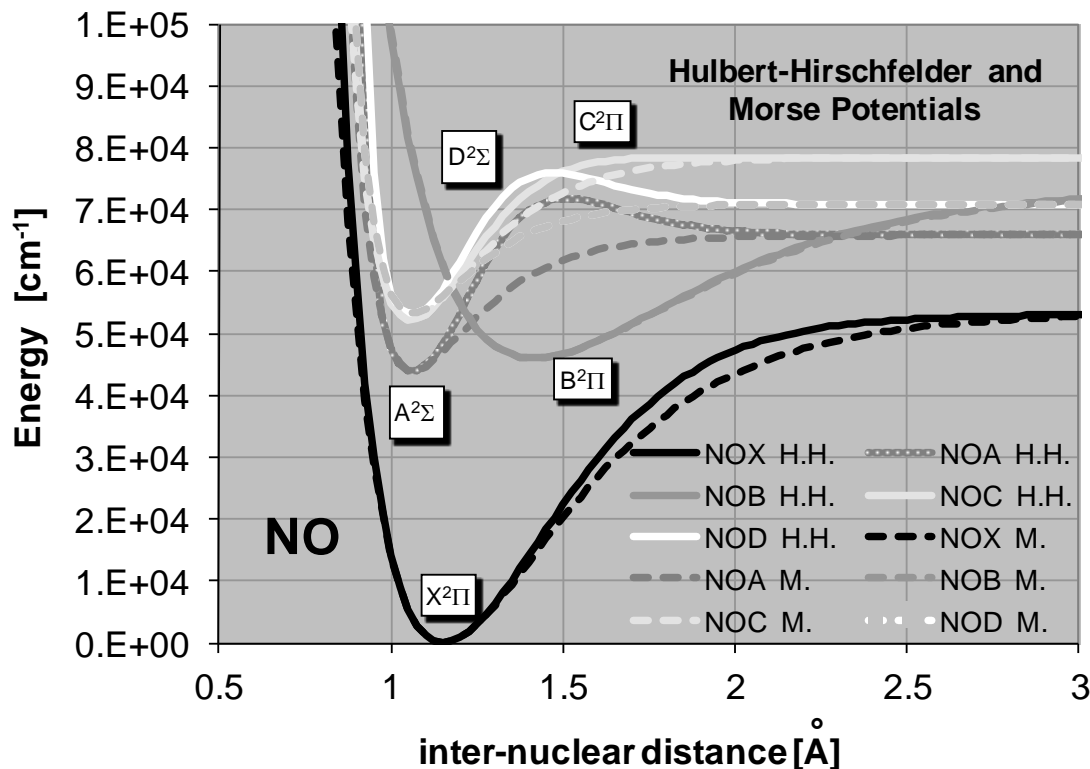
- x : distance to r_e
(r_e : equilibrium distance between the nuclei)
- D_e : Well depth of the potential
(dissociation energy- energy at minimum)

$$\beta = 1,2177 \cdot 10^{-7} \omega_e \sqrt{\frac{\mu_A}{D_e}}$$

- μ_A : reduced mass of the molecule

vibrational energy increment from V to $V+1$ now decreases with V :

$$G(V) = \omega_e \left(V + \frac{1}{2}\right) - \omega_e x_e \left(V + \frac{1}{2}\right)^2$$





Higher Order Approximations - Dunham Expansion

- Vibrational energy expressed as a polynomial function of V
- For small quantum numbers equivalent to Morse

$$G(V) = \omega_e \left(V + \frac{1}{2} \right) - \omega_e x_e \left(V + \frac{1}{2} \right)^2 + \omega_e y_e \left(V + \frac{1}{2} \right)^3 + \omega_e z_e \left(V + \frac{1}{2} \right)^4 + \dots$$

- Rotational energy contains higher orders of J
- coupling constants now depend on V

$$F_V(V, J) = B_V J(J+1) - D_V J^2(J+1)^2 + \dots$$

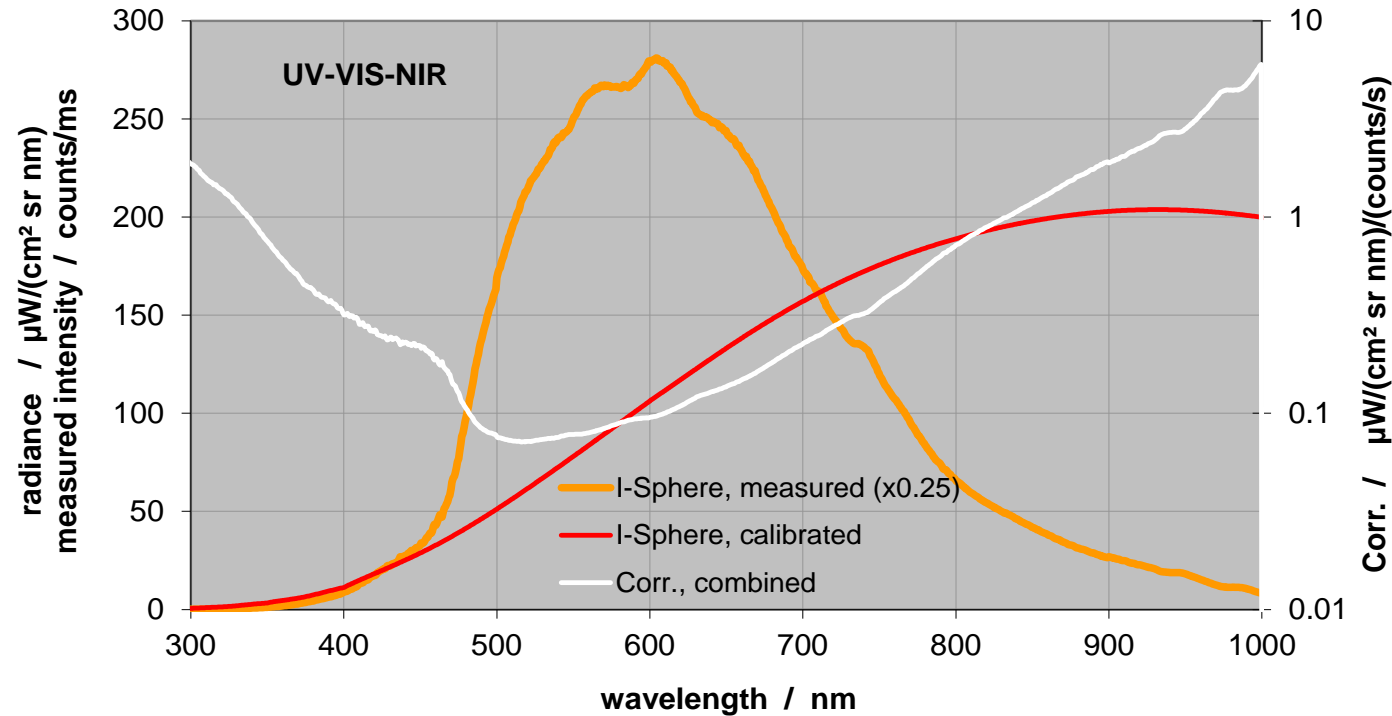
$$B_V = B_e - \alpha_e \left(V + \frac{1}{2} \right) + \gamma_e \left(V + \frac{1}{2} \right)^2 + \dots$$

$$D_V = D_e + \beta_e \left(V + \frac{1}{2} \right) + \delta_e \left(V + \frac{1}{2} \right)^2 + \dots$$

- Different sets of constants given in literature



Intensity Calibration – How?

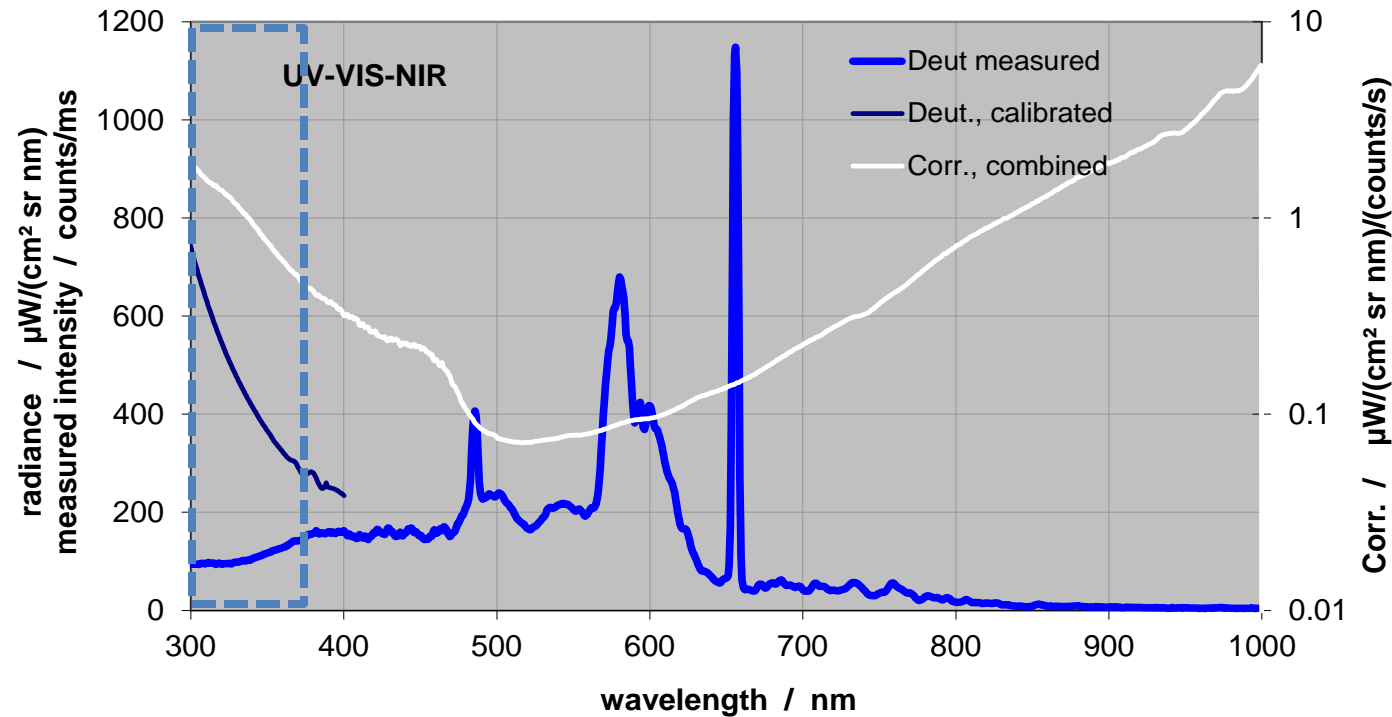


$$I_{\text{plasma,cal}}(\lambda) = \text{corr}(\lambda) * I_{\text{plasma,measured}}(\lambda) = [I_{\text{lamp,theory}}(\lambda)/I_{\text{lamp,measured}}(\lambda)] * I_{\text{plasma,measured}}(\lambda)$$

- Best calibration: place the calibration lamp at the location of the measured plasma
→ all set-up influences are covered and direct calibration is possible.
- **Lamp area must be larger than measurement spot !!!**



Intensity Calibration – How?



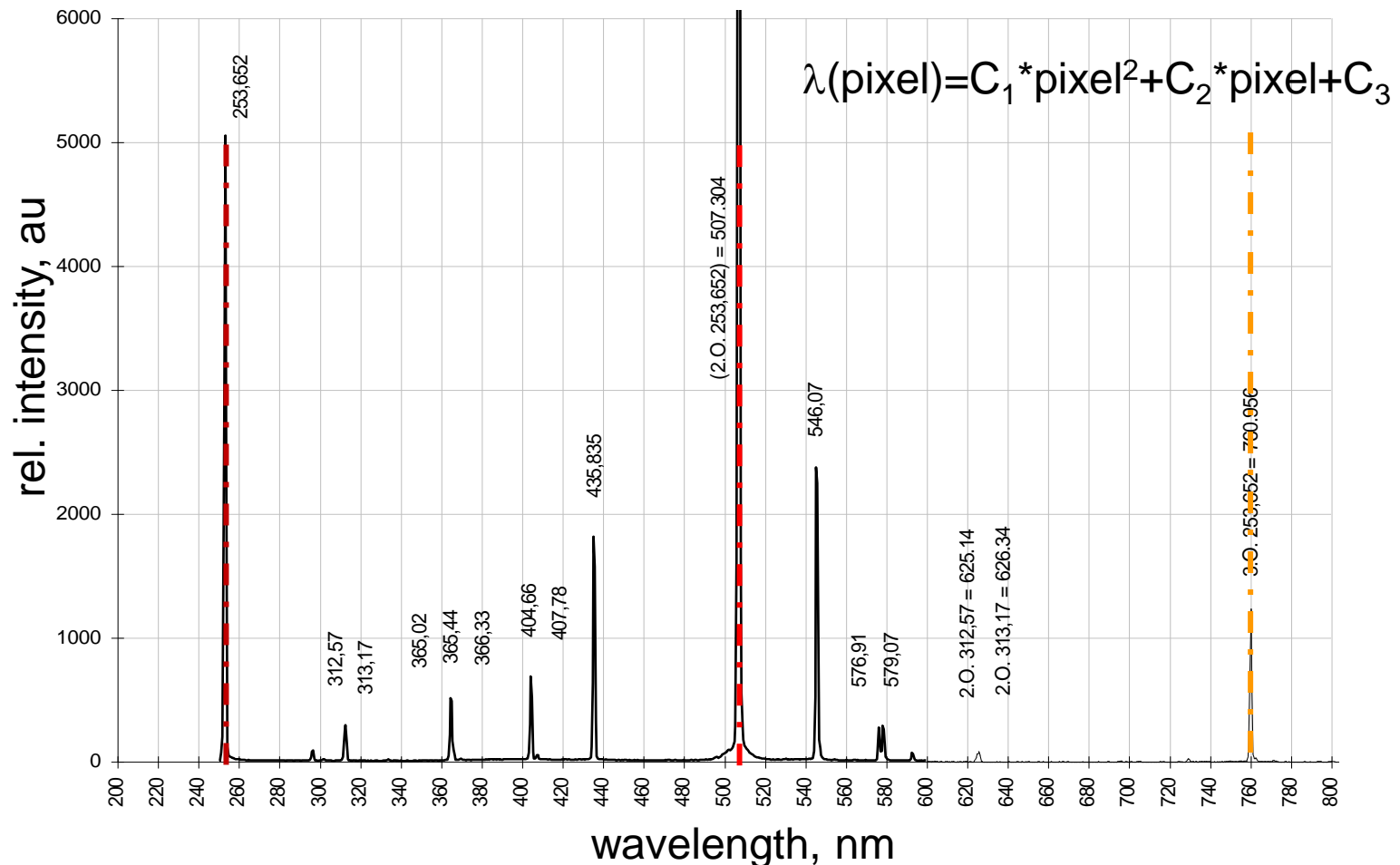
- Deuterium lamp (UV) uses a hydrogen discharge to produce high radiation in VUV-VIS
- Usually, only the continuum emission from UV down is used for calibration.
- Although calibrated to radiance in $\mu\text{W}/(\text{cm}^2 \text{sr nm})$, the dimensions of the discharge are small (~1mm) → measurement spot usually larger
- Discharge shows gradients → additional uncertainties introduced.

→ **Use of Deuterium lamp only for qualitative calibration followed by scaling (cross calibration) through halogen lamp/black-body.**



Wavelength Calibration

- Compare measured line positions (pixel) with known line positions (e.g. Hg lamp):
 - scanning spectrometer: typically linear with time → at least 2 lines needed;
 - CCD measurement: typically binomial → at least 3 lines needed.
- additional lines may serve as a calibration check ...





Electronic Excitation Temperature



The emission coefficient

$$\varepsilon = \frac{h\nu}{4\pi} A_{ki} n_k$$

With the Boltzmann distribution

$$n_k = \frac{g_k}{U(T_{ex})} n_0 \exp\left(-\frac{E_k}{kT_{ex}}\right)$$

is integrated along the line of sight

$$I_{ki} = \int \varepsilon(x) dx = \frac{h\nu}{4\pi} A_{ki} n_k l$$

follows:

$$\ln\left(\frac{I_{ki}}{\nu A_{ki} g_k}\right) + const = -\frac{E_k}{kT_{ex}}$$

Theoretically, the ratio of two lines would be sufficient, but it is often in doubt if the electronic excitation is in equilibrium.

→ Boltzmann Plot:

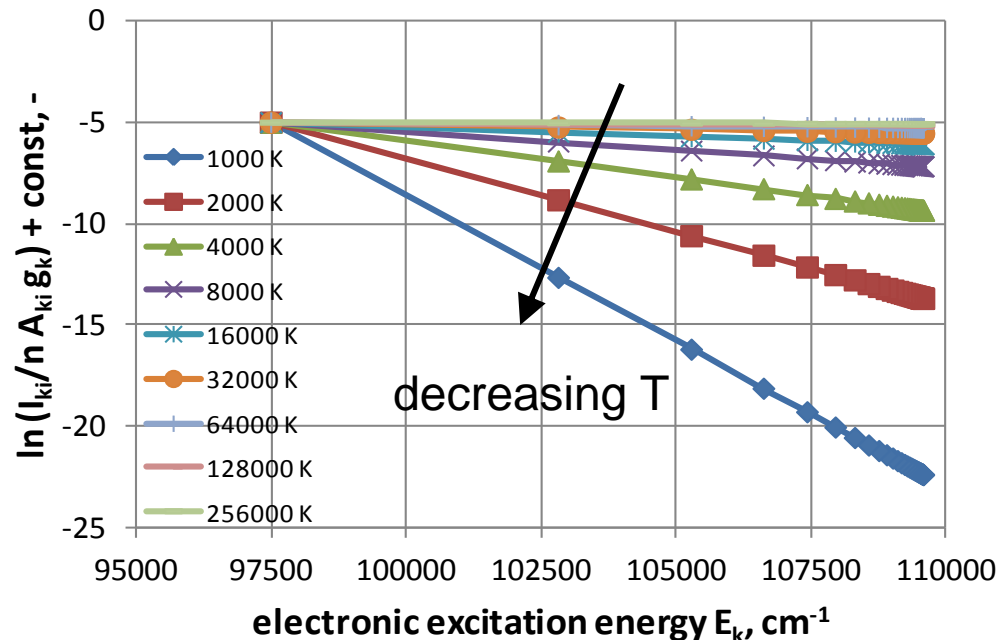
Plot $\ln\left(\frac{I_{ki}}{\nu A_{ki} g_k}\right)$ vs E_k

→ Straight line with slope $1/-kT$

If points are indeed on a straight line

→ Boltzmann valid

→ T can be determined

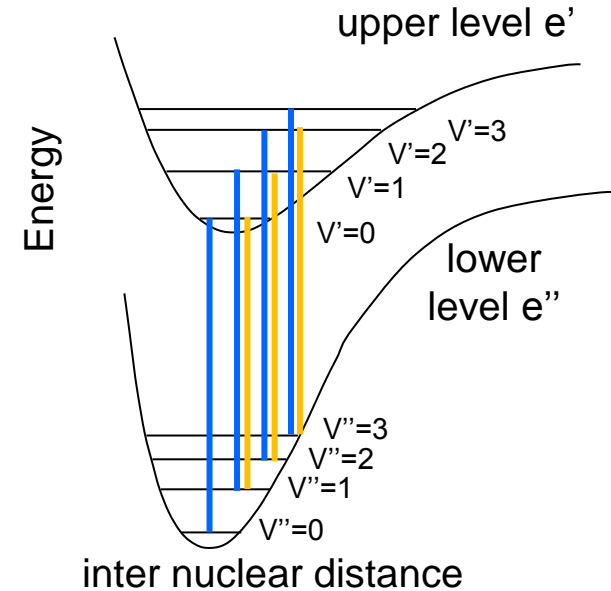
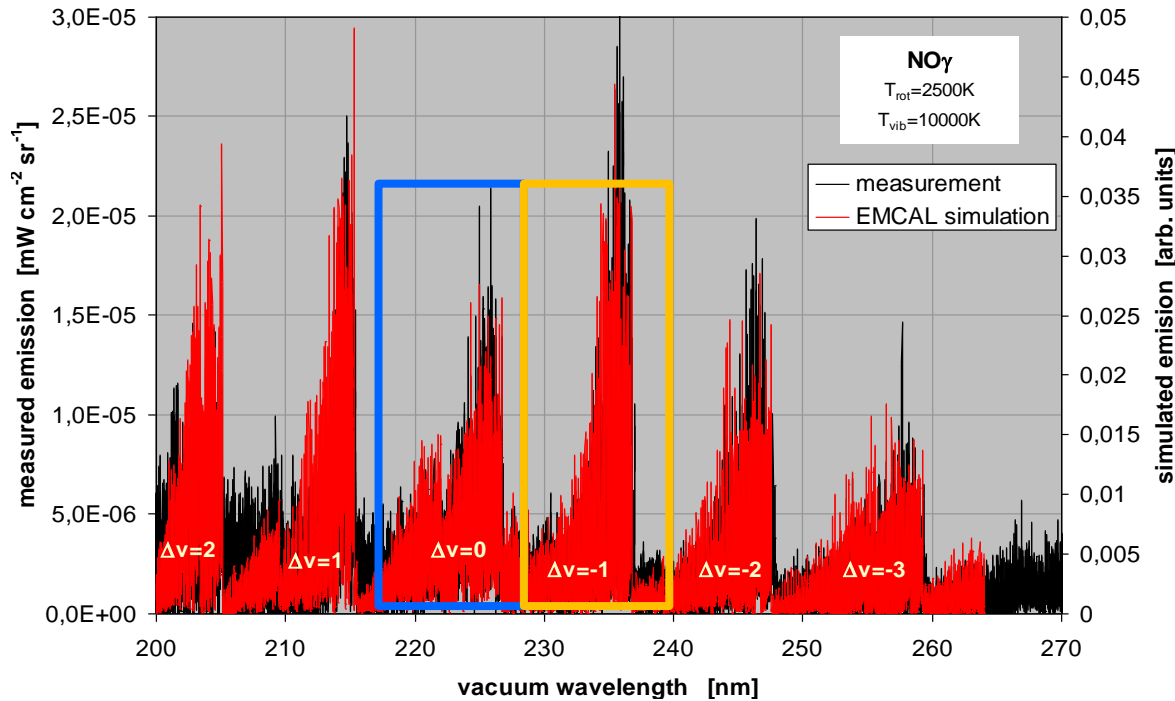




Molecular Band Structure



- Transition energies with the same difference in vibrational quantum number Δv are similar
→ The different vibrational transitions tend to group for the same Δv .
- $\Delta V = -1$: 0-1, 1-2, 2-3, 3-4, ... → lower ΔE → higher λ



$\Delta V = -1$: transition energy lower than $\Delta V = 0$



Theoretical Simulation of Molecule Radiation

➤ Intensity of one emission line:

$$\varepsilon = \frac{N' A_{\rightarrow} \Delta E_{\rightarrow}}{4\pi} = N' \frac{16\pi^3 c \bar{\nu}^4}{3} \underbrace{(R_e(\bar{r}_{VV''}))^2 q_{VV''}}_{\text{Electronic transition moment}} \frac{S_{J''\Lambda''}^{J'\Lambda'}}{2J'+1} \underbrace{\hspace{10em}}_{\text{Hönl London Factor}}$$

↓
↓
↓

Particle density in the level e' V' J' Electronic transition moment Hönl London Factor

- There are (2J+1) allowed rotational states (rotational multiplicity)
- The selection rules allow for ΔJ=-1,0,1
- The Hönl London Factor controls how the (2J+1) states are distributed among the branches



Emission of Atoms and Molecules



Line Broadening

Emission and absorption lines can be broadened through different processes:

- natural broadening (Heisenberg uncertainty principle)
- Doppler broadening (thermal motion)
- Collision broadening
 - Van-der-Waals: collisions with neutrals
 - Resonance: collisions with the 'like' species particles (perturber's state connected by an allowed transition to the upper or lower state of the transition under consideration)

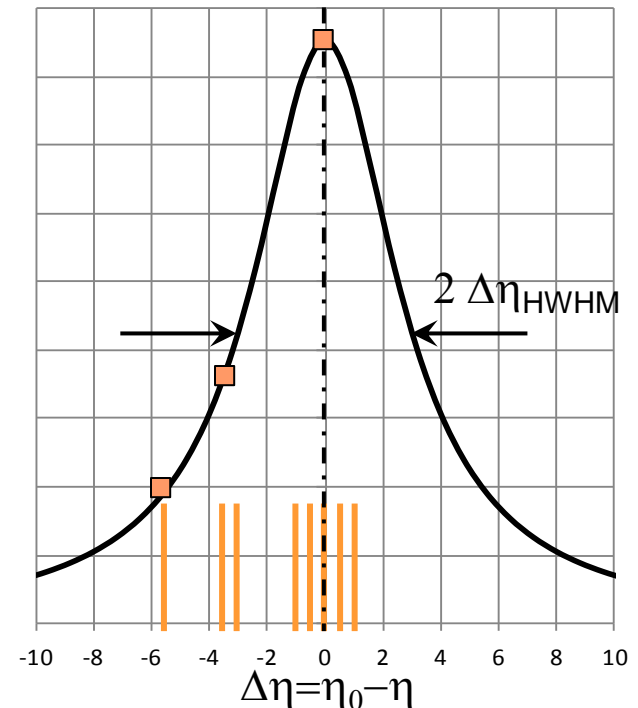
- Stark for interactions with ions or electrons, specific for each transition/line

- (Zeeman effect - interaction with magnetic fields)

- Each of these processes is actually a line shift for one photon.
- The integration over many photons with different shifts produces a broadening.
→ distributing the transition energy over a certain wavelength/wavenumber range

- Temperature measurement (low pressures, high temperatures)

- Electron density measurement (lines with large Stark coefficients, e.g. H_α or H_β)





Emission of Atoms and Molecules

Line Broadening

Emission and absorption lines can be broadened through different processes:

- natural broadening (Heisenberg uncertainty principle)
- Doppler broadening (thermal motion)
- Collision broadening
 - Van-der-Waals: collisions with neutrals
 - Resonance: collisions with the 'like' species particles (perturber's state connected by an allowed transition to the upper or lower state of the transition being studied)
 - Stark for interactions with ions or electrons, specific for each transition/line
- (Zeeman effect - interaction with magnetic fields)

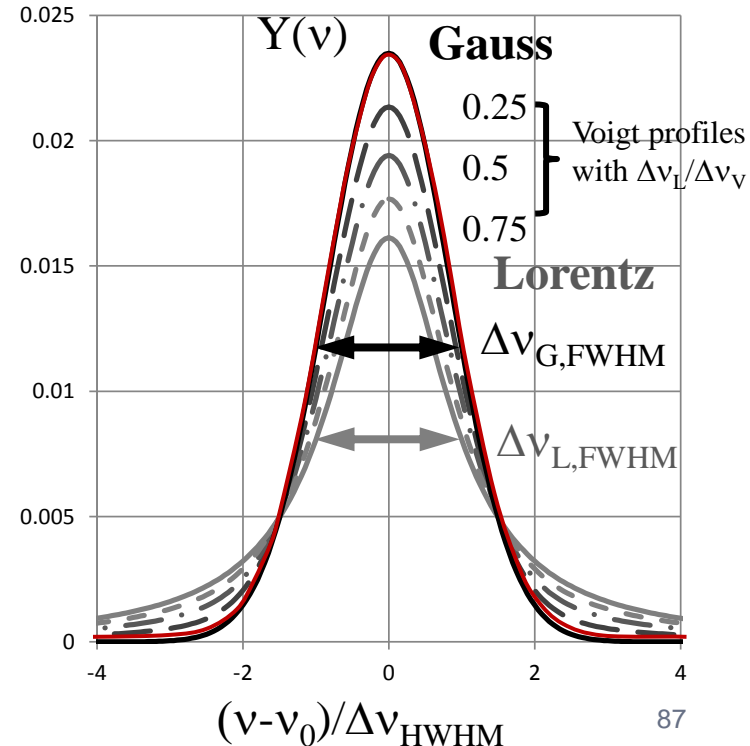
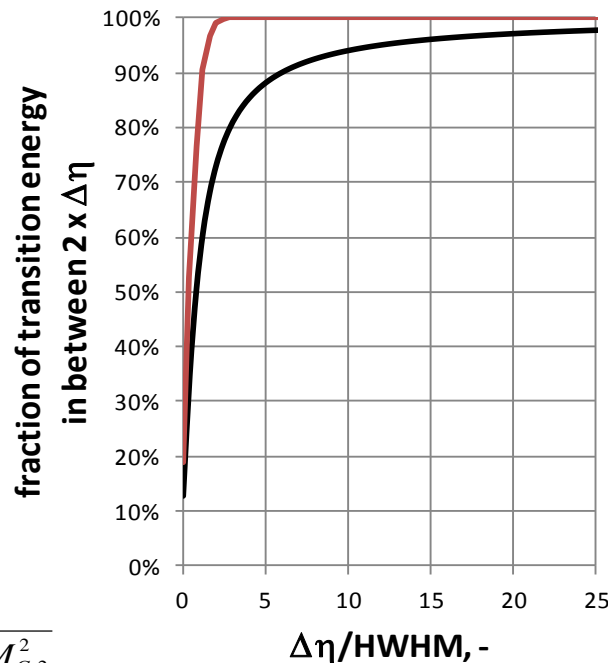
Lorentz:

- 90% of the transition energy within 6 HWHM
- 99% is reached after ~ 50 HWHM
- Half widths are added linearly.

Gauss:

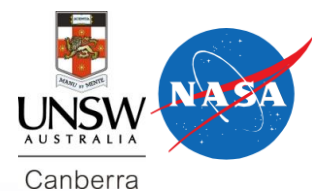
- 99% in 2 HWHM
- are combined as the geometric sum

$$FWHM_{G,total} = \sqrt{FWHM_{G,1}^2 + FWHM_{G,2}^2}$$



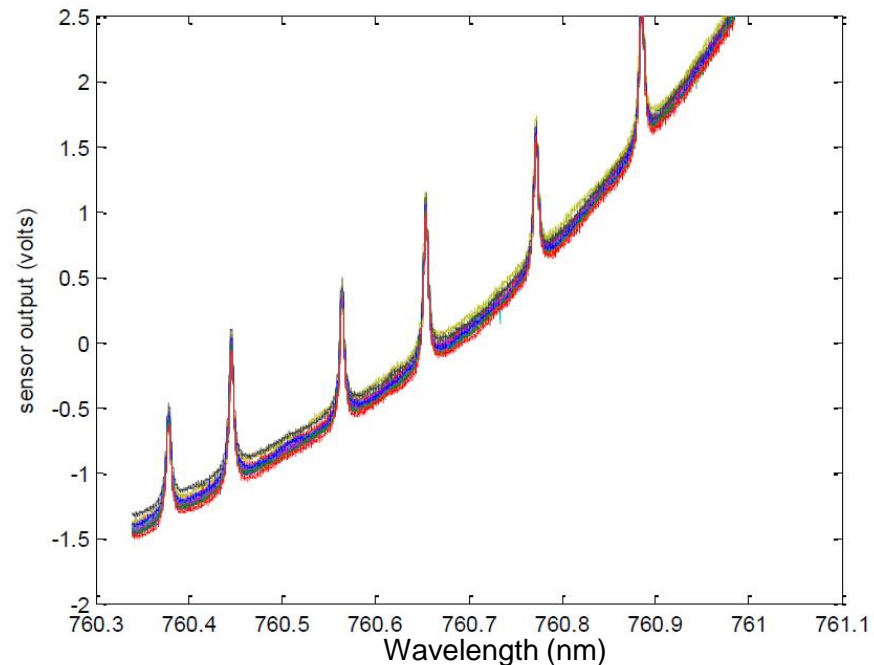
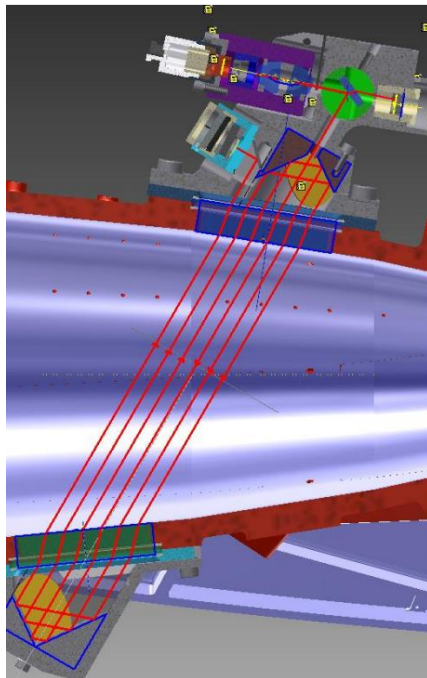


Intro to Absorption Spectroscopy in Nonequilibrium Hypersonic Flows



Craig Johansen, The University of Calgary, Canada

Sean O'Byrne, University of New South Wales
Canberra, Canberra, Australia



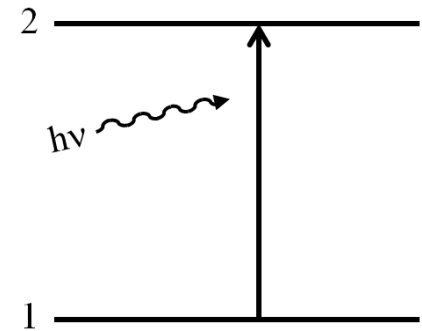
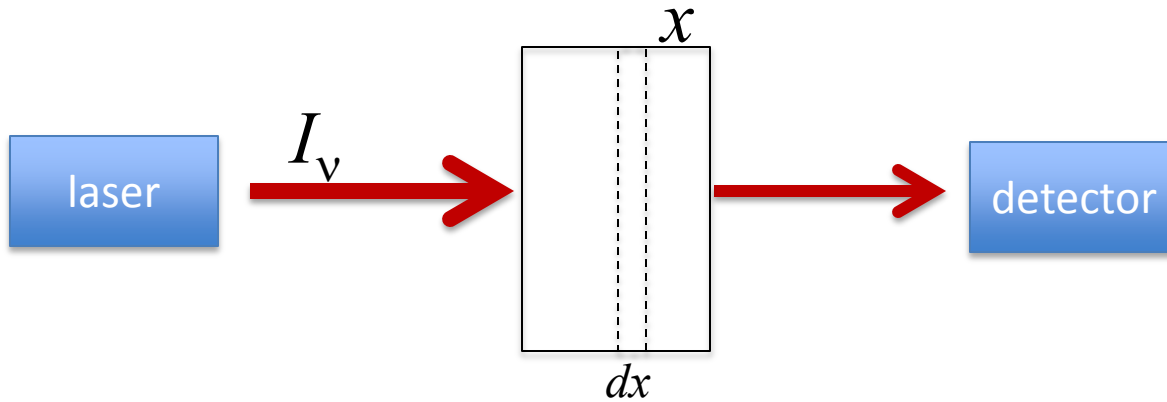
J. Kurtz, M. Aizengendler, Y. Krishna, and S. O'Byrne, S (2015) "Flight Test of a Rugged Scramjet-Inlet Temperature and Velocity Sensor," *AIAA SciTech*, 5-9 January, Kissimmee, Florida, USA.



Outline



- Introduction & Background
- Velocity measurement
- Temperature:
 - Translational
 - Rotational
 - Vibrational
- Tomography and Hyperspectral
- Flight Application



- Absorption is described by the Beer-Lambert Law:

$$-dI_\nu = I_\nu k_s(\nu) dx$$

where $k_s(\nu)$ is the spectral absorption coefficient.

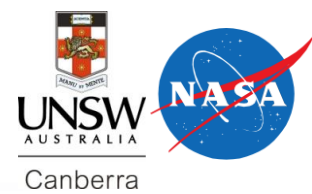
- This leads to exponential decay of laser intensity:

$$I_{\nu,x} = I_{\nu,0} e^{-k_s(\nu)x}$$

- Measure I_ν , know x , directly measure $k_s(\nu)$
- $k_s(\nu)$ contains information about temperature, concentration, velocity of gas



TDLAS: Strengths and Weaknesses



• Strengths

- Can probe non-luminous flows and ground-state populations
- Simple, rugged optical arrangements with no moving parts
- Comparatively inexpensive
- Fast wavelength scanning capability (wavelength agile)
- Can provide quantitative multi-parameter measurement with a single instrument
 - No systematic errors due to quenching

• Weaknesses

- Path-integrated technique
 - Distributions can be determined tomographically, but time consuming and analysis can be complex
- Spatial and temporal flow nonuniformity can produce bias errors in measurements unless the freestream is well characterized
- Some important diatomics (eg N_2) do not have a dipole moment and do not have a direct absorption spectrum



Broadening Mechanisms

- Spectral shape of $k_s(\nu)$ is from “broadening”
- Pressure (Homogeneous) Broadening

$$g_H = \frac{\Delta\nu_H}{2\pi} \frac{1}{(\nu - \nu_0)^2 + (\Delta\nu_H/2)^2}$$

- Caused by collisions with other atoms/molecules, a high-pressure effect causing a Lorentzian shape
- Generates a broadening

$$\Delta\nu_c = P \sum_i (\chi_i^2 \gamma_i)$$

and a shift in the transition

$$\Delta\nu_s = P \sum_i (\chi_i \delta_i)$$

P is the pressure

χ_i is the concentration

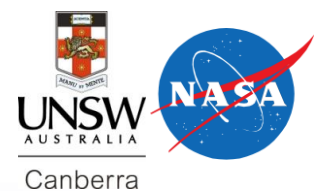
γ_i is collision width per unit pressure

δ_i is collision shift per unit pressure

If temperature can be independently determined, pressure can be measured from these quantities



Broadening Mechanisms



- Doppler (Inhomogeneous) Broadening
 - Due to thermal motion of absorbing particles towards or away from laser

$$g_D = \frac{2\sqrt{\ln 2}}{\pi^{1/2} \Delta \nu_D} e^{\left[\frac{-4(\ln 2)(\nu - \nu_0)}{\Delta \nu_D^2} \right]}$$

- $\Delta \nu_D$ is the full-width at half-maximum of the measured peak, and is given by

$$\Delta \nu_D = 2\nu_0 \sqrt{\frac{2kT_{trans}}{(MW)c^2} \ln 2}$$

ν_0 is the transition center
 k is the Boltzmann constant

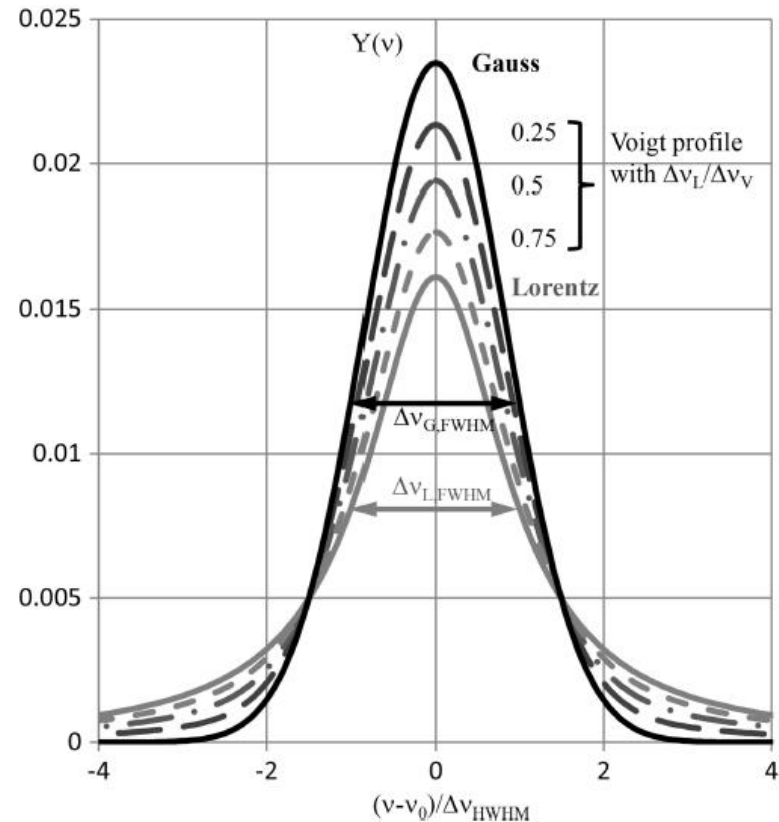


Voigt Profile

- The Voigt profile is a convolution of the two previous broadening effects

$$V(a, x) = \frac{a}{\pi} \int_{-\infty}^{\infty} \frac{e^{-y^2}}{a^2 + (x - y)^2} dy$$

$$a = \sqrt{\ln 2} \frac{\Delta v_H}{\Delta v_D}, \quad x = 2\sqrt{\ln 2} \frac{(v - v_0)}{\Delta v_D}$$





Laser Sources

- In 1970s, dye lasers were often used in visible and NIR absorption studies, and Pb salt for IR. Now mostly replaced with:
- Diode laser sources
 - **Distributed feedback (DFB) lasers**
 - Tune over ~ 0.1 nm
 - Robust and well tested in telecoms
 - Very spectrally narrow (1-30 MHz)
 - **Vertical cavity surface-emitting lasers (VCSELs)**
 - Tune over 1 nm
 - Tune very rapidly
 - Spectrally narrow (< 30 MHz)
 - **Quantum cascade lasers (QC)**
 - High-power pulsed source operating in the IR

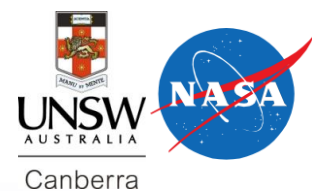


Detection Schemes

- **Direct absorption**
 - Simple, direct measurements, but poor use of dynamic range
- **Difference amplification**
 - Removes intensity modulation, but only when perfectly balanced
- **Log-ratio detection**
 - Simple circuit, and cancels common-mode electronic and laser noise very efficiently
 - Can be autobalanced, to remove offset caused by mismatch in reference and signal intensities
 - M.G. Allen *et al.* *Applied Optics* 34.18 (1995): 3240-3249
 - Bandwidth decreases as photocurrent decreases



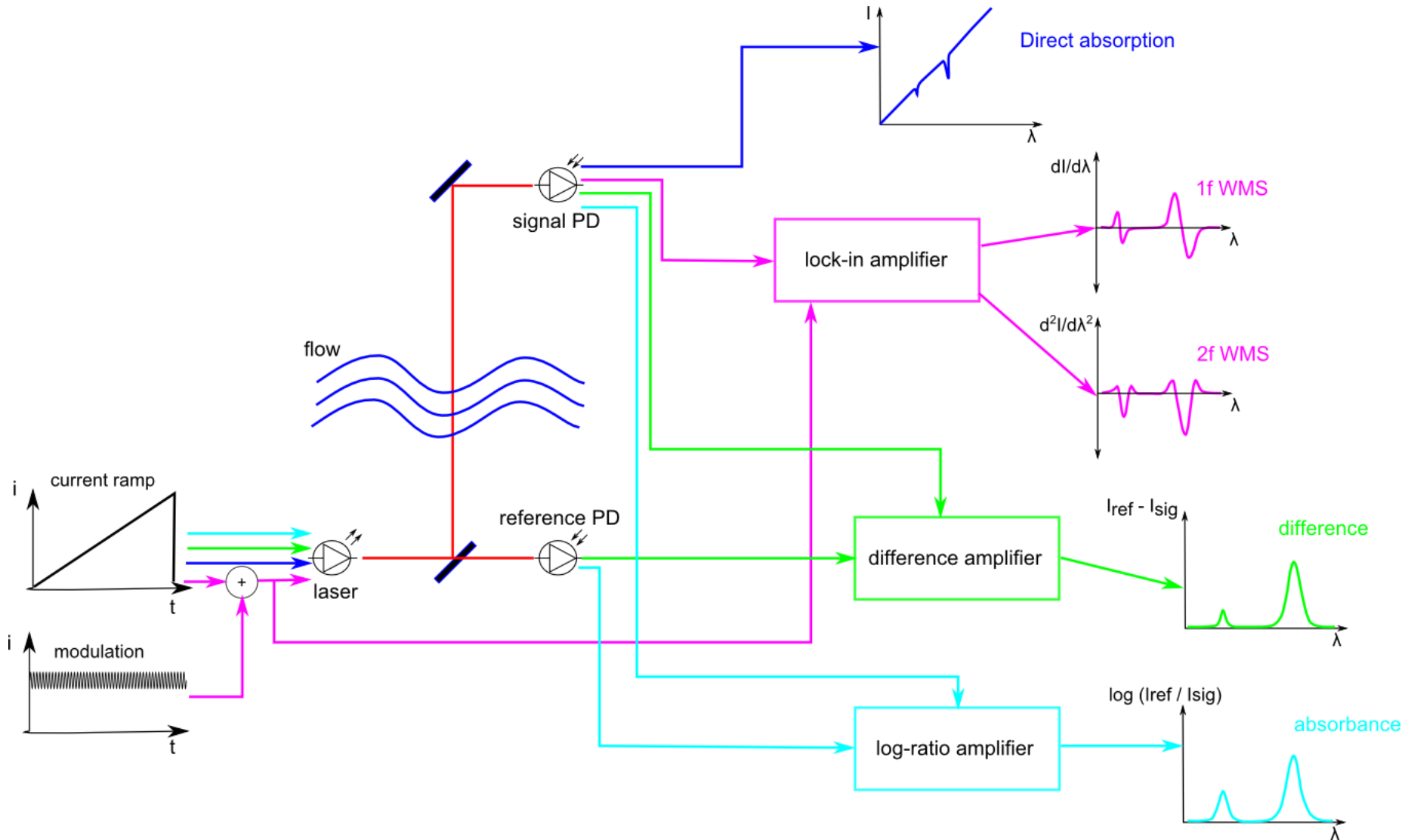
Detection Schemes



- **Wavelength modulation**
 - Removes DC offset from signal
 - Signal proportional to the derivative of the input intensity
 - Phase-sensitive detection at a multiple of the modulation frequency can reduce $1/f$ noise in the signal
 - Traditionally required careful calibration to samples under controlled conditions, but recent innovation using the ratio of second-harmonic ($2f$) and first-harmonic ($1f$) signals to account for the laser intensity
 - GB Rieker *et al. Appl. Opt.* 48.29 (2009): 5546-5560.
- **Cavity-based methods**
 - Useful for measurements of trace quantities, but practical challenges in hostile environments.



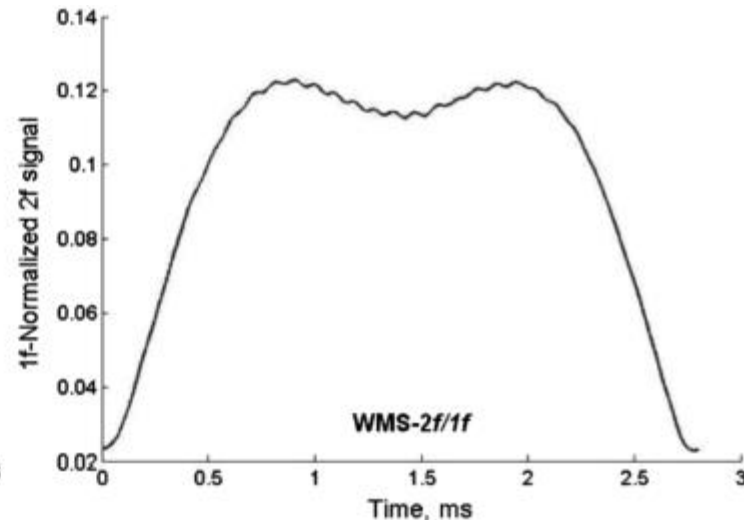
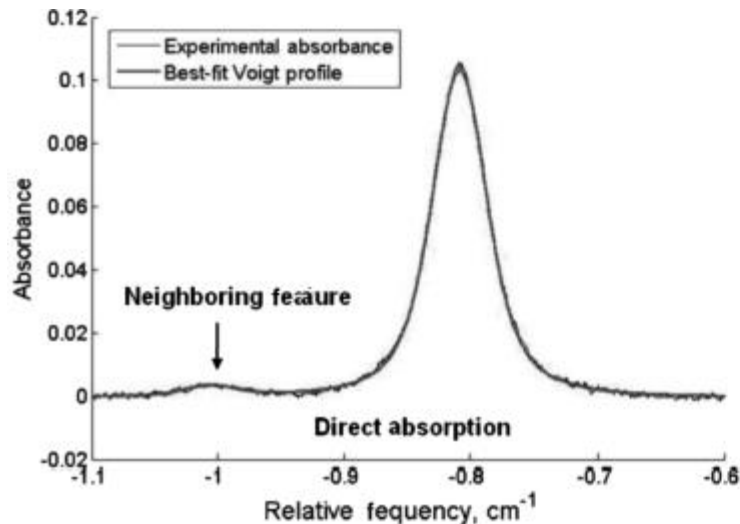
Detection Schemes





Detection Schemes

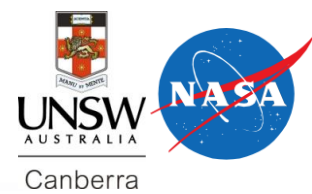
- *E.g. Goldenstein et al.*
 - Measured spectra of water vapor in UVa scramjet test facility
 - Small amplitude of second feature limits signal-to-noise ratio for direct absorption
 - $2f/1f$ ratio measurement provided consistently better signal-to-noise ratios, but both methods consistent with computational predictions



C.S. Goldenstein, I.A. Schultz, J.B. Jeffries and R.K. Hanson “Tunable Diode Laser Absorption Sensor for Measurements of Temperature and Water Concentration in Supersonic Flows,” 49th AIAA Aerospace Sciences Meeting including the New Horizons Forum and Aerospace Exposition, Orlando FL, Jan 4–7, 2011, AIAA Paper 2011–1094.



Detection Schemes

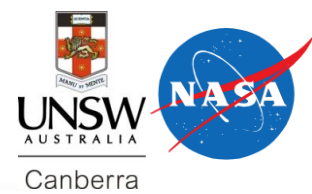


Operation Mode	Expected Value	DA	WMS
11% Steam	700–1000 K	776 ± 10 K	742 ± 9 K
(Combustor Entrance)	$11.4 \pm 0.2\%$ H ₂ O	$10.9 \pm 0.1\%$ H ₂ O	$10.8 \pm 0.1\%$ H ₂ O
9% Steam	700–1000 K	860 ± 30 K	831 ± 9 K
(Exit Plane)	$9 \pm 0.2\%$ H ₂ O	$9.1 \pm 0.2\%$ H ₂ O	$9.1 \pm 0.1\%$ H ₂ O
12% Steam	700–1000 K	875 ± 50 K	850 ± 6 K
(Exit Plane)	$12 \pm 0.2\%$ H ₂ O	$12.1 \pm 0.5\%$ H ₂ O	$11.5 \pm 0.1\%$ H ₂ O
H ₂ -Air Combustion $\varphi = 0.33$	1800–2200 K	1802 ± 94 K	1765 ± 41 K
(Exit Plane)	13% H ₂ O	$12.8 \pm 0.5\%$ H ₂ O	$13.3 \pm 0.3\%$ H ₂ O

C.S. Goldenstein, I.A. Schultz, J.B. Jeffries and R.K. Hanson “Tunable Diode Laser Absorption Sensor for Measurements of Temperature and Water Concentration in Supersonic Flows,” 49th AIAA Aerospace Sciences Meeting including the New Horizons Forum and Aerospace Exposition, Orlando FL, Jan 4–7, 2011, AIAA Paper 2011–1094.



Velocity Measurements



- Simplest quantity to measure in a high-speed flow
 - Measured through Doppler shift between beams with velocity components in two different directions relative to the flow

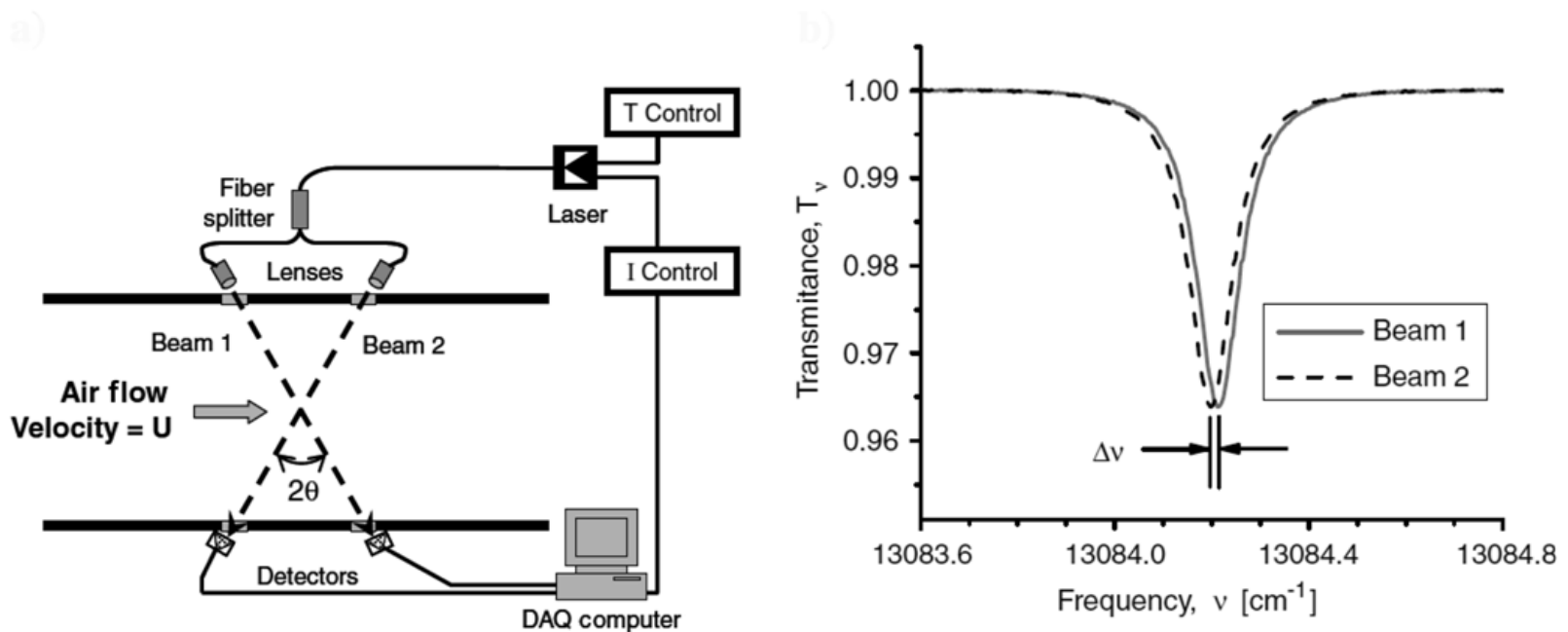
$$U = \frac{c \Delta \nu_{Dopp}}{\nu_{Source}}$$

- Shift in the peak position relatively insensitive to amplitude noise.
- Shift typically calibrated to etalon measurements



Velocity Measurements

- *E.g. Lyle et al.*, mass flux sensor based on measurements of density and velocity using oxygen A-band near 760-nm.
- Measured speed with time-averaged precision of 0.25 m/s.



K. H. Lyle, J. B. Jeffries and R. K. Hanson "Diode-laser Sensor for Air-mass flux 1: Design and Wind Tunnel Validation," AIAA Journal, 45 (9), 2204–2212, 2007.



Translational Temperature

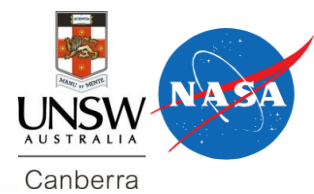
- Can be determined through the Doppler width, but as $T_{trans} \propto \left(\frac{\Delta v_D}{v_0}\right)^2$, small errors in Doppler width have a significant effect on T

$$\frac{\Delta T}{T} = \frac{2\Delta(\Delta v_D)}{\Delta v_D}$$

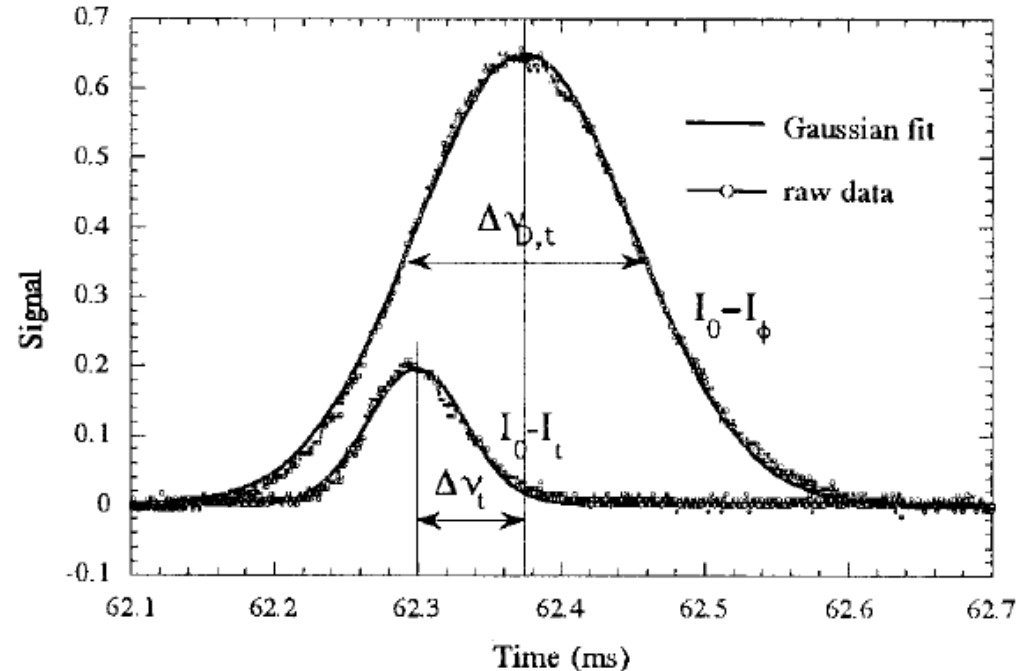
- *E.g.* An uncertainty in width measurement of 1.5% for a Doppler-broadened transition in the oxygen A-band will cause an uncertainty of 3% in temperature
- Uncertainty further increased in the presence of pressure broadening
- Measuring T through linewidth has the advantage of only requiring 1 transition for a measurement



Translational Temperature



- *E.g.* Measurements of temperature in an arcjet facility using an AR I line at 811.531 nm
- 12% uncertainty in width translated to 30% uncertainty in T_{trans} over 2000–1000 K

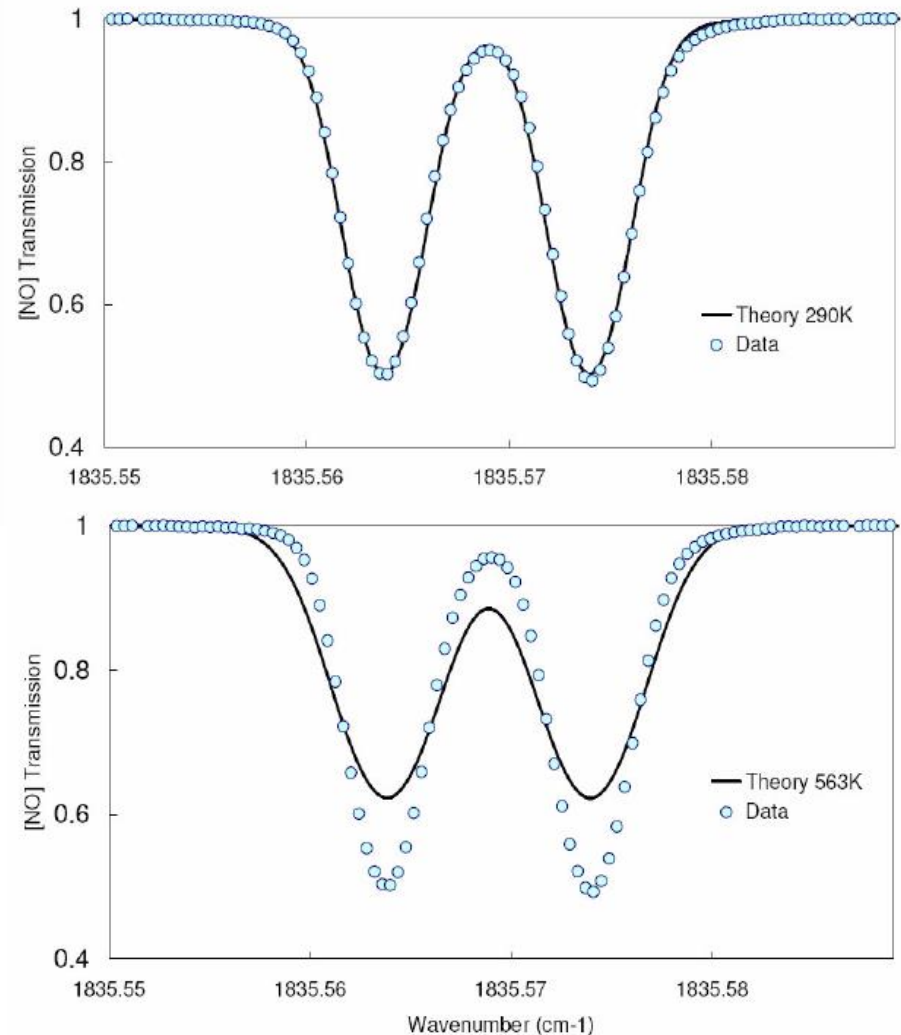


F-Y Zhang, K Komurasaki, T Iida, and T Fujiwara, "Diagnostics of an Argon Arcjet Plume with a Diode Laser," Applied Optics, 38 (9), pp. 1814–1822, 1999.



Translational Temperature

- *E.g.* Measurements of NO translational temperature at 5.44 μm in the LENS I facility, using direct absorption
- Fit temperature of 290 K significantly different to the predicted temperature of 563K



R. A. Parker, T. Wakeman, M. MacLean, and M. Holden, "Measuring Nitric Oxide Freestream Concentration using Quantum Cascade Lasers at CUBRC," 44th AIAA Aerospace Sciences Meeting and Exhibit, AIAA Paper 2006-926, 2006.



Rotational Temperature

- Typically measured using the ratio of integrated absorbance a over two lines with different linestrength variations with T

$$a_j = P\chi_iLS_j$$

- for transition j of an absorbing species i
- L is the path length and S_j is the linestrength of the transition
- All quantities other than S_j are common to the two lines and divide out

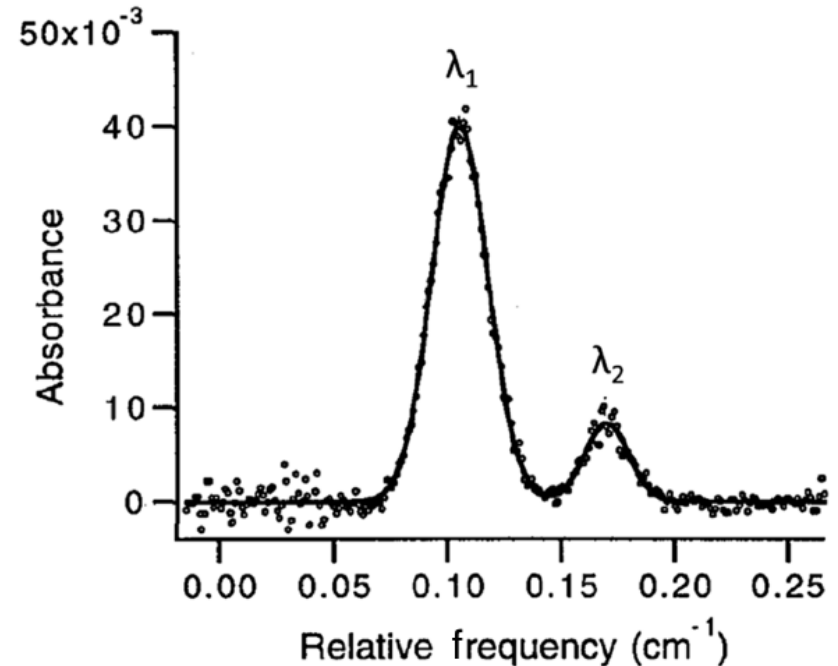
$$\frac{a_1}{a_2} = \frac{S_1}{S_2} = \frac{S_1(T_0)}{S_2(T_0)} e^{-\frac{hc\Delta E_{rot}}{k} \left(\frac{1}{T_{rot}} - \frac{1}{T_0} \right)}$$

R. A. Parker, T. Wakeman, M. MacLean, and M. Holden, "Measuring Nitric Oxide Freestream Concentration using Quantum Cascade Lasers at CUBRC," 44th AIAA Aerospace Sciences Meeting and Exhibit, AIAA Paper 2006-926, 2006.



Rotational Temperature

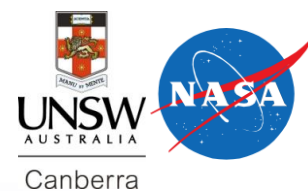
- *E.g. Wehe et al.* measured H₂O rotational and translational temperature in the 10 MJ/kg Calspan 96-inch hypersonic shock tunnel freestream
- $\nu_1 + \nu_3$ band near 1396 nm (λ_2) and 1400 nm (λ_1)
- 8 kHz scan rate
- T_{rot} uncertainty of $\pm 2.3\%$ compared with T_{trans} uncertainty of $\pm 2.7\%$ and $\pm 6.4\%$ for the T_{trans} measurements on the two lines



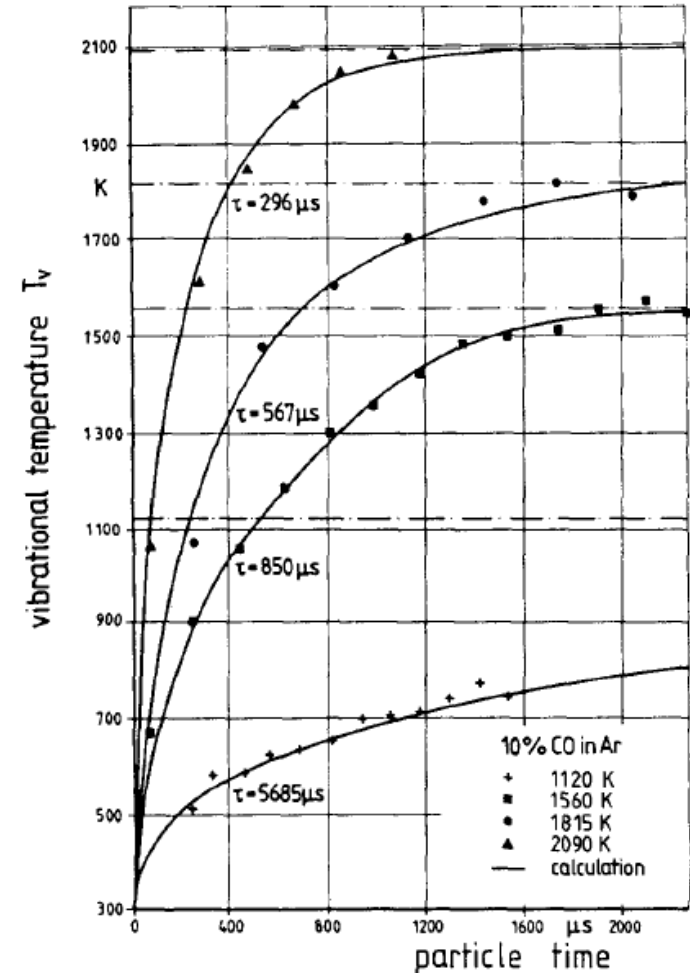
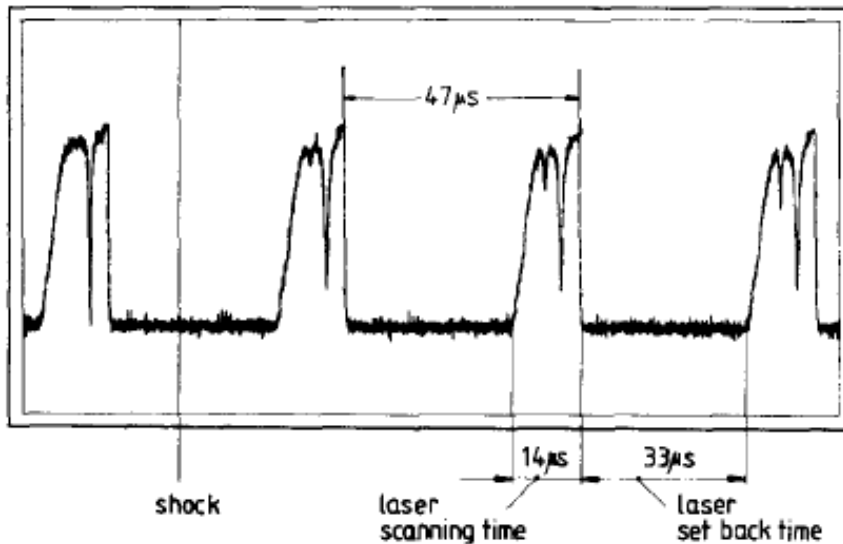
S. Wehe, D. S. Baer, and R. K. Hanson "Tunable Diode-laser Absorption Measurements of Temperature, Velocity, and H₂O in Hypervelocity Flows," 33rd Joint Propulsion Conference and Exhibit, Seattle, WA, AIAA Paper 97-3267, 1997.



Vibrational Temperature



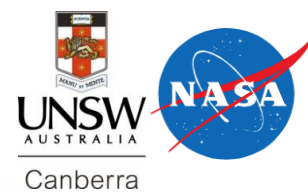
- *E.g. Brandt and Roth* measured T_{vib} and T_{trans} in CO in a reflected shock tube, using a lead salt laser operating at $2100\text{--}2200\text{ cm}^{-1}$, at 20 kHz scan rate.



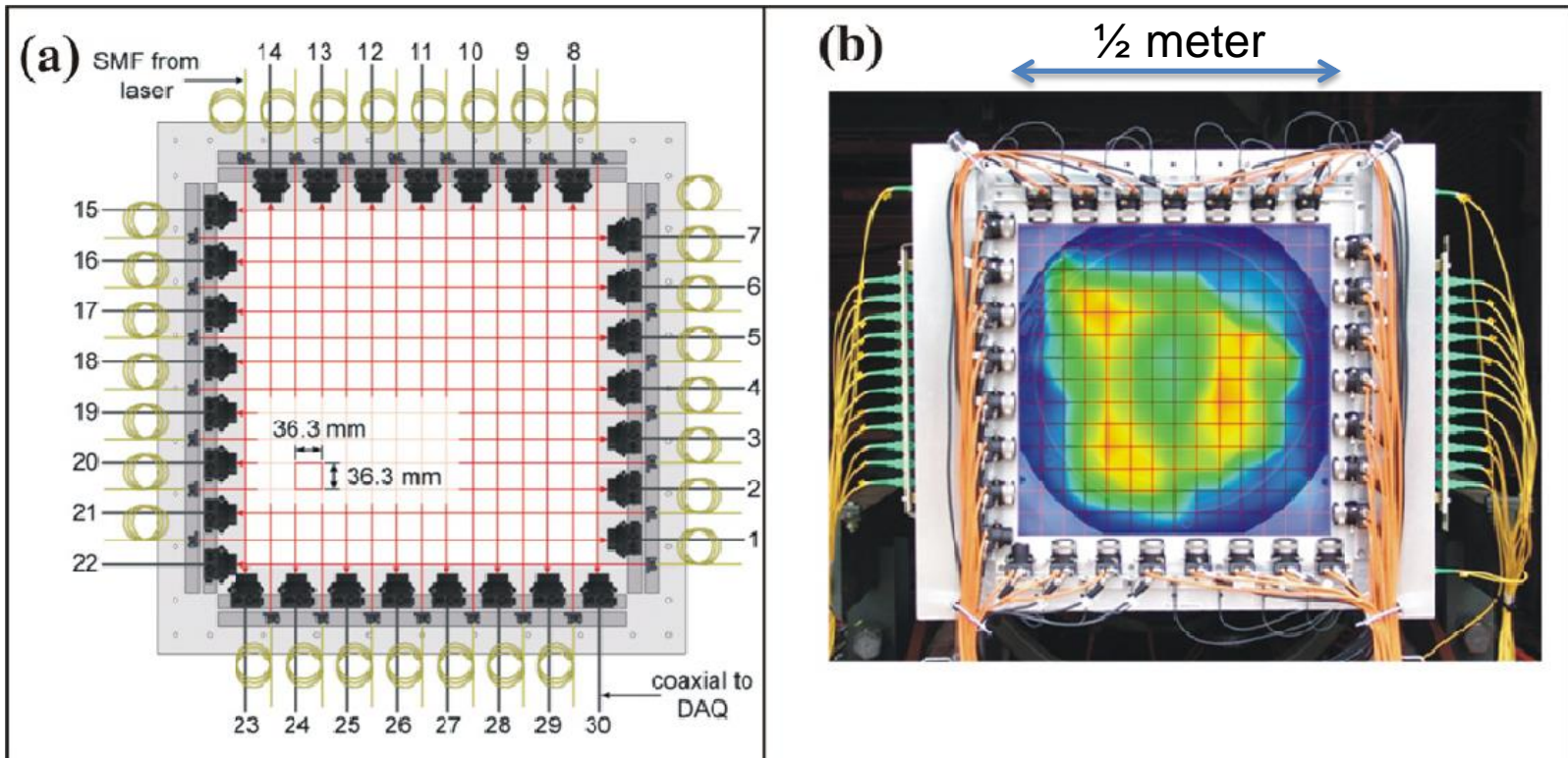
O. Brandt, and P. Roth, "Temperature Measurements behind Shock Waves using a Rapid Scanning IR-diode Laser," *Physics of Fluids*, Vol. 30, No. 5, pp. 1294–1298., 1987.



TDLAS Tomography



- Major limitation of TDLAS: path-averaged
 - Can do tomography



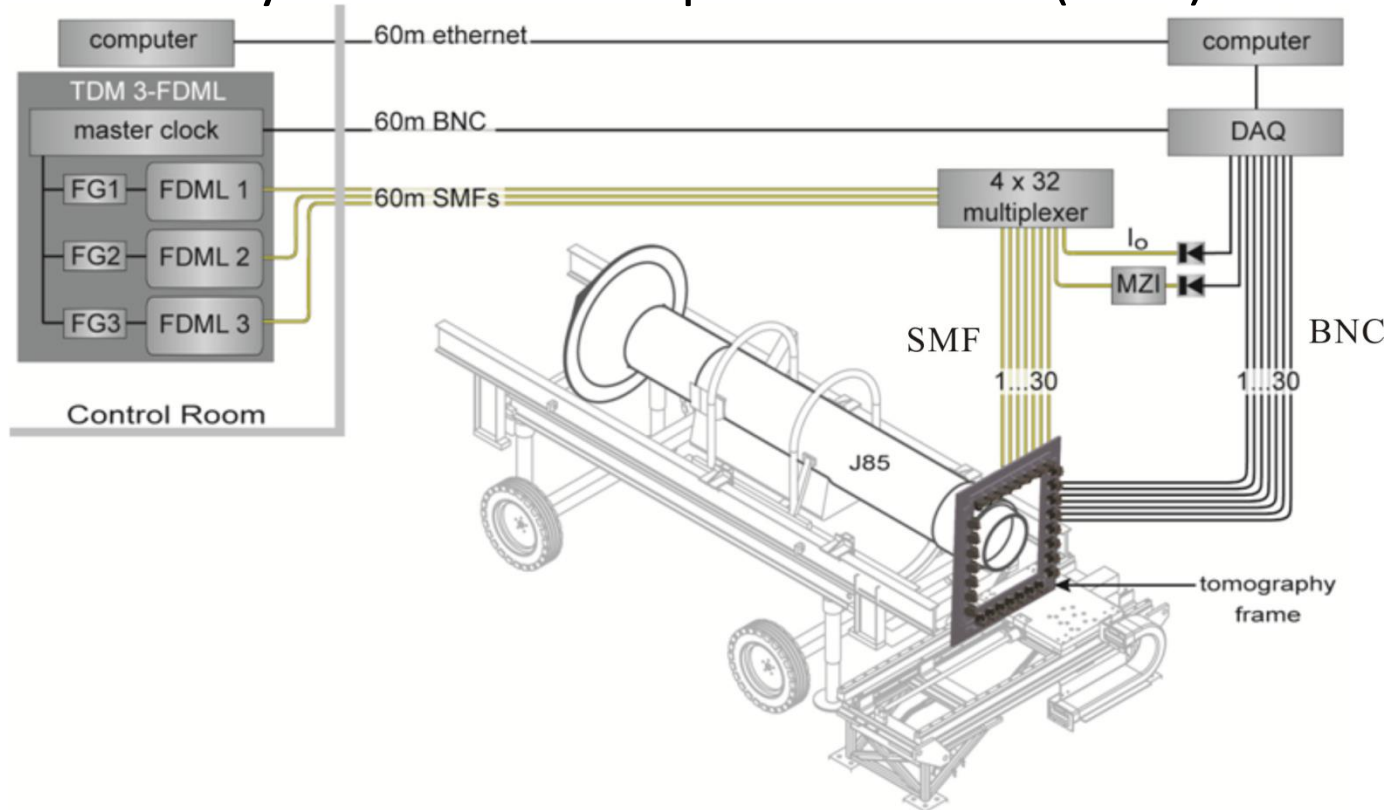
– 15x15 grid provides data at 225 points (36 mm grid)

L. Ma, X. Li, S. T. Sanders, A. W. Caswell, S. Roy, D. H. Plemmons, and J. R. Gord, "50-kHz-rate 2D imaging of temperature and H₂O concentration at the exhaust plane of a J85 engine using hyperspectral tomography," *Optics Express*, Vol. 21, Issue 1, pp. 1152-1162, 2013



TDLAS Tomography

- General Electric J85 gas turbine engine
 - University of Tennessee Space Institute (UTSI)

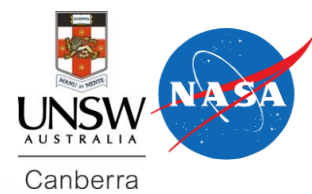


- Measure water and temperature at 50 kHz rate

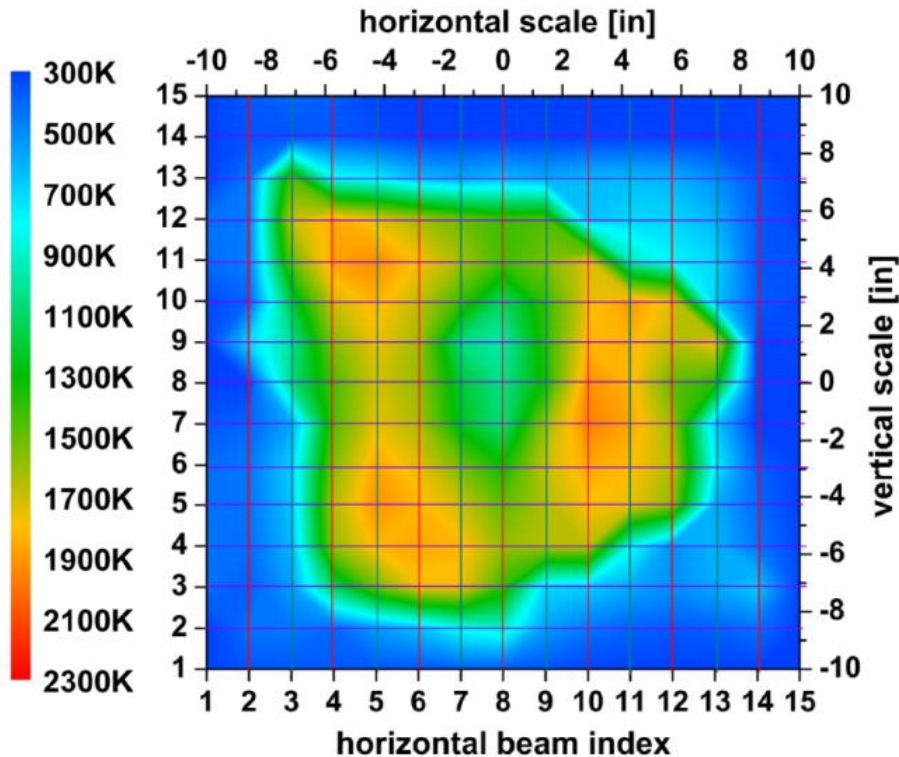
L. Ma, X. Li, S. T. Sanders, A. W. Caswell, S. Roy, D. H. Plemmons, and J. R. Gord, "50-kHz-rate 2D imaging of temperature and H₂O concentration at the exhaust plane of a J85 engine using hyperspectral tomography," *Optics Express*, Vol. 21, Issue 1, pp. 1152-1162, 2013



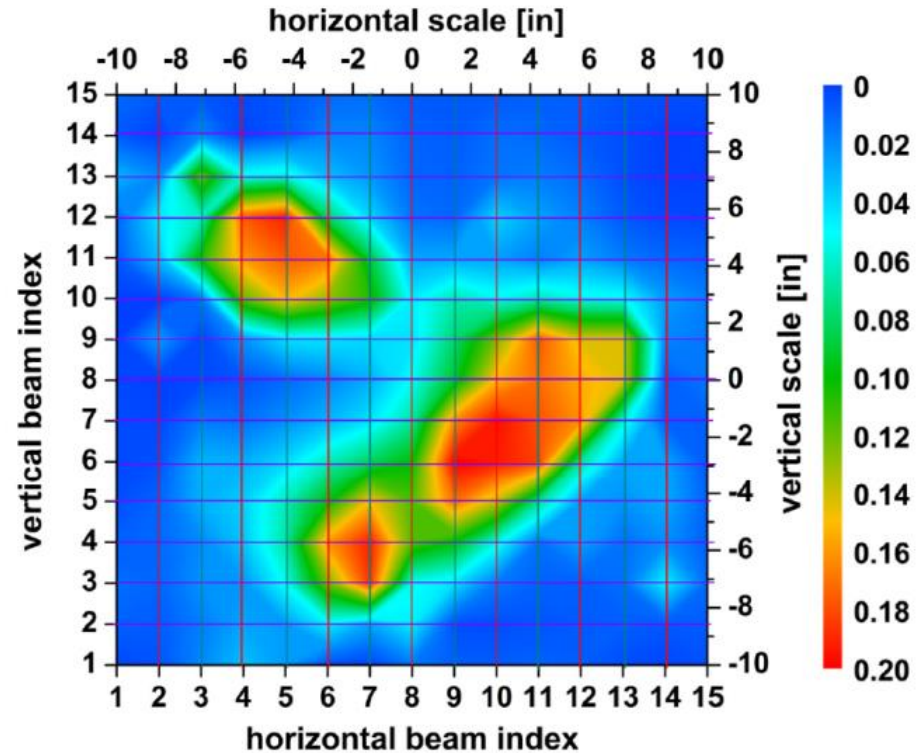
TDLAS Tomography Results



Temperature



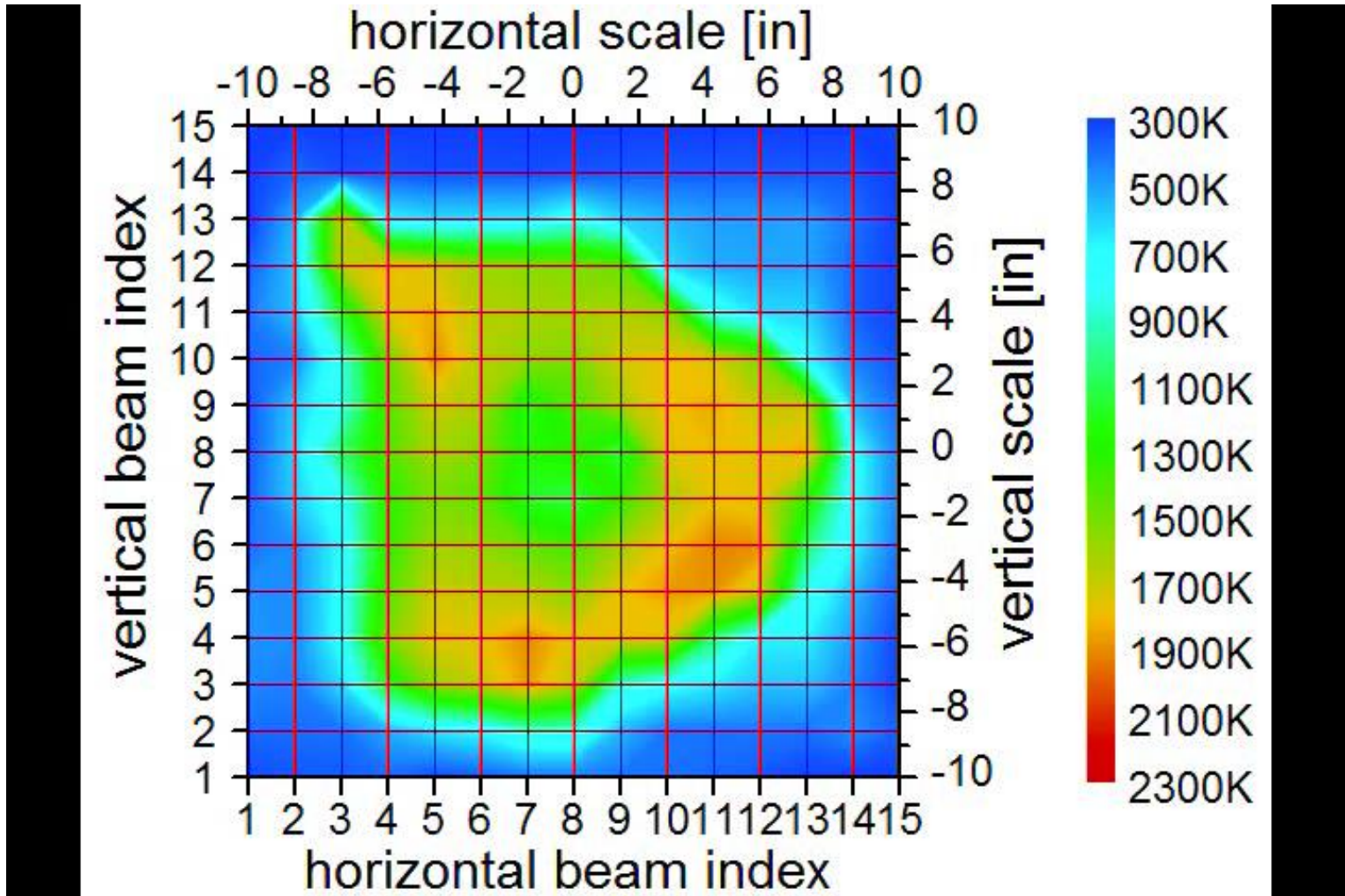
Water Vapor



- Measurement is over ~ 0.5 meter square
 - Time resolution is $20 \mu\text{sec}$ (50 kHz)
 - Spatial resolution is ~ 36 mm



TDLAS Tomography Results

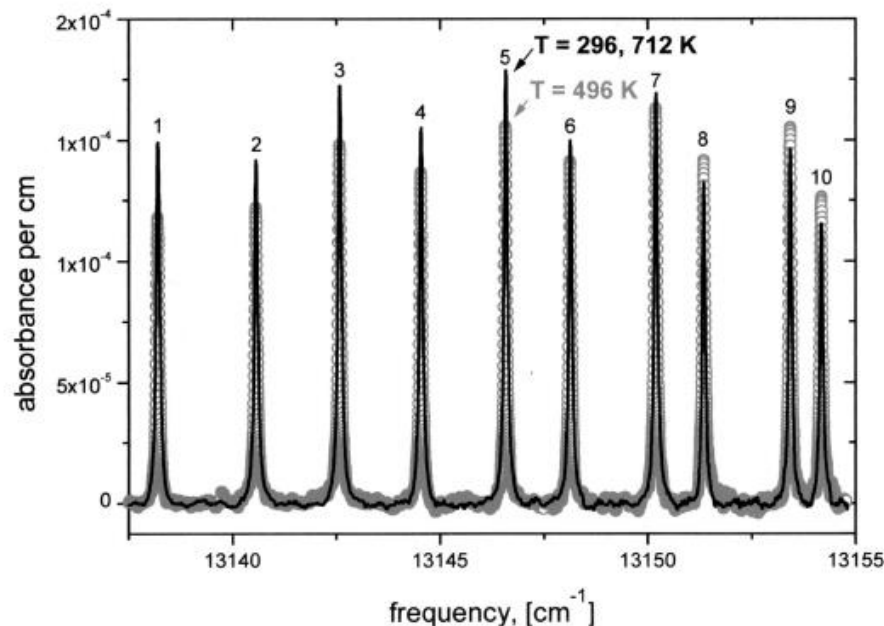


L. Ma, X. Li, S. T. Sanders, A. W. Caswell, S. Roy, D. H. Plemmons, and J. R. Gord, "50-kHz-rate 2D imaging of temperature and H₂O concentration at the exhaust plane of a J85 engine using hyperspectral tomography," *Optics Express*, Vol. 21, Issue 1, pp. 1152-1162, 2013



Using Spectral Information

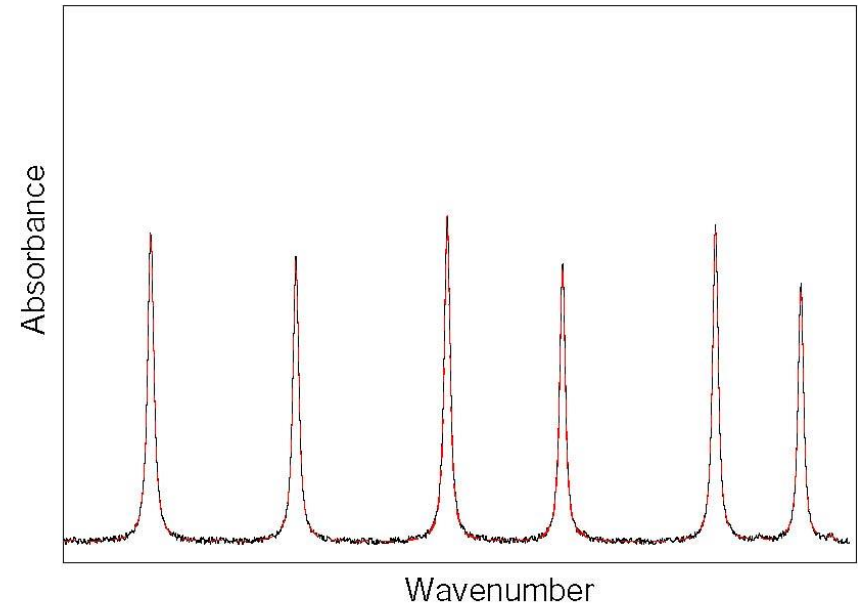
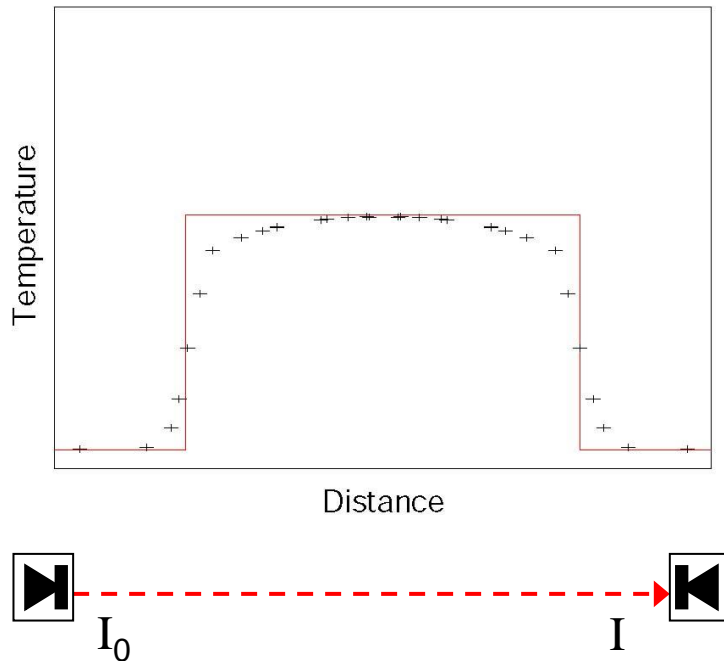
- Many hypersonic environments (flight vehicles, test facilities) have limited optical access for tomography
 - Can use spectral information to infer spatial variations of temperature.



S.T. Sanders, J. Wang, J.B. Jeffries, and R. K. Hanson. "Diode-laser absorption sensor for line-of-sight gas temperature distributions." *Applied Optics* 40,(24) 4404-4415., 2001.

Extracting Line-of-Sight Temperatures

- Example: Temperature in a tube furnace using a single VCSEL line of sight
 - The 'distribution technique' assumes *a priori* knowledge of the distribution shape.



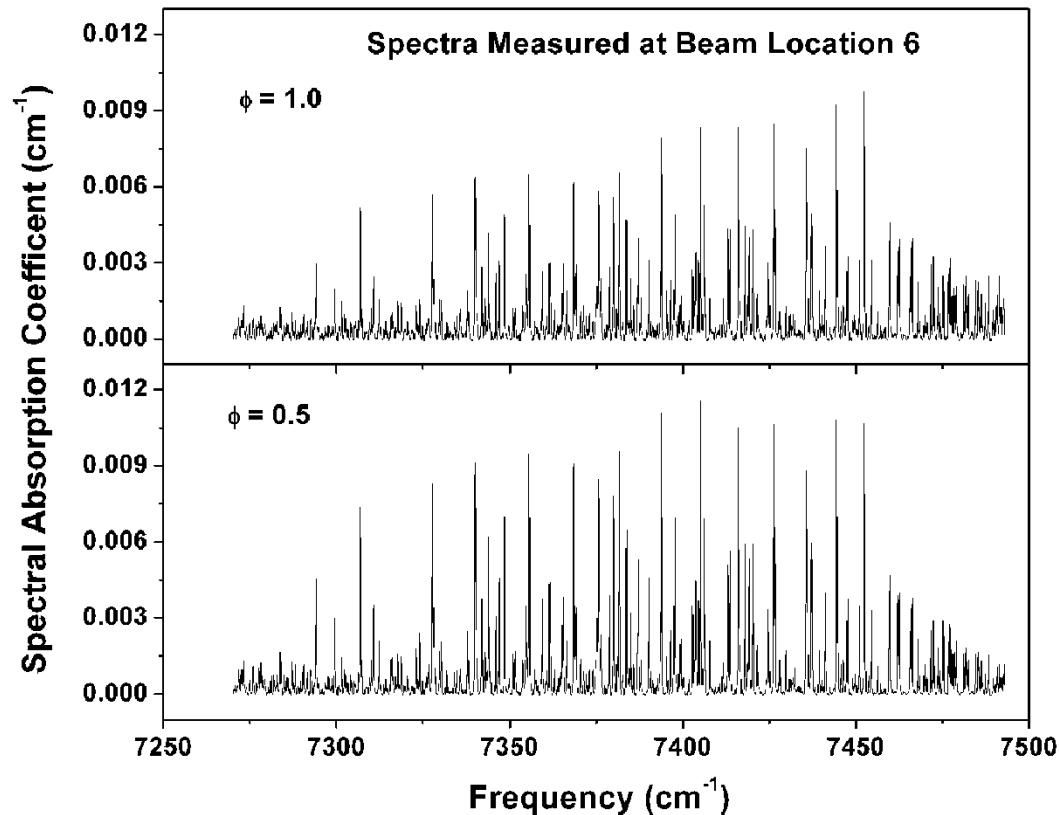
'experimental' spectrum —
theoretical spectrum - - -

L. C. Webster, S. O'Byrne, A. F. P. Houwing, "Determination of Temperature Distributions in Air using a Scanning Vertical Cavity Surface-Emitting Laser," *Proc. 4th Australian Conference on Laser Diagnostics in Fluid Mechanics and Combustion*, Adelaide, Australia, 2005.



TDLAS Hyperspectral Tomography

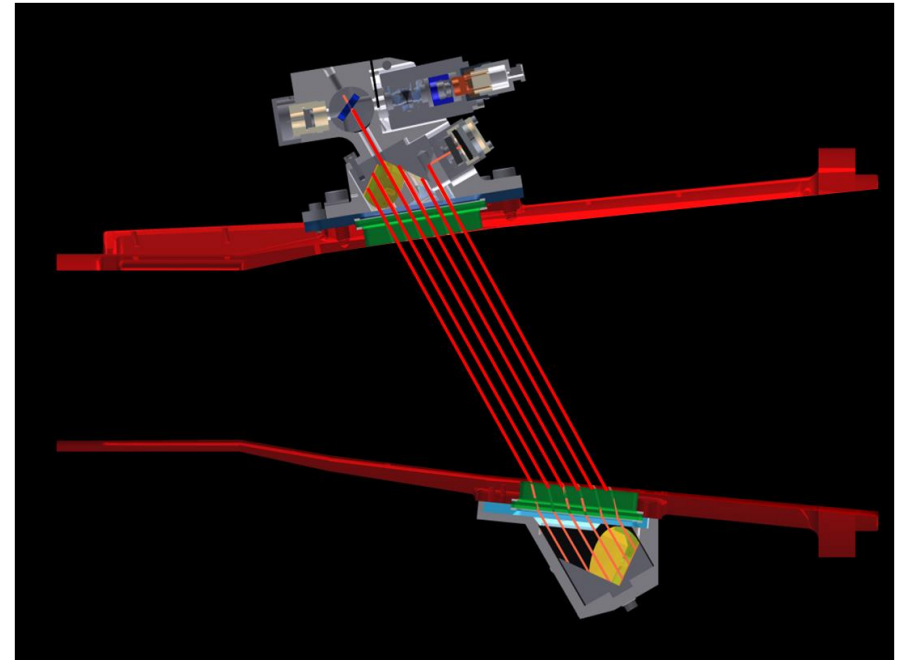
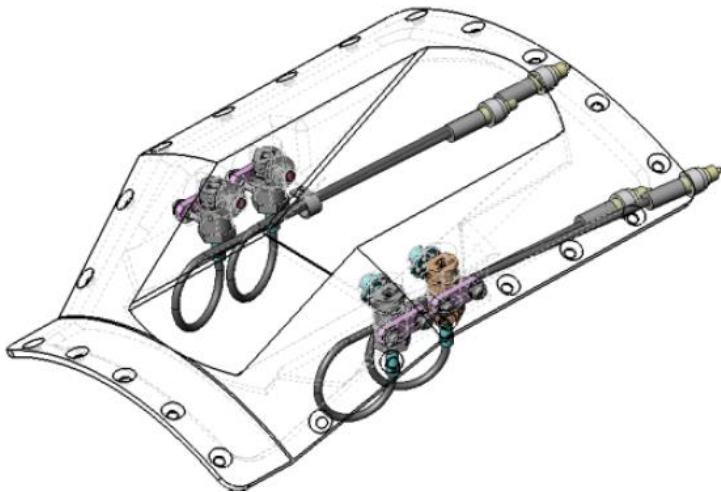
- Using hyperspectral sources, can gain spectral images over many lines, reducing number of projections



L. Ma, W. Cai, A. W. Caswell, T. Kraetschmer, S. T. Sanders, S. Roy, and J. R. Gord, "Tomographic imaging of temperature and chemical species based on hyperspectral absorption spectroscopy," *Optics Express* 17(10), 8602–8613, 2009.

Flight-Testing TDLAS Systems

- Small size and power requirements have allowed TDLAS systems to be used in hypersonic flight tests

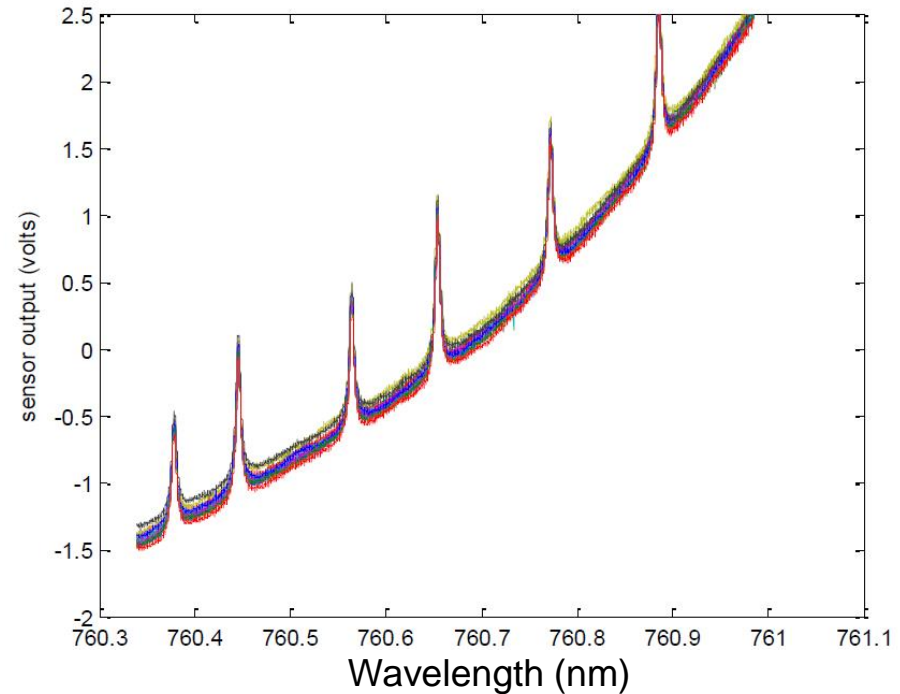
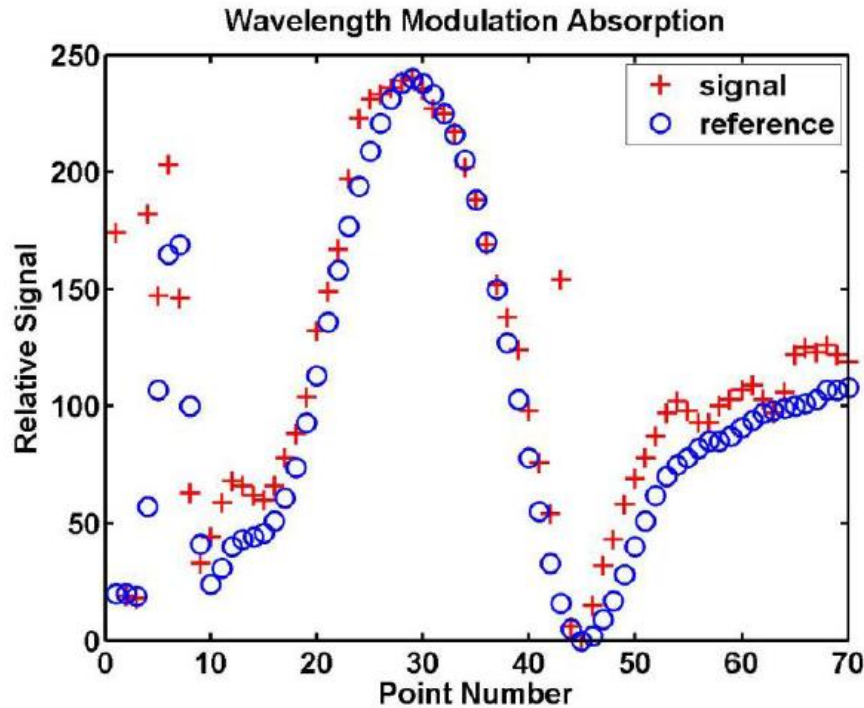
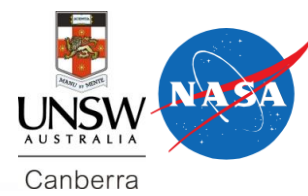


T. Barhorst and S. Williams, "Development of an In-Flight Non-Intrusive Mass Capture System," *45th AIAA/ASME/SAE/ASEE Joint Propulsion Conference & Exhibit*. AIAA, Denver, Colorado, USA, 2009.

J. Kurtz, M. Aizengendler, Y. Krishna, and S. O'Byrne, S (2015) "Flight Test of a Rugged Scramjet-Inlet Temperature and Velocity Sensor," *AIAA SciTech*, 5-9 January, Kissimee, Florida, USA.



Flight-Testing TDLAS Systems



M. S. Brown, and T.F. Barhorst. "Post-flight analysis of the diode-laser-based mass capture experiment onboard HIFiRE flight 1." In *Proceedings of 17th AIAA International Space Planes and Hypersonic Systems and Technologies Conference paper AIAA-2011-2359*. 2011.

J. Kurtz, M. Aizengendler, Y. Krishna, and S. O'Byrne, S (2015) "Flight Test of a Rugged Scramjet-Inlet Temperature and Velocity Sensor," *AIAA SciTech*, 5-9 January, Kissimee, Florida, USA.



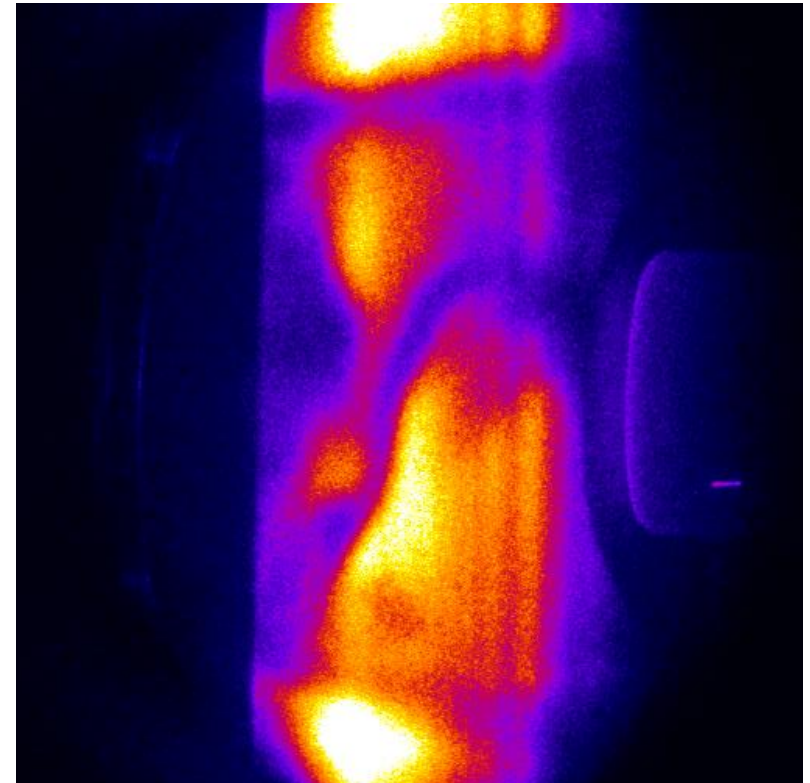
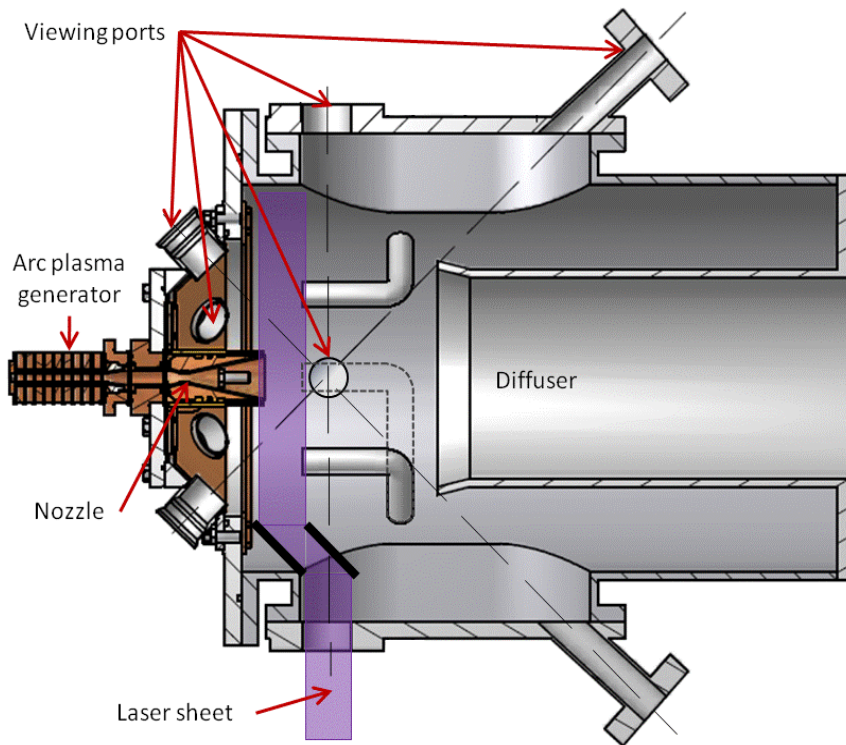
Conclusions

- TDLAS is a reliable and well established nonintrusive measurement technique, capable of precise path-averaged measurements of velocity, density and trans/rot/vib temperatures
- Availability of telecoms lasers and detectors makes it comparatively economical
- Path-averaging disadvantages can be mitigated using tomography or additional spectral information
- Particularly valuable for flight-test applications and time-resolved online facility monitoring
- Rapid development in mid-IR sources and detectors will significantly expand applications



Intro to Planar Laser-Induced Fluorescence for Hypersonic Nonequilibrium Flows

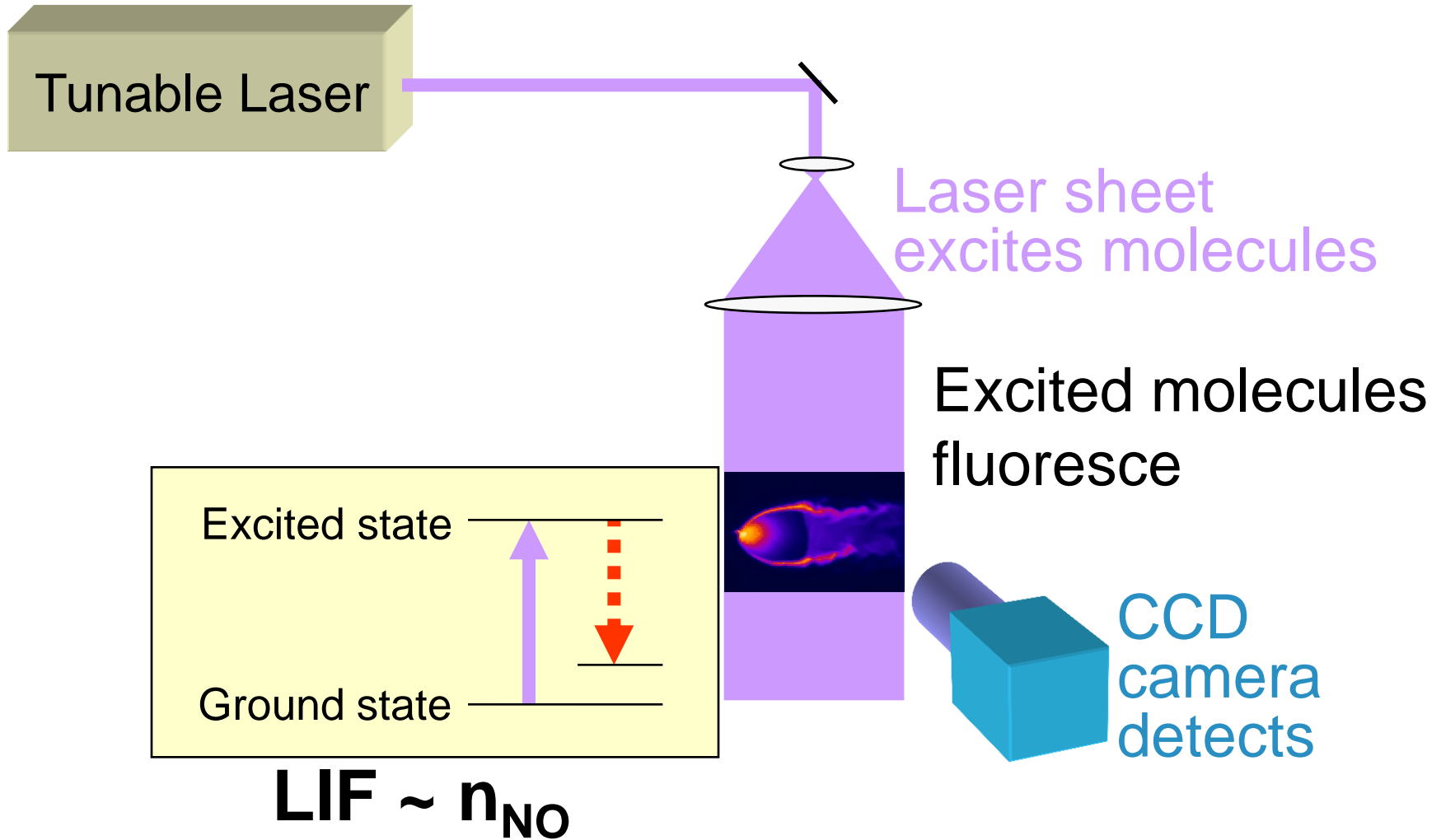
Brett Bathel, NASA Langley Research Center, Virginia, USA
Paul Danehy, NASA Langley Research Center, Virginia, USA
Craig Johansen, The University of Calgary, Canada



Figures from Inman, J., Bathel, B., Johansen, C., Danehy, P., Jones, S., Gragg, J., and Splinter, S., (2013) "Nitric oxide planar laser-induced fluorescence measurements in the Hypersonic Materials Environment Test System," *AIAA Journal*, Vol. 51, No. 10, pp. 2365-2379



Planar Laser-Induced Fluorescence (PLIF)





PLIF can probe nonequilibrium



- Commonly used in equilibrium environments
- Useful probe for thermal non-equilibrium:
 - Translational temperature
 - Rotational temperature
 - Vibrational temperature (often $T_{vib} \neq T_{rot} \approx T_{tran}$)
 - Species specific:
 - Different species can have different temperatures (especially vibrational temperatures)
- Can measure, quantify species in chemical non-equilibrium (eg. NO in shock tunnels)



LIF Theory (Two-Level Model)



2 Energy of absorbing species at excited state (2)

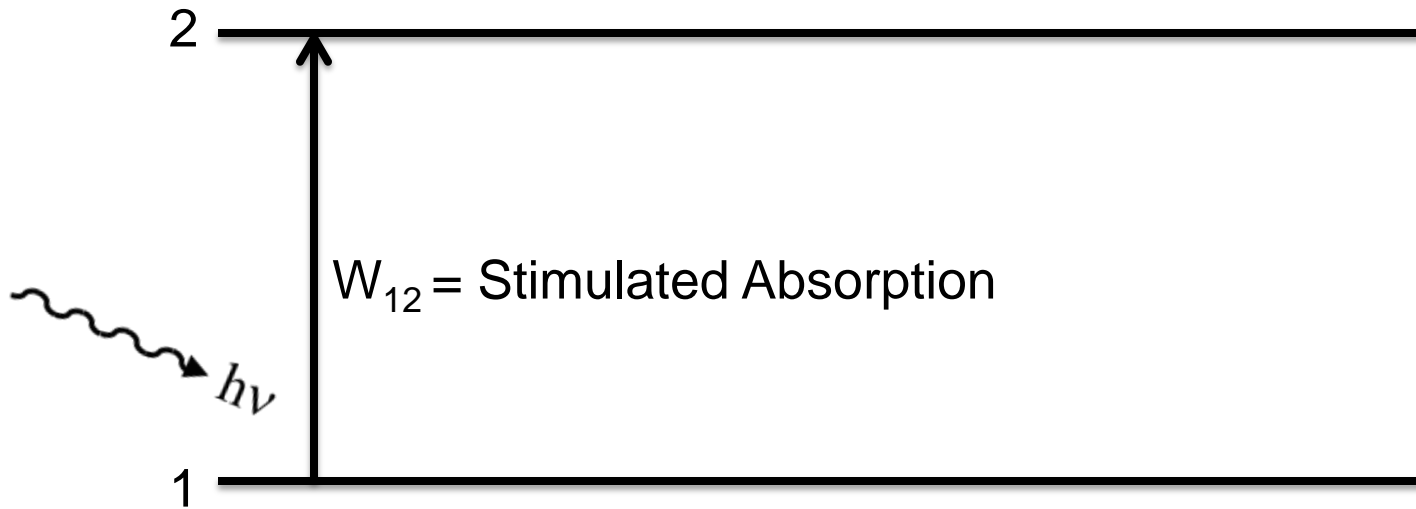
1 Energy of absorbing species at ground state (1)

Assumptions:

- A. There are only two important states to consider (ground state and excited state). Other levels (rotational and vibrational) are ignored.
- B. Prior to excitation, population of absorbers in excited state is negligible ($N_2=0$)



Two-Level Model Theory



An incident photon from the light source (e.g. laser) is absorbed and sends some of the ground state population to the excited state

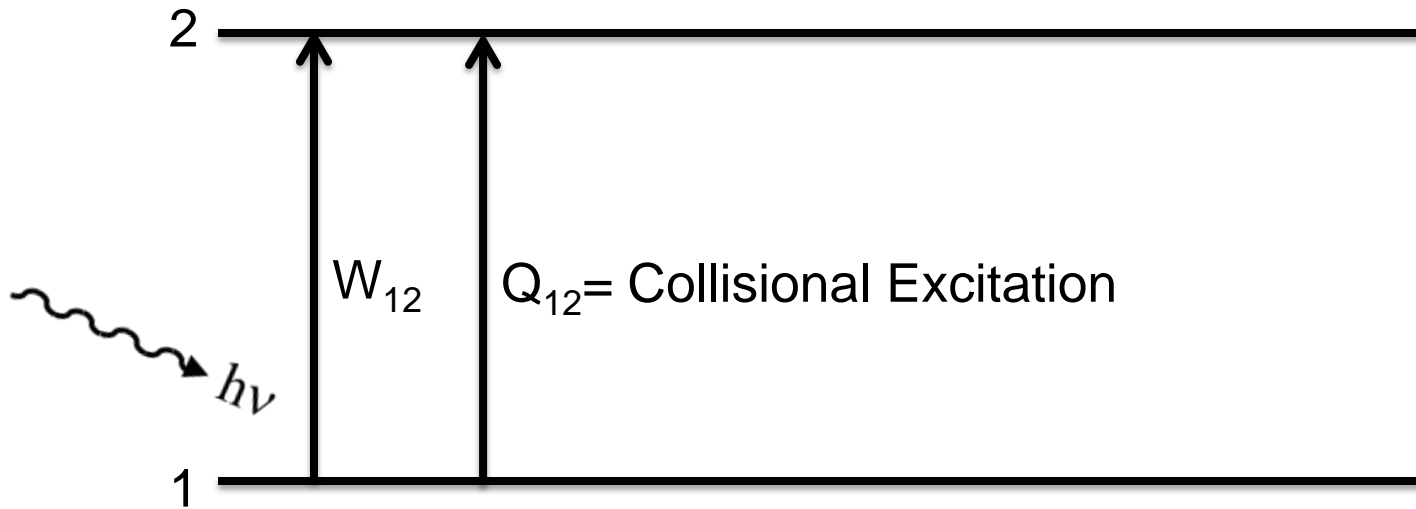
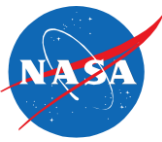
$$\frac{dN_1}{dt} = -N_1 W_{12}$$

$$\frac{dN_2}{dt} = N_1 W_{12}$$

Population rate equations
(incomplete at this point)



Two-Level Model Theory



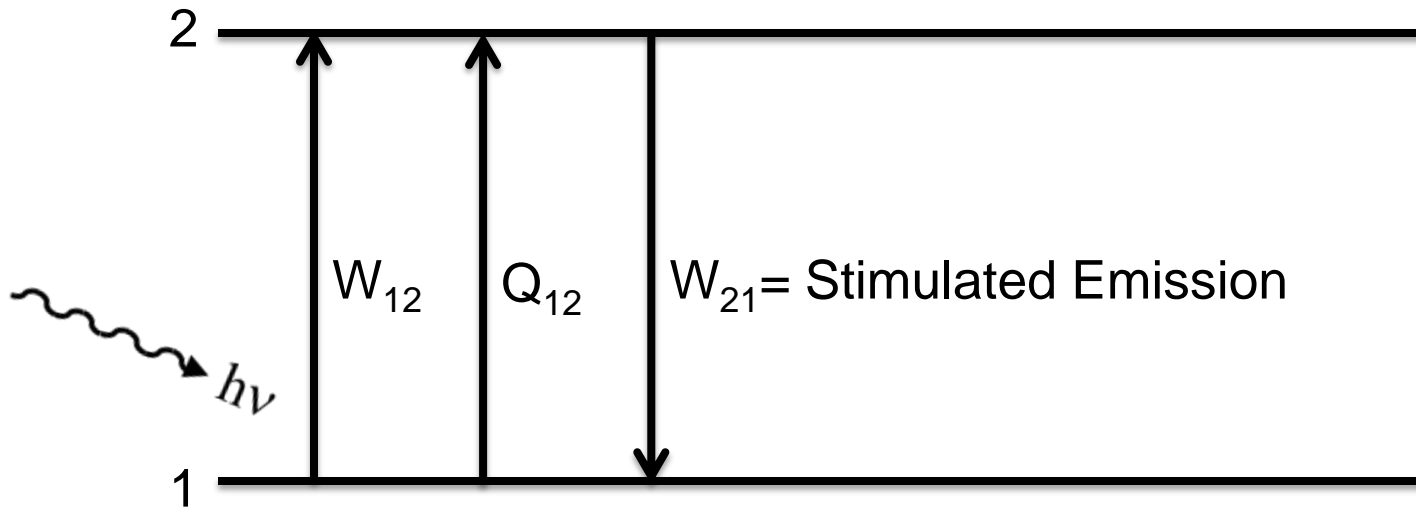
The excited state population is further increased by collisional excitation.

$$\frac{dN_1}{dt} = -N_1(W_{12} + Q_{12})$$

$$\frac{dN_2}{dt} = N_1(W_{12} + Q_{12})$$



Two-Level Model Theory



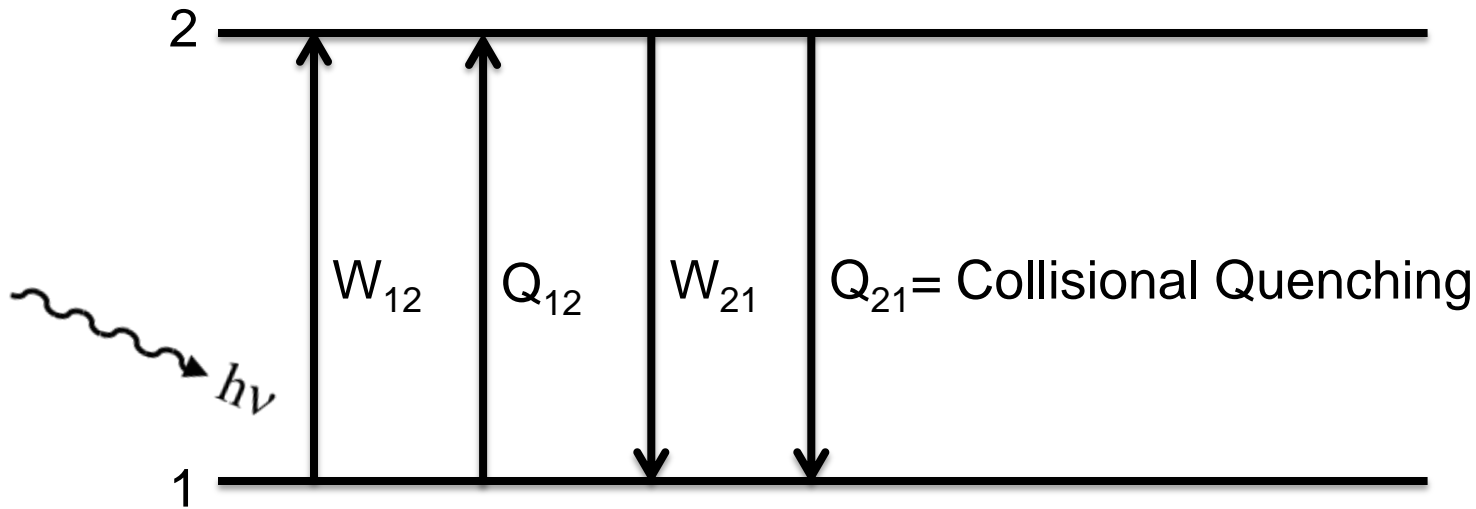
Some of the excited state population returns to the ground state through stimulated emission

$$\frac{dN_1}{dt} = -N_1(W_{12} + Q_{12}) + N_2W_{21}$$

$$\frac{dN_2}{dt} = N_1(W_{12} + Q_{12}) - N_2W_{21}$$



Two-Level Model Theory



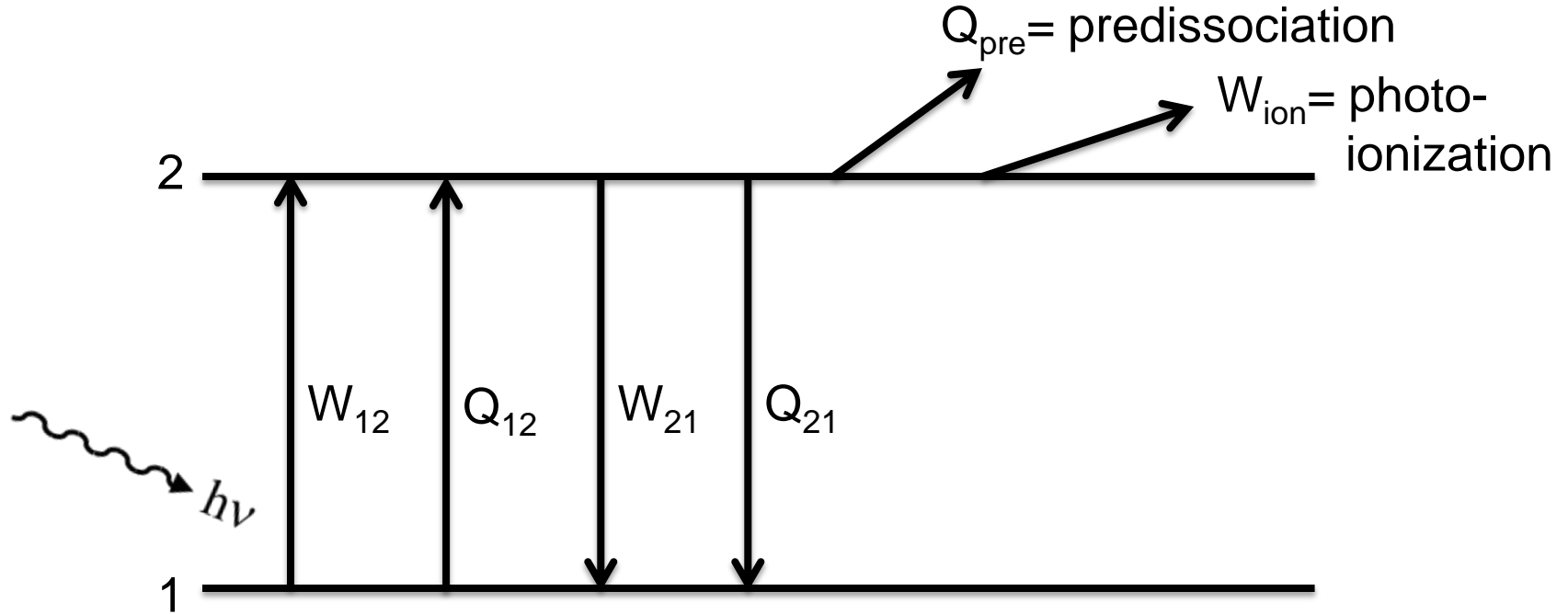
Some of the excited state population returns to the ground state through collisions (self or with other atoms/molecules)

$$\frac{dN_1}{dt} = -N_1(W_{12} + Q_{12}) + N_2(W_{21} + Q_{21})$$

$$\frac{dN_2}{dt} = N_1(W_{12} + Q_{12}) - N_2(W_{21} + Q_{21})$$



Two-Level Model Theory



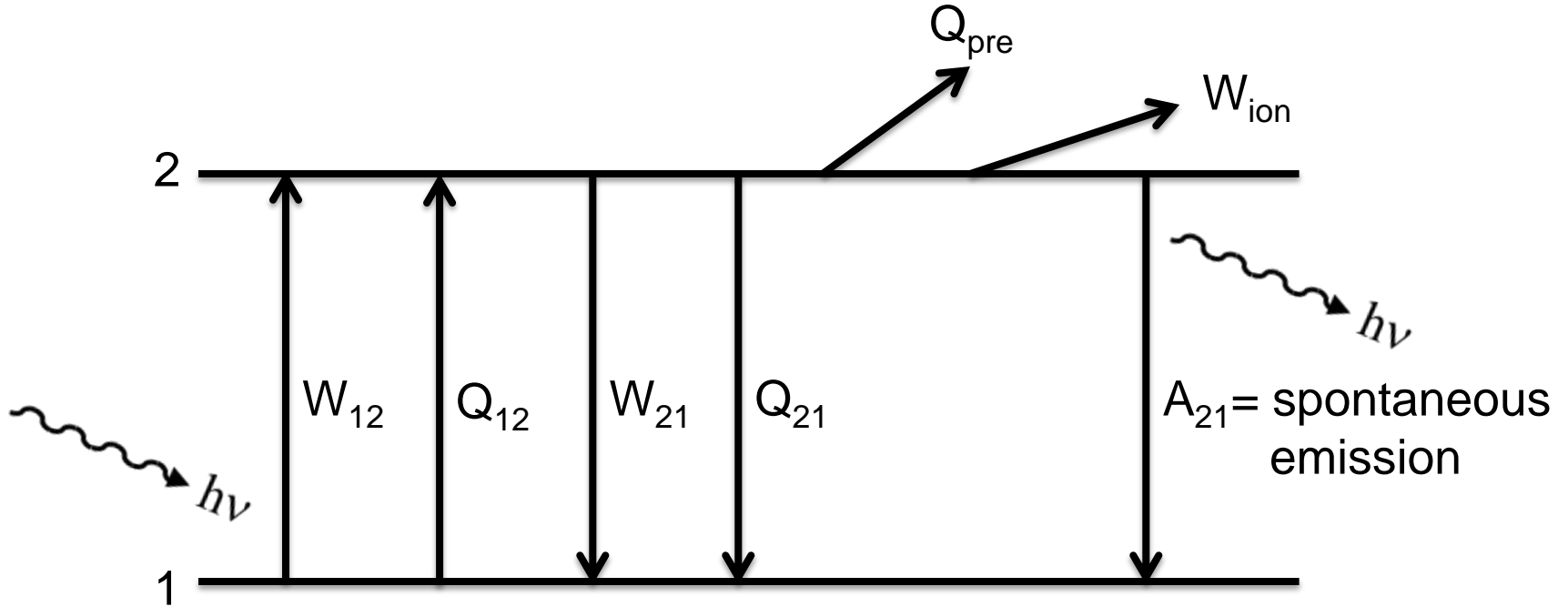
The excited state population gets depleted through dissociation and ionization (without returning to the ground state)

$$\frac{dN_1}{dt} = -N_1(W_{12} + Q_{12}) + N_2(W_{21} + Q_{21})$$

$$\frac{dN_2}{dt} = N_1(W_{12} + Q_{12}) - N_2(W_{21} + Q_{21} + Q_{\text{pre}} + W_{\text{ion}})$$



Two-Level Model Theory



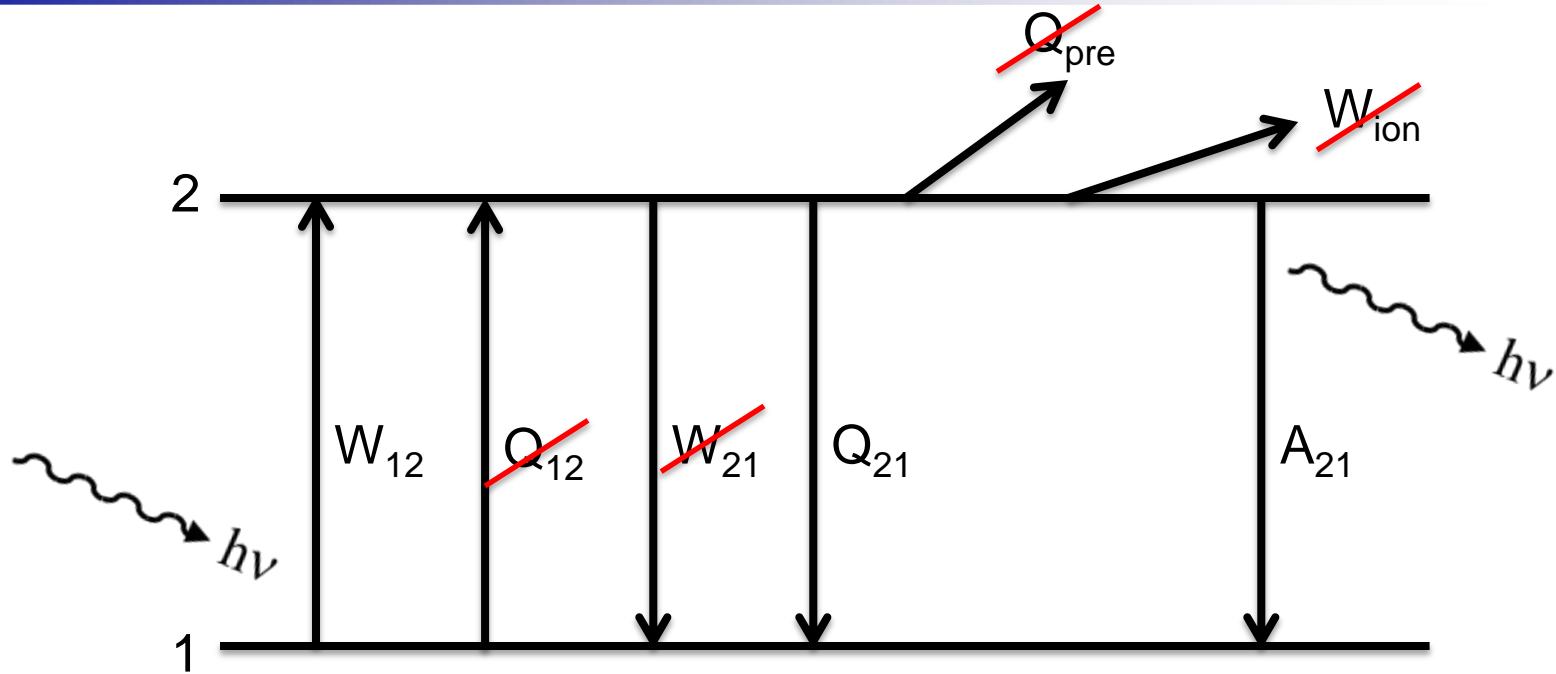
Finally, some of the excited population return to the ground state via spontaneous emission and emit a photon (**fluorescence**)

$$\frac{dN_1}{dt} = -N_1(W_{12} + Q_{12}) + N_2(W_{21} + Q_{21} + A_{21})$$

$$\frac{dN_2}{dt} = N_1(W_{12} + Q_{12}) - N_2(W_{21} + Q_{21} + Q_{\text{pre}} + W_{\text{ion}} + A_{21})$$



Two-Level Model Theory



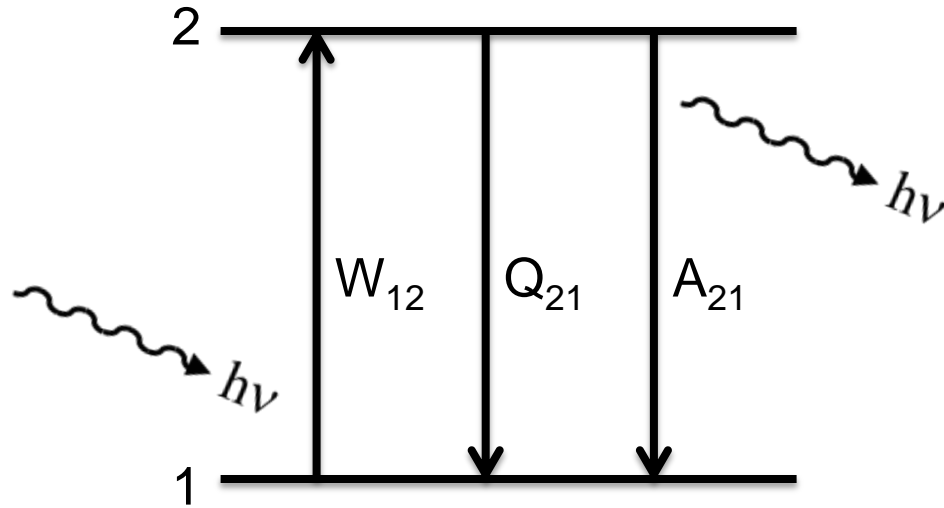
Fortunately, for many applications, Q_{12} , W_{21} , Q_{ion} , and Q_{pre} are negligible.

$$\frac{dN_1}{dt} = N_2(\cancel{W_{21}} + \cancel{Q_{21}} + A_{21}) - N_1(W_{12} + \cancel{Q_{12}})$$

$$\frac{dN_2}{dt} = N_1(W_{12} + \cancel{Q_{12}}) - N_2(\cancel{W_{21}} + \cancel{Q_{21}} + \cancel{Q_{pre}} + \cancel{W_{ion}} + A_{21})$$



Two-Level Model Theory



Simplification of rate equation:
$$\frac{dN_1}{dt} = -\frac{dN_2}{dt} = N_2(Q_{21} + A_{21}) - N_1W_{12}$$

Conservation of mass for absorbing species:

$$N_1 + N_2 = N_s = \chi_s f_B N_T$$

Mole fraction of absorbing species

Total number density

Number density of the absorbing species in the ground state prior to excitation

Boltzmann fraction



Steady State Two-Level Model



- Steady state assumption (e.g. continuous wave laser): $\frac{dN_1}{dt} = -\frac{dN_2}{dt} = 0$

- Solve for N_2 :
$$N_2 = \frac{\chi_s f_B N_T W_{12}}{W_{12} + Q_{21} + A_{21}}$$

- Weak excitation assumption: $W_{12} \ll (Q_{21} + A_{21})$

- Integrate spontaneous emission rate:
$$\int_0^{t_{det}} N_2 A_{21} dt = N_2 A_{21} t_{det}$$

- Include the optics of detection to get LIF signal:

$$S_{LIF} = \chi_s f_B N_T W_{12} \left(\frac{A_{21}}{Q_{21} + A_{21}} \right) t_{det} V \frac{\Omega}{4\pi} \eta$$

total number of photons collected (points to S_{LIF})
 fluorescence yield (Φ) (points to $\frac{A_{21}}{Q_{21} + A_{21}}$)
 detection time (points to t_{det})
 volume excited (points to V)
 solid angle (points to $\frac{\Omega}{4\pi}$)
 collection efficiency (points to η)



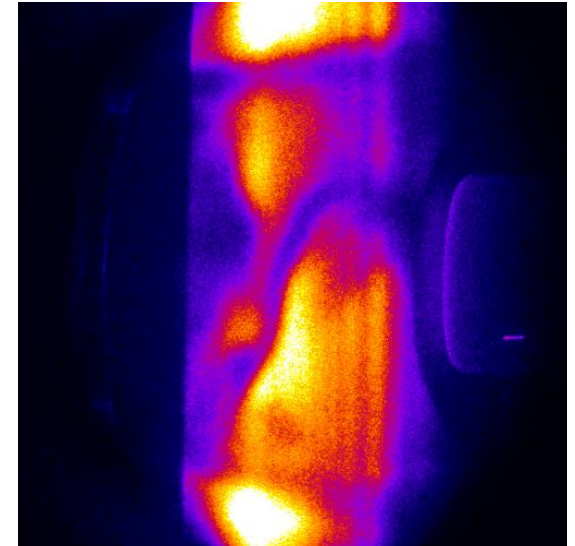
Concentration of Absorbing Species



$$S_{LIF} = \underline{\chi_S} N_T f_B W_{12} \Phi t_{det} V \frac{\Omega}{4\pi} \eta$$

- To first order, S_{LIF} is proportional to the concentration of the absorbing species
- Qualitative PLIF visualization often used to show the spatial distribution of absorbing species
- (see the text for measurement strategies for quantitative concentration)

Figure from Inman et al (2013)



$$S_{LIF} \propto \chi_{NO} N_T$$



Boltzmann Fraction



$$S_{LIF} = \chi_s N_T \underline{f_B} W_{12} \Phi t_{det} V \frac{\Omega}{4\pi} \eta$$

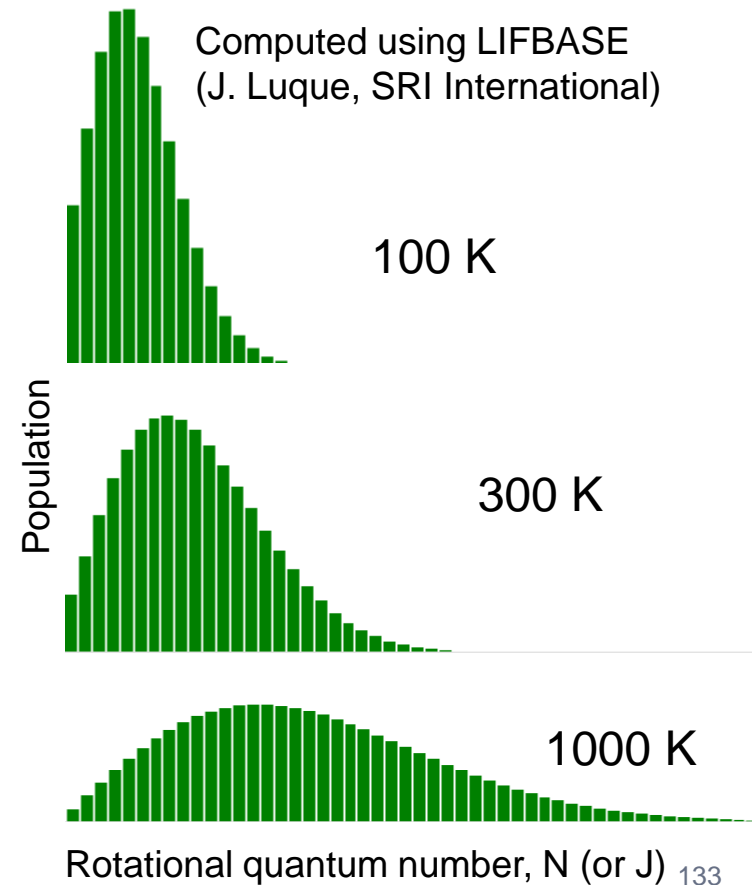
- Rotational Boltzmann fraction

$$f_B = \frac{g_j e^{-E_j/k_B T}}{\sum_j g_j e^{-E_j/k_B T}}$$

- a function of temperature only
- Peak at 300 K is ~3% for $N = 7$ ($J = 7.5$)

- Vibrational and electronic Boltzmann fractions

- Most molecules in ground state for $T < 2000$ for atoms, diatomics





Stimulated Absorption



$$S_{LIF} = \chi_s N_T f_B \underline{W}_{12} \Phi t_{det} V \frac{\Omega}{4\pi} \eta$$

W_{12} is the probability of an absorption transition per sec

$$W_{12} = B_{12} I \underbrace{\int Y_v L_v dv}_G$$

laser irradiance

absorption lineshape function

laser spectral profile

Einstein B coefficient

spectral overlap integral



Fluorescence Yield



$$S_{LIF} = \chi_s N_T f_B B_{12} I G \Phi t_{det} V \frac{\Omega}{4\pi} \eta$$

The fluorescence yield is affected by collisional quenching

$$\Phi = \frac{A_{21}}{Q_{21} + A_{21}}$$

Probability of a quenching collision per second

Probability of an atom/molecule undergoing spontaneous emission per second (Einstein A coefficient)

Collisional quenching is hard to predict since it depends on many factors



$$Q_{21} = N_T \sum_i \chi_i \sigma_{s,i} v_{s,i}$$

$$\left\{ \begin{array}{l} N_T = P/k_B T \\ \chi \text{ is mole fraction} \\ \sigma \text{ is quenching cross section} \\ v \text{ is mean relative velocity} \end{array} \right.$$



Steady State S_{LIF} dependencies



UNIVERSITY OF
CALGARY



$$S_{LIF} \propto \chi_s f_B(T) B_{12} I G(\chi_s, P, T, U) \Phi(\chi_s, \chi_i, P, T) t_{det}$$

- LIF signal is sensitive to T, P, U, χ_s, χ_i
 - Can potentially measure these parameters
 - Complicates measurement of a single parameter
- Making quantitative measurements with LIF involves finding a way to make measurement sensitive only to the parameter being measured

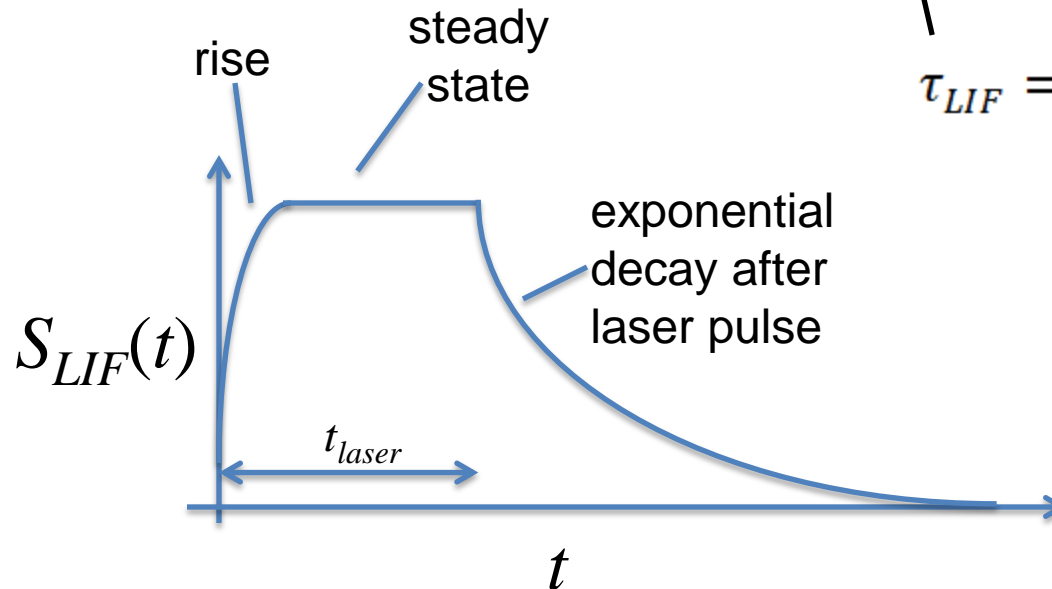


Time Dependent S_{LIF} Solution



$$S_{LIF}(t) = S_{LIF}(t_{laser}) e^{-(t-t_{laser})/\tau_{LIF}}, \quad t > t_{laser}$$

photons
collected
per time



$$\tau_{LIF} = (Q_{21} + A_{21})^{-1}$$

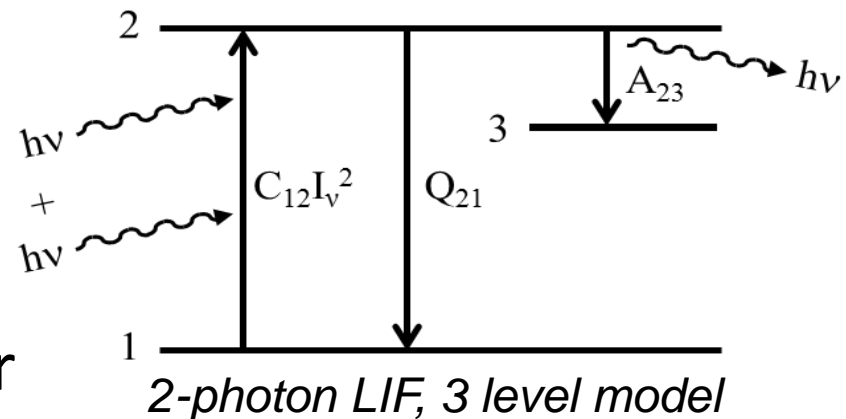
- Laser pulse length is typically ~ 10 ns
- LIF lifetimes can be a few ns to 100's of ns or longer
 - If you can measure lifetime, you can measure Q!
 - Can measure velocity from long lived decay (MTV)



More Complicated LIF Models



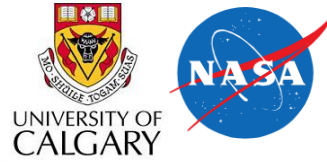
- More complete LIF theories and phenomena:
 - Saturation effects (see manuscript)
 - Line shapes
 - overlap integral, G , to be discussed below
 - Multi-level LIF models
 - 2 photon absorption
 - 3, 4, 5 level models
 - Predissociation
 - Rotational energy transfer
 - Vibrational energy transfer
- For further reference:



A. C. Eckbreth, *Laser Diagnostics for Combustion Temperature and Species 2nd Ed.*, Combustion Science & Technology Book Series, Volume 3, Taylor & Francis, New York, 1996



A real molecule: NO



- NO is a diatomic molecule
 - Electronic
 - Vibration
 - Rotation
 - Not shown
- Absorption and fluorescence take place between electronic states
 - Show rotational and vibrational structure

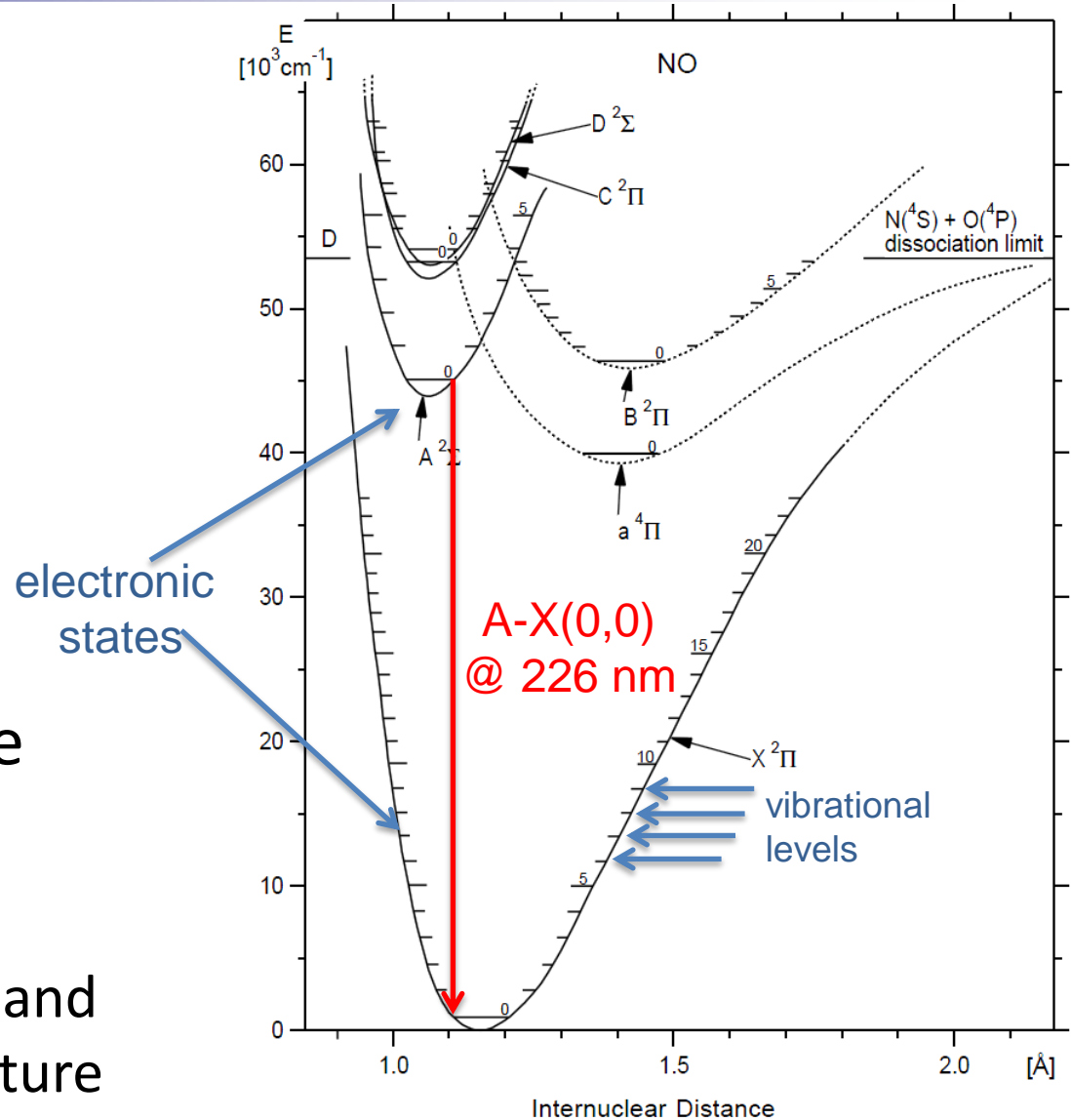
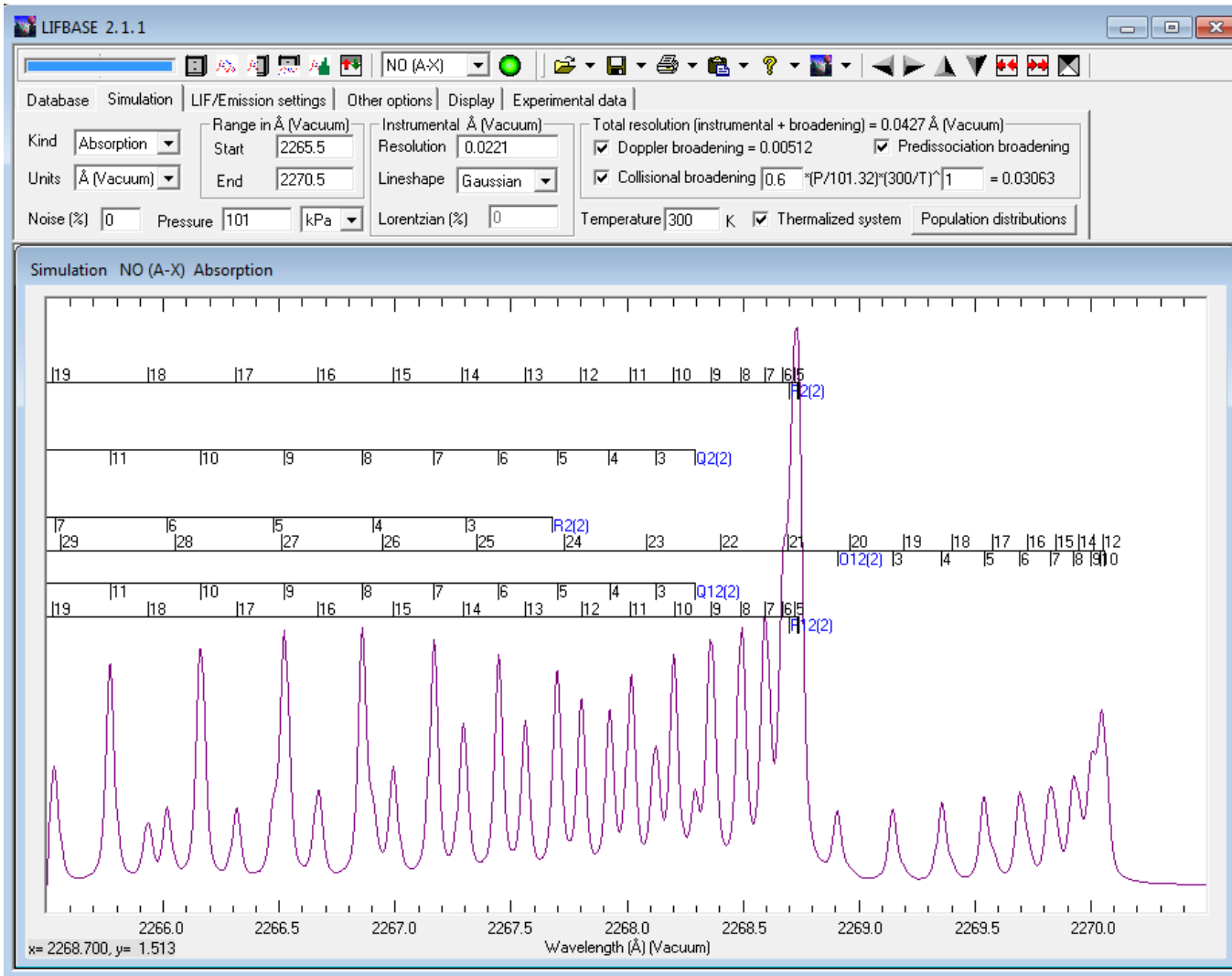
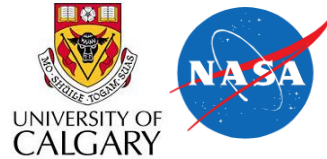


Figure A2.1. Selected potential energy curves that show the electronic structure of NO. In this experiment, we probed transitions in the A–X band of NO [adapted from (Scheingraber and Vidal, 1985)]



LIFBASE Simulation of NO



LIFBASE
freeware by
J. Luque, SRI
International
lifbase@yahoo.com

- LIF Excitation Scan between 226.6-227 nm, 1 atm, 300 K
 - Lines all have band names (*O*, *P*, *Q*, *R*, *S*) and *N*'s or *J*'s (rot quant #)



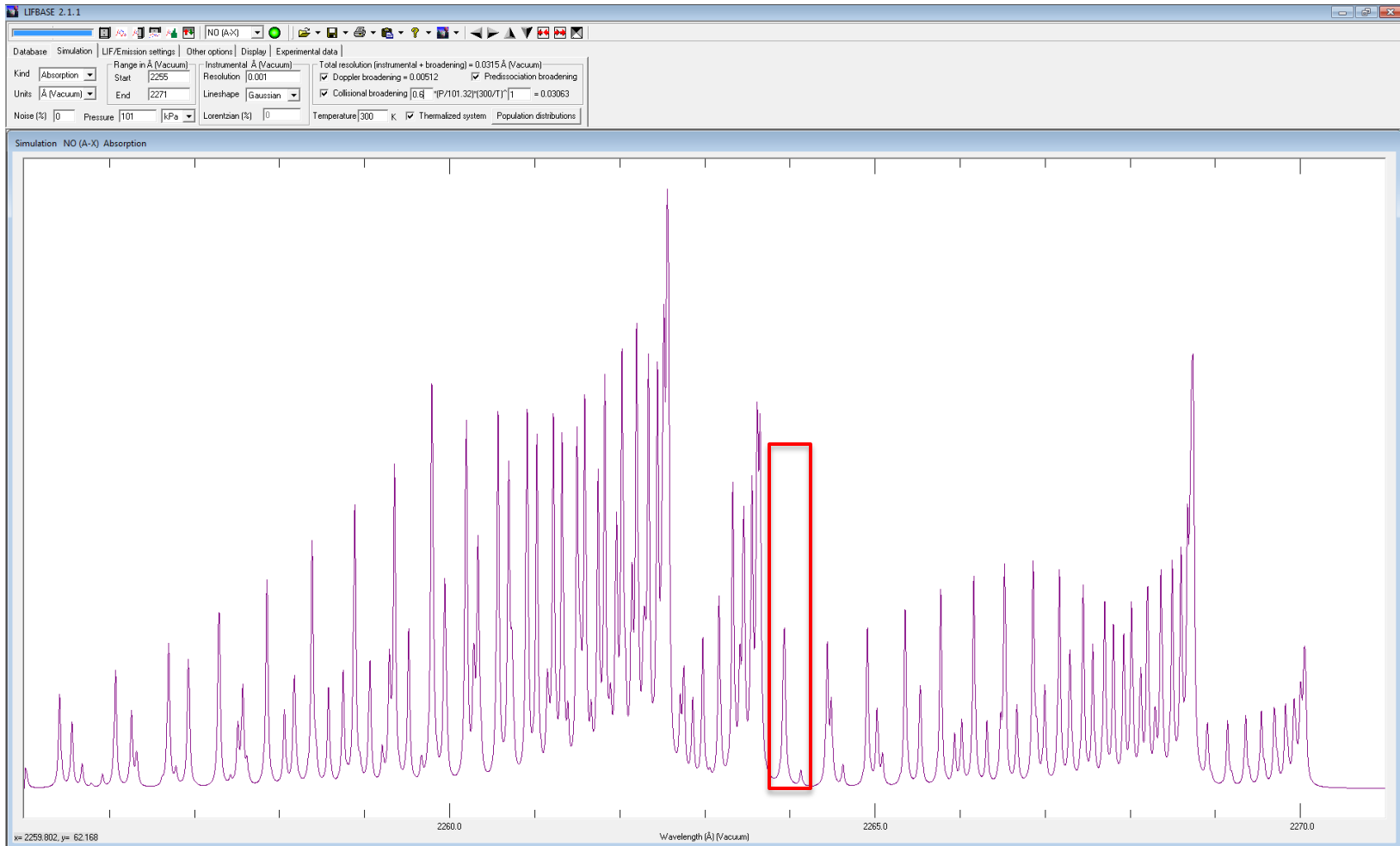
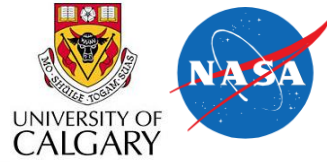
LIF Temperature Measurements



- Rotational Temperature
 - Ratio of 2 or more rotational lines
 - Describe general case
 - Example in a turbulent base flow
- Vibrational Temperature
 - Ratio of 2 or more vibrational lines
 - Example of freestream characterization
 - Boltzmann plot, where more than 2 lines used
- Translational Temperature



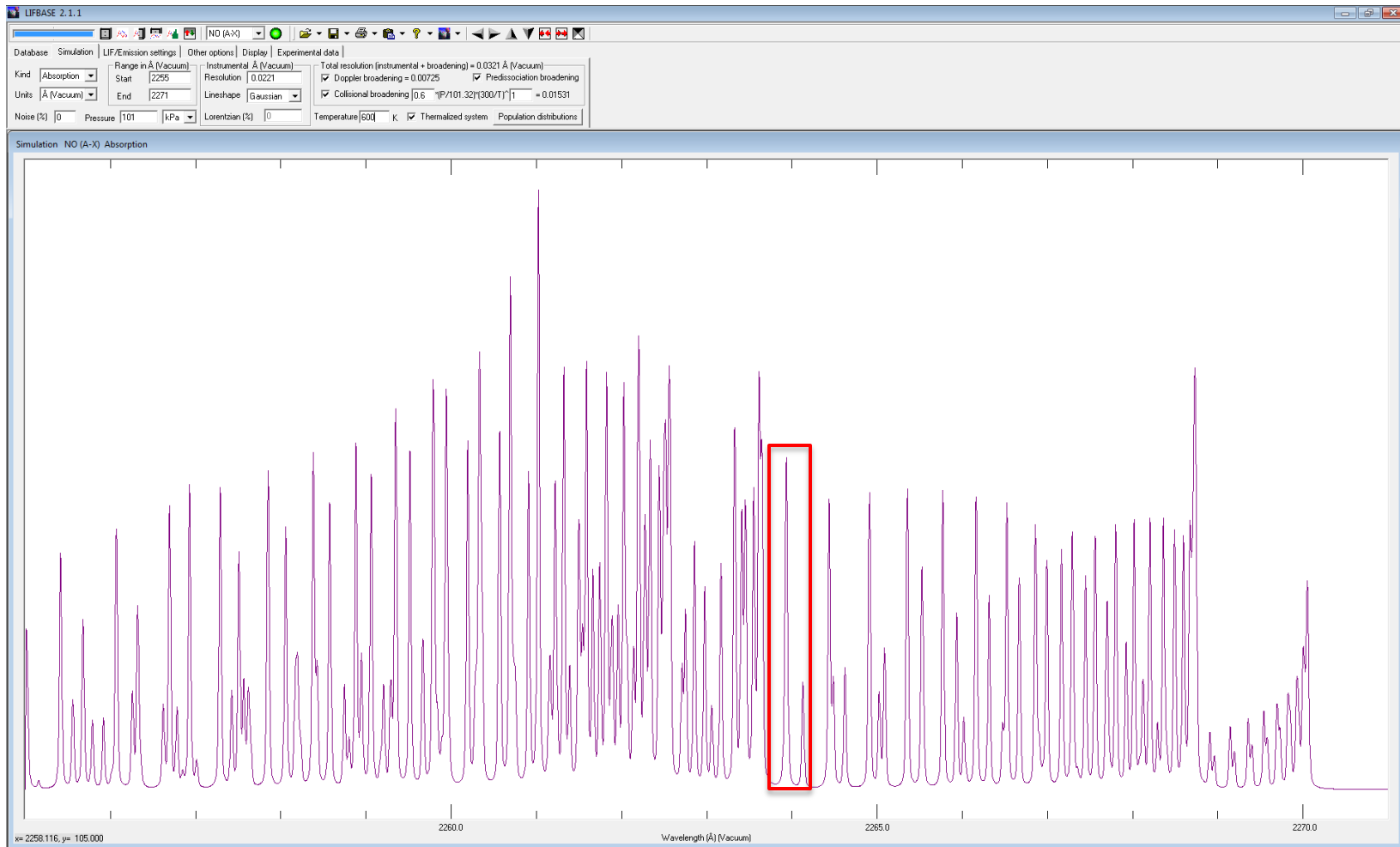
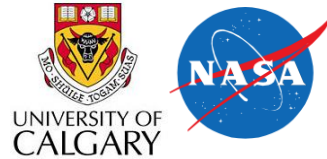
Rotational Lines of NO, 300 K



- LIF Excitation Scan between 225-227 nm, 1 atm, 300 K



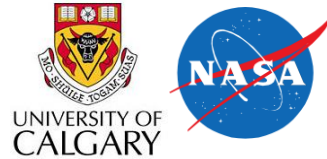
Rotational Lines of NO, 600 K



- LIF Excitation Scan between 225-227 nm, 1 atm, 600 K



LIF: Rotational Temperature, T_{rot}



- Recall:

$$S_{LIF} \propto \chi_s f_B(T) B_{12} IG(\chi_s, P, T, U) \Phi(\chi_s, \chi_i, P, T) t_{det}$$

- Obtain LIF or PLIF on two different rotational lines of a molecule: i and j . Take ratio, R:

$$\frac{S_{LIF,i}}{S_{LIF,j}} = R = C \frac{B_{12,i} E_i (2J_i + 1) \exp[-F_{J,i}/k_B T_{rot}]}{B_{12,j} E_j (2J_j + 1) \exp[-F_{J,j}/k_B T_{rot}]}$$

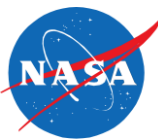
- Where:

- C is a constant
- E is the laser energy (in mJoules)
- J is the rotational quantum number
- F_J is the energy of the state
- k_B is Boltzmann's constant

$\Omega, \chi_s, \eta, G, V, N_T$ and Φ
(including Q_{21})
cancel out!



LIF: Rotational Temperature, T_{rot}



- Solve for T_{rot} :

$$T_{rot} = \frac{-\Delta E_{rot}}{k_B \ln \left[CR \frac{B_{12,j} E_j (2J_j + 1)}{B_{12,i} E_i (2J_i + 1)} \right]}$$

- Where:

$$\Delta E_{rot} = (F_{J,i} - F_{J,j})$$

- Temperature sensitivity:

$$\frac{\delta T_{rot}}{T_{rot}} = \frac{k_B T_{rot}}{\Delta E_{rot}} \frac{\delta R}{R}$$

- Suggests to maximize ΔE_{rot} (as long as signals still strong) to minimize error in temperature, δT_{rot}
 - Should choose widely separated states: e.g. $J = 3.5$ & 35.5



Typical Strategies for T_{rot}



UNIVERSITY OF
CALGARY



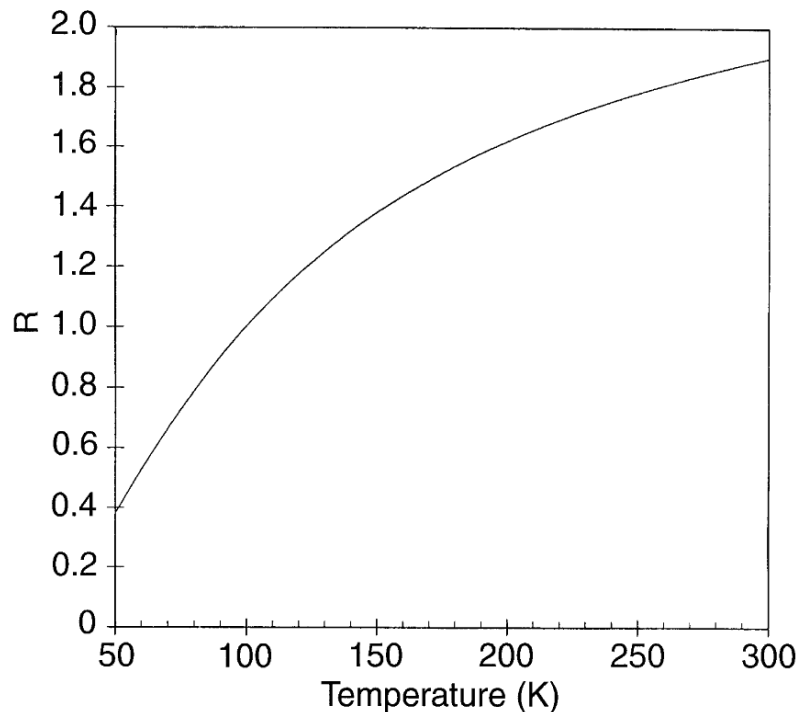
- Typically two approaches:
 - Steady laminar flow
 - Obtain images on one J, then scan laser to another J
 - Ratio images, determine temperature
 - Turbulent flow
 - Two lasers, two cameras (Cumbersome! Expensive!)
 - Acquire two images nearly simultaneously, different J's
 - Need to do this because ratio is a nonlinear function of temperature:
$$\frac{S_{LIF,i}}{S_{LIF,j}} = R = C \frac{B_{12,i}E_i (2J_i+1)\exp[-F_{J,i}/k_B T_{rot}]}{B_{12,j}E_j (2J_j+1)\exp[-F_{J,j}/k_B T_{rot}]}$$
 - Typical single-shot temperature measurement precision is ~20% at flame temperatures (Seitzman, 1994)
 - If you use 1 laser/1 camera, → bias errors in turb. Flows
 - (E. R. Lachney, and N. T. Clemens, "PLIF imaging of mean temperature and pressure in a supersonic bluff wake," Experiments in Fluids, 24, pp. 354-363, 1998.)
 - Average many measurements to reduce uncertainty



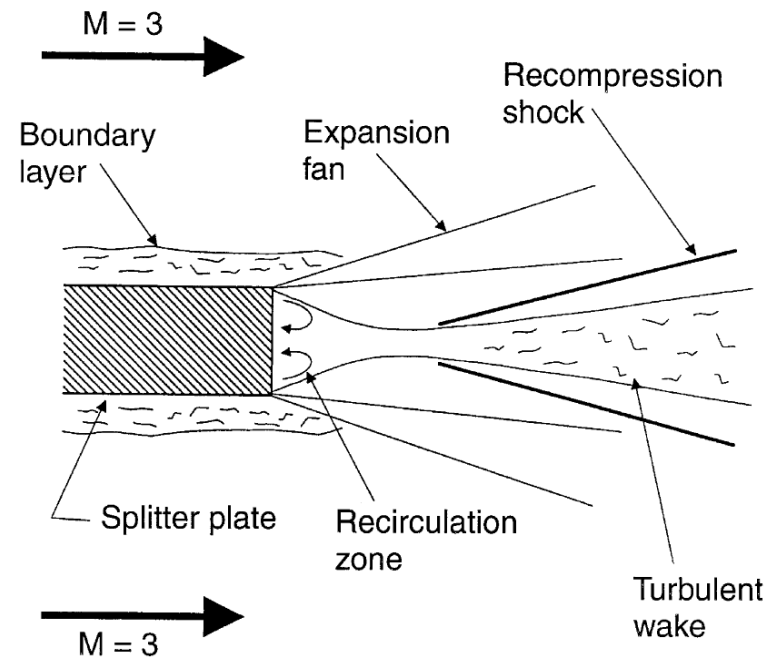
Single laser/camera for T_{rot} in turbulent flow



- Lachney and Clemens (1998) used 1 laser / 1 camera to map mean T_{rot} in a base flow.
- NO seeded N_2 at Mach 3
- Chose: $J = 8.5$ and $J = 10.5$

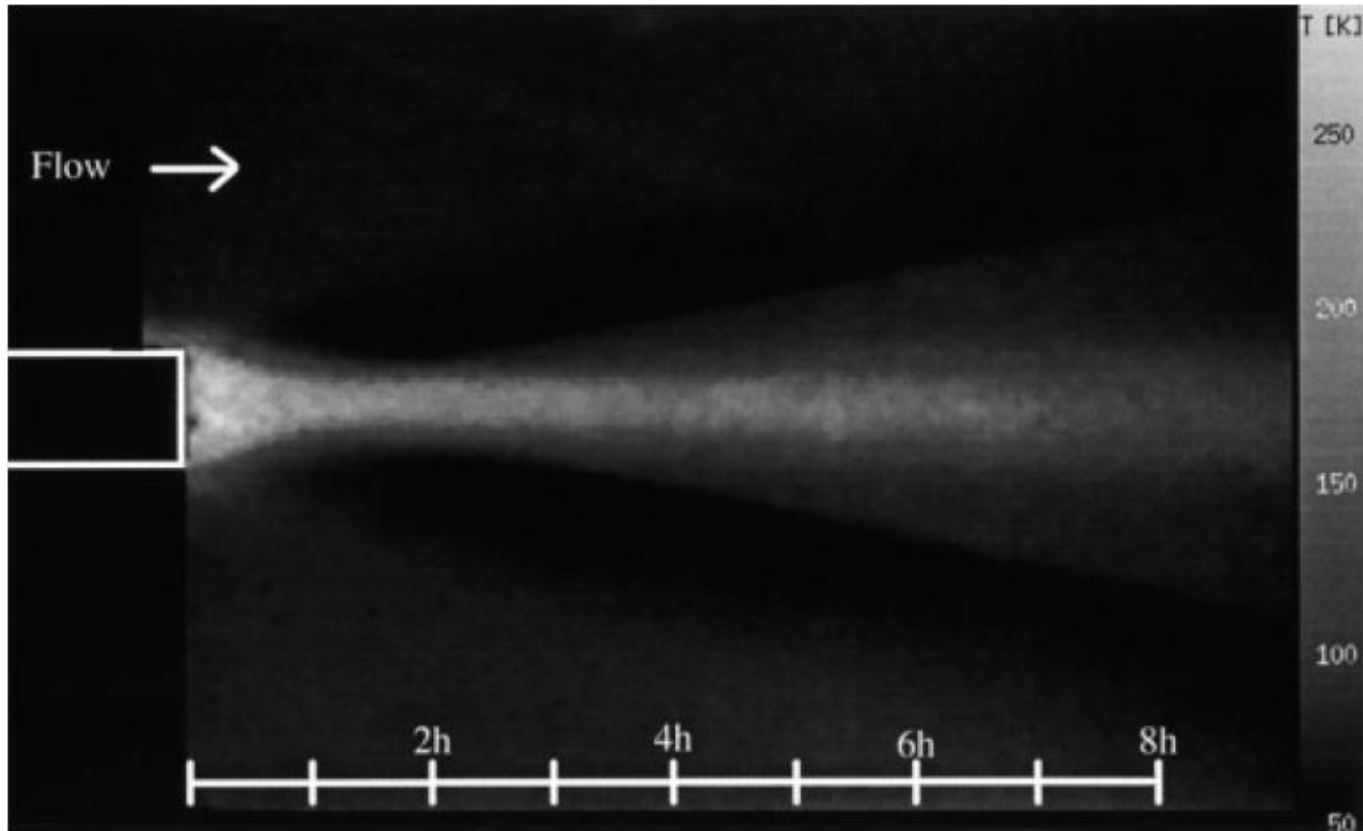


Ratio of lines, used to measure T_{rot}



Turbulent supersonic wake flow

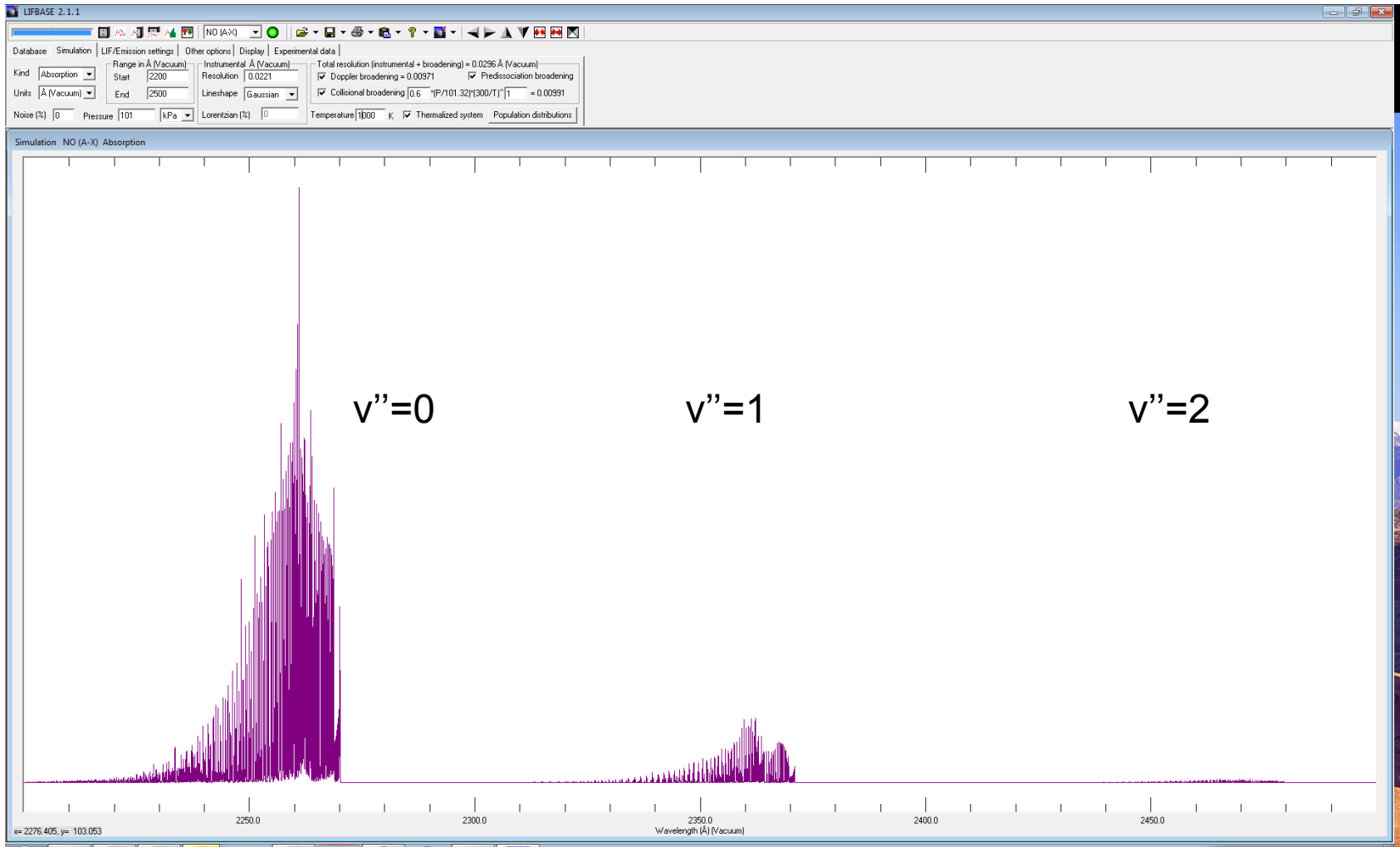
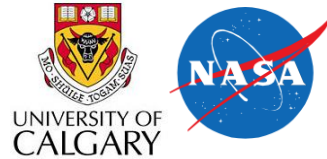
- Lachney and Clemens (1998):



Turbulent supersonic wake flow temperature measurement
Agreed with temperatures inferred from probe measurements to within 11%



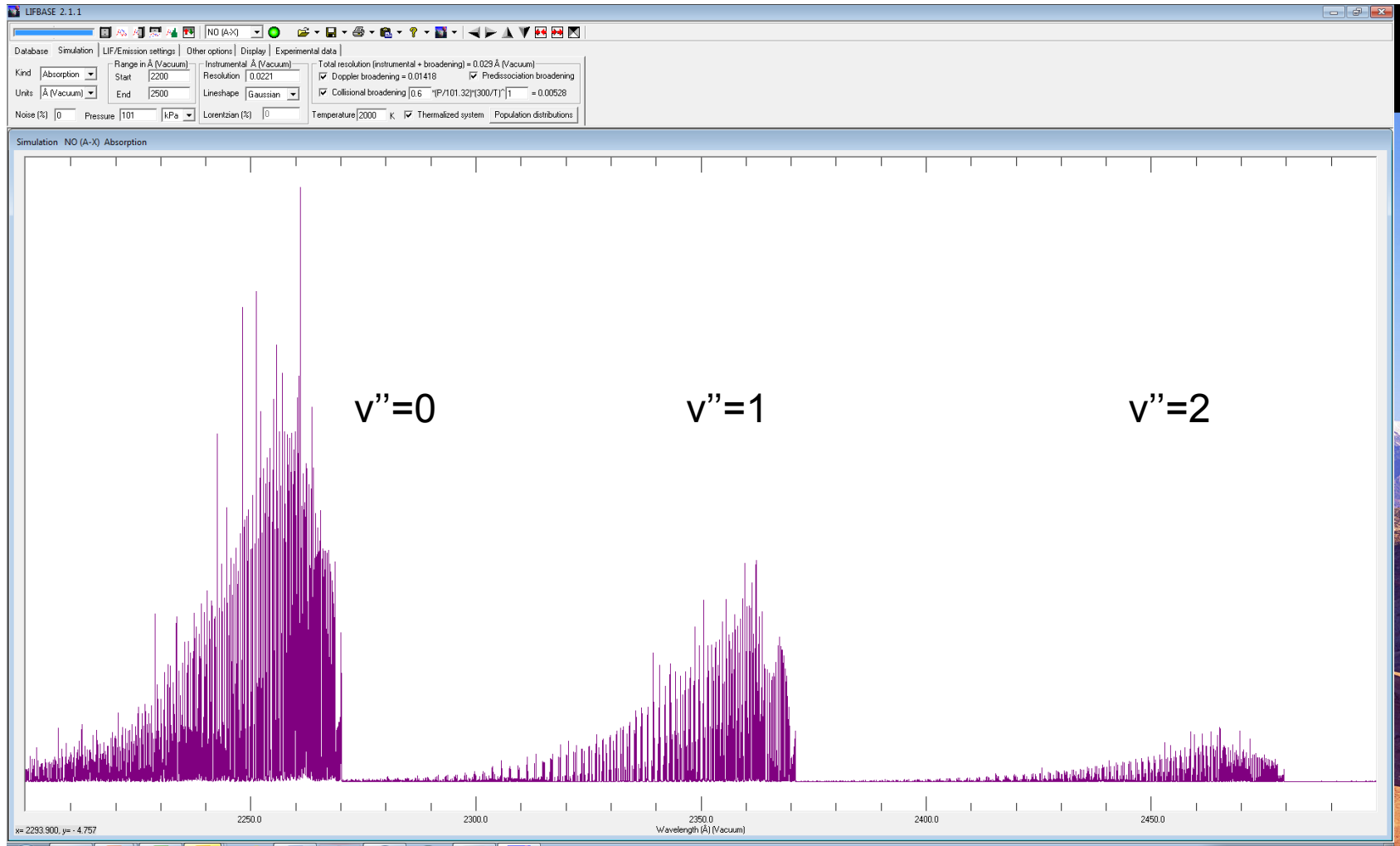
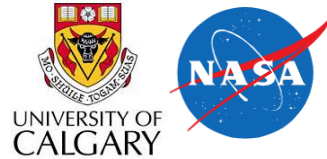
Vibrational Bands of NO



- Three vibrational bands: $T = 1000$ K
 - Vibrational bands have quantum number, v



Vibrational Bands of NO



- Three vibrational bands: T = 2000 K



Vibrational Temperature T_{vib} Measurement



- A similar approach can be made to obtain vibrational temperature measurements
 - Typically excite the same rotational line (J) in 2 or more vibrational bands ($F_j \approx \text{constant}$)
 - Can do 2 line measurements as before
 - Can use a Boltzmann Plot:

- Graph:

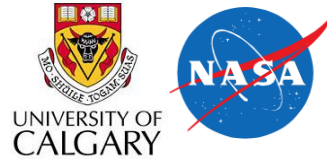
$$\ln \left[\frac{S_{LIF,i}}{B_{12,i} E_i (2J_i + 1) \exp[-F_{J,i}/k_B T_{rot}]} \right]$$

versus $G_{v,i}$ vibrational energy of states probed

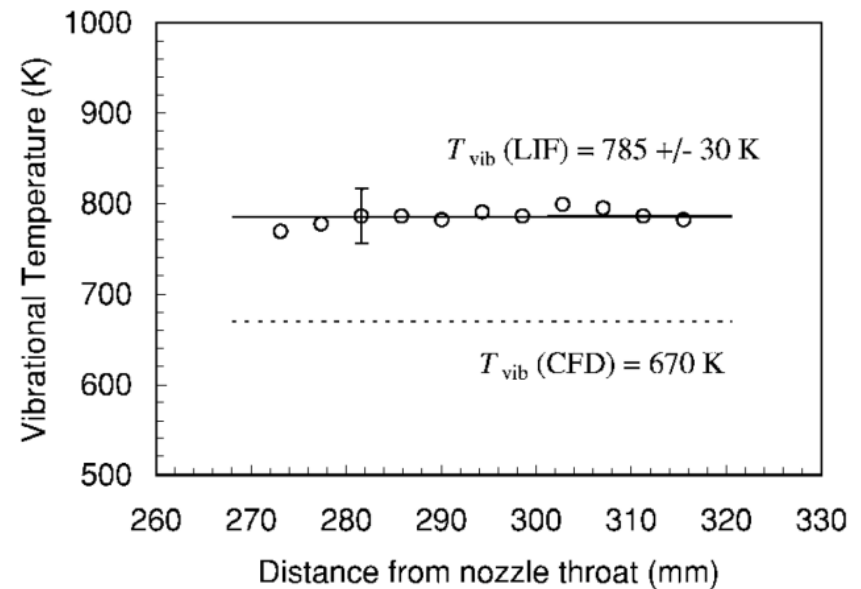
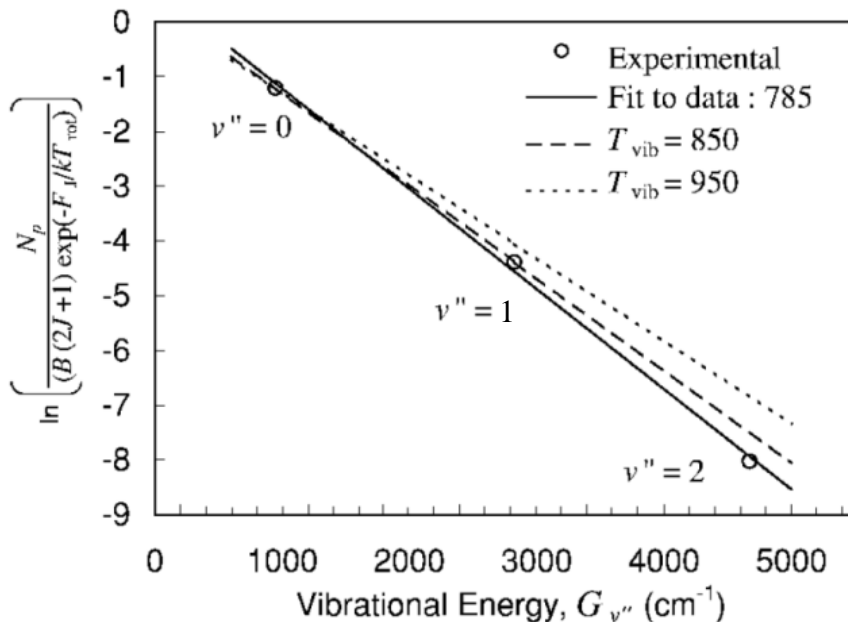
- Slope is: $-1/(k_B T_{vib})$

If $F_j \approx \text{constant}$ then T_{vib} can be determined independent of T_{rot}

Vibrational Temperature T_{vib} Measurement



- Vibrational temperature measured in a nozzle exit flow verifying vibrational nonequilibrium ($T_{vib} \neq T_{rot}$)

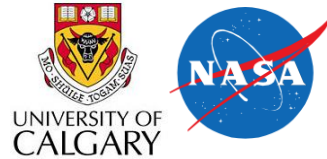


$T_{rot} \approx 400 \text{ K}$ and decreasing with distance

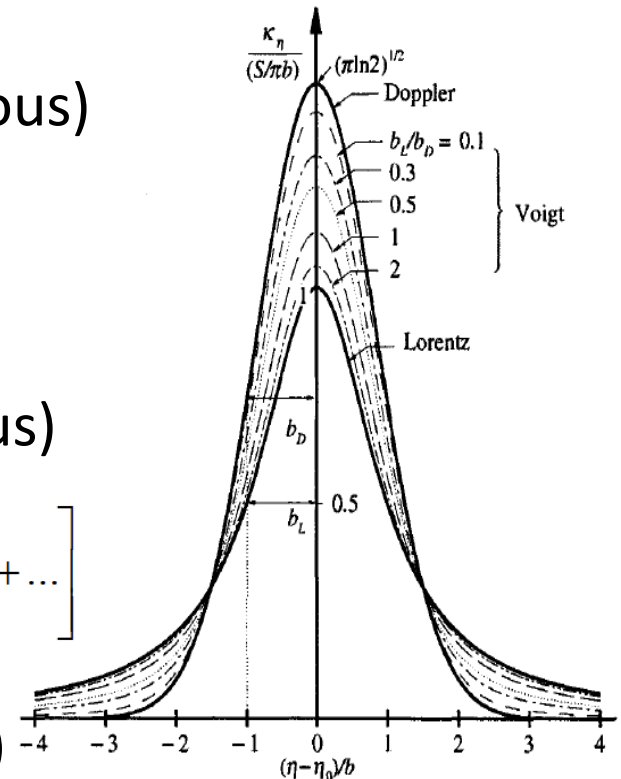
P. C. Palma, P. M. Danehy, and A. F. P. Houwing, "Fluorescence Imaging of Rotational and Vibrational Temperature in Shock-Tunnel Nozzle Flow," AIAA Journal, 41(9), September 2003



Translational Temperature

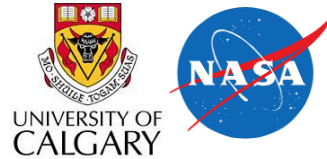


- Can measure T_{trans} (and P) from width and shapes of spectral lines
- Spectral lines have a shape
 - Molecular motion leads to:
 - Doppler Broadening (inhomogeneous)
 - Gaussian shape
 - FWHM:
$$\Delta v_D = \frac{v_0}{c} \sqrt{\frac{8 \ln(2) k_B T}{m}}$$
 - Collisions lead to:
 - Pressure Broadening (homogeneous)
 - Lorentzian shape
 - FWHM:
$$\Delta v_P = \frac{P}{101,325} \cdot \left[2\gamma \cdot \chi_i \cdot \left[\frac{295}{T} \right]^{0.75} + \dots \right]$$
 - Combination is: Voigt
 - Convolution (if $\Delta v_P, \Delta v_D$ comparable)
 - Formulas in manuscript





Translational Temperature

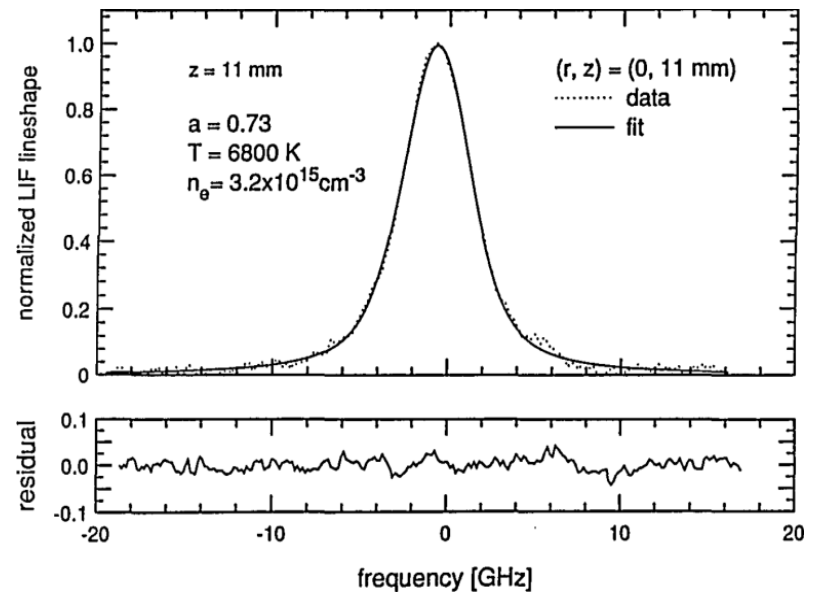
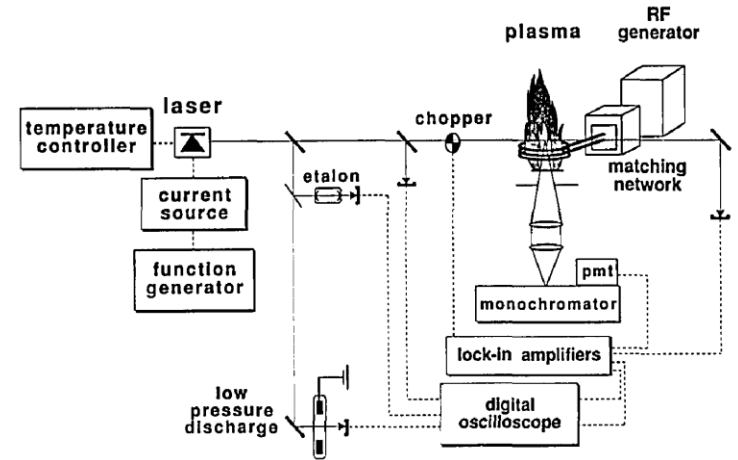


- If using a very narrow linewidth laser...

$$\Delta \nu_L \ll \Delta \nu_P, \Delta \nu_D$$

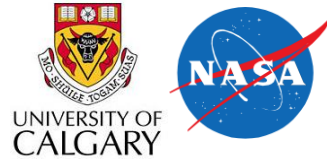
...can neglect laser width

- Semiconductor diode laser
- Scan laser frequency across a transition
 - Argon atom at 810.4 nm
 - Turbulent inductively coupled plasma (ICP) torch
- Fit measured LIF spectrum
 - Have homogeneous (Stark) and Doppler broadening
 - Determine n_e and T





Species Concentrations



- Problem: How to deal with unknown Q_{21} ?

- Solutions:

- Saturated LIF: $(W_{12} + W_{21}) \gg (Q_{21} + A_{21})$

- Q_{21} is negligible compared to W 's
 - Hard to achieve

- Predissociation

- $Q_{pre} \gg Q_{21}$

- Measure τ_{LIF}

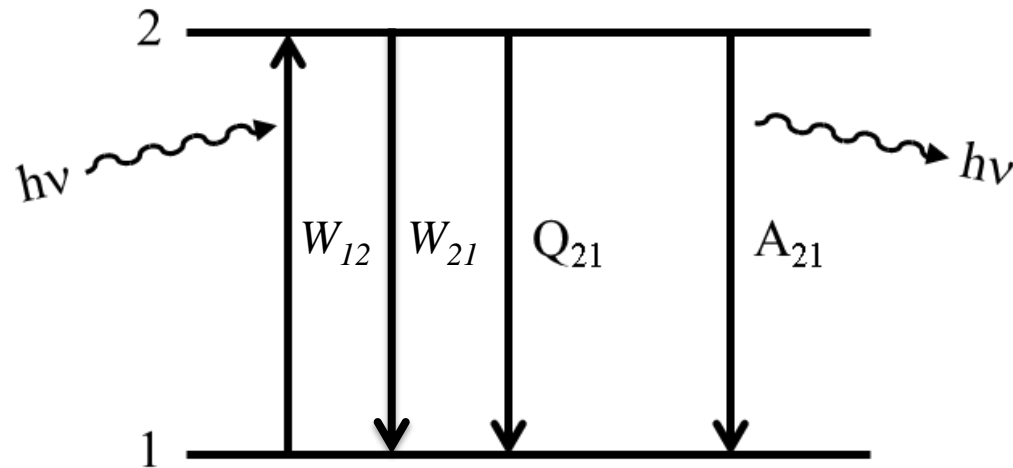
- Determine Q_{21} from τ_{LIF}

- Measure other species present and predict τ_{LIF}

- Raman/Rayleigh/LIF (Sandia and DLR)

- Counter-propagating beams, take ratio (Versluis, 1997)

- Potential problems: absorption, rad. trapping





LIF Advantages/Disadvantages



- Advantages
 - Relatively easy to make planar measurements (PLIF)
 - Provides flow visualization simultaneously
 - Relatively easy to perform
 - Can probe many different parameters (T, V, concentration)
 - Velocity measurements (MTV) can have with 1-2% precision
- Disadvantages
 - Precision of single-shot temperature measurements (~20%) is not good compared to CARS (2-3%) or LITA (1%)
 - Difficult to do quantitative concentration measurements, especially planar

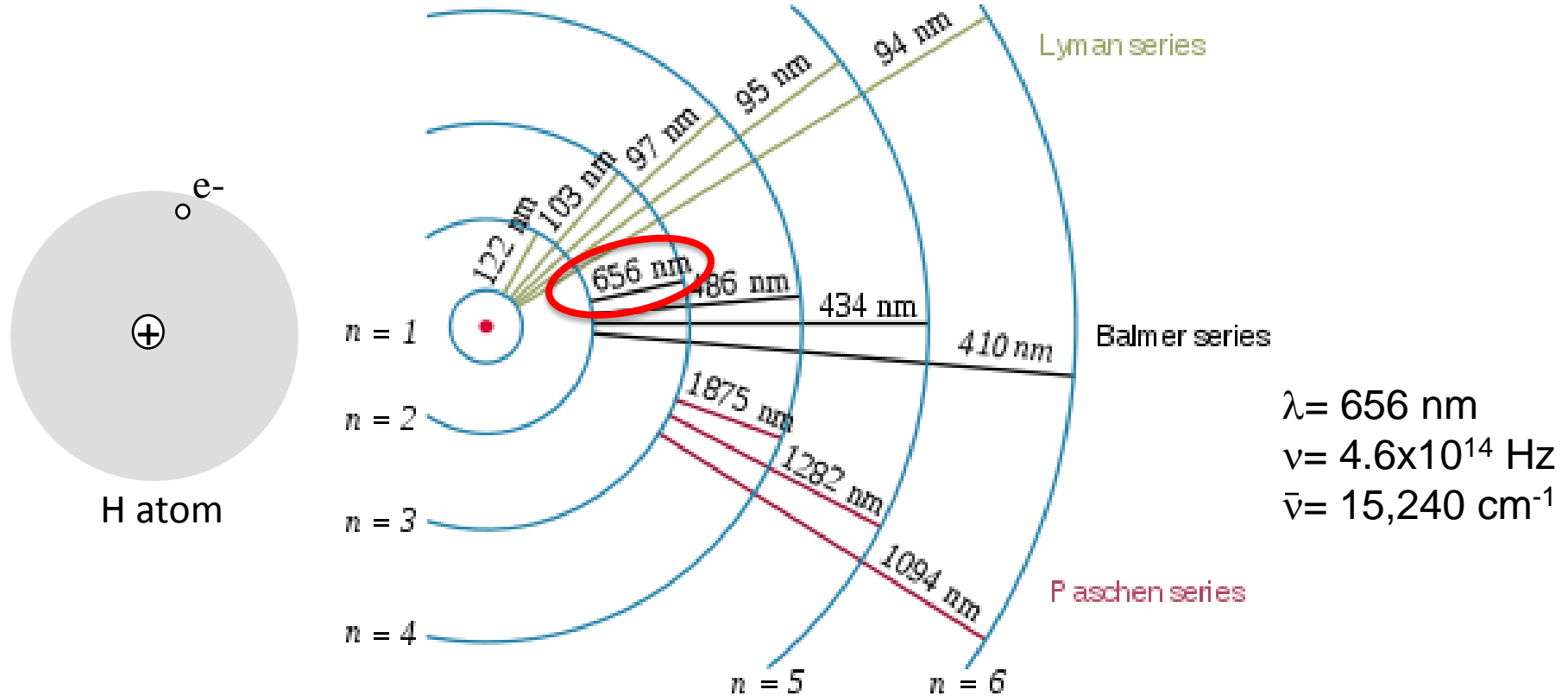


PLIF Backup Slides





LIF Theory: Atoms



$$\lambda = 656 \text{ nm}$$

$$\nu = 4.6 \times 10^{14} \text{ Hz}$$

$$\bar{\nu} = 15,240 \text{ cm}^{-1}$$

- Two level model
 - e.g. Hydrogen atom
- Photon energy = $h\nu$
 - $c = \lambda\nu$

Hydrogen atom energy levels
 (from Wikipedia, "hydrogen spectral series")
<http://creativecommons.org/licenses/by-sa/3.0/deed.en>

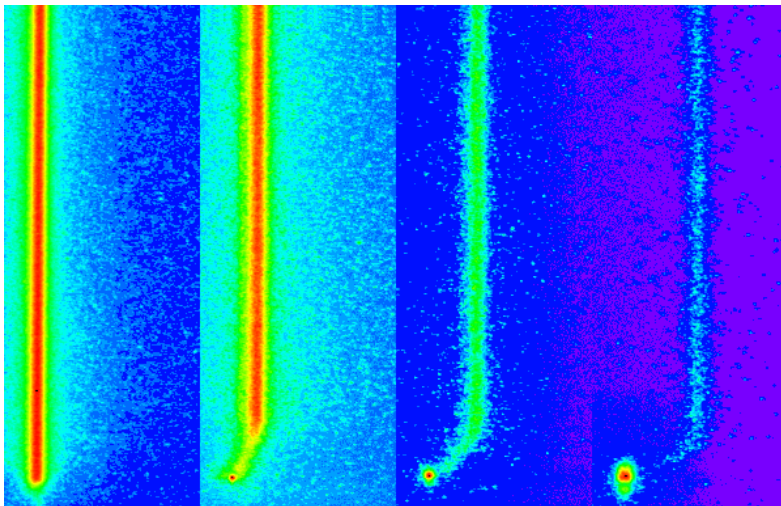
wavenumbers = $\bar{\nu} = 1/\lambda \text{ cm}^{-1}$



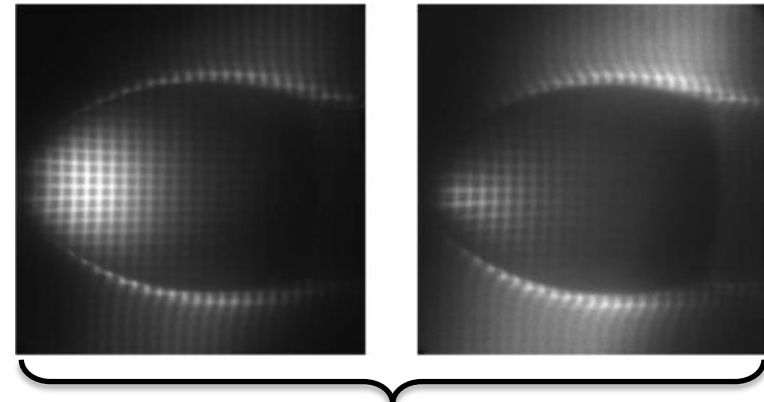
Introduction to LIF Velocimetry Techniques for Hypersonic Nonequilibrium Flows



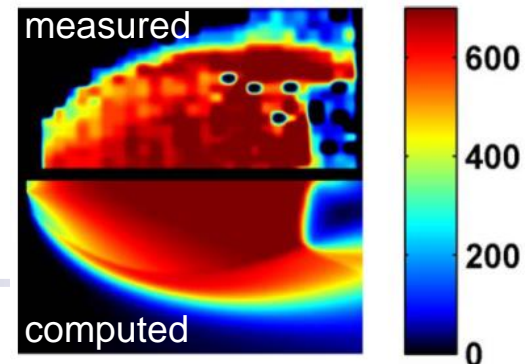
Brett Bathel, NASA Langley Research Center, Virginia, USA
Paul Danehy, NASA Langley Research Center, Virginia, USA
Craig Johansen, The University of Calgary, Canada



NASA and The Australian National University



U-Velocity (m/s)



Texas A&M





Outline: Velocimetry Techniques



- LIF-Based Velocimetry Techniques
 - Doppler shift
 - Based on laser frequency relative to absorption line
 - Molecular tagging velocimetry (MTV)
 - aka Flow tagging velocimetry
 - Time of flight
 - Single-laser method requires lifetime long enough for flow to move while light is being emitted
 - Summary
- Other Techniques
 - Particle: Particle Image Velocimetry (PIV), Laser Doppler Velocimetry (LDV)
 - Interference/Scattering: Laser-Induced Thermal Acoustics (LITA)
 - Schlieren: Density Tagging Velocimetry (DTV)
 - Scattering: Rayleigh



Doppler Shift Velocimetry



Doppler Shift Velocimetry



- The Doppler shift:



$$\Delta\nu = \frac{U}{c} \nu_0$$

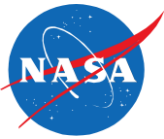
Wikipedia "Doppler Shift"
<http://creativecommons.org/licenses/by-sa/3.0/deed.en>

- Can be used to measure velocity with LIF
 - Relative shift between laser and absorbing molecules
 - Angle of detection does not matter for LIF
- The overlap integral, G , which describes the overlap of the laser's spectrum with a line
 - L_ν is laser's spectral shape, typically modeled as Gaussian or Lorentzian
 - Y_ν is the transition's absorption line shape, can be shifted by Doppler shift

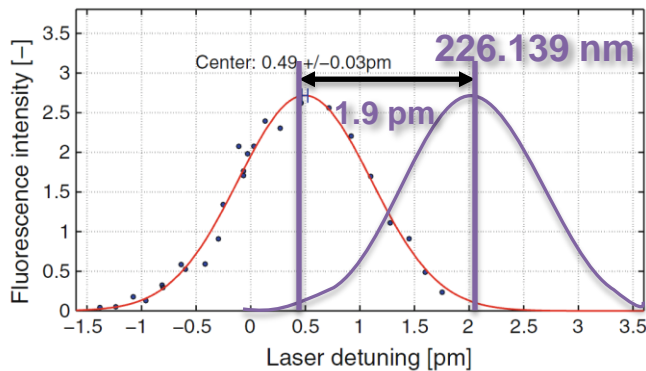
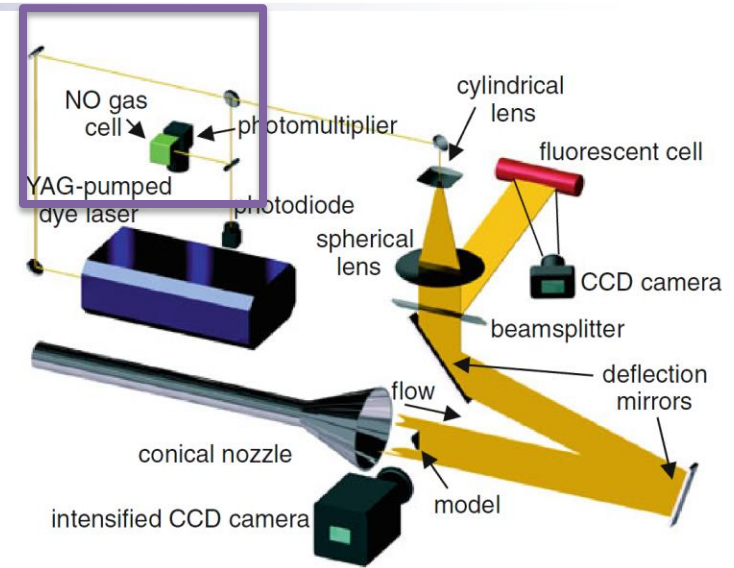
$$G = \int L_\nu Y_\nu d\nu$$



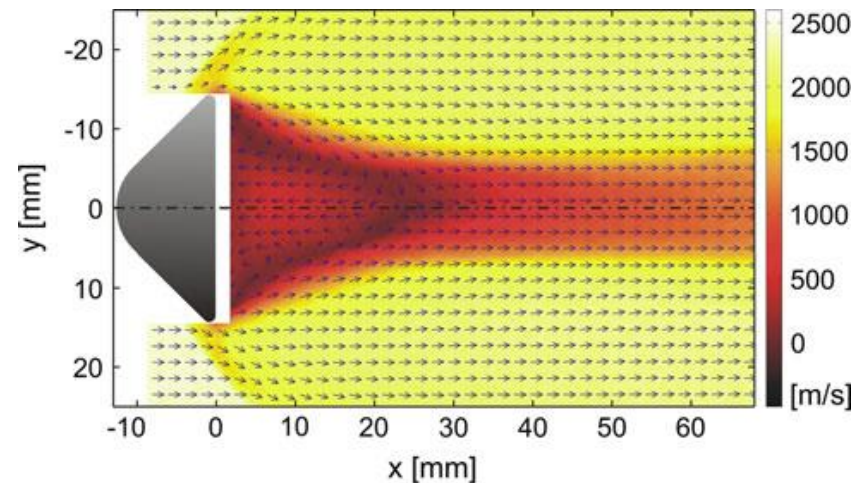
Doppler-based LIF Velocimetry



- Direct laser sheet into the flow
- Acquire images or signal at different laser frequencies
 - Choose frequencies near an absorption line
 - Measure absorption lineshape at each point
 - Reference data acquired simultaneously



- Measure from two different directions to get two different velocity components
- Do need to consider pressure shift



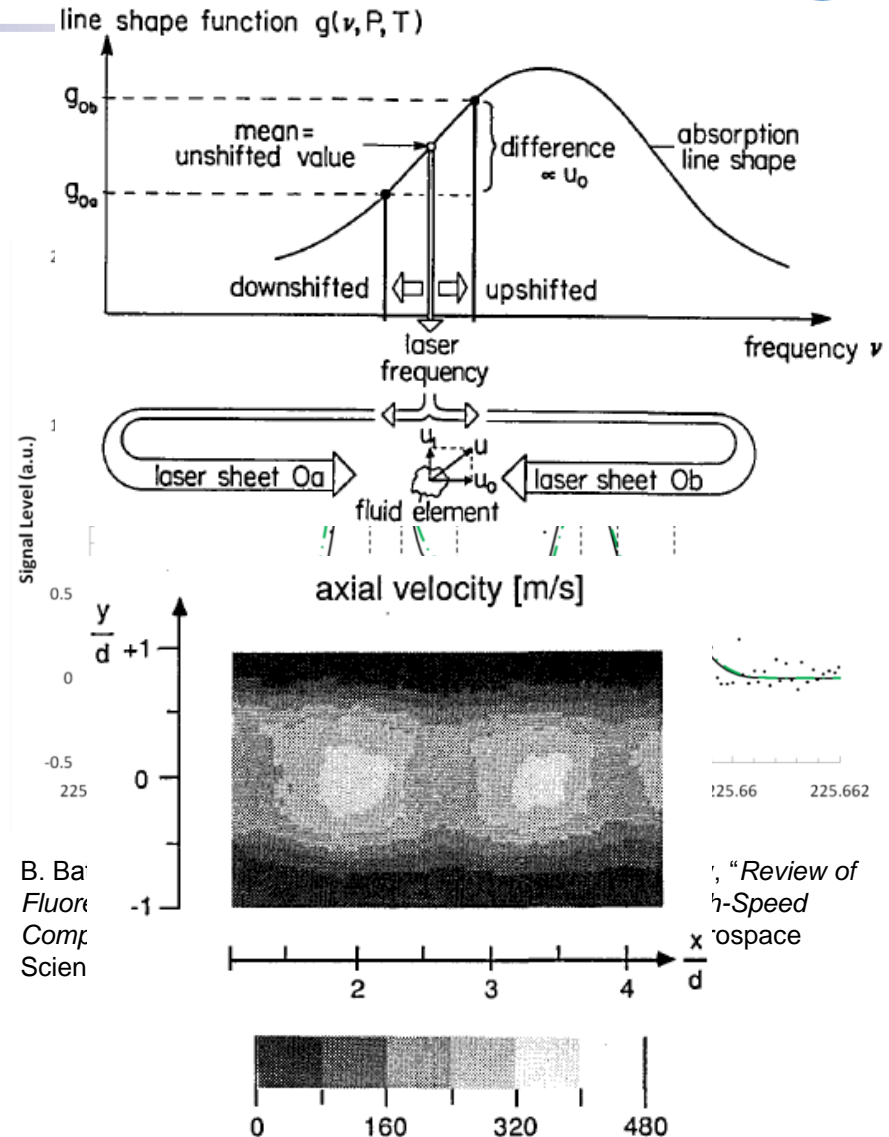
R. Hruschka, S. O'Byrne, and H. Kleine, "Two-component Doppler-shift fluorescence velocimetry applied to a generic planetary entry probe model," *Experiments in Fluids*, 48, pp. 1109-1120, 2010



Doppler-based LIF Velocimetry



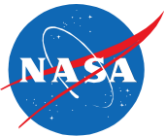
- Self-referenced tuning Doppler velocimetry
 - Does not require reference cell measurement
 - $v_0 = \frac{v_f + v_r}{2} \rightarrow U = \frac{c}{\cos \theta} \cdot \frac{(\Delta\nu/2)}{[(v_f + v_r)/2]}$
 - Laser passed through measurement volume, followed by a delay line that returns beam along original path
 - Requires high-speed measurement device (e.g. photomultiplier tube) to resolve forward and return signals
- Fixed frequency (single-shot)
 - Potential for time resolved velocity
 - Less accurate – estimating Doppler shift with few measurements



B. Hiller and R. Hanson, "Simultaneous planar measurements of velocity and pressure fields in gas flows using laser-induced fluorescence," *Applied Optics*, 27(1), January 1, 1988.



Doppler Shift Velocimetry



- Benefits
 - Capable of providing 1- or 2-component velocity maps
 - Relatively easy to implement
- Drawbacks
 - Typically not time resolved
 - Typically requires reference measurement
 - Spectral shift resulting from increased pressure needs to be accounted for
 - Requires a gas ‘seed’ to either be naturally present or introduced into the flow



Molecular Tagging Velocimetry



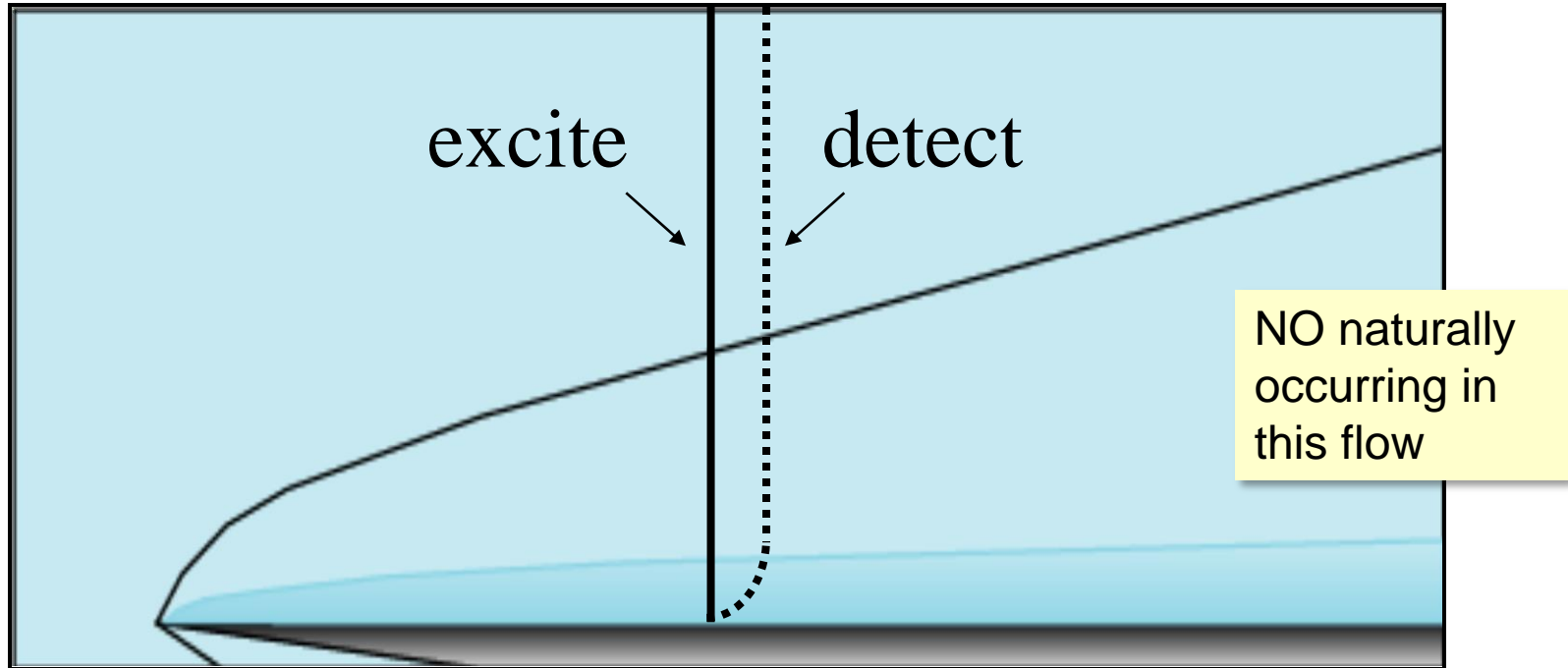
Single-Laser MTV



- Biacetyl (Hiller et al, 1984; Koochesfahani, 2007)
- Acetone (Lempert, 2002)
- NO (Danehy, 2003; Hsu, 2009; Bathel, 2011)
- I₂ (Balla, 2013)
- N₂ using FLEET (*Femtosecond laser electronic excitation tagging*) (Michael, 2011)
 - Does not require seeding
 - Does require an expensive fs laser
- *LIF lifetime must be long enough so molecules still emit light after (slightly) moved*



Single-laser LIF MTV

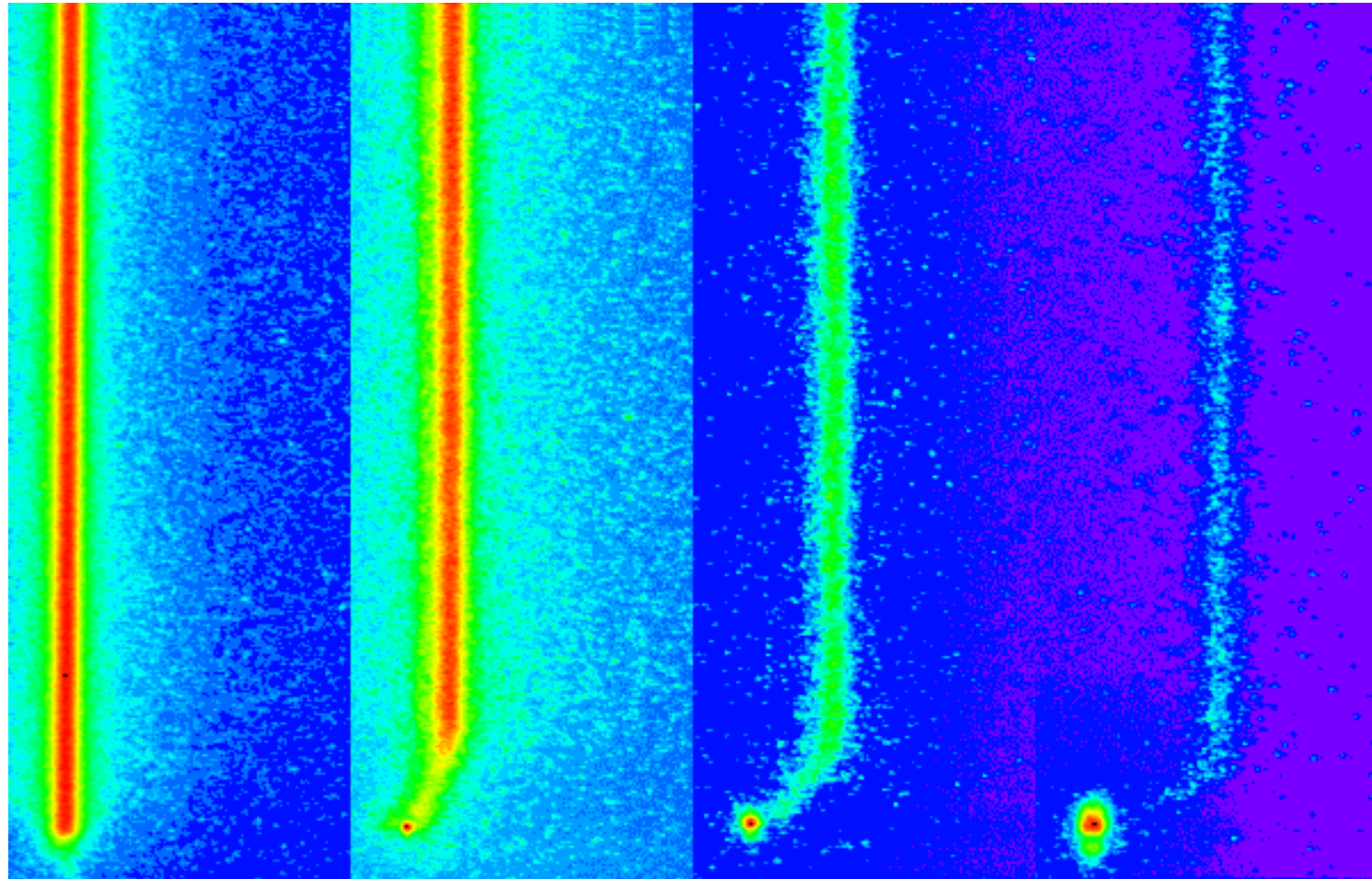


- Boundary layer: slow moving gas near surface
 - Important: heat transfer, drag, separation, etc.
- Instantaneous measure of 1 velocity component
 - Can be extended to 2 or 3 components

P. M. Danehy, S. O'Byrne, A. F. P. Houwing, J. S. Fox, and D. R. Smith, "Flow-Tagging Velocimetry for Hypersonic Flows Using Fluorescence of Nitric Oxide," AIAA Journal, 41(2), February 2003



MTV: Delayed Images



Delay = 0

250 ns

500 ns

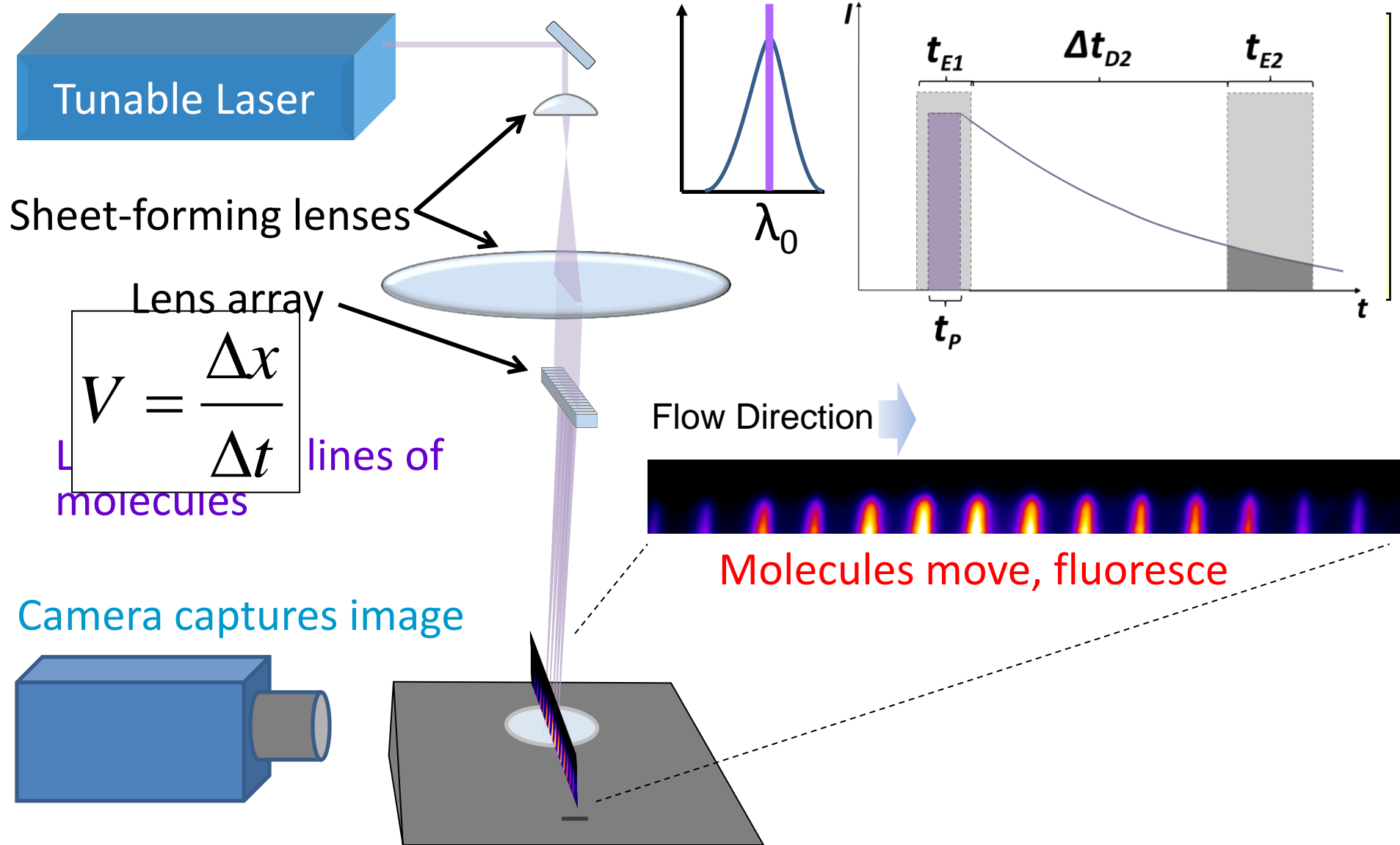
750 ns

In(data)
shown here

- Measurements performed on successive tunnel runs

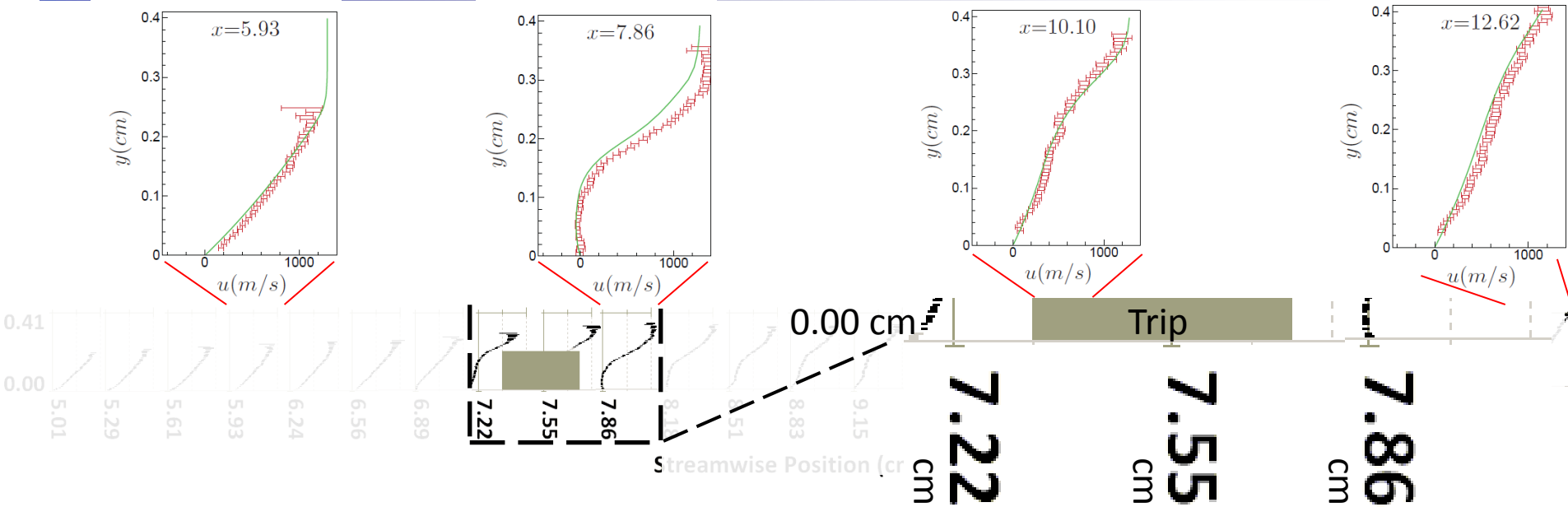


Single-laser MTV





Single-laser MTV



• Velocity Measurement

- Instantaneous ($<1 \mu\text{s}$), single-component measure of 25 profiles simultaneously
- Developed through uncertainty analysis methodology
- Data used in subsequent CFD study by Iyer et al. of Univ. of Minnesota (AIAA 2011-566)

B. F. Bathel, P. M. Danehy, J. A. Inman, S. B. Jones, C. B. Ivey, C. P. and Goyne, "Velocity Profile Measurements in Hypersonic Flows Using Sequentially Imaged Fluorescence-Based Molecular Tagging," AIAA Journal, 49(9), September 2011



Single-laser MTV

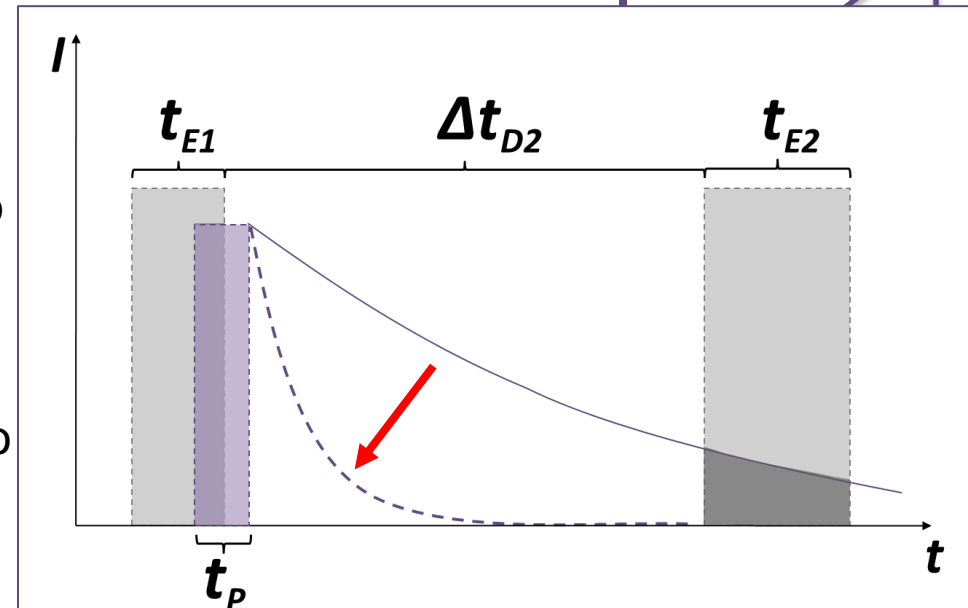
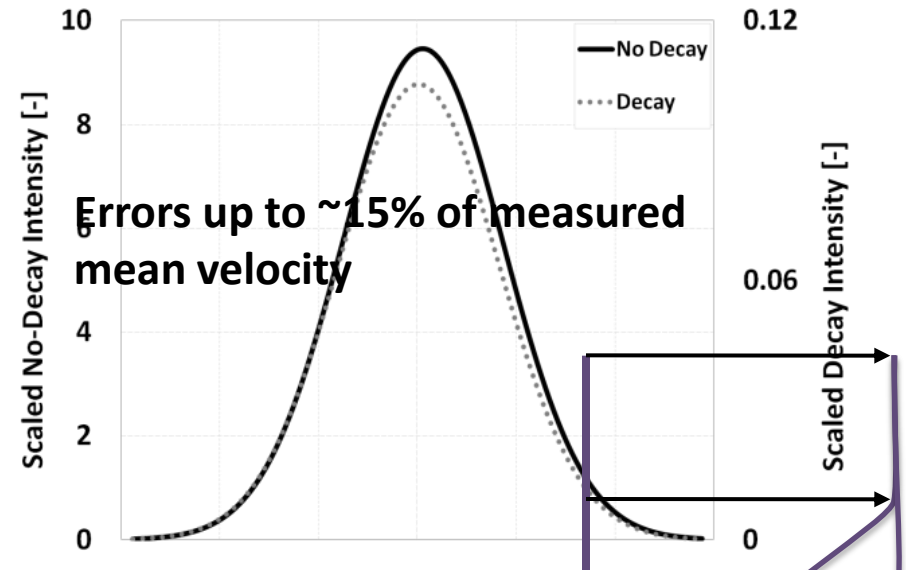


- **Analysis**

- Uncertainties in mean: as good as 3% of freestream (~ 1000 m/s) for 38 images
- Modeled error from intensity decay, exposure duration, motion blur
- Error from velocity component parallel to MTV profiles quantified

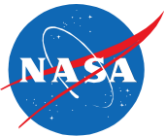
- **Study conclusions**

- Velocity gradients can bias measurement
- Scatter off of the model surface limited proximity of measurement to the wall
- Limited to low-pressure conditions
- Need higher pressure capability for higher Reynolds number required to study laminar-to-turbulent transition at least on this short model

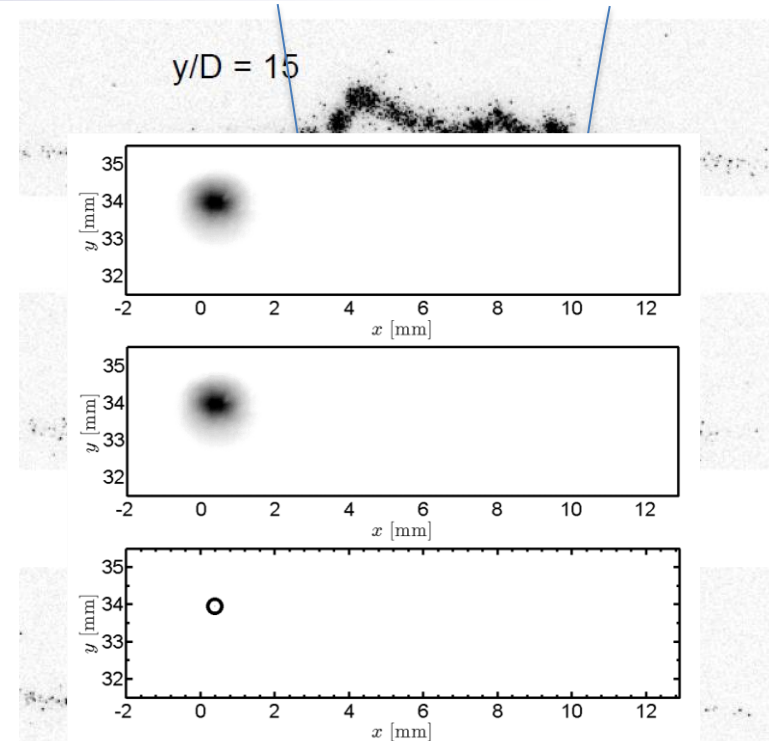




Single-laser MTV: FLEET



- Simple principle:
 - Works with N_2 seed
 - Femtosecond laser is focused down to a line or spot
 - Gas glows for 10's of μs
- Originally developed at Princeton:
 - Air jet at room temperature, atmospheric pressure
 - Non-linear process
- Recently applied to transonic cryogenic flow at NASA Langley
 - Tracking of spot provided 2-D velocimetry
 - ~ 1 m/s accuracy and precision



R. Burns, P. Danehy, S. Jones, B. Halls, and N. Jiang, "Application of FLEET Velocimetry in the NASA Langley 0.3-Meter Transonic Cryogenic Tunnel," AIAA Paper 2015-2566, 31st AIAA Aerodynamic Measurement Technology and Ground Testing Conference, June 2015.

J. Michael, M. Edwards, A. Dogariu, and R. Miles, "Femtosecond laser electronic excitation tagging (FLEET) for quantitative velocity imaging in air," *Applied Optics*, 50(26), September 10, 2011.

N_2
Jet



Single-laser MTV



- Benefits

- Instantaneous measurement
- Capable of providing velocity information along a line (1-component) or at grid points (2-component)
- ‘Seedless’ methods available
- Relatively simple to setup

- Drawbacks

- Reduced spatial resolution compared to Doppler shift approach
- Operational limits often dictated by fluorescence lifetime
- Potential for model damage
- Potential for altering thermodynamic state of gas



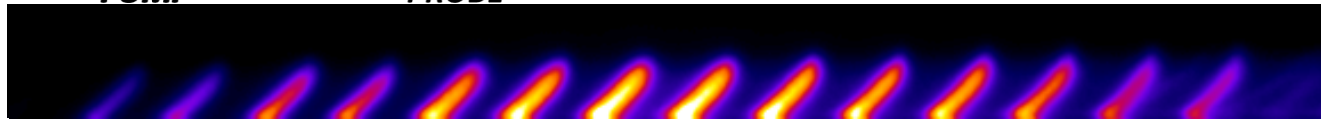
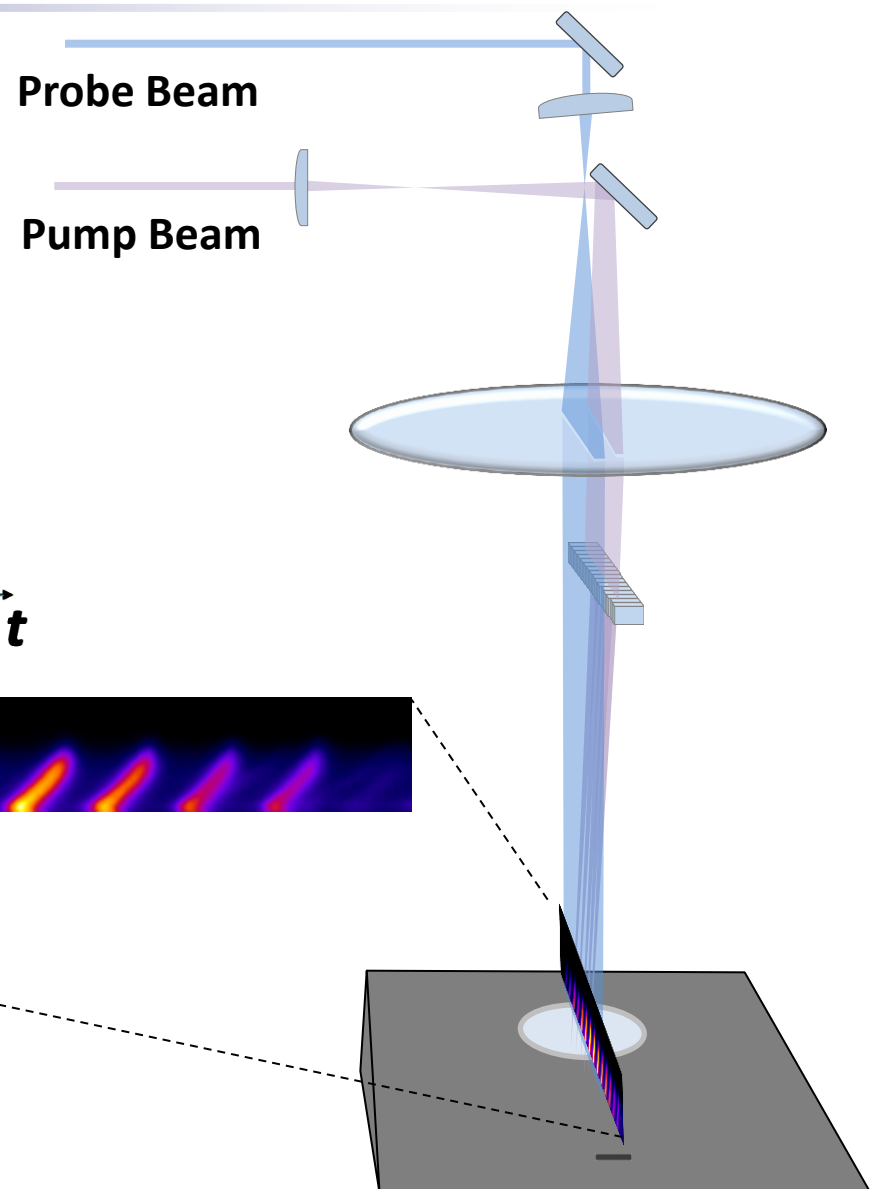
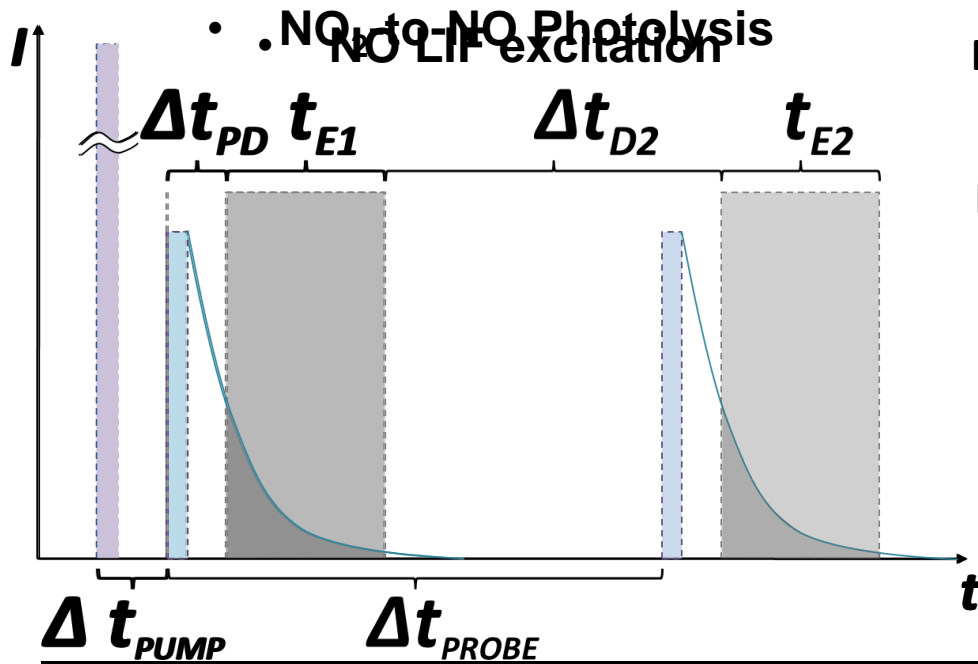
Multilaser MTV



- Typically, one laser generates a line, series of lines or a grid pattern by, ionization ($\text{LEI}^{126-128}$), vibrational excitation (RELIEF¹²⁹⁻¹³¹), photolysis, bleaching or other process. Additional laser(s) read out pattern.
 - Example: Excimer laser at 193 nm + $\text{N}_2 + \text{O}_2 \rightarrow \text{NO}$
 - Air Photolysis and Recombination Tracking (APART)
 - Dam et al, Optics Letters, 26 (1), pp. 36-38 2001
- A list of partner species used in the photolysis writing and reading process includes:
 - $\text{H}_2\text{O}-\text{OH}$,¹³³⁻¹³⁹ $\text{N}_2\text{O}-\text{NO}$,¹⁴⁰ O_2-O_3 ,^{141,142}
 - $\text{N}_2/\text{O}_2-\text{NO}$,¹⁴³⁻¹⁴⁶ and NO_2-NO .^{116,147-154}
- Method can use air constituents (N_2/O_2 , O_2 , N_2) or can be seeded (H_2O , N_2O , NO_2 , Na, etc.).
 - We have used $\text{NO}_2 \rightarrow \text{NO}$ to study transition

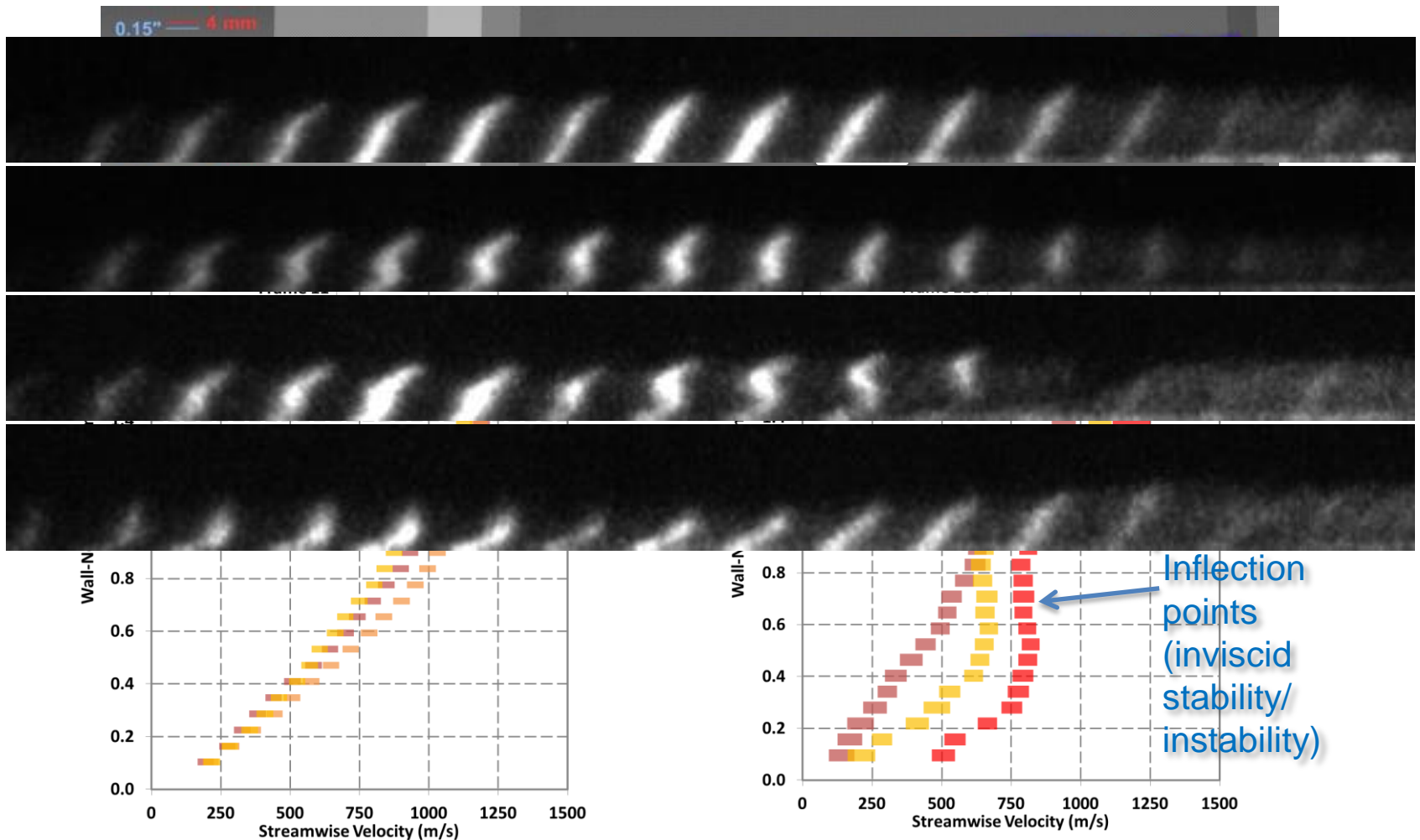


Multilaser MTV





Velocimetry: 1-mm Tall Trip (centerline)



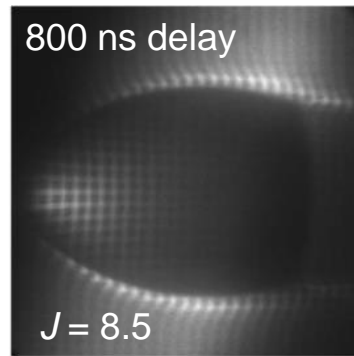
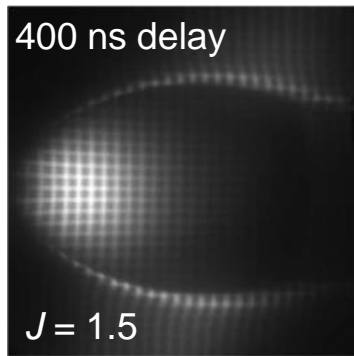
- Transition-to-turbulence study (Bathel et al. AIAA-2011-3246)
 - Reynolds number requirement necessitated higher operating pressures
 - Signal lifetime too short for single-laser NO LIF MTV



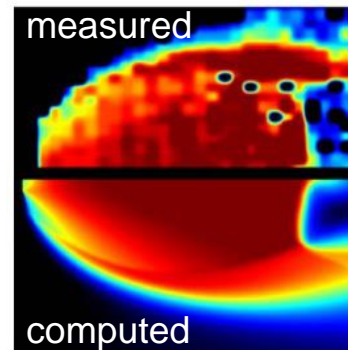
3 laser MTV: measure u , v , T



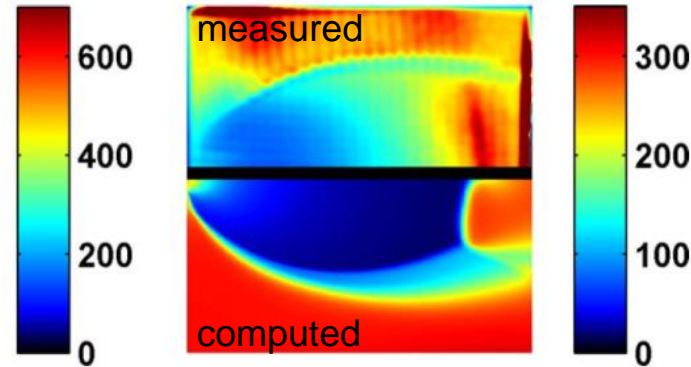
- Texas A&M has used 3 laser technique with crossed beam pattern for 2-component velocity and temperature in an underexpanded N_2 jet flow with NO_2 :
 - VENOM: **vibrationally excited nitric oxide monitoring**
 - Excite to $v' = 1$ state



Raw data images



U-Velocity (m/s)
(~5% uncertainty)

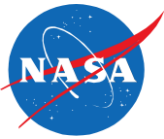


Temperature (m/s)
(~9-35% uncertainty)

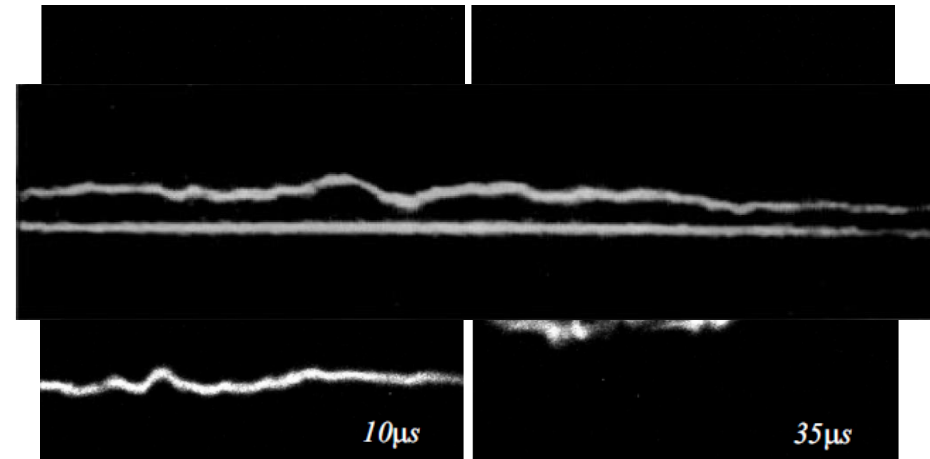
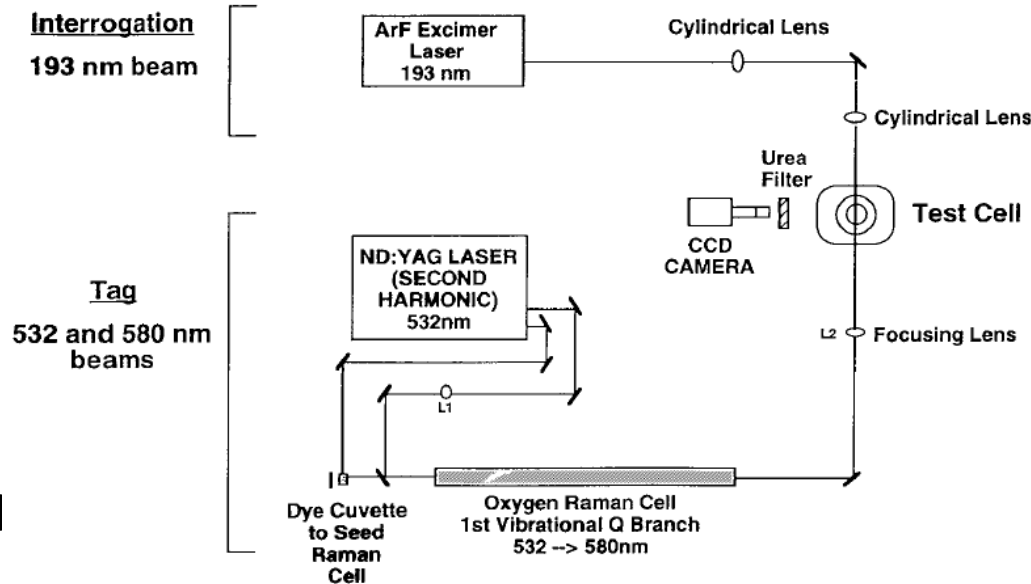
R. Sánchez-González, R. Srinivasan, R. D. W. Bowersox, and S. W. North, “Simultaneous velocity and temperature measurements in gaseous flowfields using the vibrationally excited nitric oxide monitoring technique: a comprehensive study,” *Applied Optics*, 51(9), pp. 1216-1228, March 20, 2012



Multilaser MTV: Unseeded



- **Air *P*hotolysis And *R*ecombination Tracking (APART)**
 - Nitric oxide generated in unseeded air via dissociation by UV excimer laser beam
 - NO then probed with LIF excitation wavelengths
- **Raman *E*xcitation and *L*aser-Induced *E*lectronic *F*luorescence (RELIEF)**
 - O₂ vibrational excitation via Raman pumping
 - UV Excimer laser used to probe 1st vibration state of oxygen
 - Works for flows where $T < \sim 750$ K



R. Miles, J. Grinstead, R. Kohl, and G. Diskin, "The RELIEF flow tagging technique and its application in engine testing facilities and for helium-air mixing studies," *Measurement Science & Technology*, 11, pp. 1272-1281, 2000.



Multi-laser MTV



- Benefits
 - Capable of providing instantaneous velocity along a line (1-component) or at grid points (2-component)
 - Several ‘seedless’ methods available
 - Not limited by fluorescence lifetime (works in high P)
- Drawbacks
 - Reduced spatial resolution compared to Doppler shift approach
 - More complicated setup – requires multiple lasers
 - Potential for model damage
 - Altering thermodynamic state of gas



Summary



Velocimetry Techniques



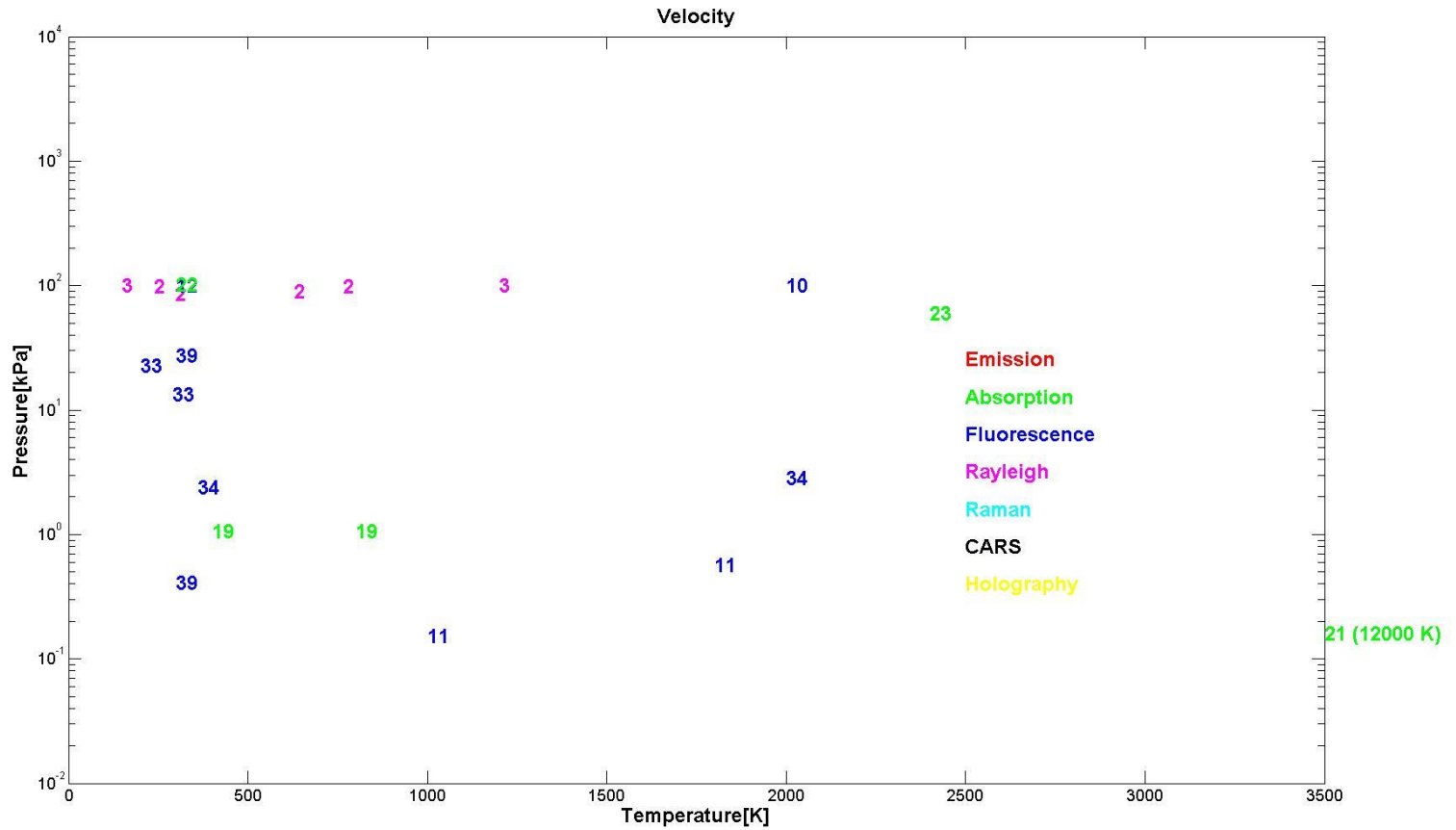
- Introduced three fluorescence-based techniques
 - Doppler shift velocimetry
 - Single-laser molecular tagging velocimetry
 - Multi-laser molecular tagging velocimetry
- Provided representative examples for each of the techniques
- Discussed benefits and drawbacks for each approach
- Following presentation will provide a more in-depth discussion of laser-induced fluorescence used for many of these MTV techniques.



Backup Charts

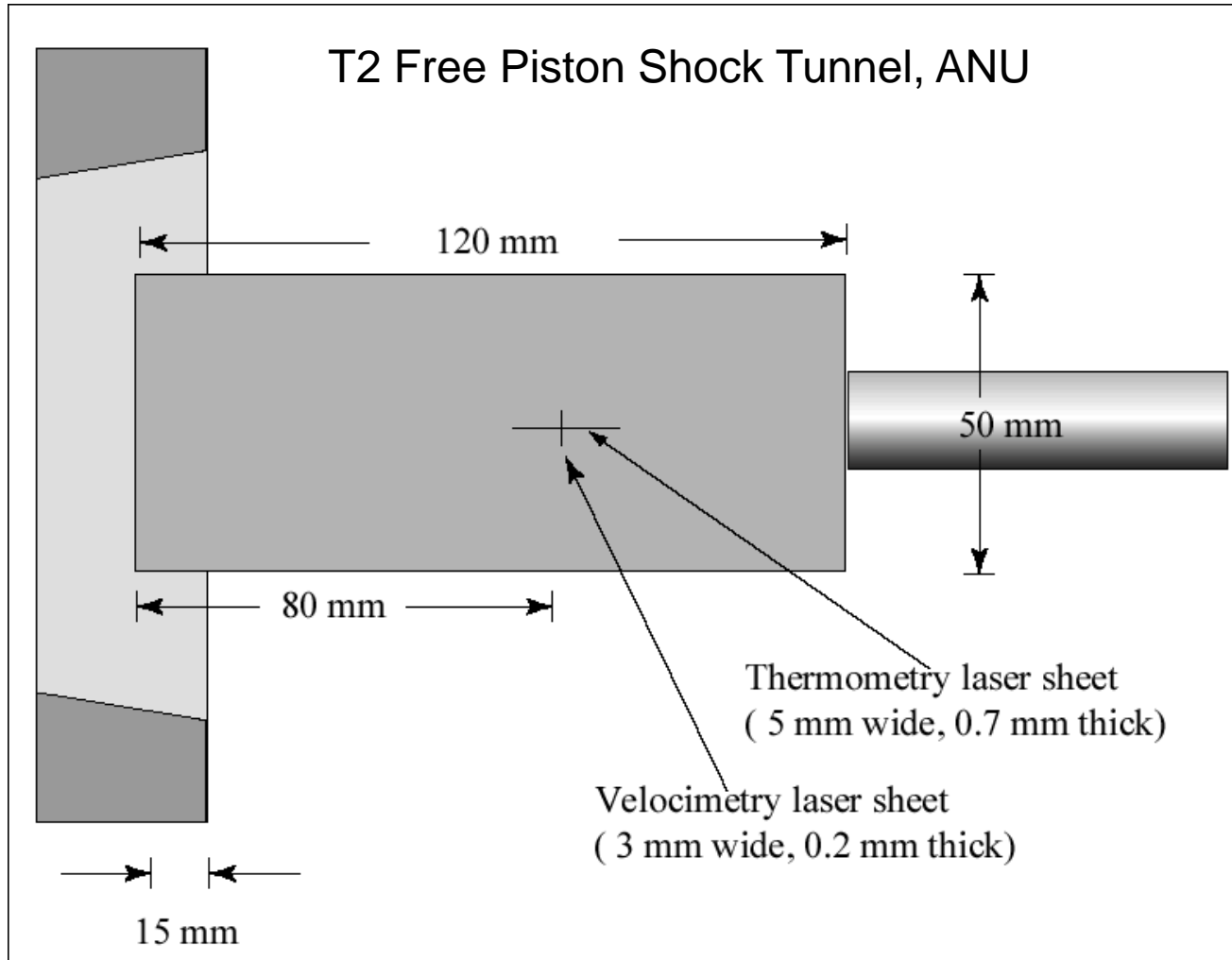


Velocity





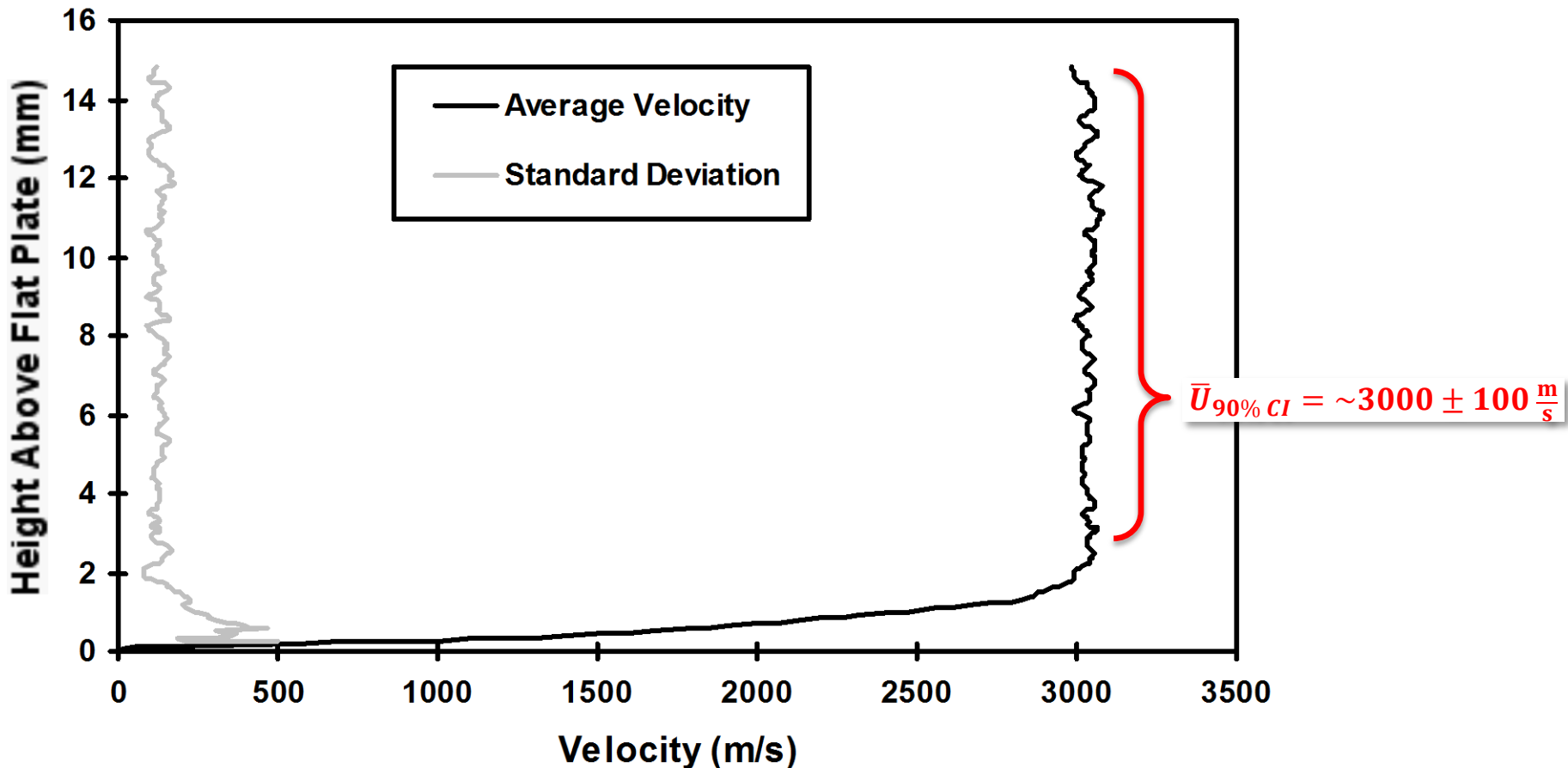
Experimental Setup: Top View



Velocity ~ 3000 m/s; Mach Number = 7, laminar boundary layer



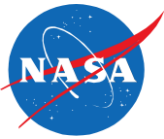
Average of Single-Shot Measurements



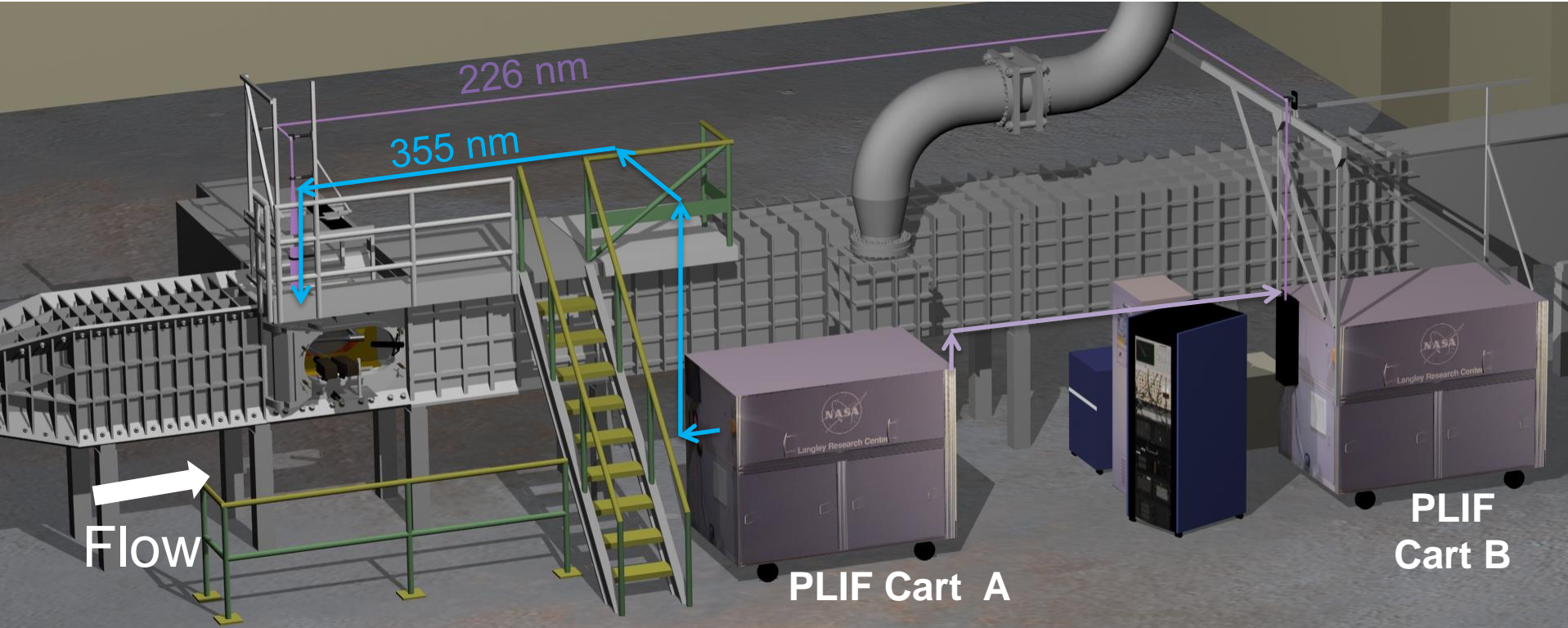
- Freestream velocity is uniform at 3035 ± 60 m/s.
- 95% boundary layer thickness is 1.4 ± 0.1 mm.
- Single shot measurement precision: ~ 60 m/s out of ~ 3000 m/s (2%)
 - spatially averaged uncertainty (freestream region) ~ 100 m/s (3%)



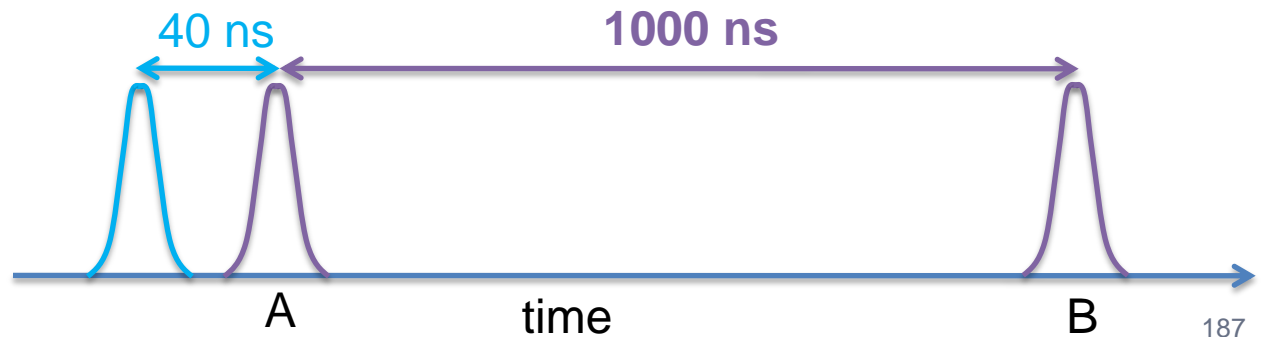
Three-Laser MTV ($\text{NO}_2 \rightarrow \text{NO}$ velocimetry)



(for details of velocimetry method, see Bathel et al, AIAA-2011-3246 and others incl. TAMU¹⁴⁹, OSU¹⁵⁰, etc.)

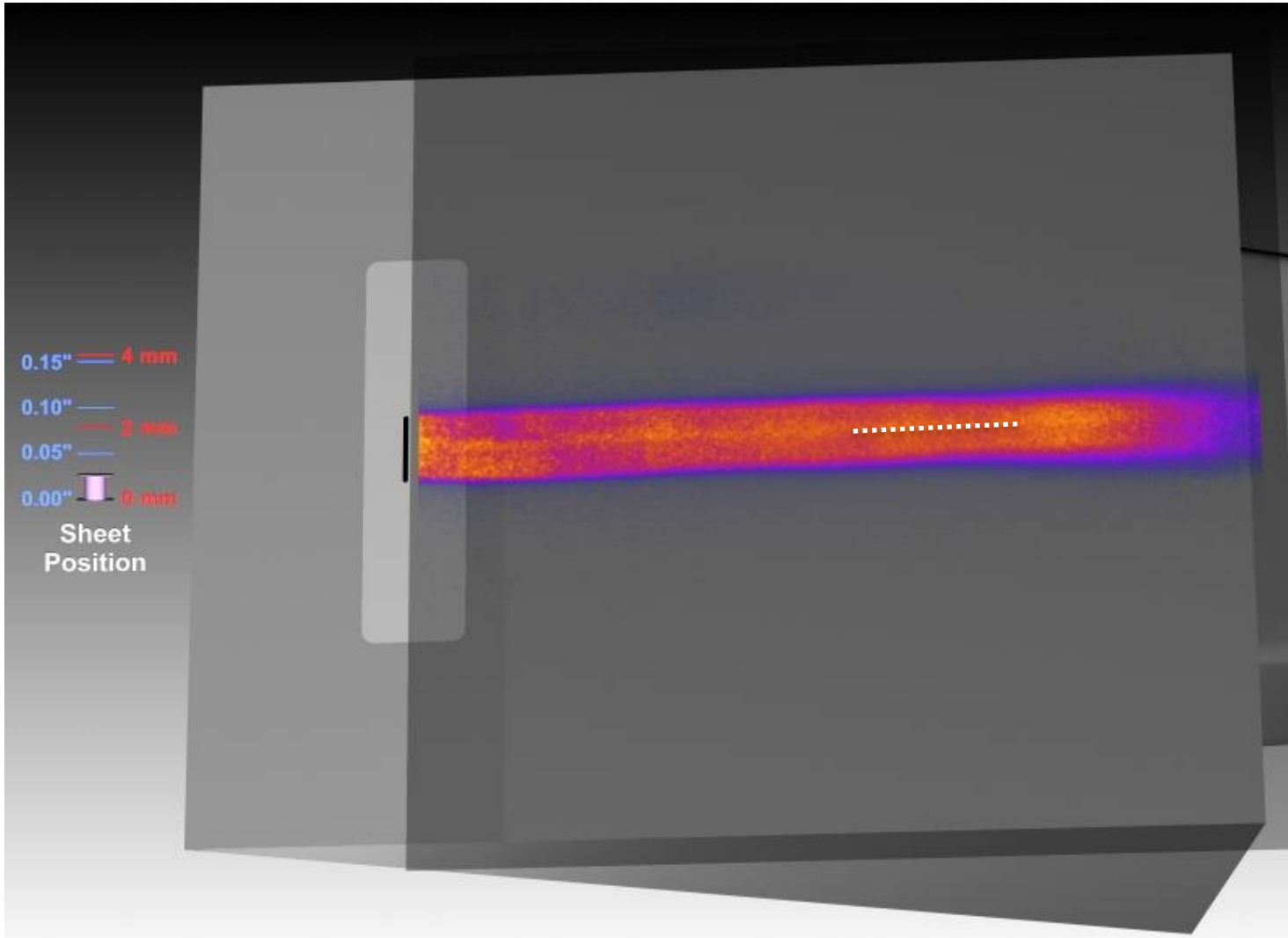


$\text{NO}_2 + 355 \text{ nm} \rightarrow \text{NO}$
Write lines of NO into
 NO_2 seeded in the flow





Flow Visualization: No trip



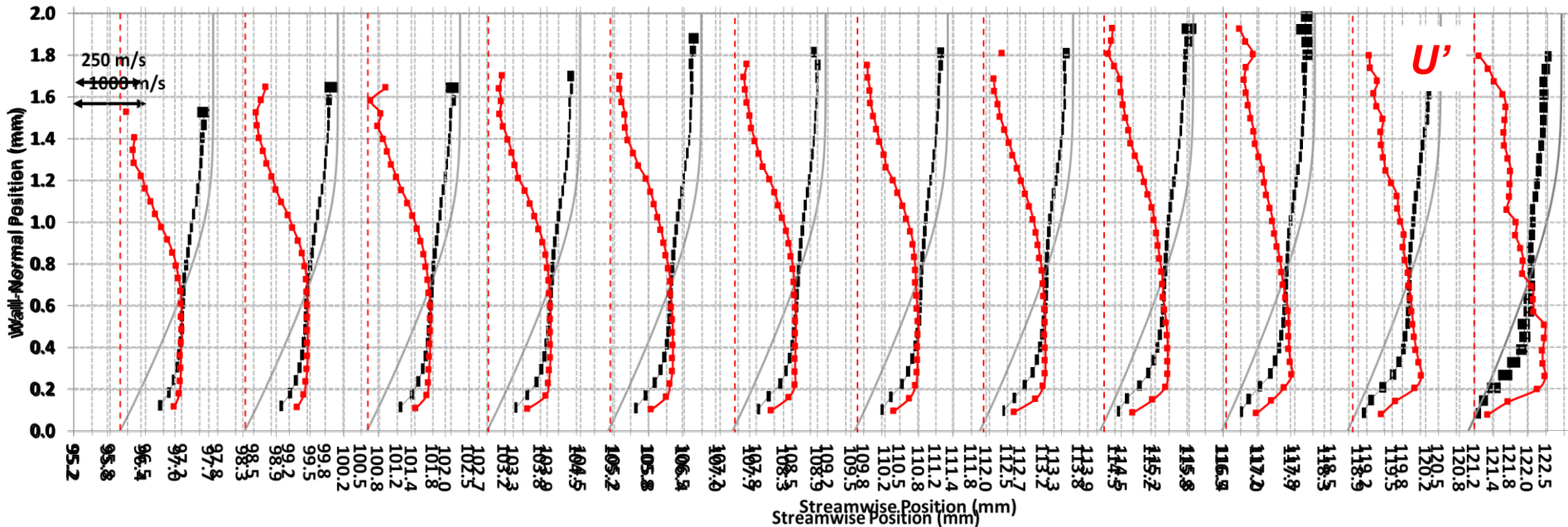
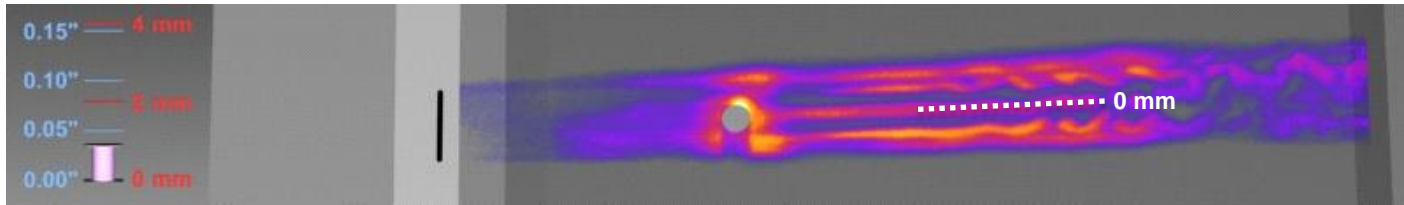
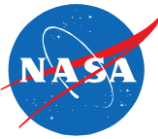
PA = 20°
mid-Re

$M_e \approx 4.2$

- Flow appears laminar when no trip is present



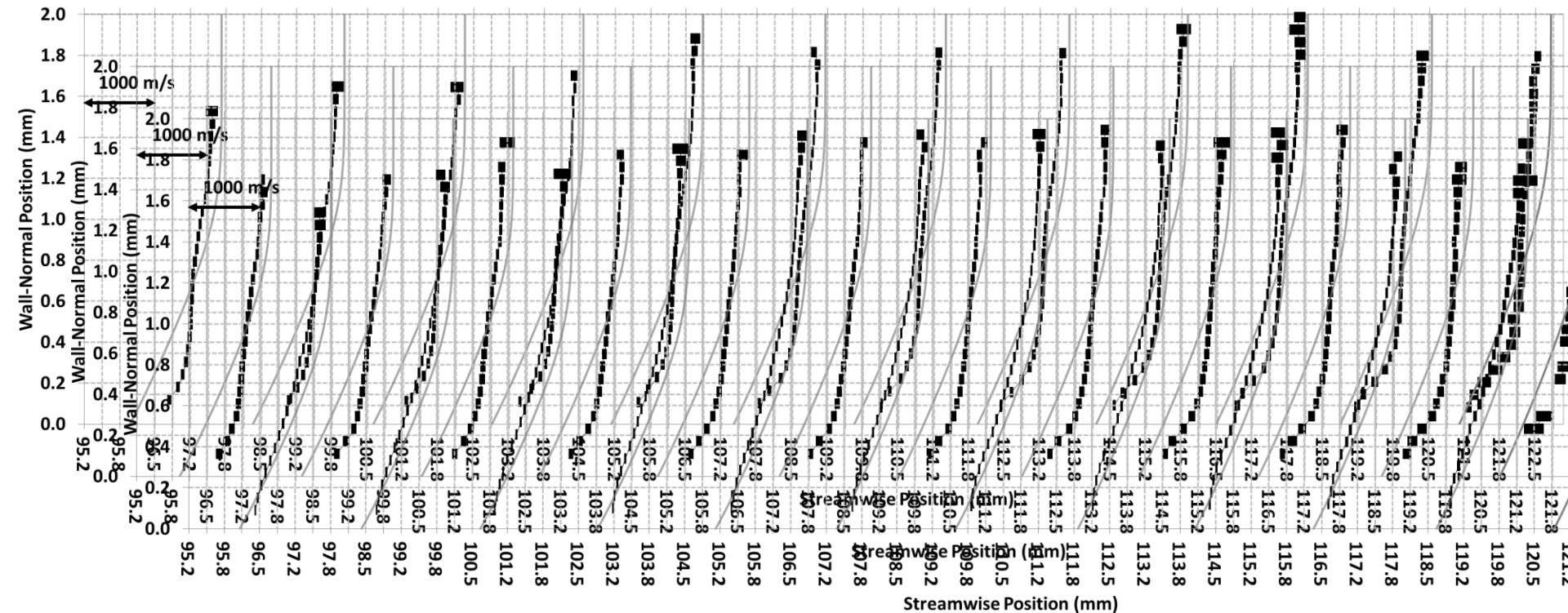
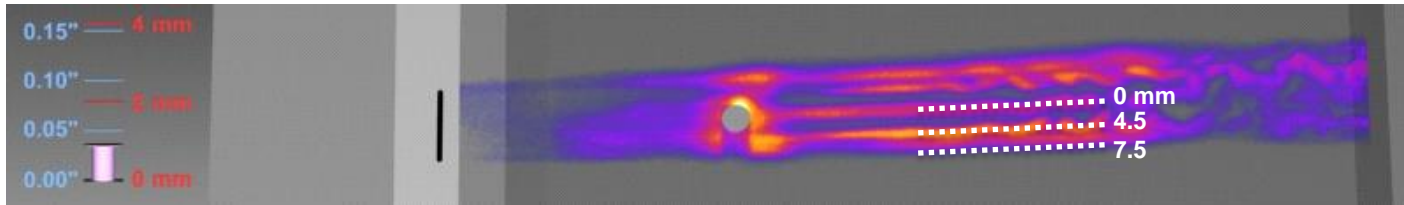
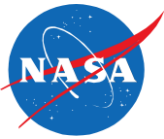
Velocimetry: 1-mm Tall Trip (centerline)



- Velocity profile is full near flat plate with a deficit near edge of BL
 - Note: 2x lower flowrate in this run compared to no-trip case previously shown.
- U' data has increased to peak ~ 250 m/s (3x larger than laminar case).
- Shape of U' profile changes slightly with distance downstream.



Velocimetry: 1-mm Tall Trip



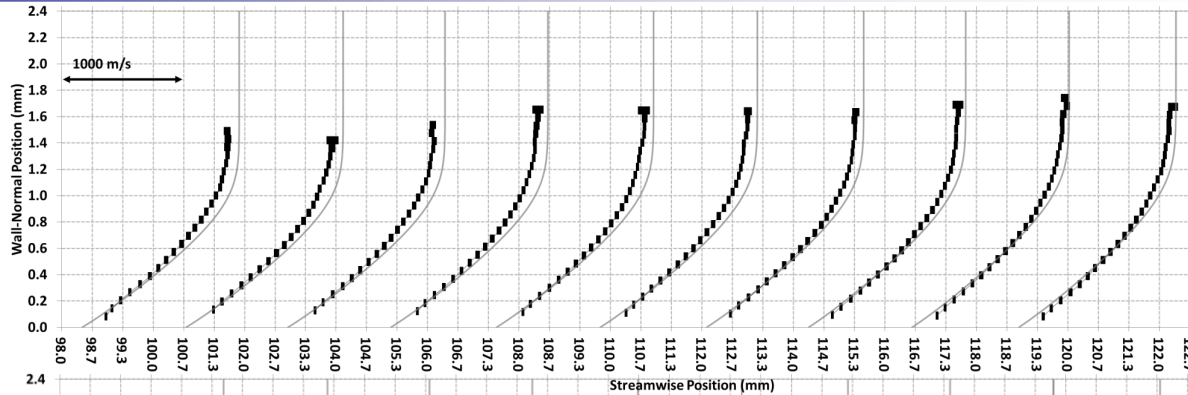
- 4.5 mm profiles show profiles most different from laminar
- Flow becomes more laminar far from centerline (similar to flow vis)
 - U' drops back to ~ 80 m/s



Comparison of U for different trip heights

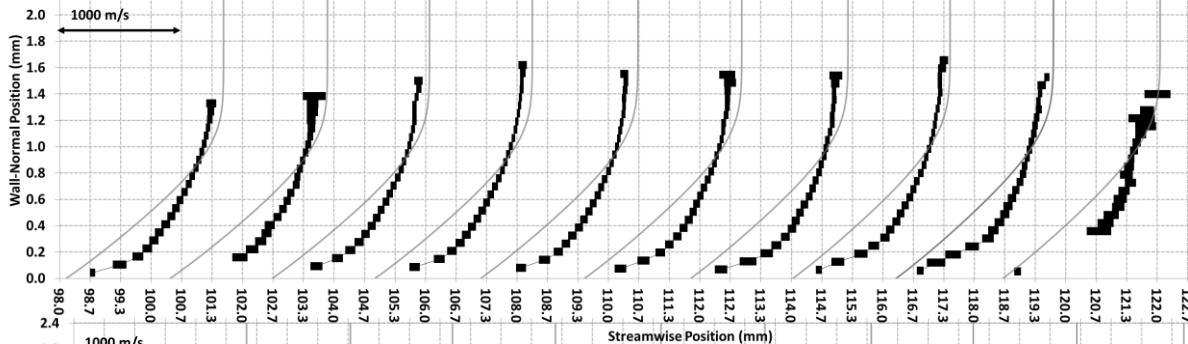


No Trip



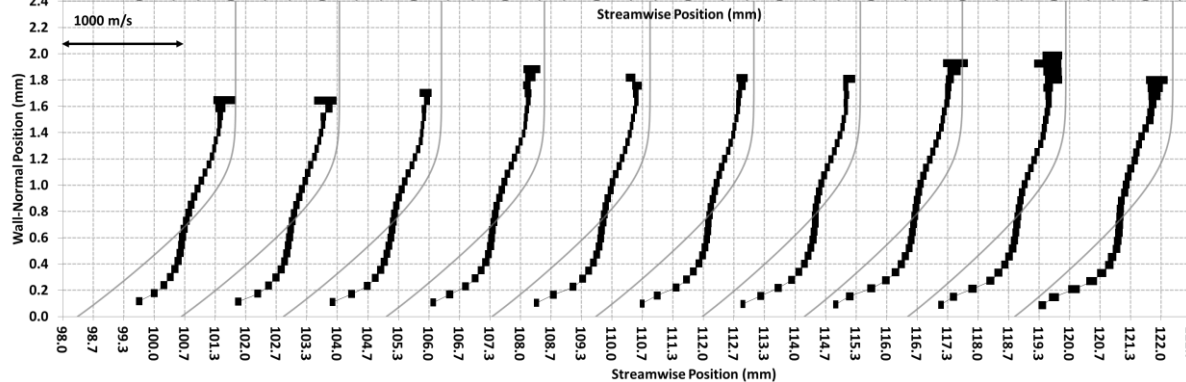
*measurements
on centerline*

0.53-mm Trip



$Re_{kk} \approx 400$

1.0-mm Trip

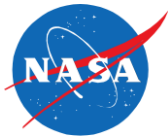


$Re_{kk} \approx 2000$

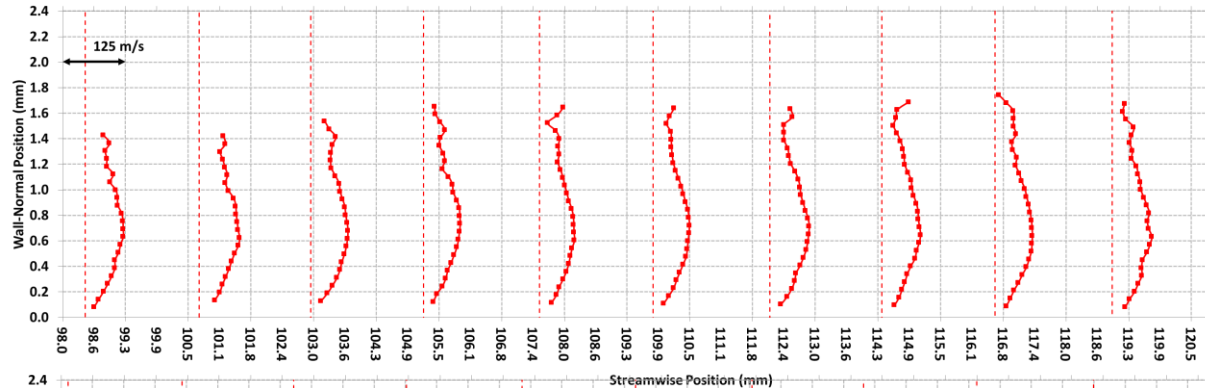
- 0.53 mm trip profile is between no and 1-mm but no inflection point.



Comparison of U' for different trip heights

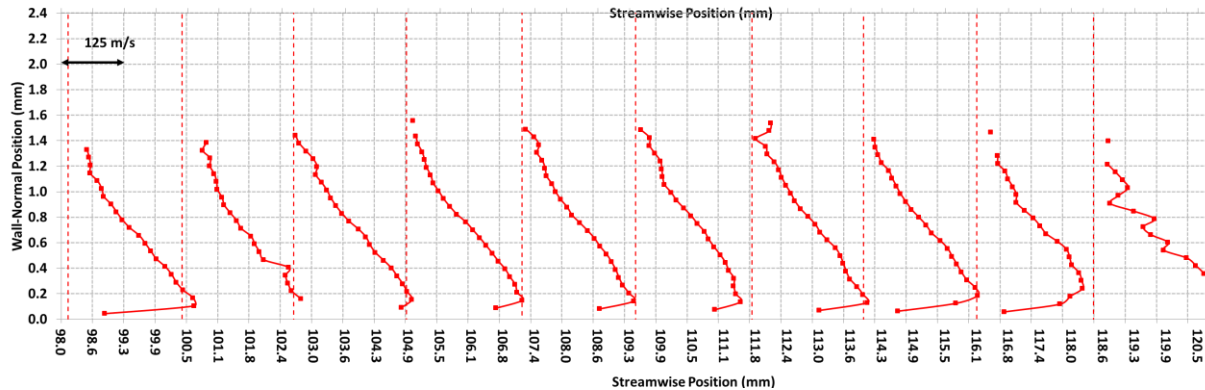


No Trip

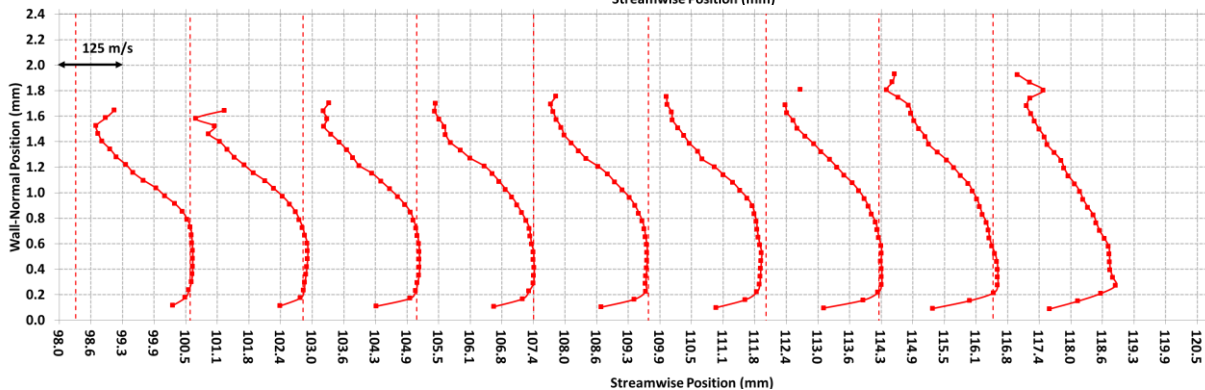


*measurements
on centerline*

0.53-mm Trip



1.0-mm Trip



- 0.53 mm trip U' peak much closer to plate.



Three-laser MTV: uncertainty & design



• Analysis

- Uncertainty for high s/n data
 - Mean: 1% of edge velocity (~1300 m/s) in 200 images
 - Single-shot: 1-2% of edge velocity
- Measurement within 100 μm from wall

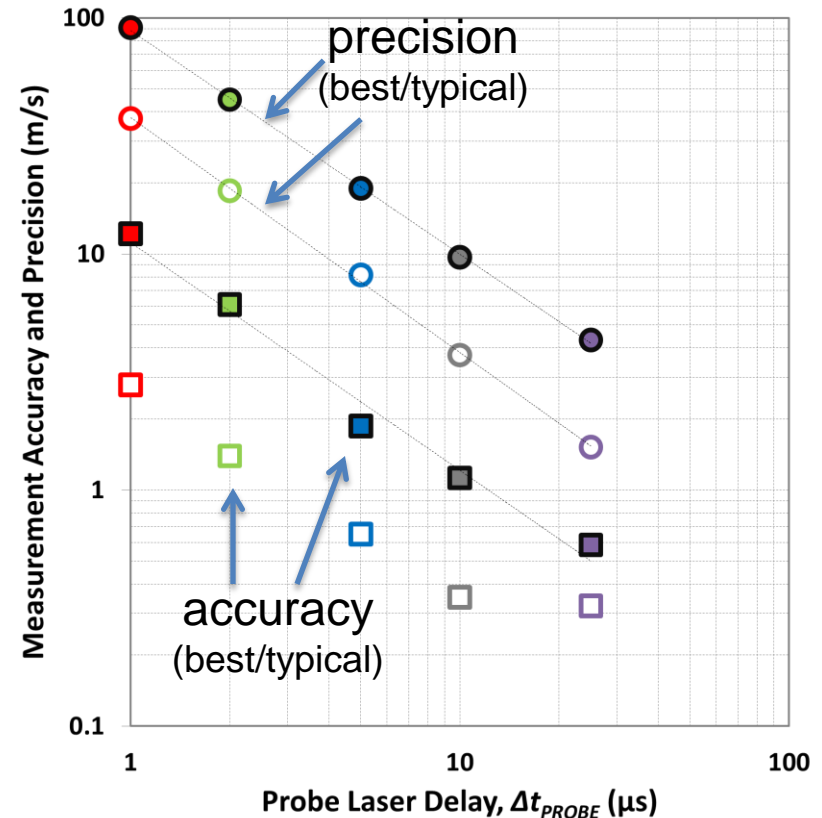
• Tradeoffs for experiment design

- Accuracy and precision improve with probe delay
- Spatial resolution worse with longer probe delay
 - Can use longer delay for slow flow
- Current configuration requires relatively large blowing rates for adequate signal-to-noise
 - May be significant wall-normal velocity component

1 μs

2 μs

5 μs

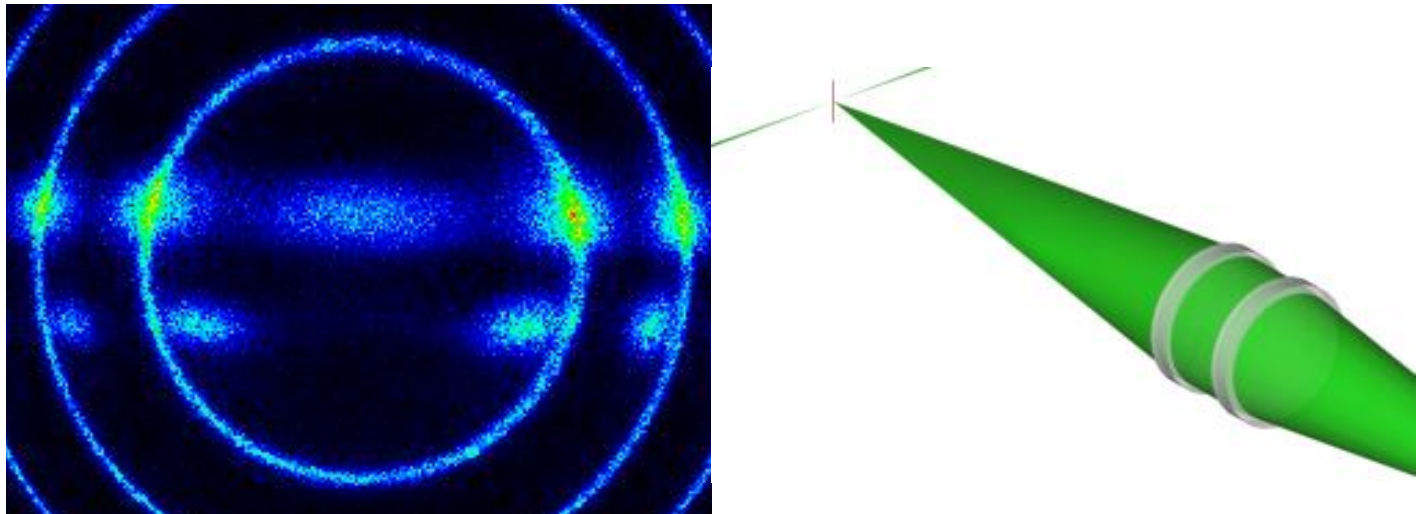




Intro to Rayleigh and Raman Spectroscopy for in Hypersonic Nonequilibrium Flows

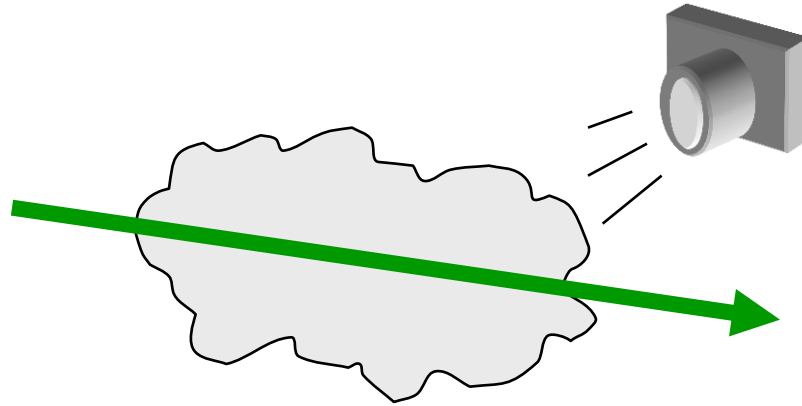


Paul Danehy, NASA Langley Research Center, Virginia, USA





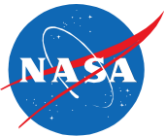
Rayleigh and Raman Scattering



- When light passes through a gas:
 - LIF is a *resonant* absorption/emission process
 - Mie, Rayleigh and Raman are scattering processes
 - Mie Scattering: $d \geq \lambda$ (d is the particle size)
 - Spontaneous Rayleigh and Raman scattering: $d \ll \lambda$
- Will explain Rayleigh and Raman two ways
 - Physical interpretation
 - Classical description
 - (Not going to discuss quantum treatment)



Rayleigh Scattering

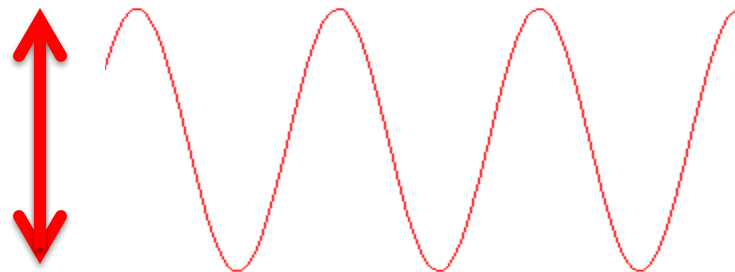


- Rayleigh scattering:
 - Electric field causes electron cloud to oscillate with respect to the nucleus: induced dipole



<http://www.timkelf.com/Research/ResearchSERS.html>

- An oscillating dipole acts like an antenna: radiates!
 - Radiation is perpendicular to oscillation

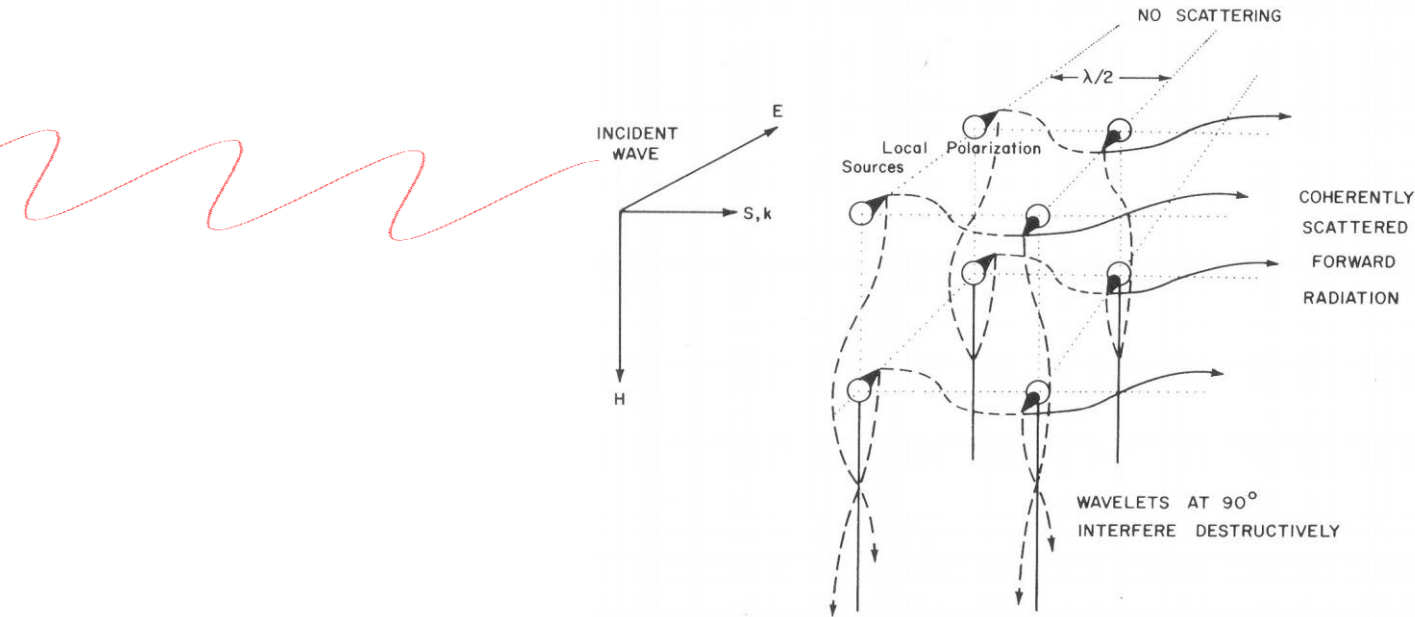




Many Particle Scattering



- A plane-wave perturbs many particles: they radiate
 - Interfere constructively in direction of propagation
 - Interfere destructively in other directions



G.C. Baldwin "An introduction to nonlinear optics." New York: Plenum Press, (1969).

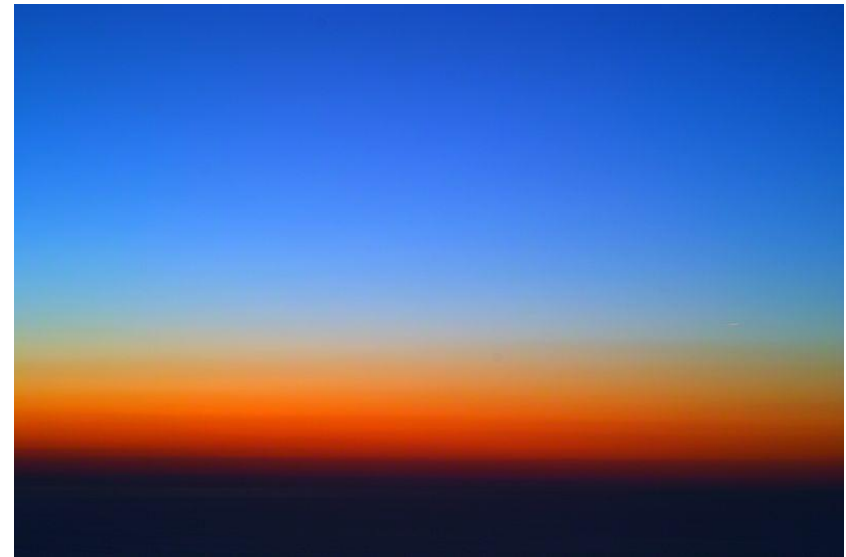
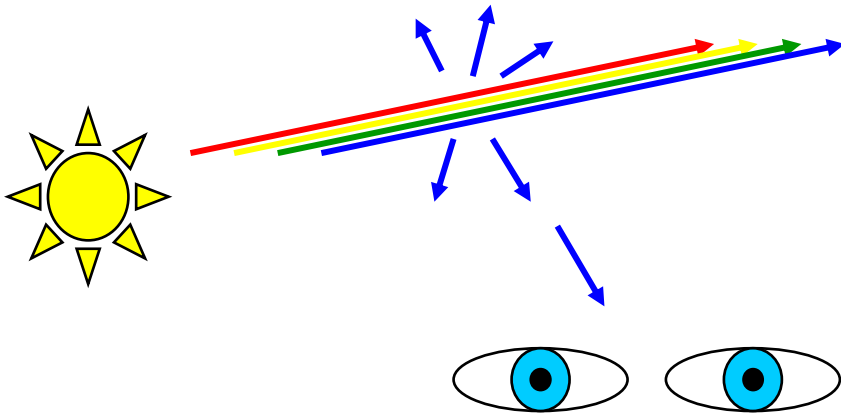
- If exact same number of particles everywhere in gas, destructive interference would give no side scatter
 - But random statistical variation in particle concentration: deconstructive interference is incomplete: Rayleigh Scattering!



Rayleigh Scattering



- Very weak process
 - 1 photon in 0.1 million scatters / meter at STP
- Wavelength dependence: $1/\lambda^4$



Rayleigh scattering in the atmosphere after sunset, picture taken over the ocean, at 500m altitude.

http://ms.wikipedia.org/wiki/Selerakan_Rayleigh

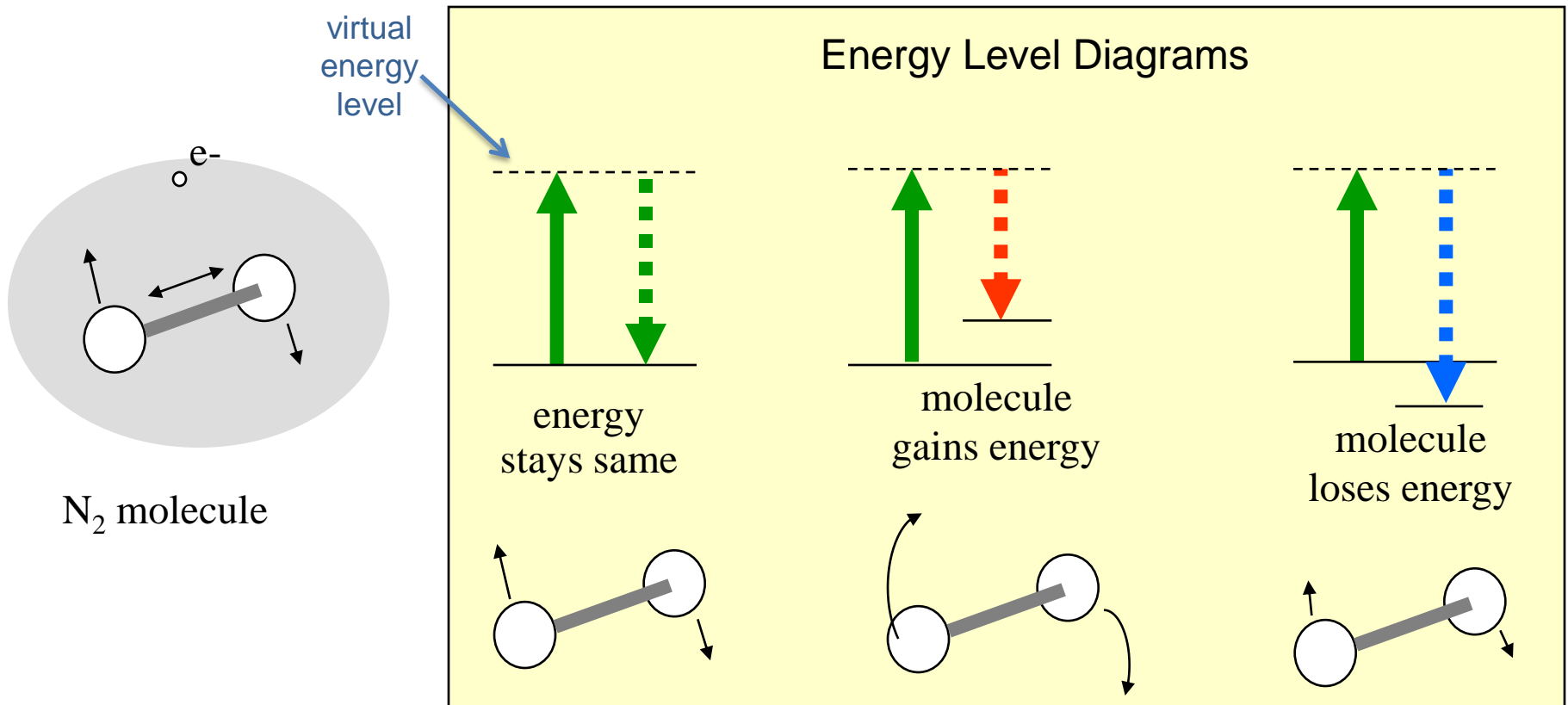
- Causes blue sky and red sunsets
 - Mie scattering from aerosols also contributes



Raman Scattering



- Similar to Rayleigh scattering but molecules gain or lose energy during scattering process
- Raman x1000 lower probability than Rayleigh



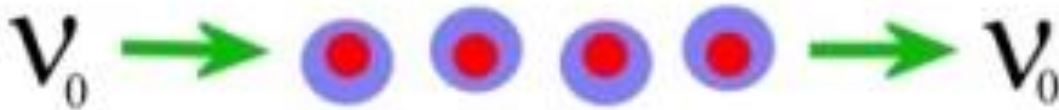


Raman Scattering

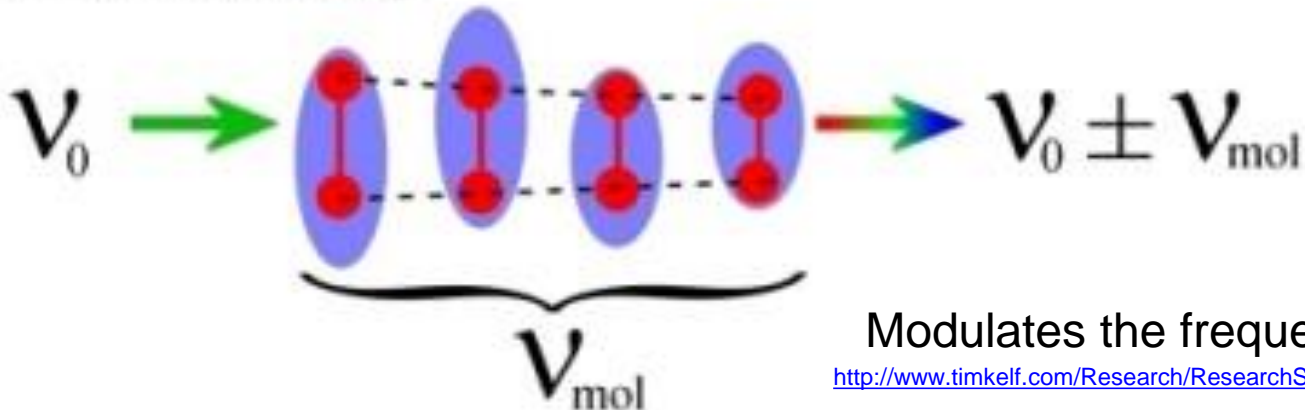


- Raman scattering results in a frequency shift
 - Molecule vibrating at frequency ν_{mol}

Rayleigh Scattering



Raman Scattering

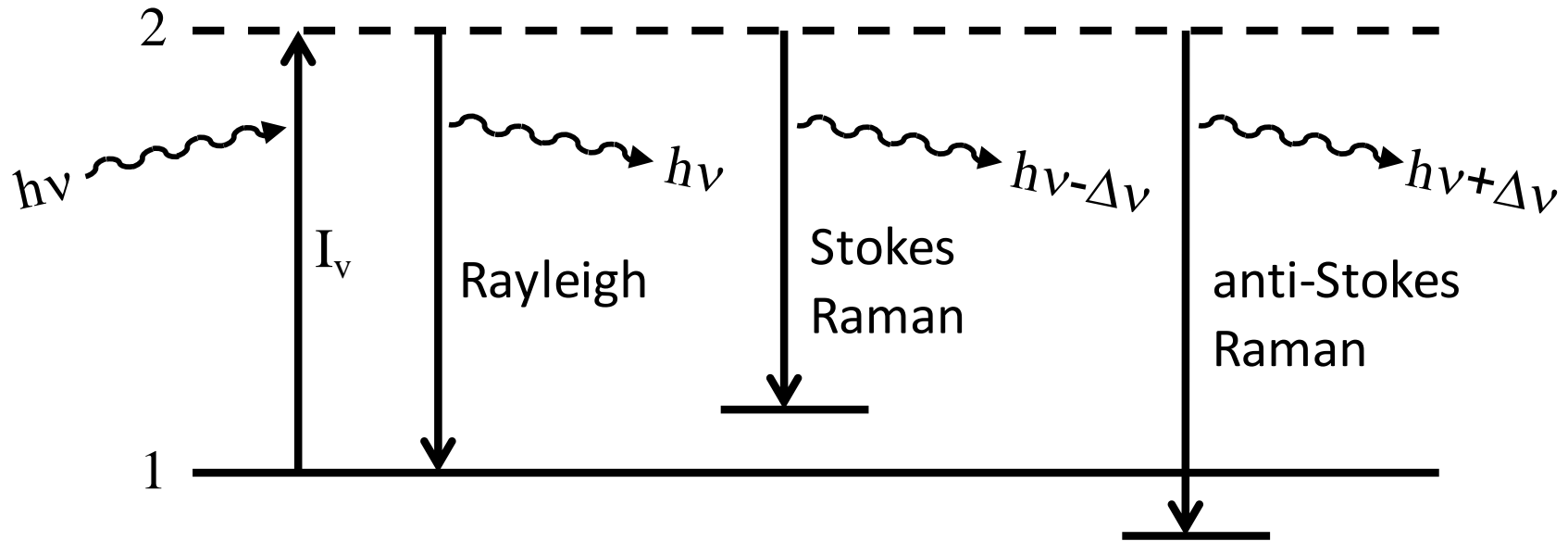


Modulates the frequency

<http://www.timkelf.com/Research/ResearchSERS.html>



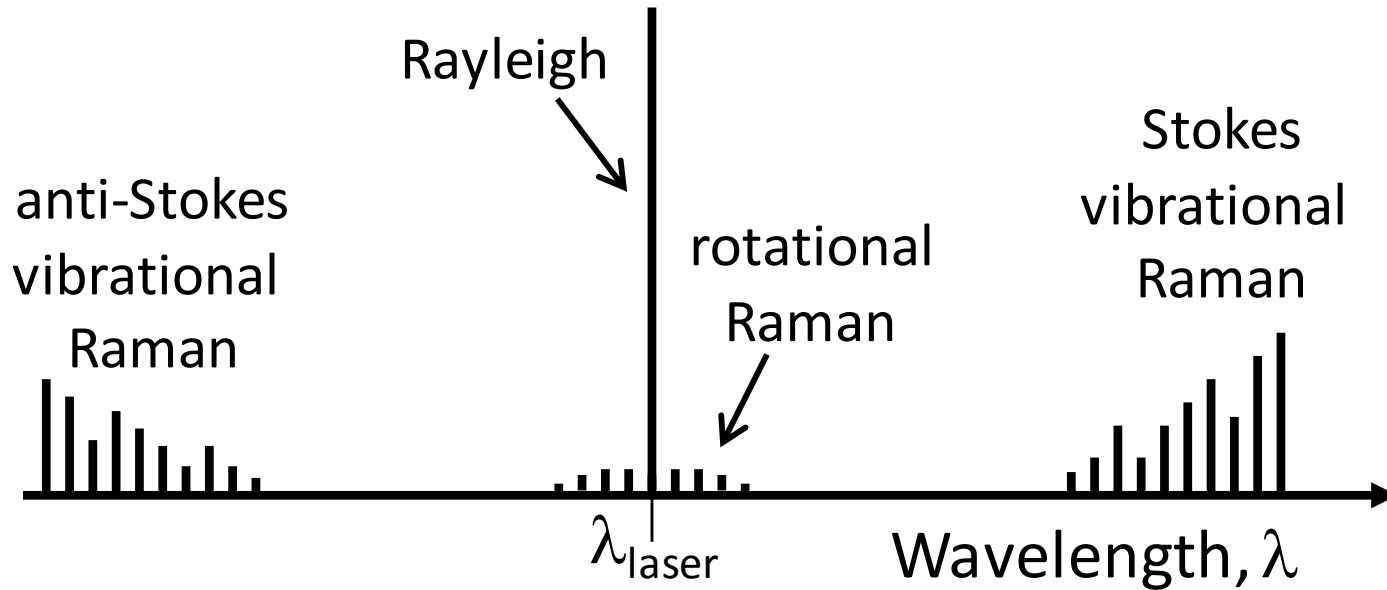
Rayleigh and Raman Scattering



- Energy level diagram:
 - Stokes Raman: energy absorbed by molecule
 - anti-Stokes Raman: energy lost by molecule
 - Initial state must not have been a ground state



Rayleigh and Raman Spectra



- Rayleigh: near laser's wavelength
- Raman: frequency shift depends on molecule, state (sensitive to concentration and temperature)
 - Rotational Raman
 - Vibrational Raman



Rayleigh and Raman Theory 1



- Scattered intensity, I , is proportional to the square of the induced dipole moment, \vec{p} :

$$\vec{p} = \epsilon_0 \alpha \vec{E}$$

where ϵ_0 is the permittivity of free space, α is the molecular polarizability and \vec{E} is the incident electric field given by:

$$\vec{E} = \vec{E}_0 \cos(\omega_0 t).$$

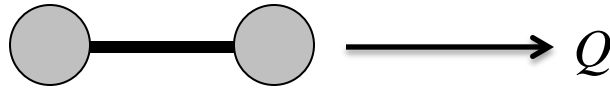
where \vec{E}_0 is the amplitude of the electric field, ω_0 is the frequency of the laser light and t is time.



Rayleigh and Raman Theory 2



- Polarizability, α , depends on internal structure
 - varies with time during vibrational oscillations at the natural frequency of the molecule, ω_v



- α varies with spatial coordinate, Q
 - More loosely held electrons \rightarrow more polarizable
 - Taylor Series Expansion:

$$\alpha = \alpha_0 + \left(\frac{\partial \alpha}{\partial Q} \right)_0 dQ$$

where dQ is small displacement about equilibrium positions which occurs during normal vibration

$$dQ = Q_0 \cos(\omega_v t)$$



Rayleigh and Raman Theory 3



- Substituting previous equations into $\vec{p} = \epsilon_0 \alpha \vec{E}$:

$$\vec{p} = \left[\alpha_0 + \left(\frac{\partial \alpha}{\partial Q} \right)_0 Q_0 \cos(\omega_v t) \right] \epsilon_0 \vec{E}_0 \cos(\omega_0 t)$$

- Expanding and using trig identity:

$$\vec{p} = \alpha_0 \epsilon_0 \vec{E}_0 \cos(\omega_0 t) + \frac{1}{2} \left(\frac{\partial \alpha}{\partial Q} \right)_0 \epsilon_0 Q_0 \vec{E}_0 [\cos(\omega_0 - \omega_v)t + \cos(\omega_0 + \omega_v)t]$$

Rayleigh Scattering

Stokes Raman

anti-Stokes Raman

- Resulting induced dipole moment (and scattering) is at three frequencies
- Amplitude is usually determined empirically:

$$\left(\frac{\partial \sigma}{\partial \Omega} \right)_{ZZ} \equiv \frac{I_{ZZ}^{\Omega}}{NI}$$

Differential Cross Section

(varies by molecule and with I but not with P, T)
(zz indicates polarization of laser and detection)

$$I_{ZZ}^{\Omega} = \left(\frac{\partial \sigma}{\partial \Omega} \right)_{ZZ} NI$$

scattered power
per solid angle

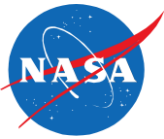
diff. cross
section

number
density

laser
irradiance



Rayleigh and Raman Theory 4



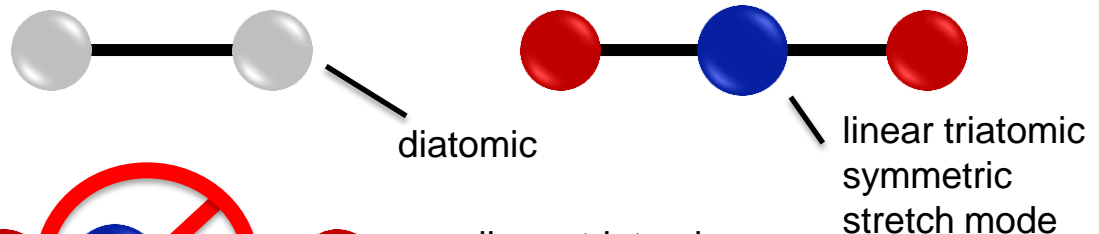
- Selection Rules: Raman Activity

- Not every molecule or vibrational mode produces Raman

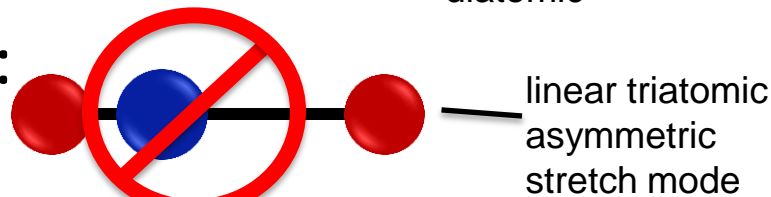
$$\vec{p} = \alpha_0 \epsilon_0 \vec{E}_0 \cos(\omega_0 t) + \frac{1}{2} \left(\frac{\partial \alpha}{\partial Q} \right)_0 \epsilon_0 Q_0 \vec{E}_0 [\cos(\omega_0 - \omega_v)t + \cos(\omega_0 + \omega_v)t]$$

- Amplitude of Raman is proportional to the magnitude of: $\left(\frac{\partial \alpha}{\partial Q} \right)_0$
- Polarizability, α , must *change* during vibrations to be Raman active

- Raman active:



- Raman inactive:





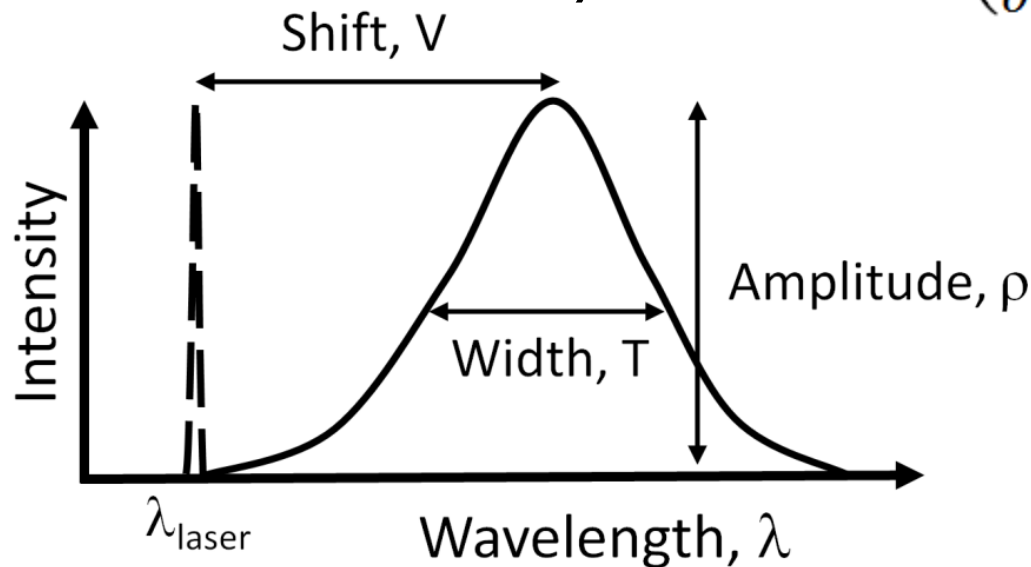
Rayleigh and Raman Theory 5



- Rayleigh Scattering is at or near the laser's wavelength.

- Doppler broadened ($\sim T^{1/2}$)
- Can be Doppler shifted ($\sim V$)
- Signal proportional to N ($\sim \rho$)

$$I_{ZZ}^{\Omega} = \left(\frac{\partial \sigma}{\partial \Omega} \right)_{ZZ} NI$$



- Can potentially measure these simultaneously
 - Requires high spectral resolution



Rayleigh and Raman Examples



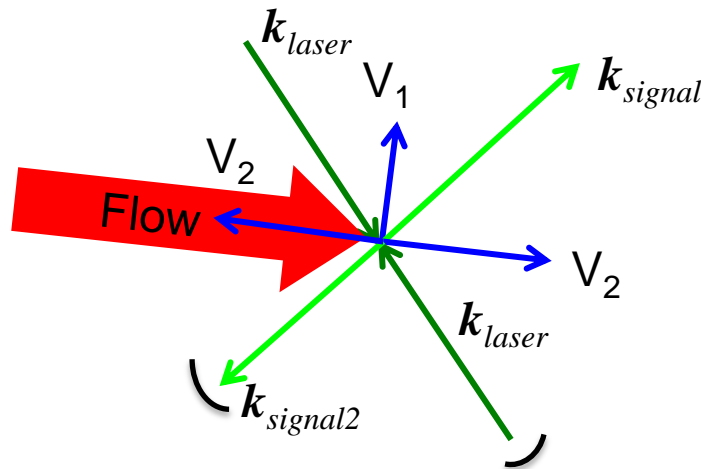
- Rayleigh
 - Velocimetry, multi point
 - V , T , ρ , single point
 - V , T , ρ , imaging
 - ρ measurement (and infer T)
- Raman
 - Concentration
 - Temperature



Rayleigh Velocimetry



- Rayleigh scattering velocimetry can measure selected velocity components
 - Measured component is bisector between incident laser and collection optics



Wave vector:
 $k = 2\pi/\lambda$

D. Bivolaru, P. M. Danehy, R. L. Gaffney, Jr. and A. D. Cutler, "Direct-View Multi-Point Two-Component Interferometric Rayleigh Scattering Velocimeter," 46th AIAA Aerospace Sciences Meeting and Exhibit, Reno, Nevada, AIAA Paper 2008-236, January 7-10, 2008

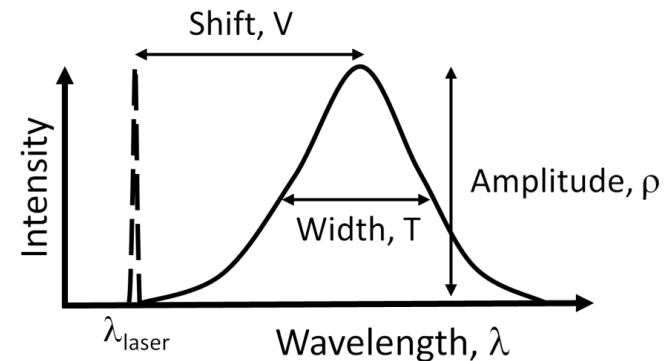
- Can measure multiple velocity components by adding additional detection angles or laser beams



Rayleigh Velocimetry

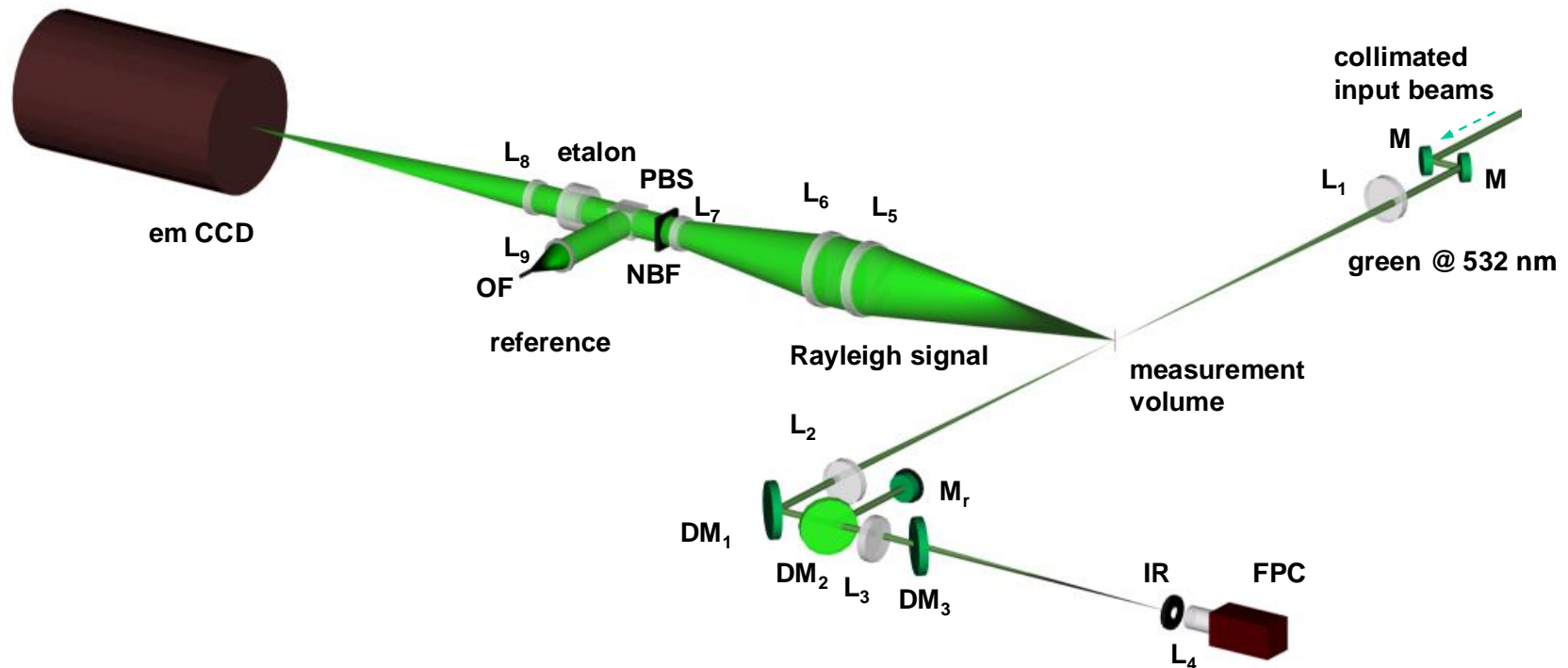


- Rayleigh scattering velocimetry has been performed different ways, always requiring a high resolution device to resolve the Doppler shift
 - I_2 filter in front of CCD
 - Imaging capability
 - limited dynamic range
 - Fabry Perot etalon
 - PMT based (faster)
 - CCD based (multi-point)
 - Combined I_2 filter and Fabry Perot etalon
 - See manuscript for references





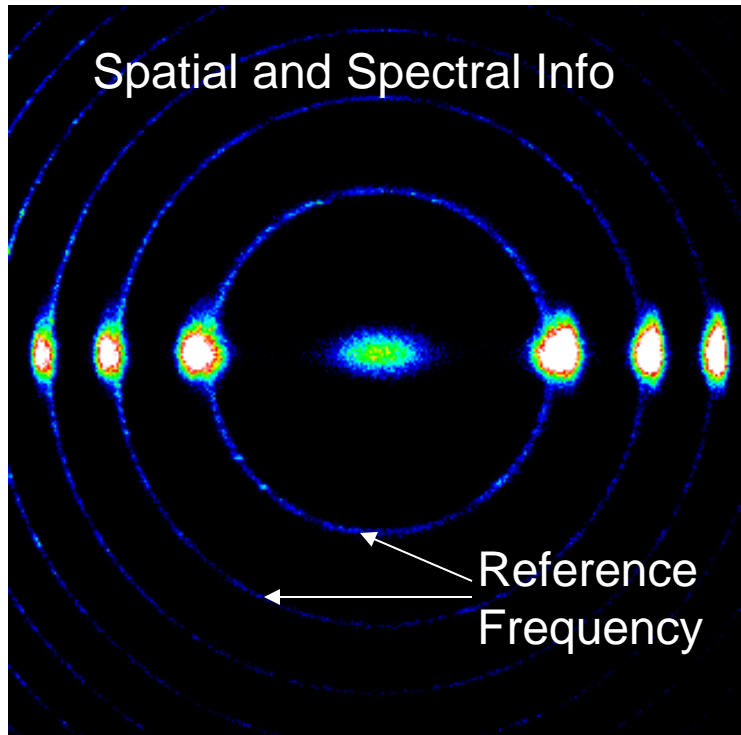
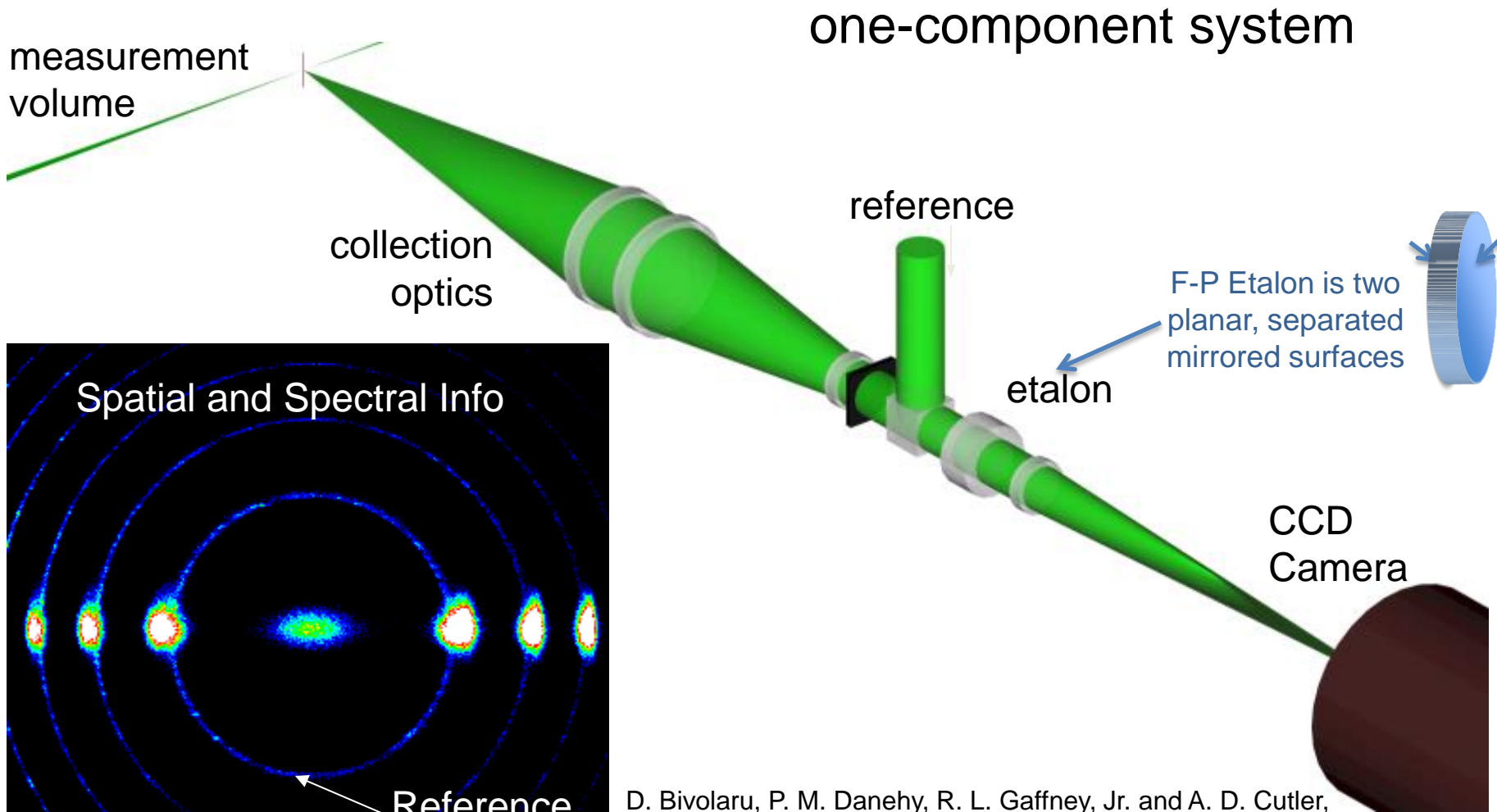
- Velocimetry using a Fabry Perot Interferometer (FPI) with CCD camera



- D. Bivolaru, P. M. Danehy, R. L. Gaffney, Jr. and A. D. Cutler, "Direct-View Multi-Point Two-Component Interferometric Rayleigh Scattering Velocimeter," 46th AIAA Aerospace Sciences Meeting and Exhibit, Reno, Nevada, AIAA Paper 2008-236, January 7-10, 2008



Rayleigh Velocimetry using Fabry-Perot Etalon



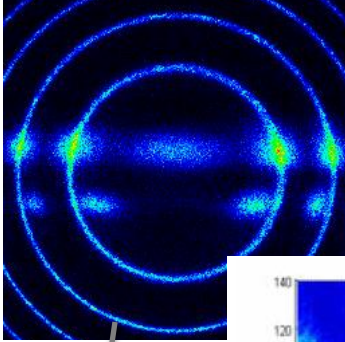
D. Bivolaru, P. M. Danehy, R. L. Gaffney, Jr. and A. D. Cutler, "Direct-View Multi-Point Two-Component Interferometric Rayleigh Scattering Velocimeter," 46th AIAA Aerospace Sciences Meeting and Exhibit, Reno, Nevada, AIAA Paper 2008-236, January 7-10, 2008



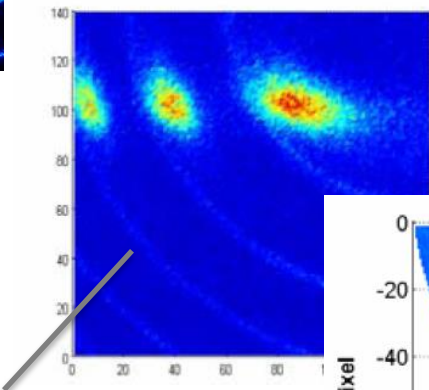
Rayleigh Scattering Image Processing



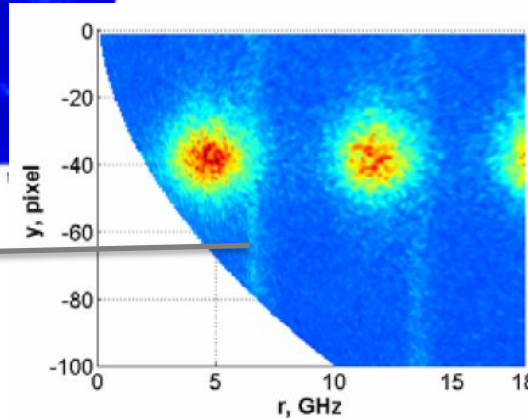
Raw image data



Import to Matlab®

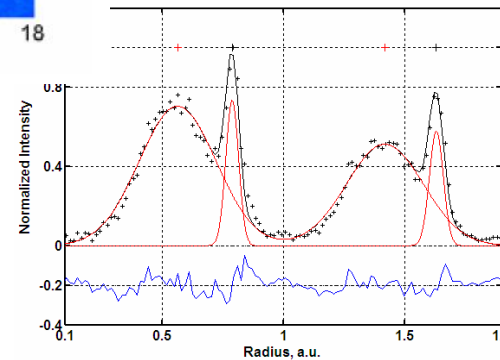


x - y to r - y transform



Circles provide reference
(7.5 GHz etalon)

Combine to spectrum and fit

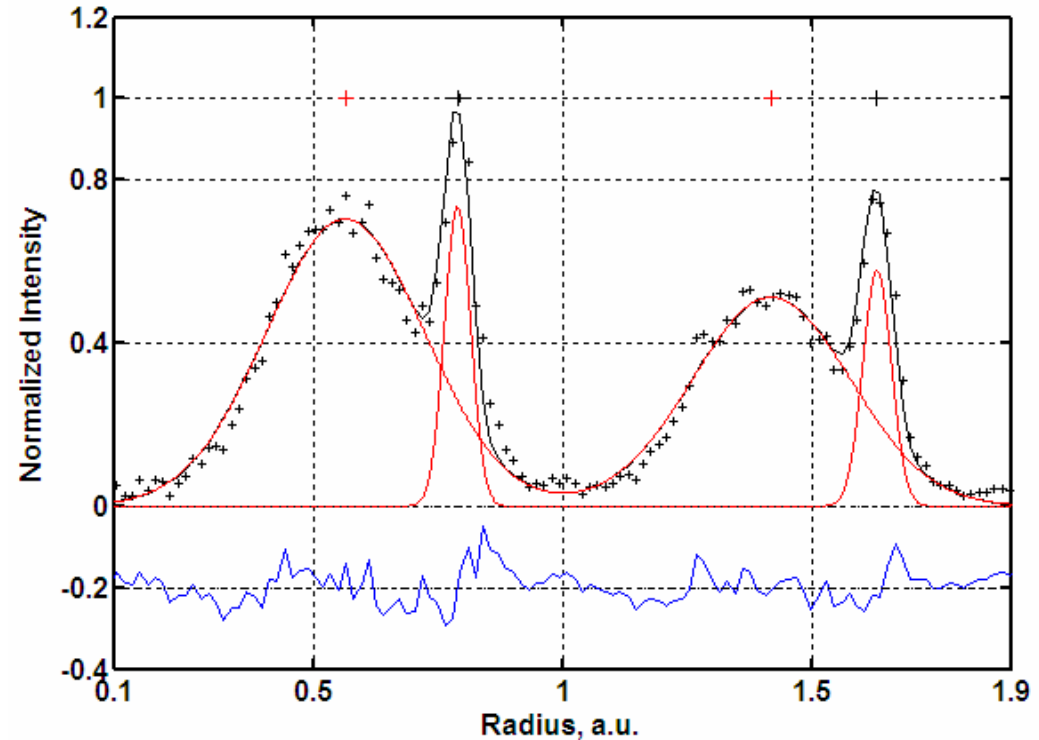
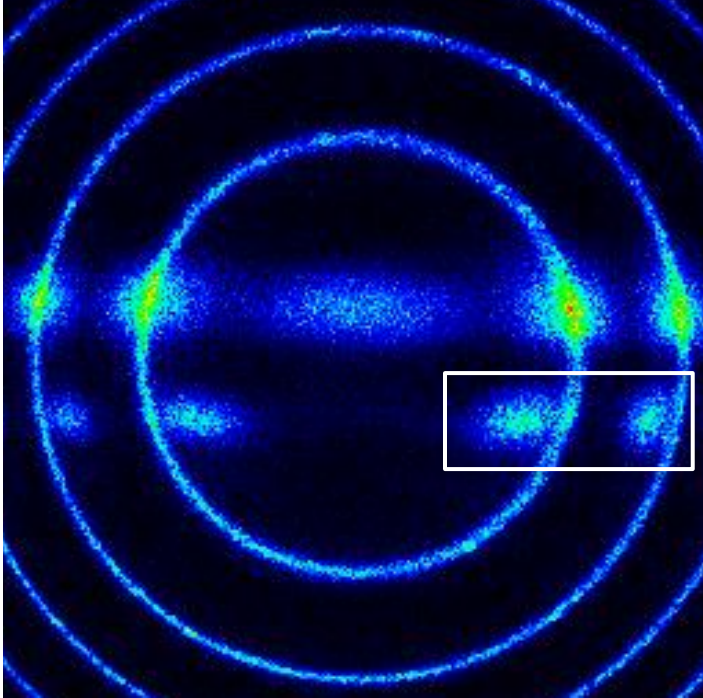
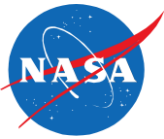


- Significant image processing is required

D. Bivolaru, P. M. Danehy, R. L. Gaffney, Jr. and A. D. Cutler, "Direct-View Multi-Point Two-Component Interferometric Rayleigh Scattering Velocimeter," 46th AIAA Aerospace Sciences Meeting and Exhibit, Reno, Nevada, AIAA Paper 2008-236, January 7-10, 2008



Rayleigh Scattering Velocity Results



- *Rayleigh scattering in a large scale (6 cm diameter) Mach 1.6 H₂-air combustion heated jet operating at Mach 5.5 enthalpy at NASA Langley*

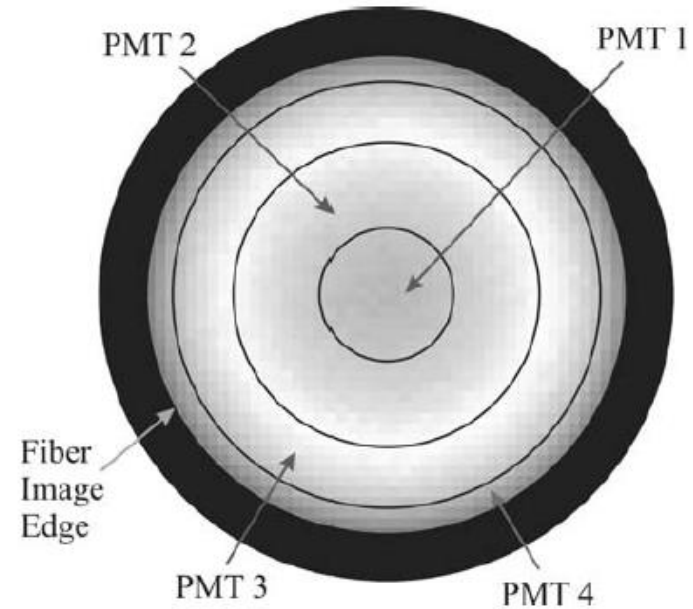
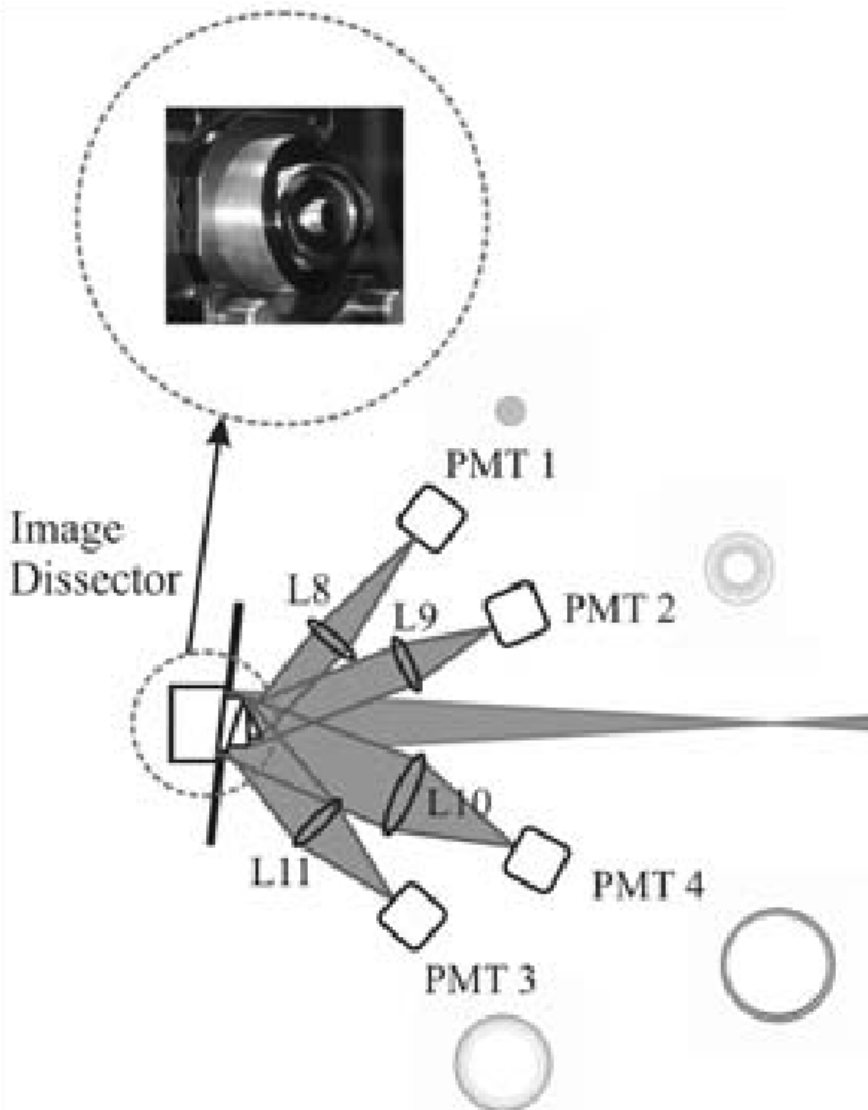
Velocity precision of ~40 m/s out of 1200 m/s, (3%)

The dynamic range of the instrument was ~3000 m/s

- precision 1% of dynamic range



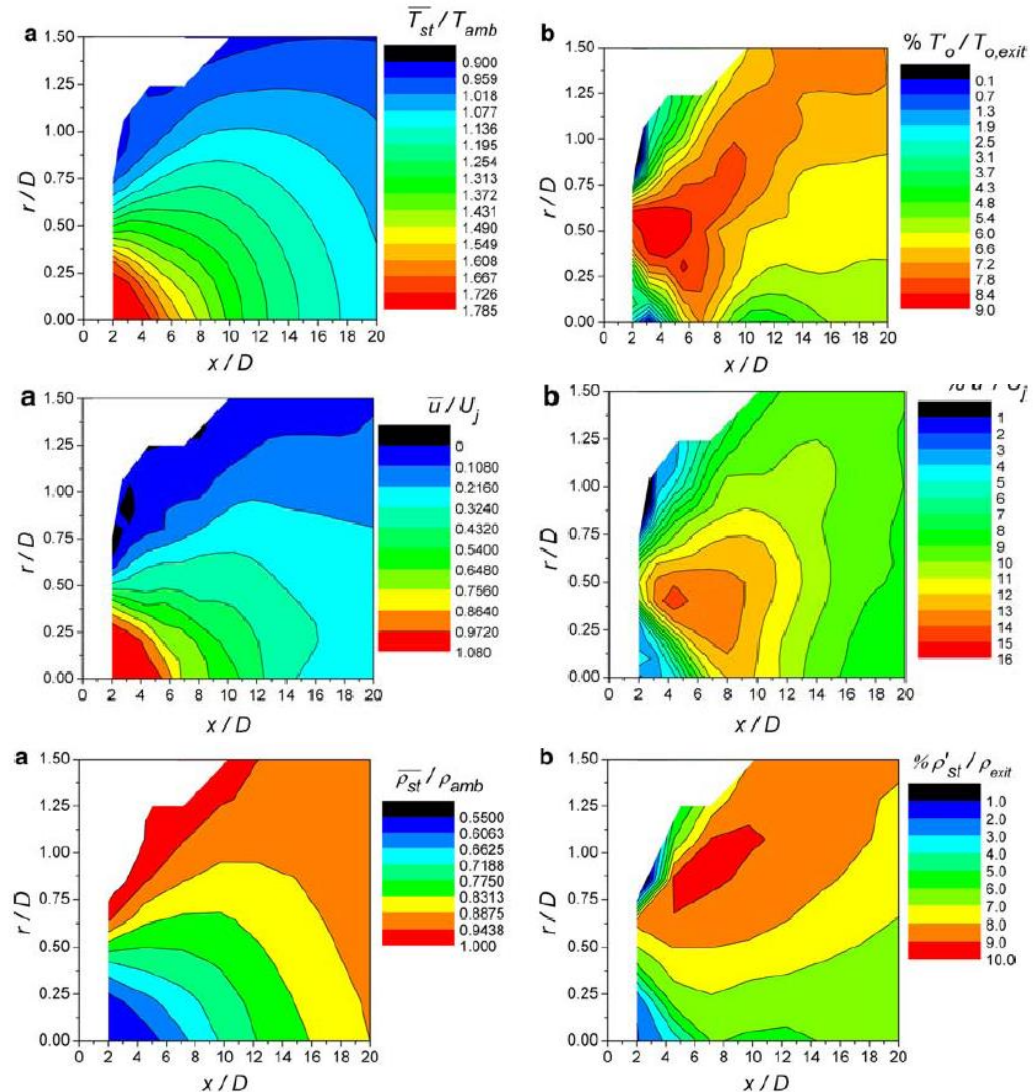
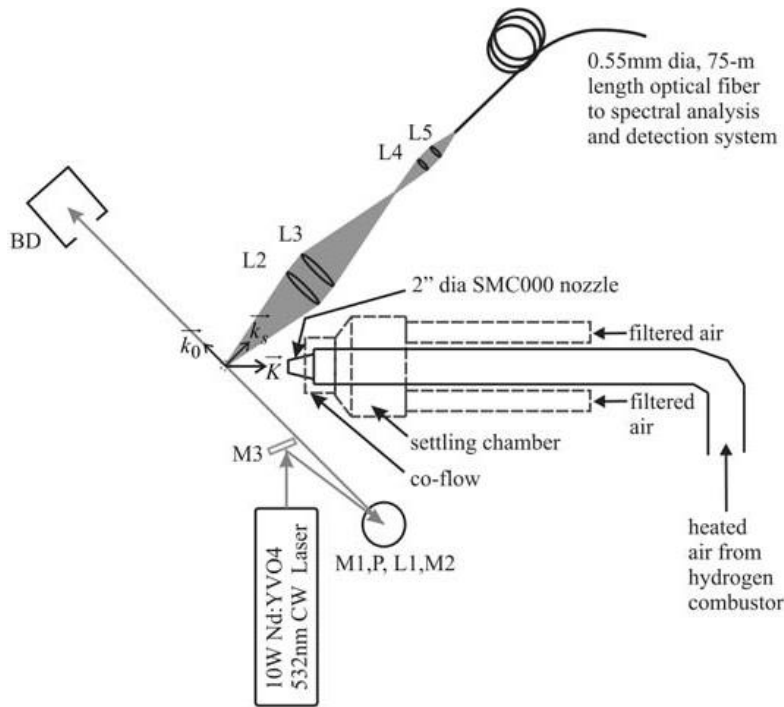
Rayleigh Scattering: T , V , ρ



- Continuous laser excitation
 - 10 W at 532 nm
- Fiber optic collection
- Data rate: 10 kHz
- Single point measurement



Rayleigh Scattering: T , V , ρ



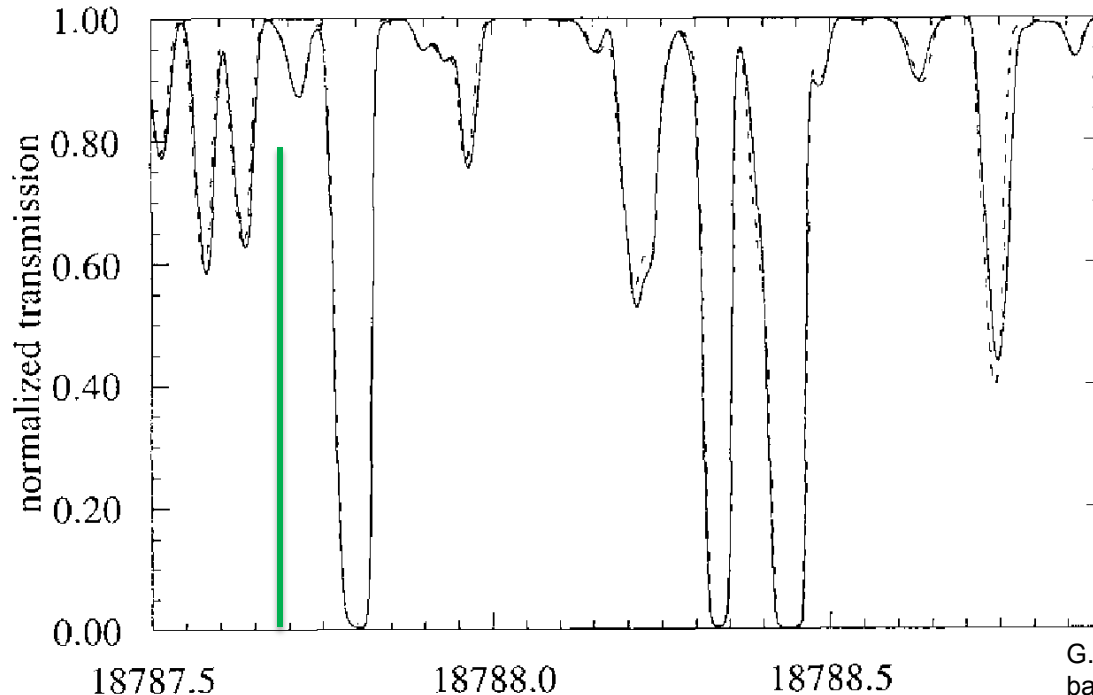
- Heated, 2" (50 mm) diameter axisymmetric near-sonic jet at NASA Glenn Research Center



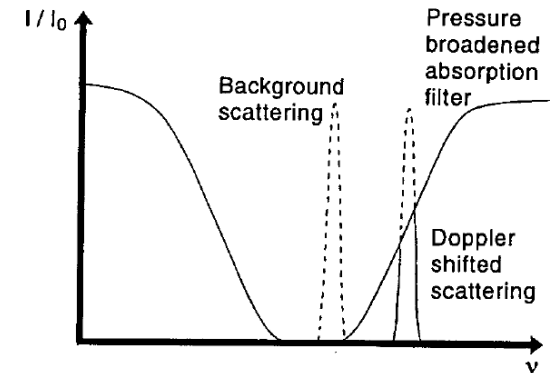
Rayleigh Velocimetry (I_2 filter)



- Instead of an etalon, use I_2 filter \rightarrow 2D imaging



I_2 absorption near 532 nm



G. S. Elliott, M. Samimy, S. A. Arnette "A molecular filter based velocimetry technique for high speed flows," Experiments in Fluids, Volume 18, Issue 1-2, pp 107-118, December 1994

R. B. Miles, W. R. Lempert and J. N. Forkey, "Laser Rayleigh Scattering," Meas. Sci. Technol. p. R33-R51, v.12, 2001

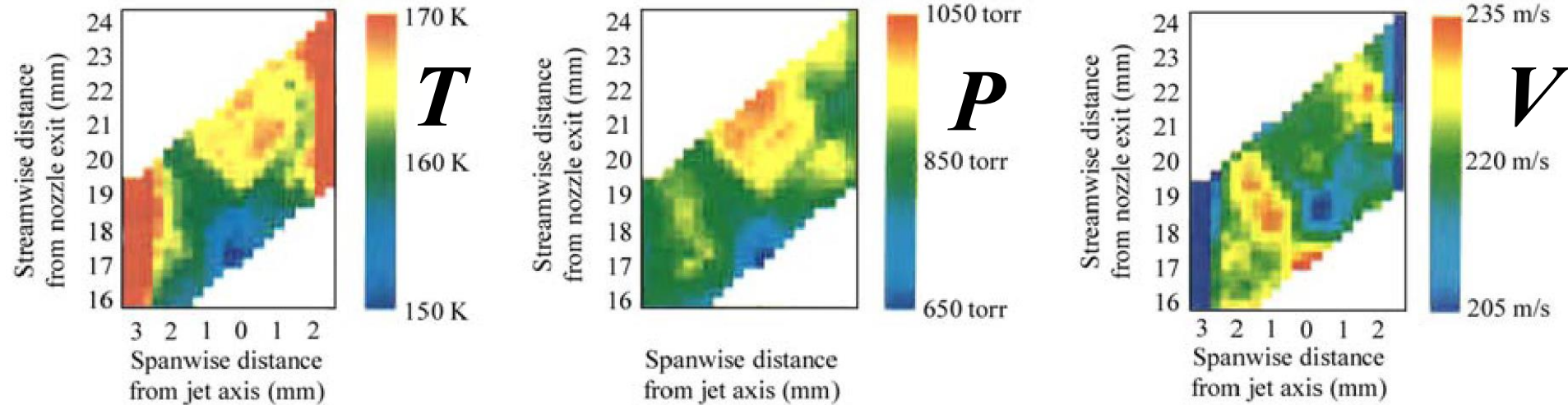
- Gas cell, filled with low-pressure N_2 plus some I_2 crystals; control temperature to determine absorption
- Scan Nd:YAG laser frequency (or fixed)



Rayleigh Imaging of T , V , ρ (or P)



- Direct YAG laser sheet into a Mach 2 jet



R. B. Miles, W. R. Lempert and J. N. Forkey, "Laser Rayleigh Scattering," Meas. Sci. Technol. p. R33-R51, v.12, 2001

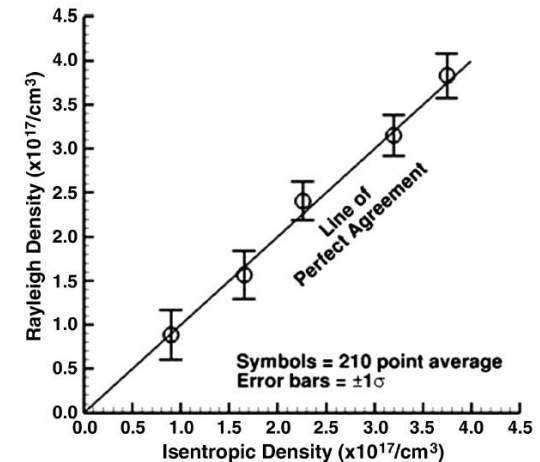
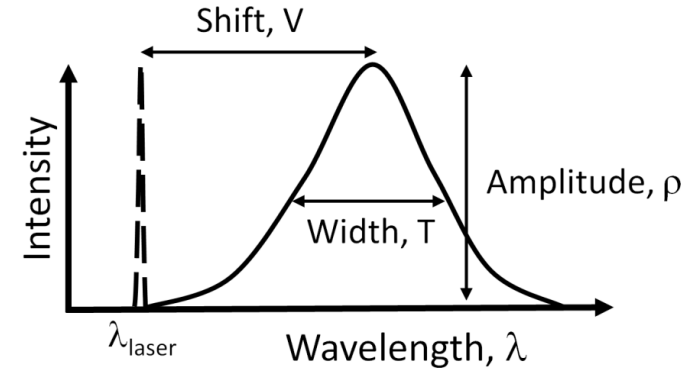
- Scanned laser frequency, determine T , V , ρ (report P) based on measured spectrum at each pixel
- Same method can be used for velocimetry from particles (usually fixed frequency, multiple detection angles)
 - Planar Doppler Velocimetry (PDV) or Doppler Global Velocimetry (DGV)



Rayleigh Scattering: ρ



- Rayleigh scattering has a spectrum:
 - Sensitive to T , V , ρ
 - Prior examples used Fabry Perot Etalon or I_2 cell to observe spectrum
 - These devices reject signal, making them less sensitive detectors of ρ .
- Collect *all* of the scattering
 - Less equipment/less setup/simpler
 - Bigger signal
 - Can do single point or imaging
 - Only sensitive to ρ .
 - (If you know P and composition you can convert ρ to T .)



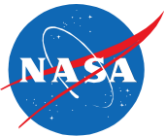
Using a UV laser (e.g. ArF at 193 nm) allows measurements to be made at low pressures (e.g. 1/300 atmospheric density)

Balla, R. Jeffrey, and Joel L. Everhart. "Rayleigh scattering density measurements, cluster theory, and nucleation calculations at Mach 10."

AIAA Journal 50, no. 3 (2012): 698-707.²²⁰



Raman Spectroscopy



- Raman spectrum obtained in a CH₄-air flame:
 - Average of 500 pulses using stretched 0.5 J/pulse, 532 nm
 - Stretch 10 ns pulse to 500 ns to avoid laser-induced breakdown

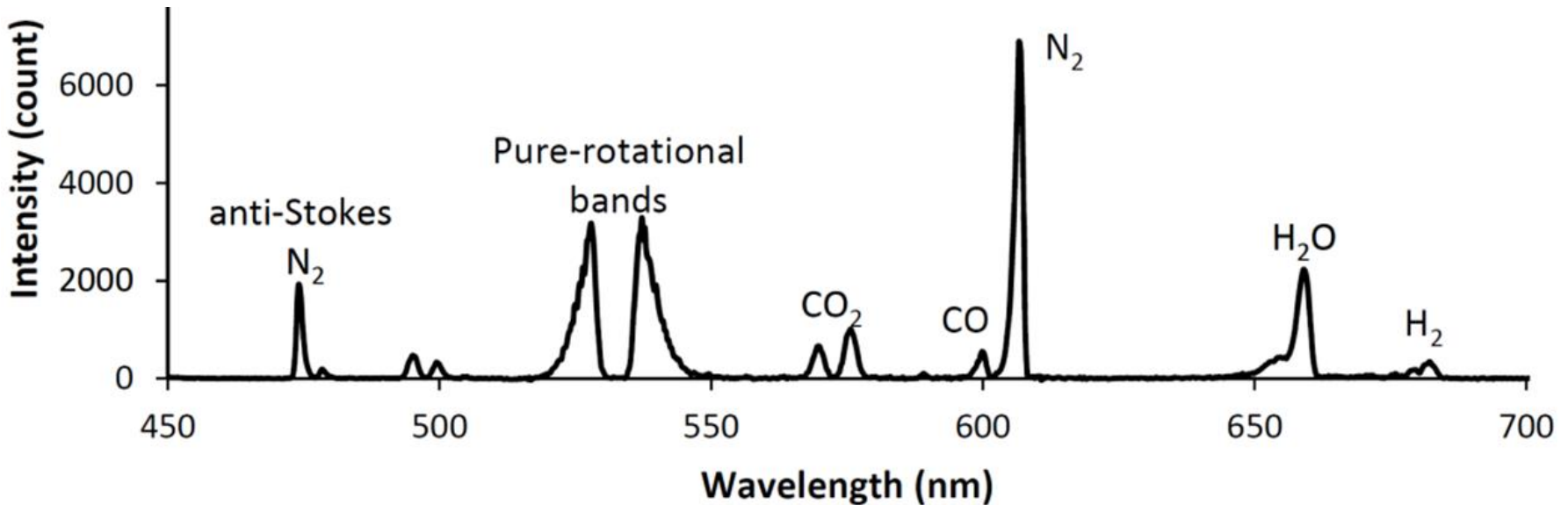
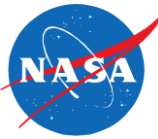


Figure courtesy of Jun Kojima, NASA Glenn Research Center (Jun.J.Kojima@nasa.gov)

- Can measure species (N₂, CO, CO₂, H₂, H₂O) from such spectra & temperature from Stokes/anti-Stokes

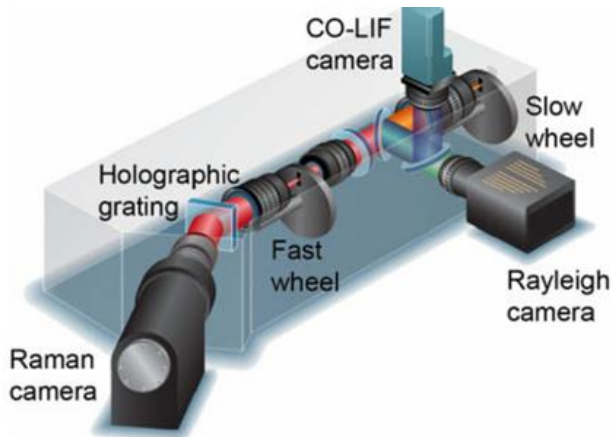


Raman Concentration Measurement

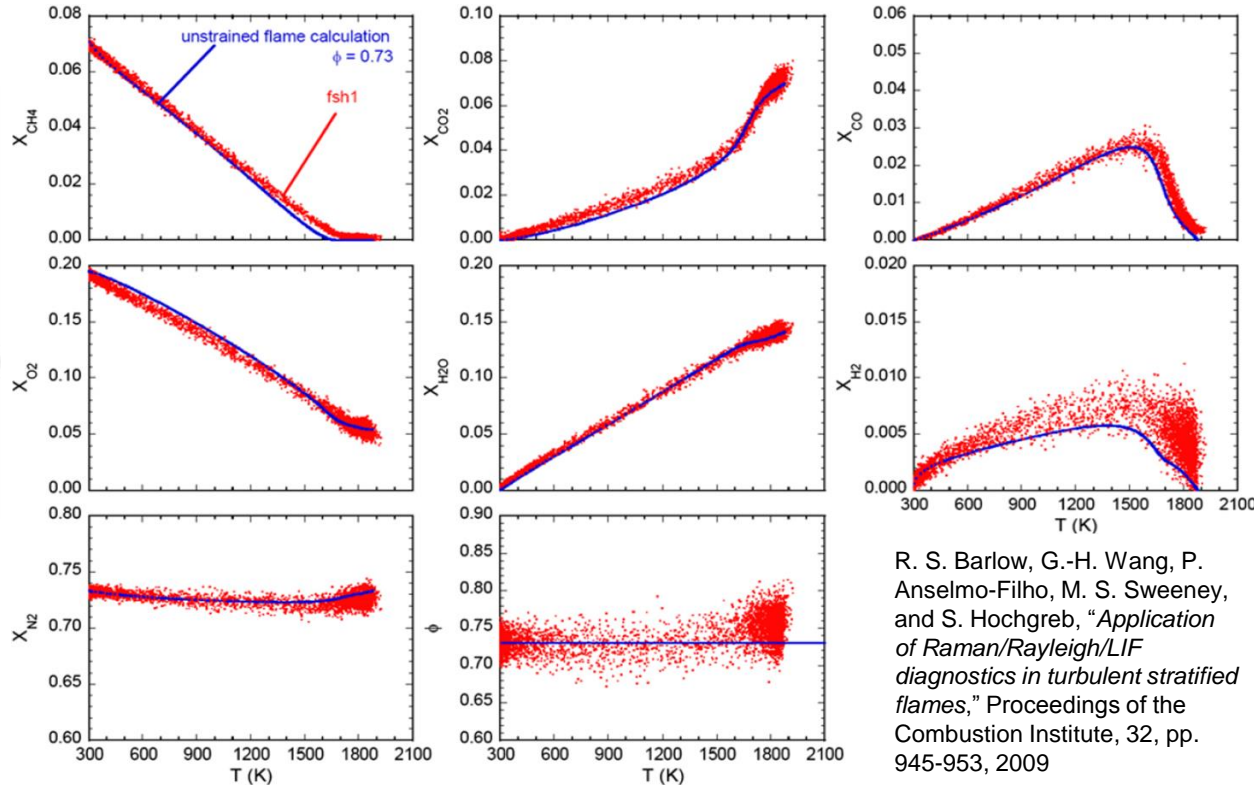


(and Rayleigh Temperature and LIF concentration)

- Example of Raman concentration measurements in a subsonic turbulent CH₄/air flame at Sandia National Laboratories, California
 - 4 Nd:YAG lasers at 532 nm to produce 1.8 Joules/pulse, focused to a point



χ_i precision ~0.7% to 7.5%
 T precision ~0.75%



R. S. Barlow, G.-H. Wang, P. Anselmo-Filho, M. S. Sweeney, and S. Hochgreb, "Application of Raman/Rayleigh/LIF diagnostics in turbulent stratified flames," Proceedings of the Combustion Institute, 32, pp. 945-953, 2009

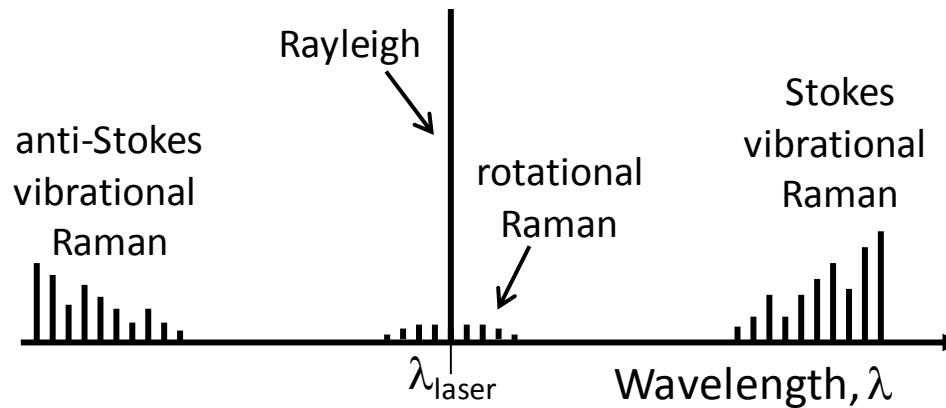
- Raman/Rayleigh/LIF line imaging (~10 pixels / mm along the 6-mm-long probe volume)
 - N₂, O₂, CH₄, CO₂, H₂O and H₂ from Raman, CO from 2 photon LIF
 - Temperature from Rayleigh density measurement (idea gas law)



Raman Temperature Measurement



- Several ways to measure temperature with Raman
 - none as precise as CARS (3%)



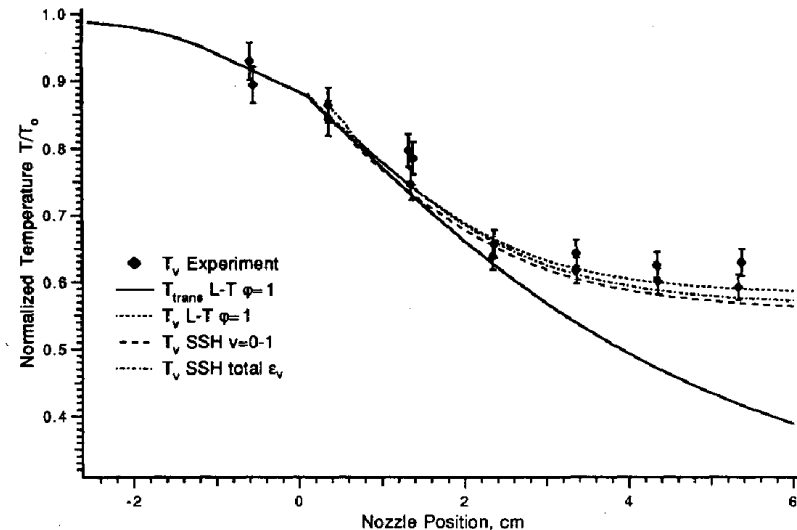
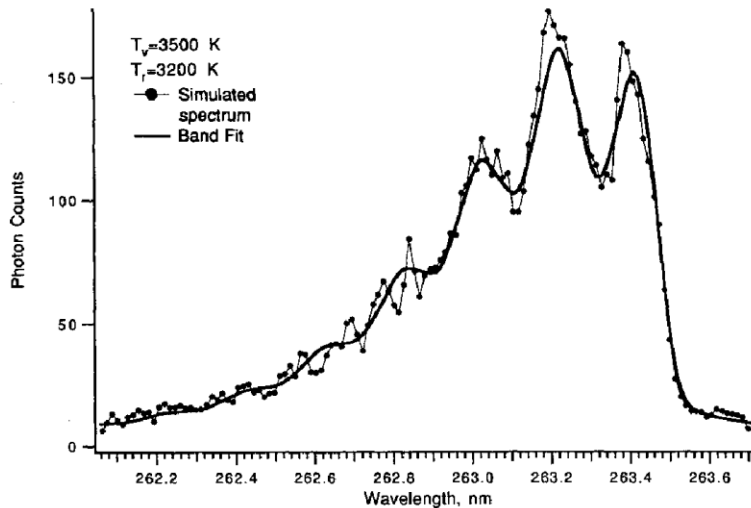
- Rotational Temperature from pure-rotational Raman
- Vibrational temperature measurements (see Kojima, 2008)
 - Only good above 700 K
 - Stokes / anti-Stokes vibrational Raman
 - Low resolution, so can measure concentrations at same time
 - ~20% precision in measurements along a line (Wehrmeyer, 1996)
 - Spectrally resolved vibrational band (Sharma et al, 1993)



Raman Temperature Measurement



- Raman temperature measurement from spectrally resolved vibrational N_2 band.
 - Excited with KrF Excimer laser 0.25 J at 248 nm (25 ns pulse)



S. P. Sharma, S. M. Ruffin, W. D. Gillespie and S. A. Meyer, "Vibrational Relaxation Measurements in an Expanding Flow Using Spontaneous Raman Scattering," J. of Thermophys. and Heat Trans. Vol. 7, No. 4, Oct.-Dec. 1993

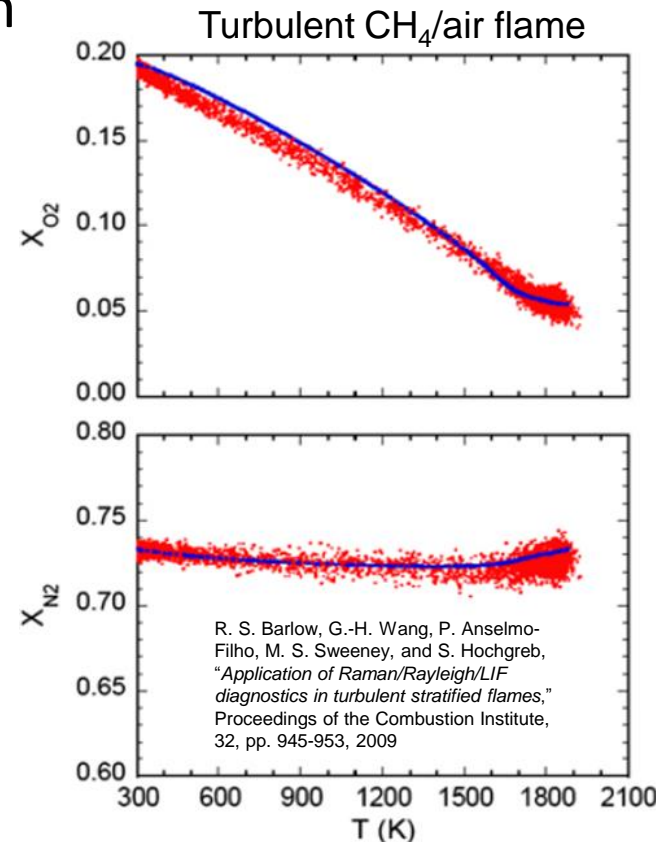
- Single shot precision $\sim 5\%$ (not explicitly stated)
 - More precise than Stokes/anti-Stokes T but cannot measure species concentrations with same instrument.



Rayleigh Scattering: ρ

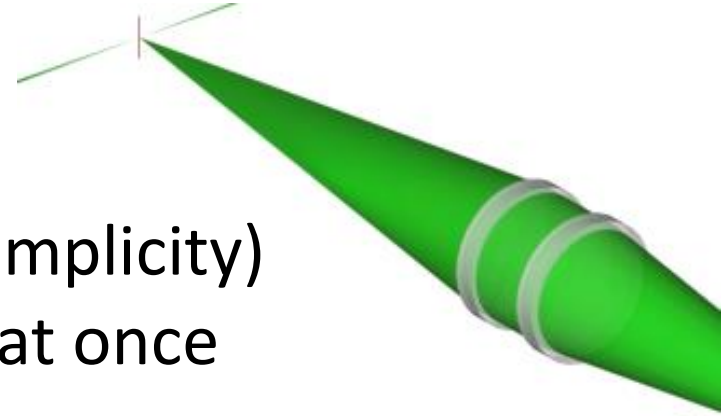


- When precise measurements are required, high S/N is needed
 - Use high powered lasers, focused to a point
 - If too high: laser-induced breakdown
- Sandia, Livermore, Calif.:
 - Raman/Rayleigh/LIF line imaging at $P = 1$ atm
 - 4 double-pulse Nd:YAG lasers: 1.8 J/pulse
 - Camera images Rayleigh along line
 - ~ 10 pix / mm along 6-mm-long probe volume
 - N_2 , O_2 , CH_4 , CO_2 , H_2O and H_2 from Raman
 - CO from 2 photon LIF
 - Temperature from Rayleigh density, ρ_2
 - Need composition to determine $\left(\frac{\partial \alpha}{\partial Q}\right)_0$
 - If known P , idea gas law give T
 - T precision reported: $\sim 0.75\%$
 - (ρ precision is probably same)
 - Cutting edge MHz laser: 40x lower energy (Jiang, 2011)





- Advantages:
 - No seeding required
 - Only one color of laser used (simplicity)
 - Multiple properties measured at once
 - T , V , ρ for Rayleigh
 - T , many species for Raman
 - Can do Raman and Rayleigh together and with LIF
- Disadvantages:
 - Weak signal:
 - Requires very high power laser
 - stretched to avoid laser induced breakdown
 - Requires large windows, big, close collection optics
 - Usually single point or line measurements
 - Temperature less accurate & precise than CARS

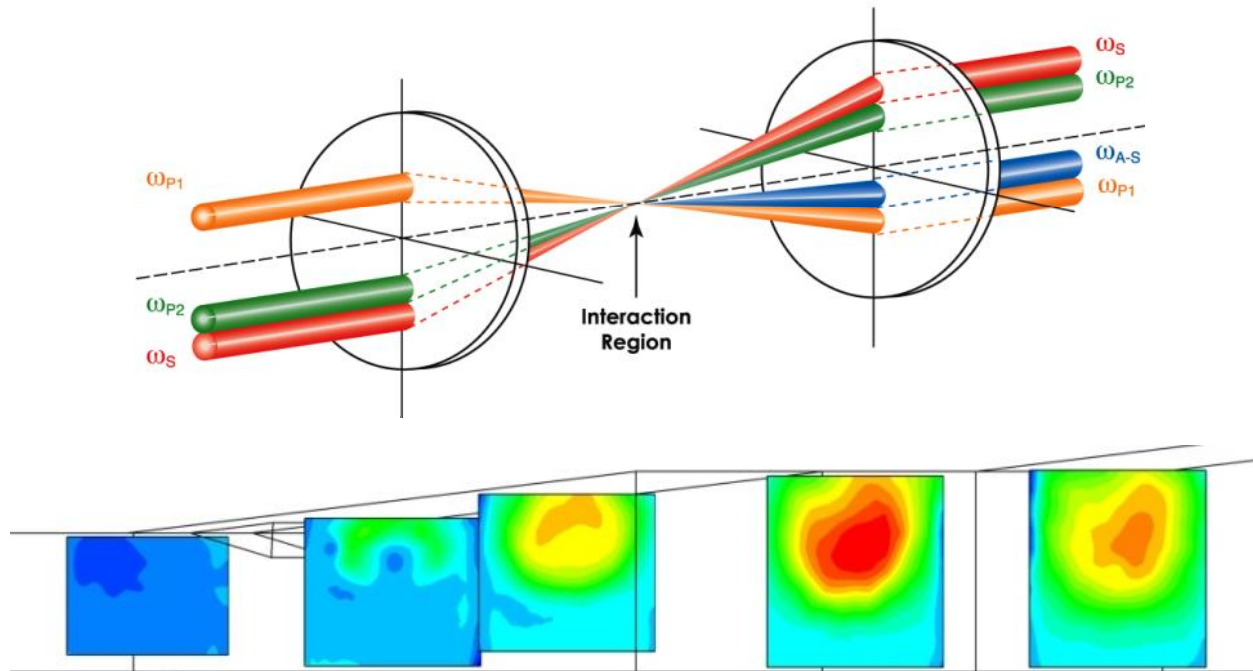




Intro to Coherent anti-Stokes Raman Spectroscopy (CARS) for Hypersonic Nonequilibrium Flows



Andrew Cutler, The George Washington University, USA
Paul Danehy, NASA Langley Research Center, Virginia, USA





Outline



- Brief introduction to nonlinear optics
- Introduction to CARS and basic theory
- NASA / GWU CARS System
 - Temperature and composition measured in UVa dual mode scramjet
 - Thermometry shows vibrational nonequilibrium
- CARS in a non-thermal plasma
- Concluding remarks



Nonlinear Optics



- First, a few words about nonlinear optics
 - Conservation of energy
 - Conservation of momentum
 - Wave equation from Maxwell's equations
- Second Harmonic Generation as an Example
 - 2nd order nonlinearity (solid)
 - CARS is a 3rd order nonlinearity (gas)



Intro: Nonlinear Optics

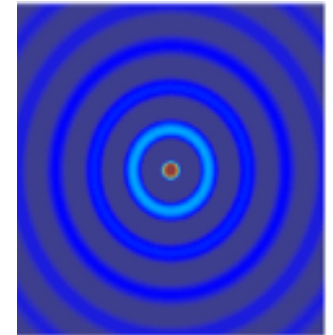


– Second Harmonic Generation (SHG)



– Solved using the Wave Eqn:

$$\nabla^2 \mathbf{E} - \frac{1}{c^2} \frac{\partial^2 \mathbf{E}}{\partial t^2} = \mu_0 \frac{\partial^2 \mathbf{P}_{\text{NL}}}{\partial t^2}$$



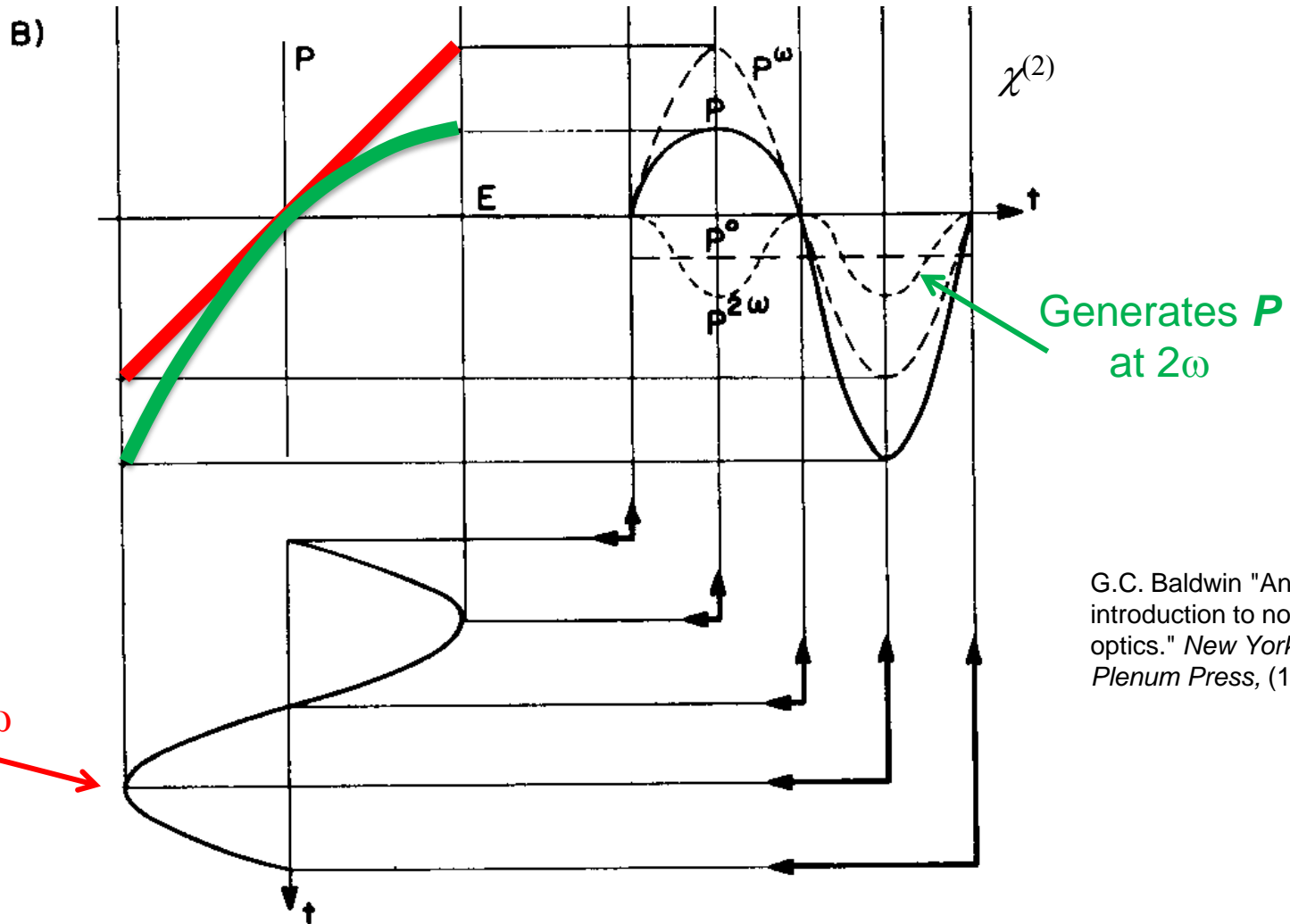
– Assume SVEA and 1st Born Approx:

$$I_{\omega_2} \propto \frac{d^2 P_{\omega_1}^2 L^2}{A^2}$$

– d is a coefficient, P is power, L is length, A is area



Non-linear Susceptibility

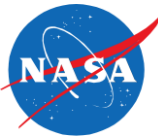


G.C. Baldwin "An introduction to nonlinear optics." New York: Plenum Press, (1969).

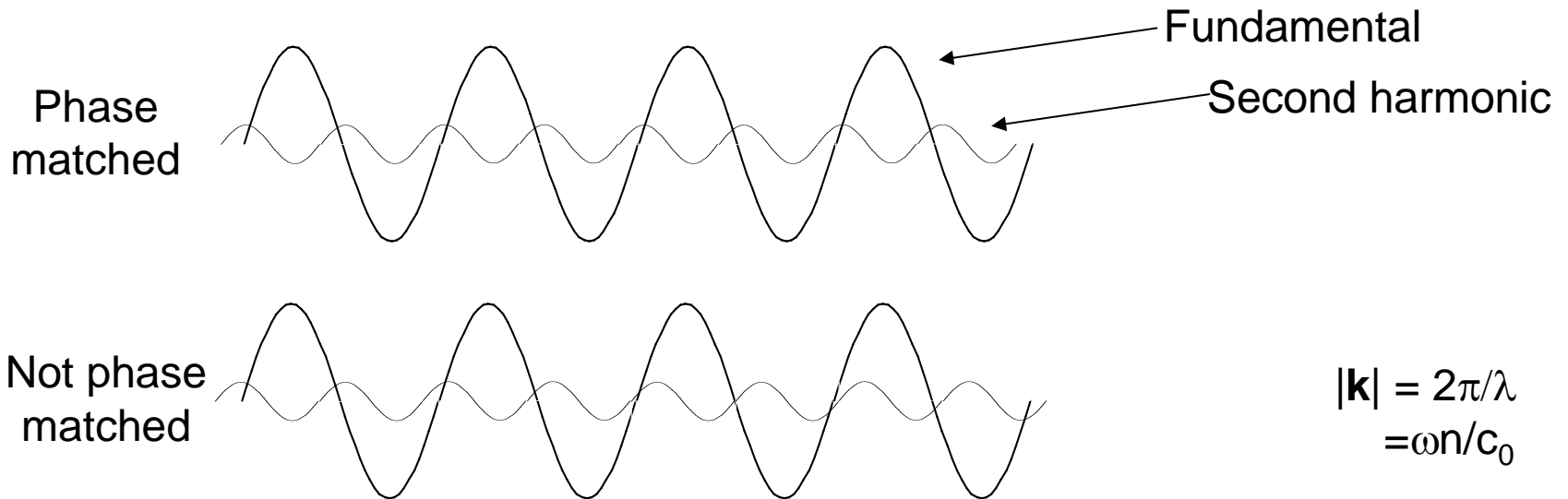
- Non-linear effects: Intense electric fields of one frequency can generate a P at another



Phase Matching



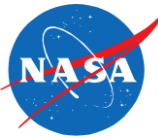
- What is Phase Matching?
 - *Ensuring that the light wavefronts ‘match up’.*



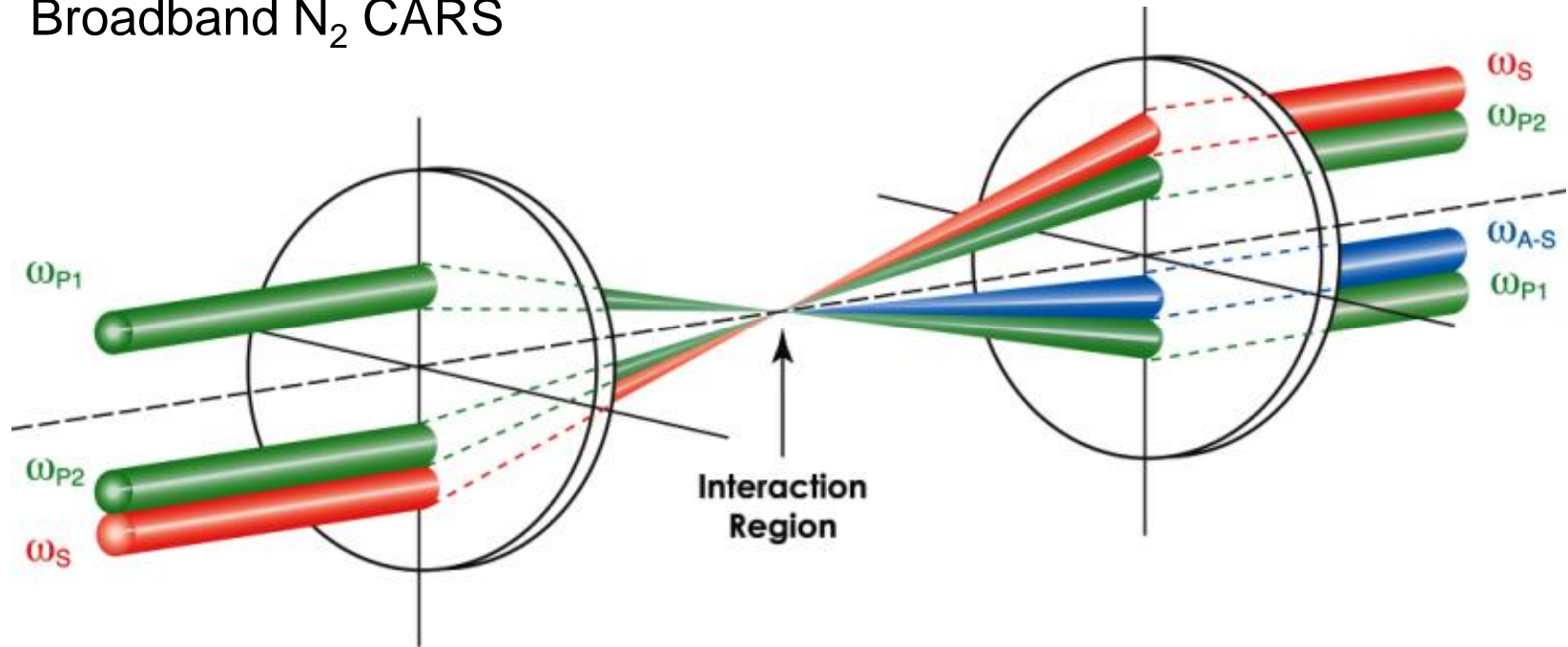
- Dispersion causes deconstructive interference
- New photons generated are out of phase with previous ones: resulting in loss
- For SHG there are tricks to make it phase matched
- Conservation of momentum: phase matching
- Conservation of energy: $\omega_2 = 2\omega_1$



What is CARS?



Broadband N₂ CARS



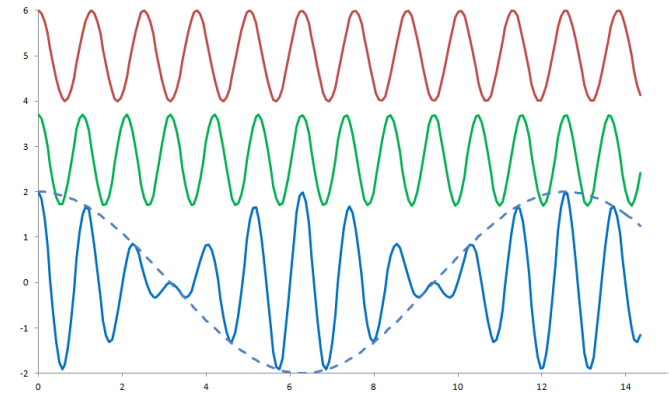
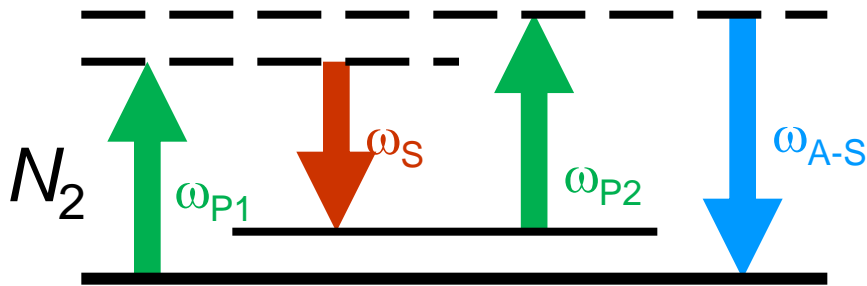
Spectrally-broad red beam +
Spectrally-narrow green beams =
Single-shot blue CARS spectrum



CARS Energy Level Diagram (conservation of energy)



- Lasers: **2 Green (532 nm)** and **1 Red (607 nm)**
 - Frequency difference between **Green** and **Red**
- Probes N_2 vibrational Raman Shift

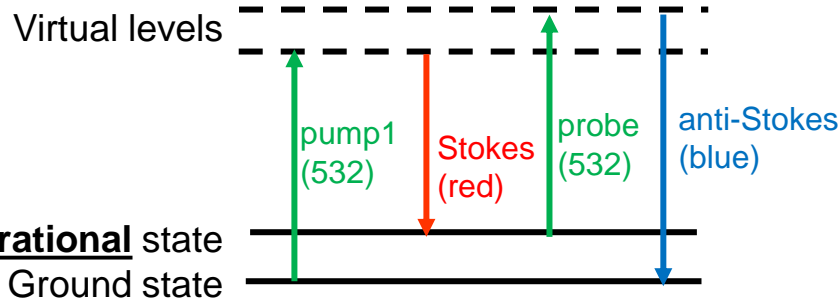


- Result: Blue signal beam at **473 nm**.
 - Spatially, spectrally, temporally filter this signal
 - Good technique for luminous flows
 - Send to spectrometer equipped with CCD camera
 - Measured CARS spectra is best fit to a library of theoretical spectra on a single-shot basis (10 ns)

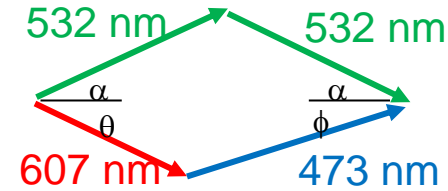




CARS Phase Matching (conservation of momentum)



Planar Boxcars Geometry



$$k_{p1} + k_{p2} = k_S + k_{A-S}$$

It is straight forward to compute the CARS phase matching angles:

N2 cars	lambda	wavenum	angle (degrees)
stokes	607	16474.46	3.963
pump 2	532	18796.99	3.500
pump 1	532	18796.99	3.500
anti stokes	473.4956	21119.52	3.091
			0.023576939
N2 Raman =	2322.528	cm-1	0.023576939
(nominal N2 = 2330 cm-1)			3.00927E-20

Different molecules
require different angles
(can get multiple signals
at different spatial
locations: Dual-Stokes)

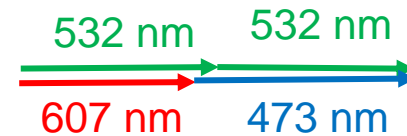


CARS Phase Matching Geometries

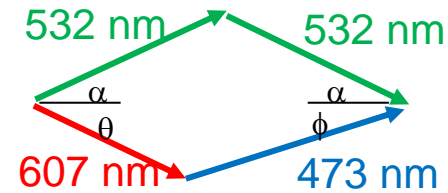
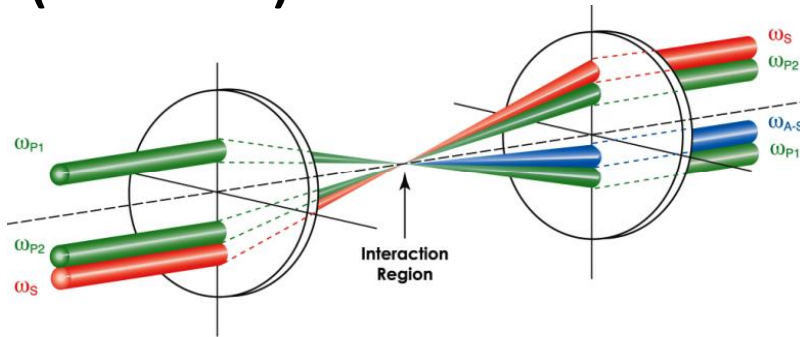


- Collinear CARS:
 - Poor spatial resolution

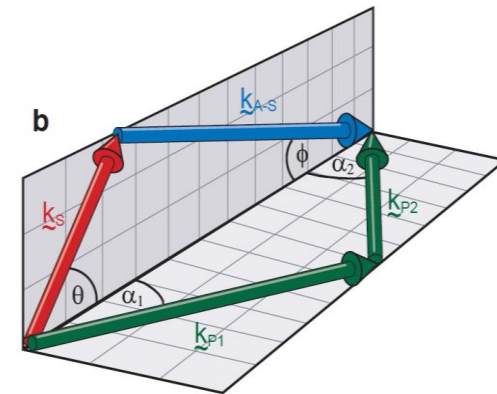
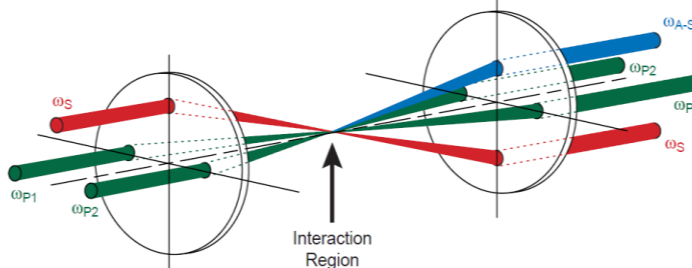
$$k_{p1} + k_{p2} = k_S + k_{A-S}$$



- (Planar) BoxCARS:



- Folded BoxCARS:



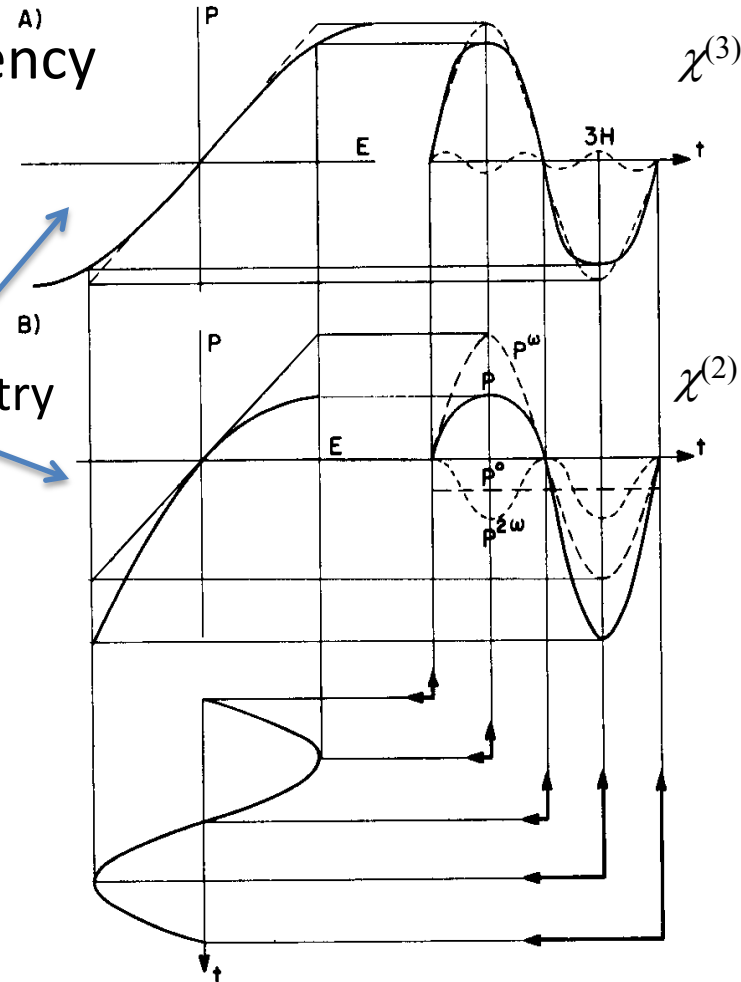
- Best spatial resolution (1.5 mm x 0.1 mm x 0.1 mm) but lower signals and affected by beam steering from turbulence



CARS Theory 1



- Non-linear effects:
 - Intense electric fields of one frequency can generate a P at another
 - $P = \epsilon_0 (\chi E + \chi^{(2)} E^2 + \chi^{(3)} E^3 + \dots)$
 - $\chi^{(2)}$ = 2nd order susceptibility
 - Only media lacking a centre of symmetry (ie, no gases, liquids)
 - $\chi^{(3)}$ = 3rd order susceptibility
 - All dielectric media
 - Generally $(\chi E \gg \chi^{(2)} E^2 \gg \chi^{(3)} E^3)$



G.C. Baldwin "An introduction to nonlinear optics." New York: Plenum Press, (1969).



CARS Theory 2



- Polarization generated at CARS signal frequency:

$$P^{(3)}(\omega_{signal}) = \epsilon_0 \chi_{CARS} E(\omega_{pump}) E(\omega_{stokes}) E(\omega_{probe})$$

- Substitute into the wave equation. Result:

$$I_{signal} \propto I_{pump} I_{stokes} I_{probe} |\chi_{CARS}|^2 L^2$$

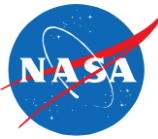
- To obtain large signals, want long L , high laser power (tight focus) and strong resonance

$$\chi_{CARS} = \sum_j \frac{K_j \Gamma_j}{2\Delta\omega_j - i\Gamma_j} + \chi_{nr} \text{ where } K_j \propto N \Delta_j \left(\frac{\partial \sigma}{\partial \Omega} \right)_j$$

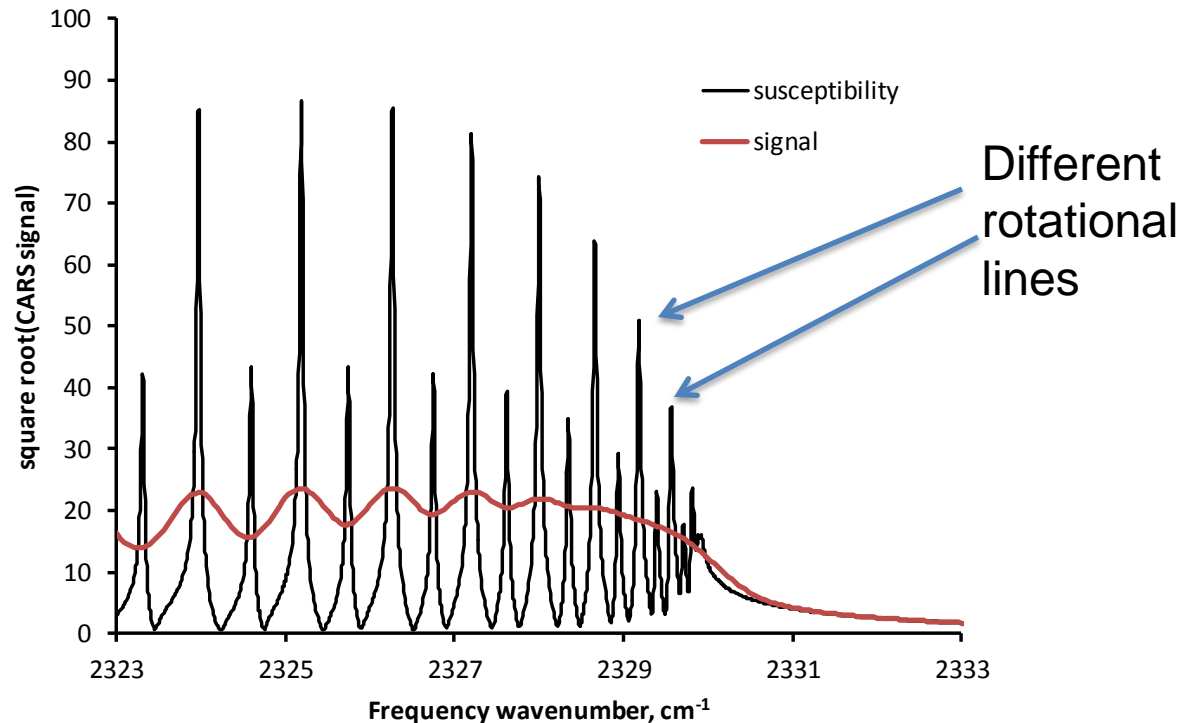
- Γ_j is damping coefficient, N is number density, Δ_j is the population difference
 - $N \rightarrow$ concentration; $\Delta_j \rightarrow$ Temperature sensitivity



CARS Theory 3



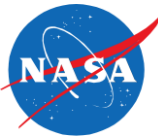
- Instructive to graph example N_2 spectra:



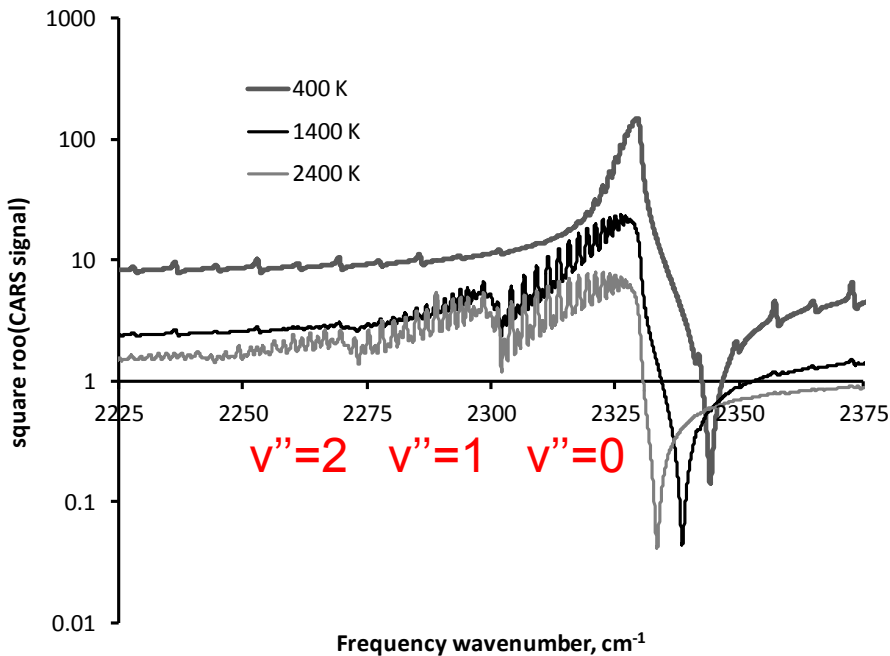
- N_2 is commonly probed with CARS because it is often present and spectroscopy is well known
- CARS spectrum at 1 atm., 1400 K, $v'' = 0$ band.
 - N_2 Q-branch ($\Delta v = +1$, $\Delta J = 0$)
 - CARS signal spectrum is convolved with lasers used



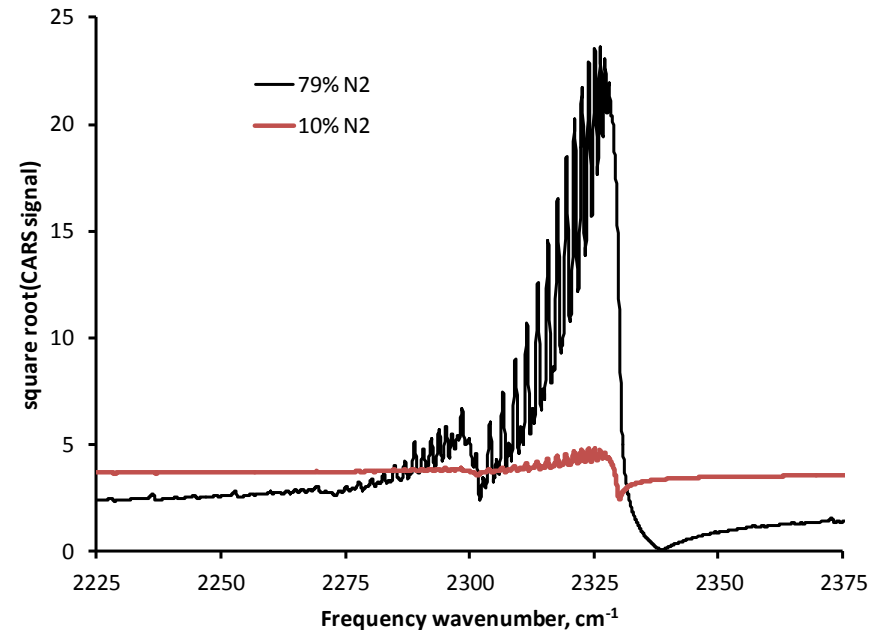
CARS Theory 4



- Effects of temperature (left) and composition (right):

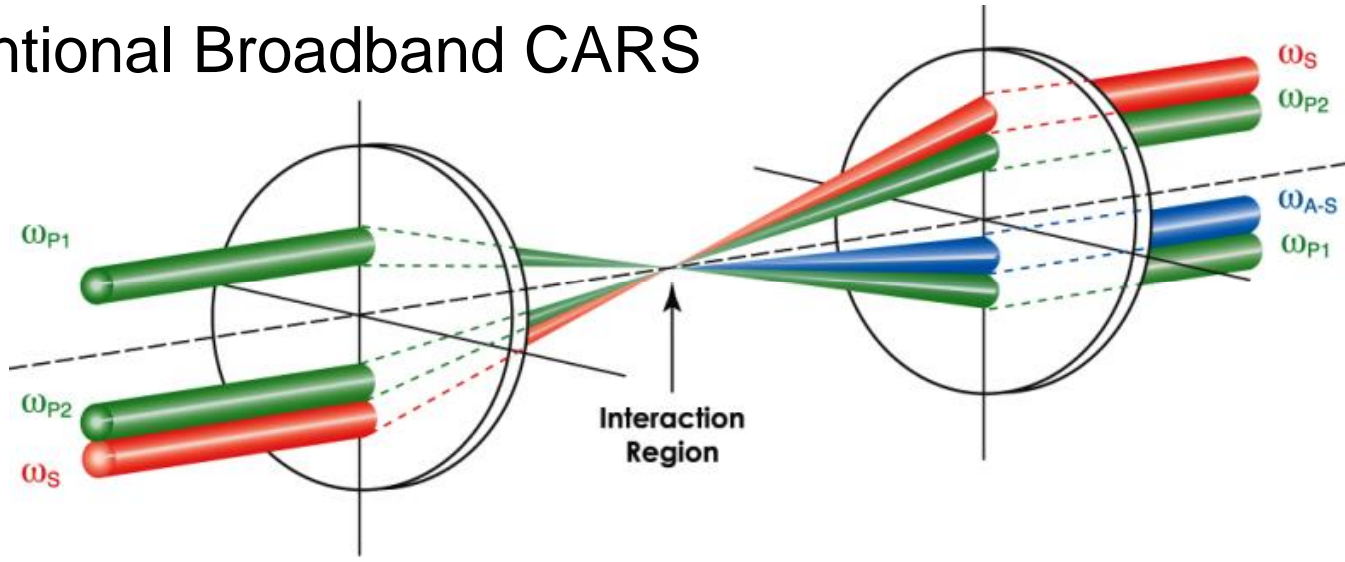


Vibrational “hot band” becomes populated above 700 K

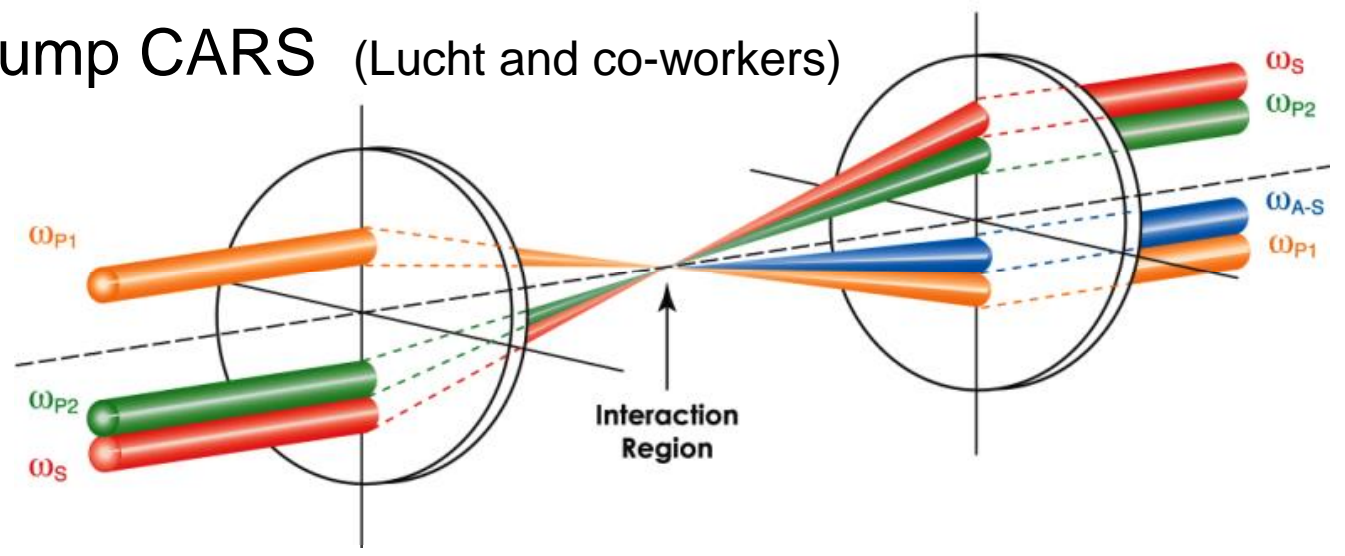


CARS spectra are sensitive to the gas composition through resonant and nonresonant parts

Conventional Broadband CARS

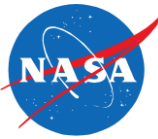


Dual-Pump CARS (Lucht and co-workers)

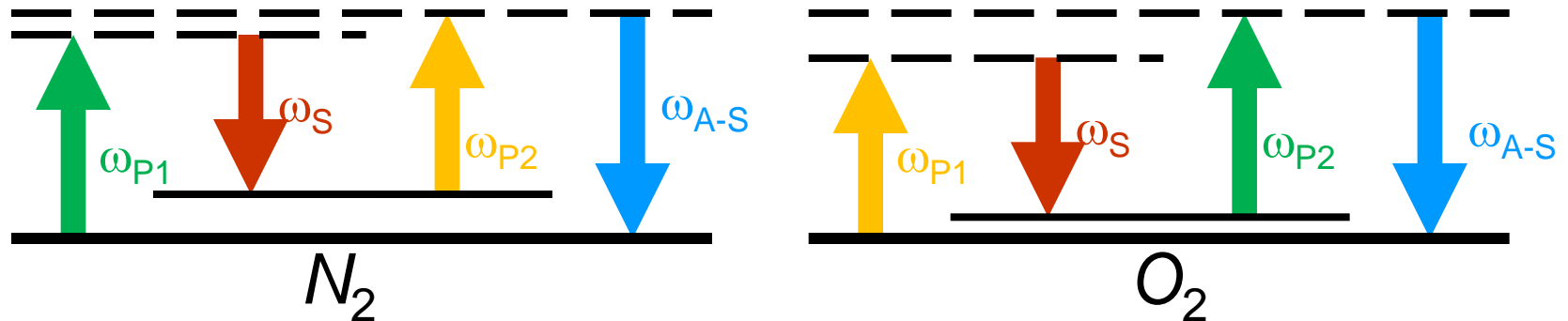




Dual-Pump CARS: N_2 , O_2 , H_2



- Green and Red Probe N_2 Raman Shift
- Red and Yellow Probe O_2 Raman Shift



- Result: Two different spectral regions of Raman Shift appear coincident in the 490 nm CARS beam.
 - ‘self calibrating’ compared to other methods
 - H_2 pure rotational Raman lines present

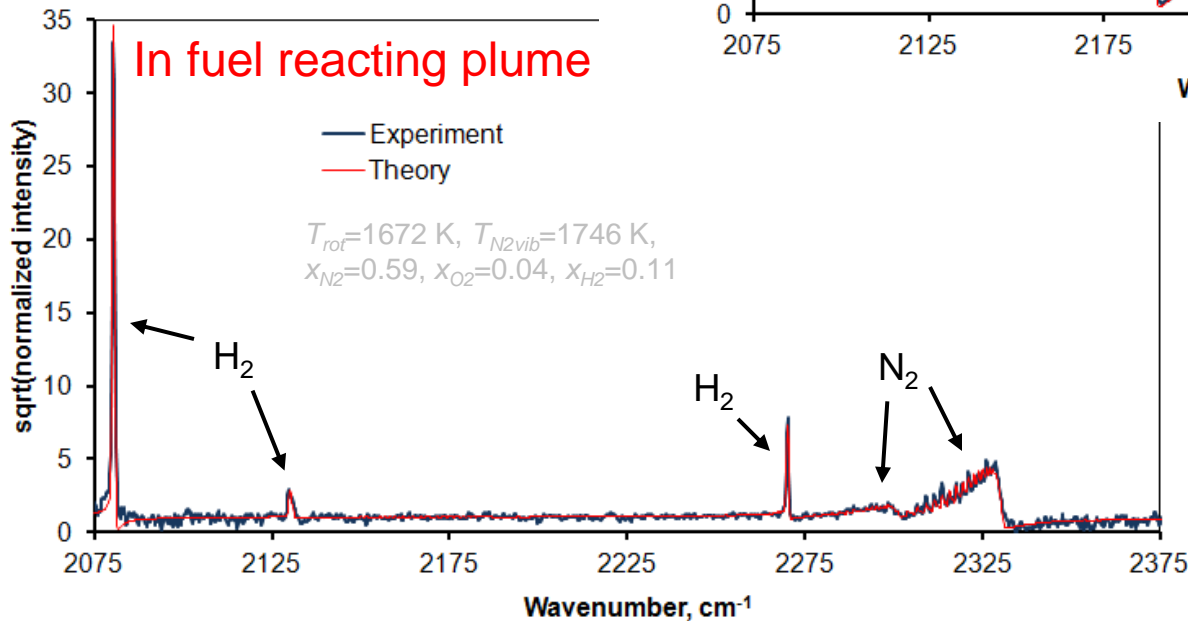
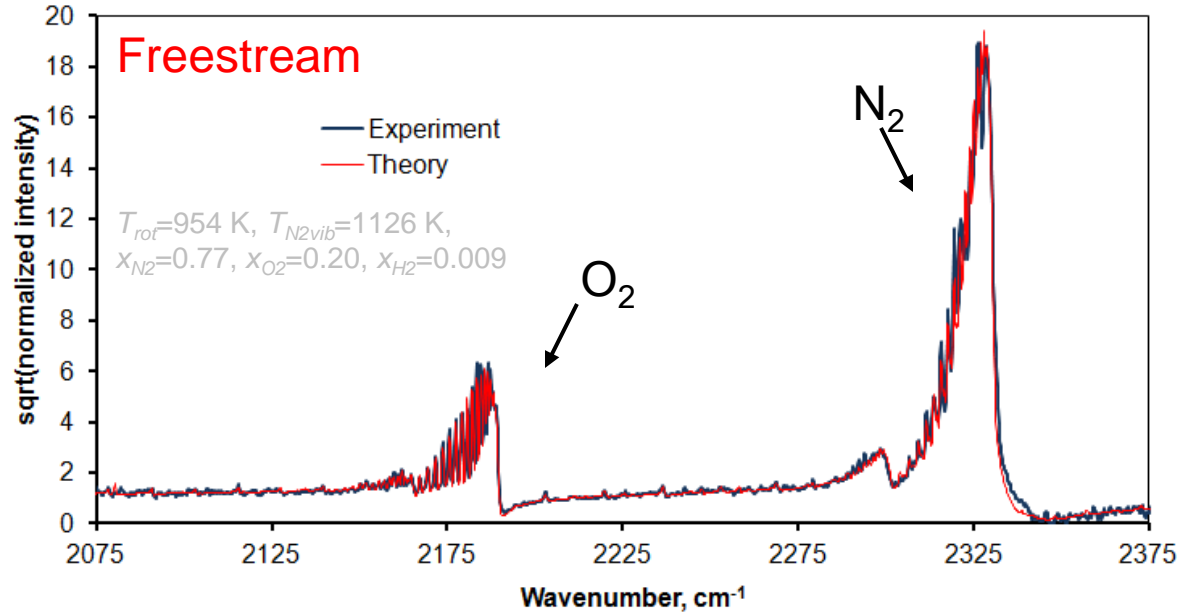
O’Byrne et al AIAA Journal v. 45, 2007



Typical Dual-Pump CARS Spectra and Fits



- Single-shot spectra obtained in combustor shown with best fit
- Absolute measurement of rotational, vibrational temperature, N_2 , O_2 , and H_2 mole fractions

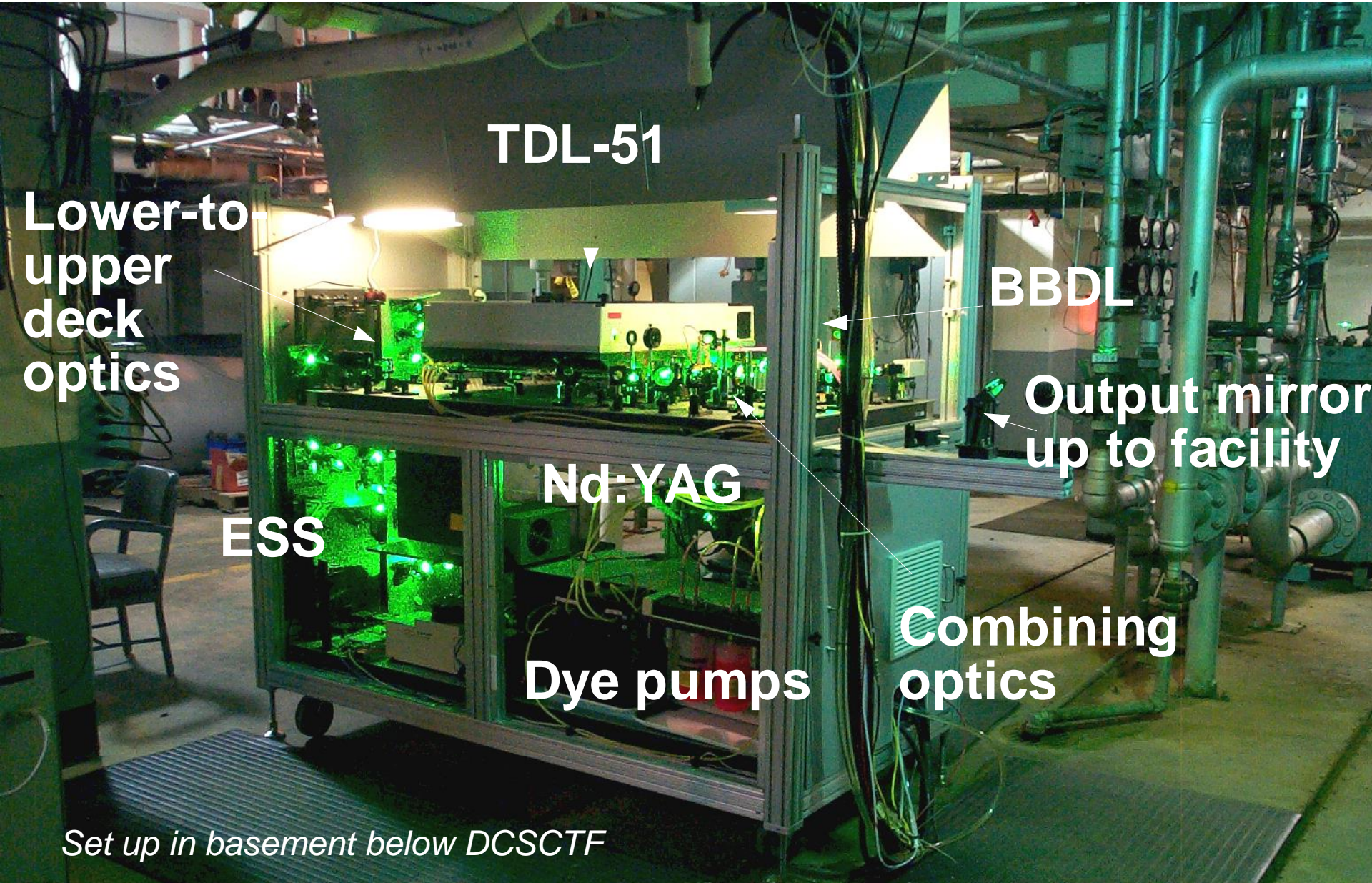


- Measurement obtained:
 - In UVa Scramjet (Conf C)
 - $\phi=0.18$, Plane 2, $z/H=0$
 - in 10 ns (instantaneous)
 - at 20 Hz repetition rate
 - Measurement volume = $1.7 \times 0.2 \times 0.2$ mm^3



NASA/GWU Mobile CARS System

→ Simplifies/speeds set up in facility



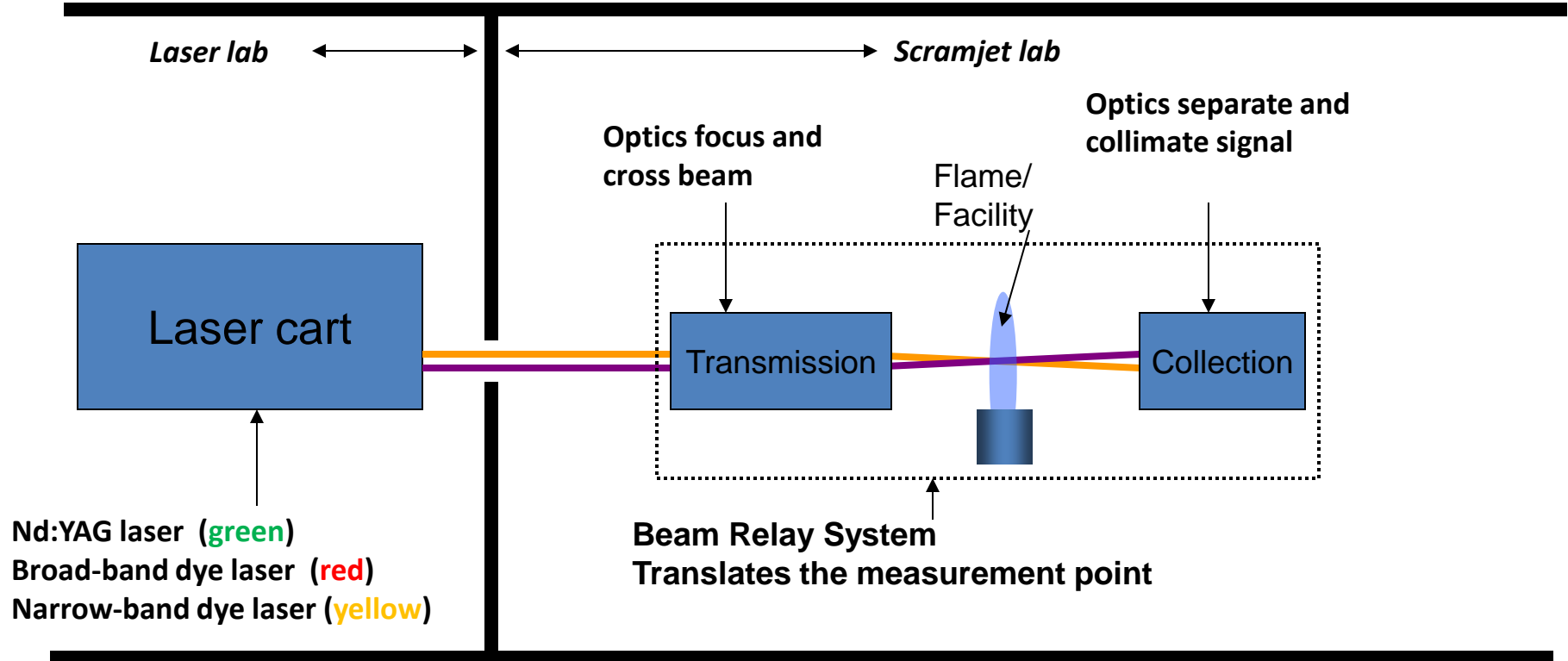
Set up in basement below DCSCCTF



- YAG laser plus 2 dye lasers on single cart
- Transmission and receiving optical stages
- Can put system on a truck and moved to facilities
- Measures T_{rot} , T_{vib} , N_2 , O_2 , H_2 mole fractions at 20 Hz.
 - Quantified accuracy, precision
- Fully automated data acquisition
 - Remote operation of system
 - X-Y (-Z) probe volume traverse capability
 - Input test matrix; then system acquires and automatically saves data for hours until complete
 - Laser power automatically adjusted to prevent saturation effects (detector saturation, Stark broadening, Raman pumping)
 - Beam alignment monitors; remote control alignment
- Beam shaping capability to maintain alignment measurement in turbulent/vibration flows
 - 10x improvement compared to USED CARS

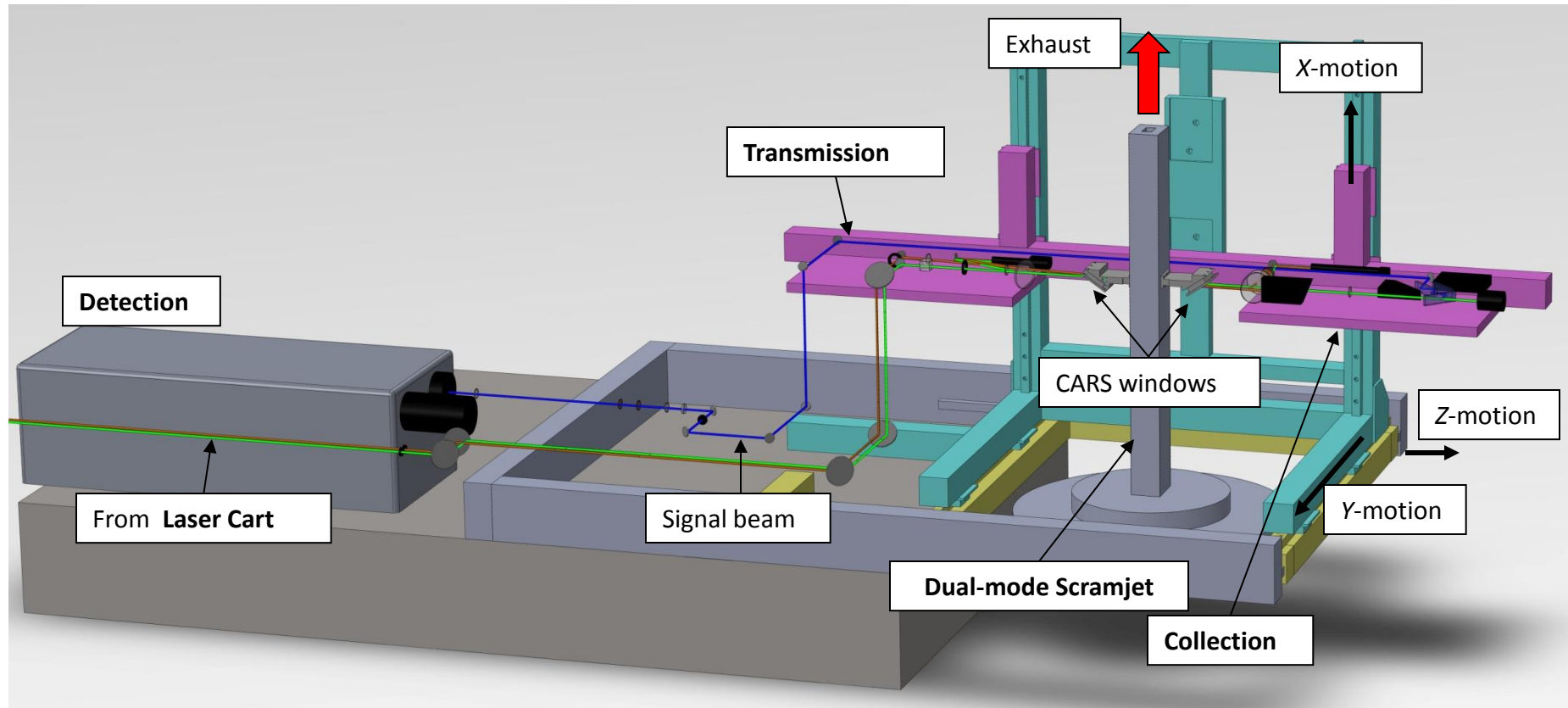


Setup at UVa: Optical System 1



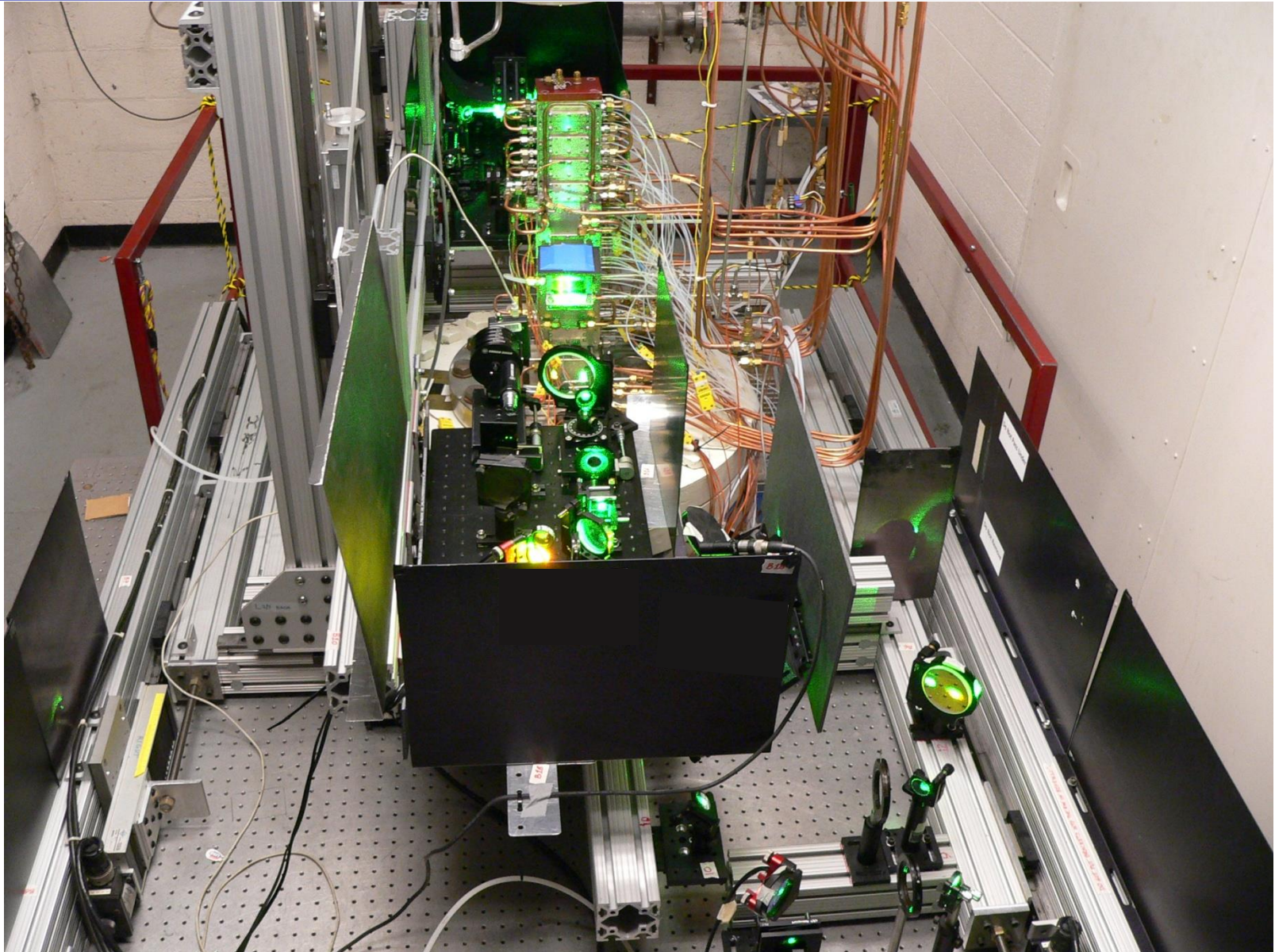


Setup at UVA: Optical System 2

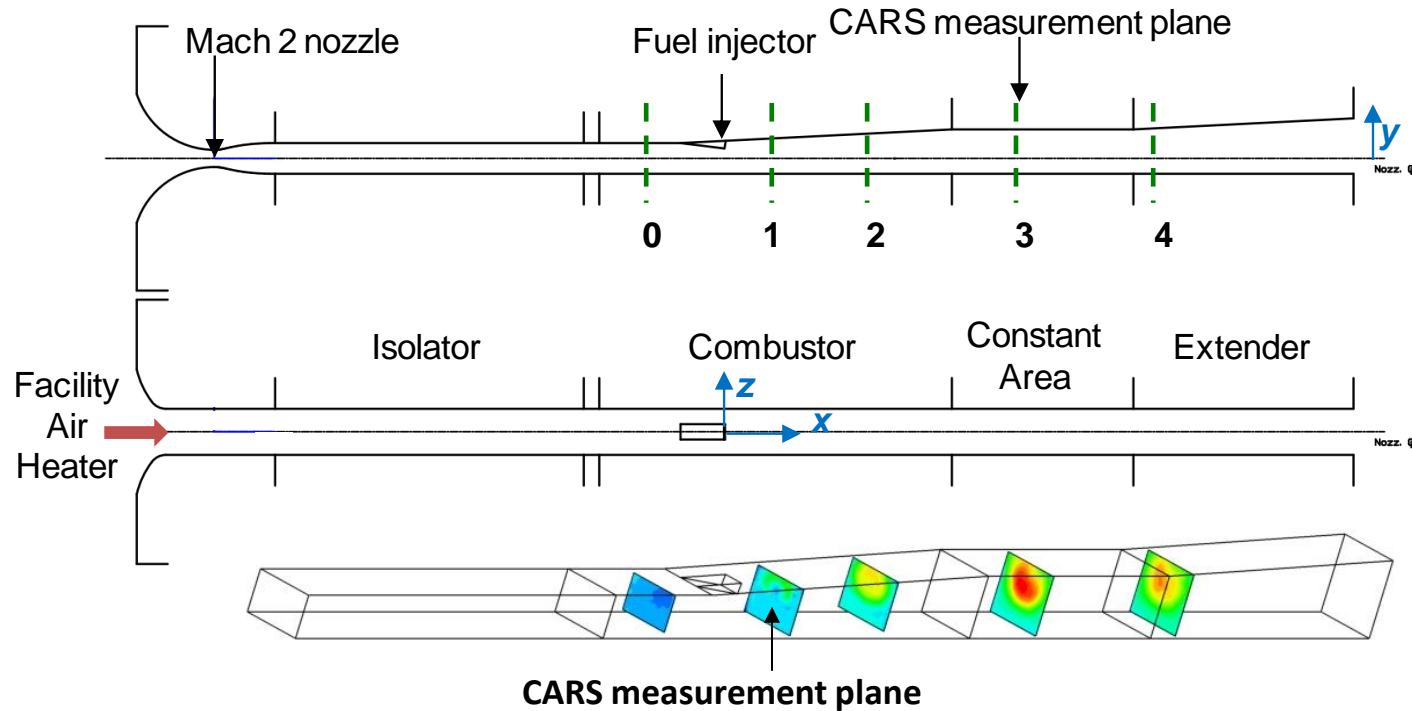




Transmission stage and test section at UVa



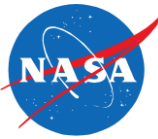
Facility / Dual Mode Scramjet at UVA



- Electrically heated clean air, nominal $T_t = 1200$ K, $M = 2$ nozzle
- Long test times allow large data sets at steady inflow conditions
- Highly turbulent flowfield
- Good optical access



Nonequilibrium: CARS T_{rot} and T_{vib}



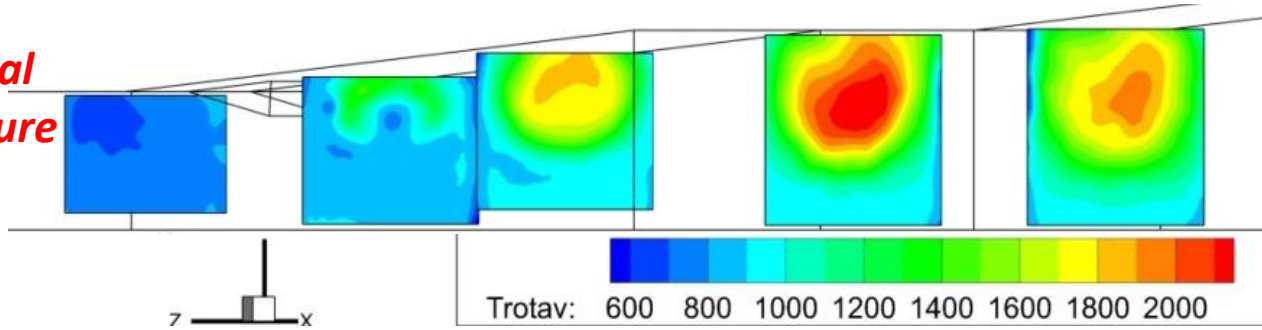
H₂ fuel, Config. C

A. D. Cutler, G. Magnotti, L. Cantu, E. Gallo, P. M. Danehy, R. Rockwell, C. Goynes, and J. McDaniel, "Dual-Pump CARS Measurements in the University of Virginia's Dual-Mode Scramjet: Configuration C," Paper AIAA-2013-0335, 2013.

A.D. Cutler, L. M. L. Cantu, E. C. A. Gallo, R. Baurle, P. M. Danehy, R. Rockwell, C. Goynes, and J. McDaniel, "Nonequilibrium Supersonic Freestream Studied Using Coherent Anti-Stokes Raman Spectroscopy," AIAA Journal (in press) 250

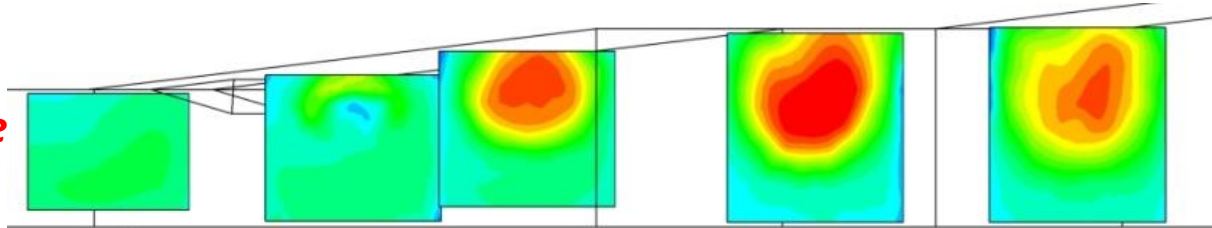
Mean Rotational Temperature

$\phi=0.18$

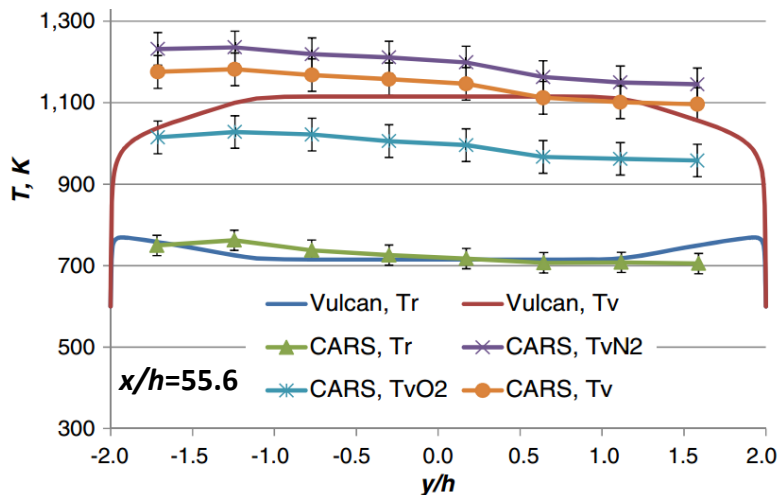


Mean Vibrational Temperature

$\phi=0.18$



T_{N_2vib} observed to be 600 K higher than T_{rot} in facility freestream; not anticipated before experiment



Vibrational Temperature
CARS vibrational O₂ and N₂ temperatures "lumped" together and used to validate the vibrational nonequilibrium model implemented in VULCAN code by R. Baurle (NASA).

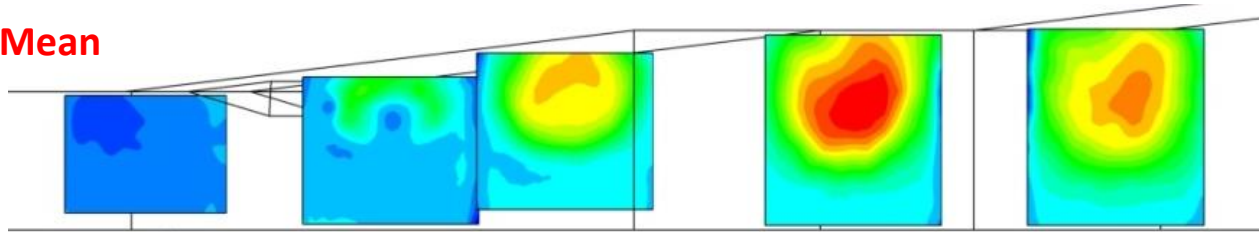
Temperature Mean, Standard Deviation



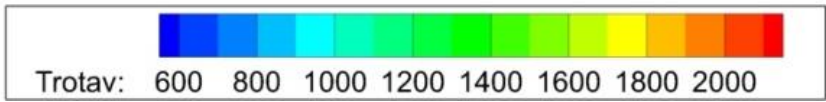
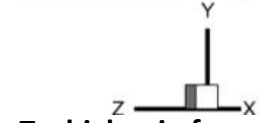
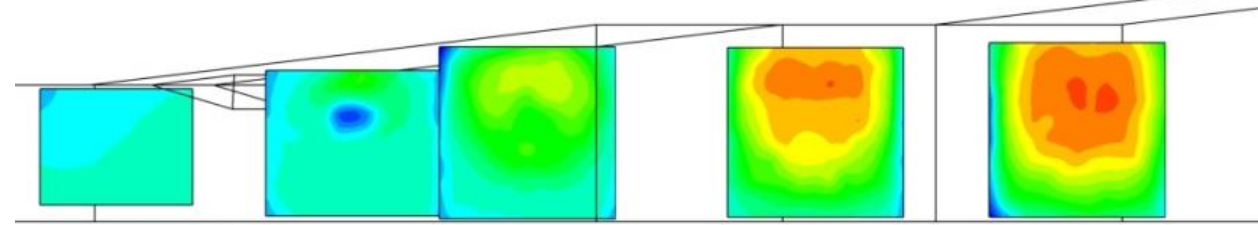
Rotational Temperature

Mean

$\varphi=0.18$



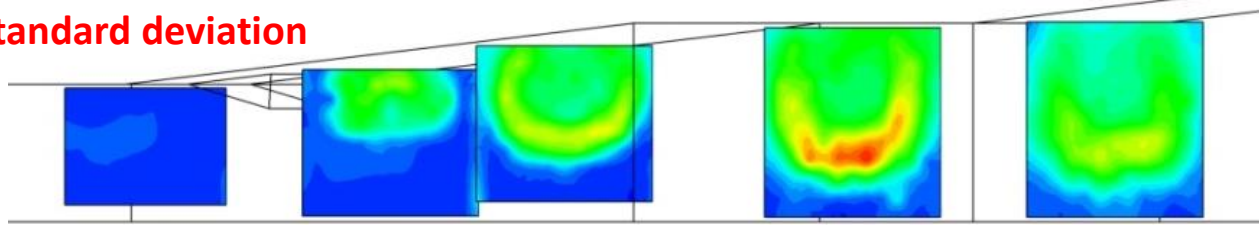
$\varphi=0.49$



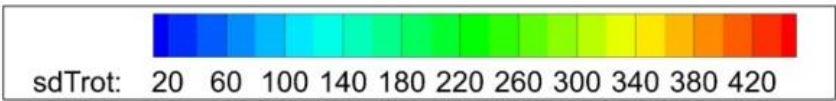
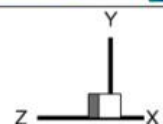
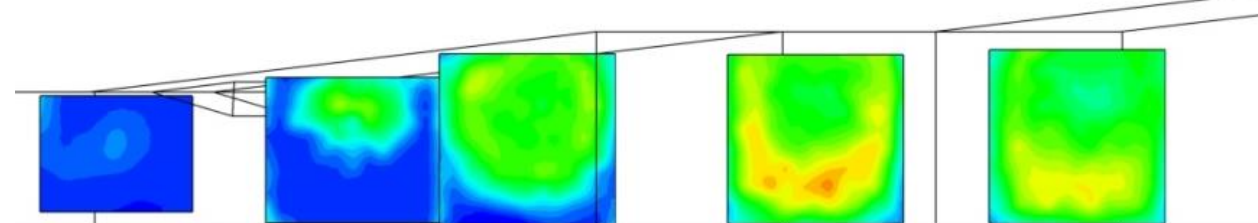
T_{rot} higher in free stream for $\varphi=0.49$ due to ram mode

Standard deviation

$\varphi=0.18$

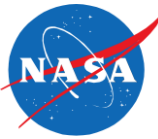


$\varphi=0.49$

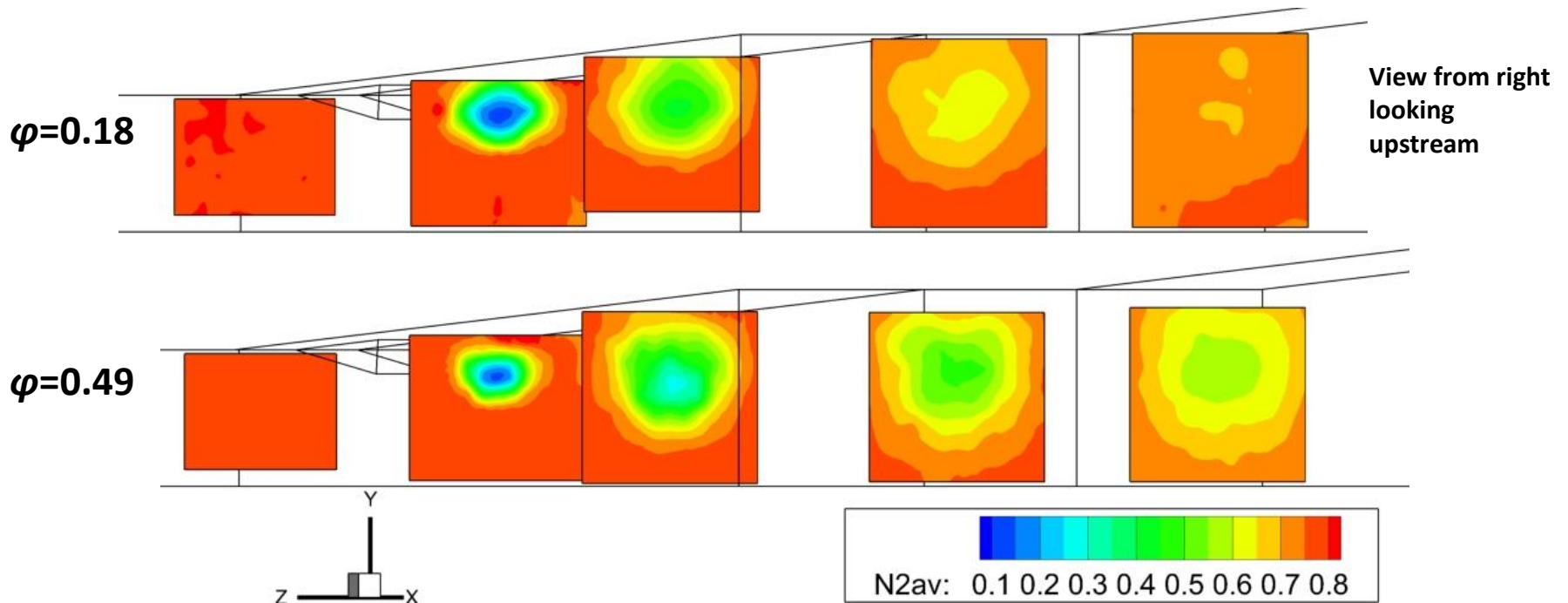
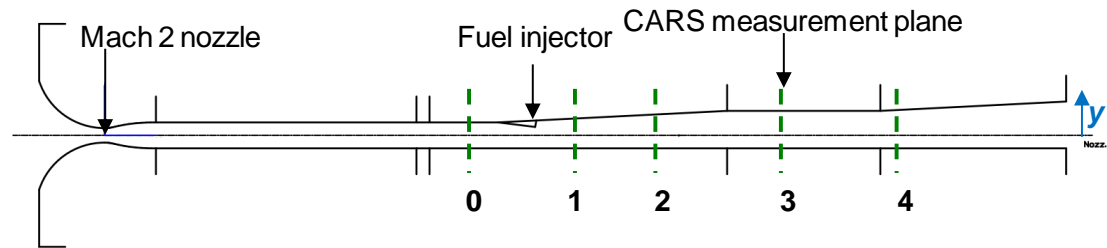




Contours of Mole Fraction N_2



- Since inert shows overall mixing



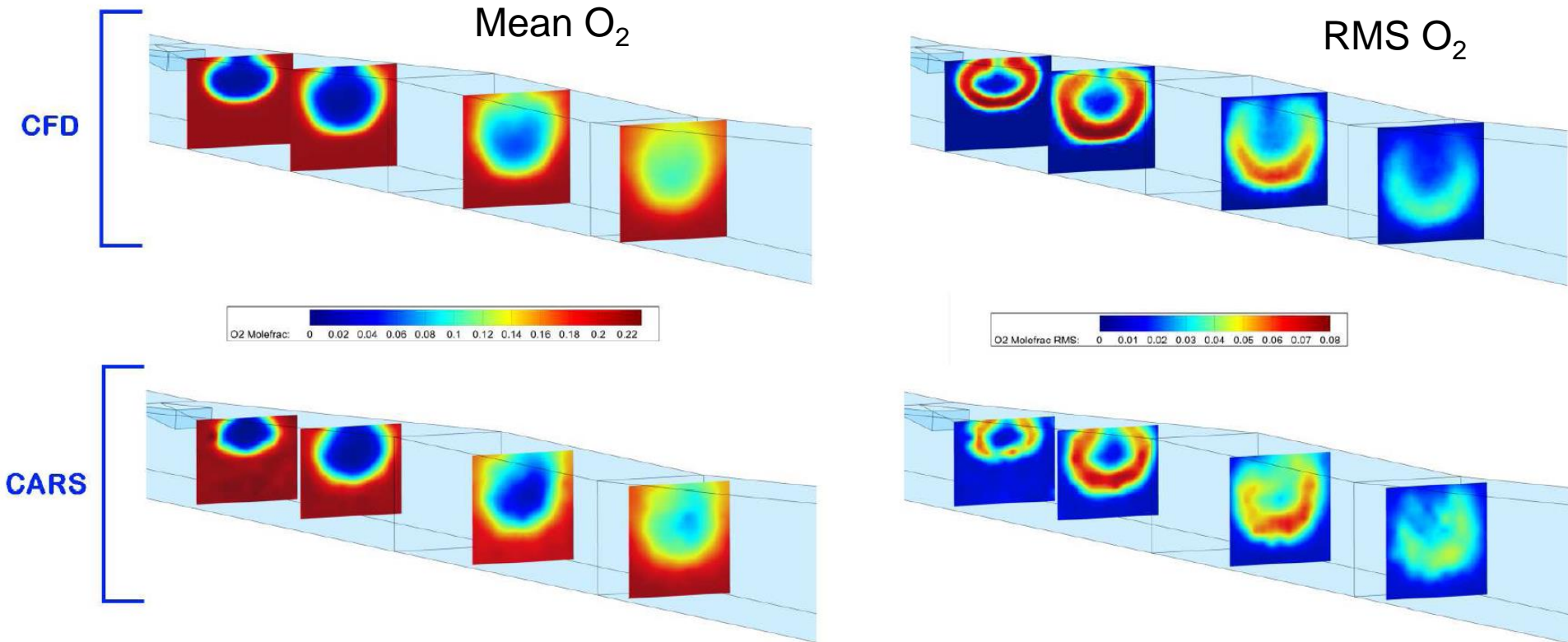


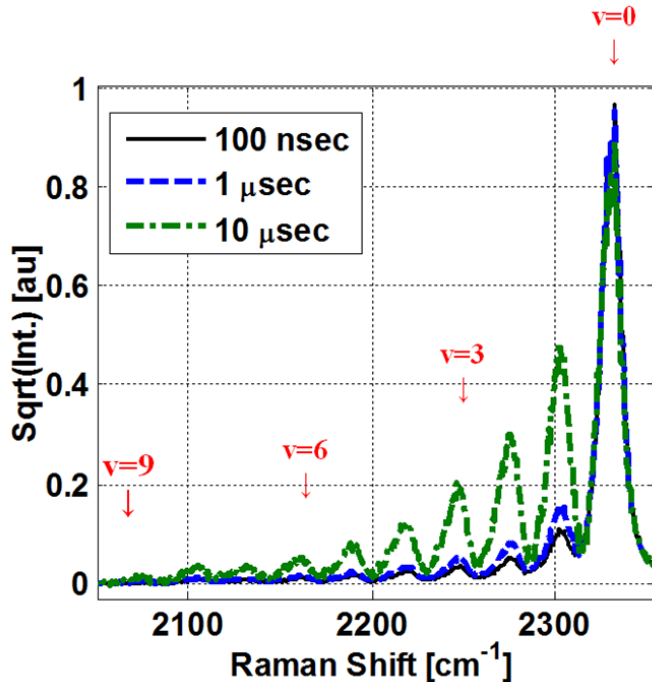
Figure 9. Comparison between CARS and O₂ concentrations and RMS fluctuations for '0.17' equivalence ratio.

- CARS provides valuable quantitative comparison data
 - Fulton, Edwards, et al, (Configuration C) AIAA-2013-0117, 2013
 - *The comparisons are not always this good!*

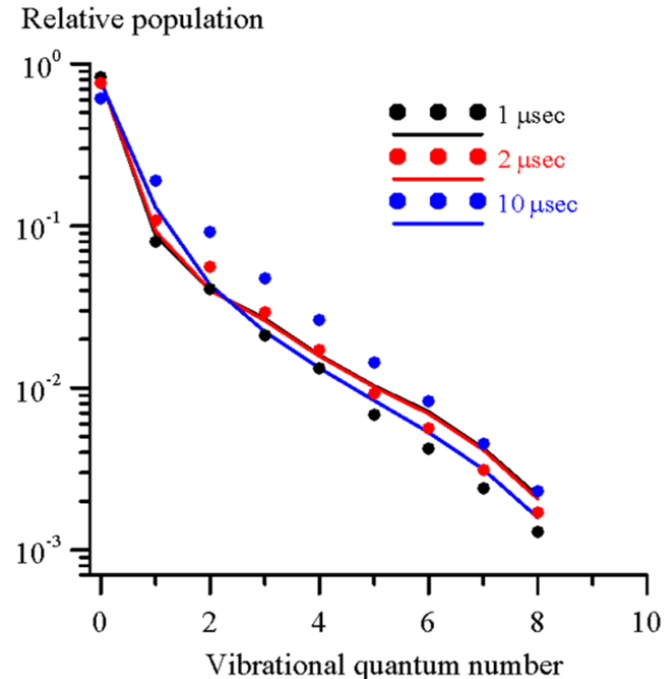


CARS for nonthermal plasma

- 100 Torr pulsed discharge at Ohio State



(a)



(b)

- CARS can measure individual state populations for model validation.
- A. Montello, Z. Yin, D. Burnette, I.V. Adamovich, and W.R Lempert, "Picosecond CARS Measurements of Nitrogen Vibrational Loading and Rotational/Translational Temperature in Nonequilibrium Discharges," J. Phys. D: Appl. Phys., Sept, 2013.

Additional Thoughts on CARS



- CARS is a relatively accurate and precise high-temperature and species measurement technique in reacting and nonequilibrium flow
 - Temp. Accuracy 2-3%; Precision 2-3% (Magnotti, 2012)
- CARS can be performed through small windows or slots but need access on 2 sides.
- It is a relatively complicated technique, theoretically and experimentally, though seedless.
 - Takes months to analyze data carefully.
- Is being extended to much faster measurements ~10 kHz with fs CARS
 - Very recently: 2 beam CARS, CARS imaging (Sandia)
- Has been performed using optical fibers to deliver the laser beams, both in ns and ps regimes



Conclusion



- Variety of different molecular-based measurement technologies are available for measuring hypersonic nonequilibrium flows.
 - Can measure temperature, density, velocity, species concentrations, etc.
 - Which is best? Which technique to use?
- Must start measurement campaign with an interview of “customer” to determine the requirements
 - How do different measurement technique capabilities satisfy the requirements?



Conclusion



- Variety of different molecular-based measurement technologies are available for measuring hypersonic nonequilibrium flows.
 - Can measure temperature, density, velocity, species concentrations, etc.
 - Which is best? Which technique to use?
- Must start measurement campaign with an interview of “customer” to determine the requirements
 - How do different measurement technique capabilities satisfy the requirements?
 - Also consider practical issues:
 - Experience of the research team
 - Available equipment / budget
 - Schedule, difficulty of method, etc.
 - Rarely a perfect match, but a match can provide the data needed to advance or validate theory or computations



The interview: prior to getting started



- What parameter(s) need to be measured?
- Must multiple parameters be obtained simultaneously to determine correlations?
- What spatial resolution is required?
- Is imaging required or are single-point or line measurements sufficient?
- What temporal resolution is required? (e.g. time required for a single measurement)
- Do measurements need to be time resolved? (e.g. a continuous sequence of data)
- What accuracy is needed?
- What precision is needed?
- What quantity of data is required?
- When is the data needed? Is instant (real-time) data required?
- Where in the flow are measurements required? (inflow, exit, near walls, etc.)
- What type of optical access is available?
- Can (toxic) seed gases be introduced? Will they influence the properties being measured?
- What is the ordered priority of the above requirements?